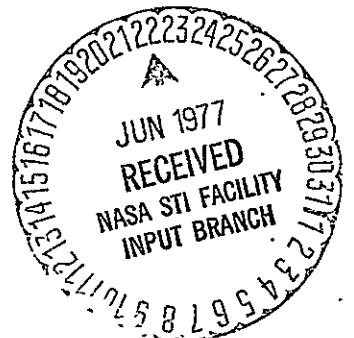
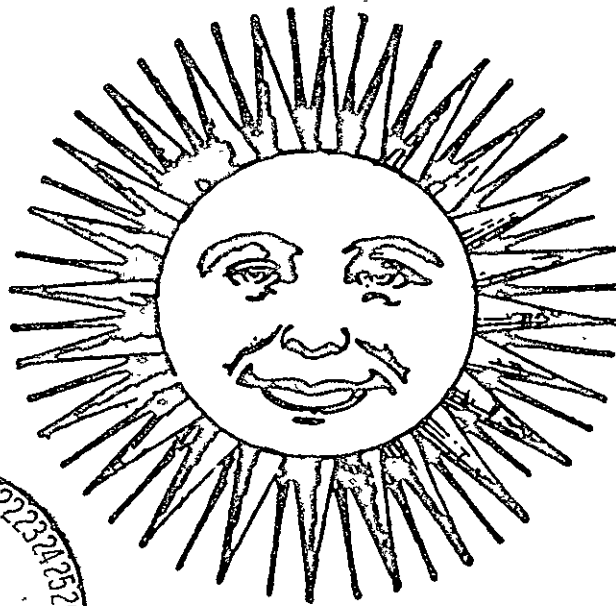


SPACE-BASED SOLAR POWER CONVERSION AND DELIVERY SYSTEMS STUDY

VOLUME II ENGINEERING ANALYSIS OF ORBITAL SYSTEMS

(NASA-CR-150295) SPACE-BASED SOLAR POWER N79-22618
CONVERSION AND DELIVERY SYSTEMS STUDY.
VOLUME 2: ENGINEERING ANALYSIS. Final
Report (Grumman Aerospace Corp.) 264 p HC Unclas
A12/MF A01 CSCL 10B G3/44 19216



FINAL REPORT

**SPACE-BASED SOLAR POWER
CONVERSION AND DELIVERY
SYSTEMS STUDY**

VOL. II
ENGINEERING ANALYSIS
OF ORBITAL SYSTEMS

MARCH 1977

Submitted to ECON Inc. in fulfillment of
ECON Agreement E-100 as part of Contract
NAS 8-31308 to NASA/MSFC.

Grumman Aerospace Corporation
Bethpage, N.Y. 11714

FOREWORD

This document is the final report covering Grumman's portion of the "Space-based Solar Power Conversion and Delivery Systems" study, performed under a subcontract to ECON, Inc. The information contained in this report deals primarily with the analyses conducted during the second follow-on effort (Phase III) of the contract. Previous documentation has been provided for Phases I and II of this study effort.

The study activities and related sections of the report, were principally the result of the dedication and untiring efforts of the following Grumman people: Messrs. Ed Magnani, Bruce Clark, Joe Rothenberg, Ken Johnson, Sima Miluschewa, Joe Bundy, Roy Olsen, Marcy Romanelli, and Bert Dawkins.

Special acknowledgment and thanks go to the NASA COR, Mr. Walter Whitaker, for his guidance and direction during the course of the study. In addition, we would like to express our gratitude to Mr. Charles Gutmann, whose valuable critique and encouragement of Grumman's efforts herein, are greatly appreciated.

SUBMITTED BY: *R. J. Adornato*

Rudolph J. Adornato, Study Manager

APPROVED BY: *J. Mockovciak Jr.*

John Mockovciak, Jr., SPS Program Manager

Table of Contents

Section	Title	Page
1.0	Introduction	1
2.0	Study Objectives and Scope	2
3.0	Summary of Engineering Analyses	7
3.1	Major Findings and Conclusions	7
3.2	Recommendations	14
4.0	Updating the Baseline Configuration	21
5.0	Phase III Engineering Studies	26
5.1	Analysis of LEO and GEO Construction/ Assembly Approach	26
5.1.1	Construction Base Concepts	31
5.1.2	Construction/Assembly Transportation Scenarios	57
5.1.3	Impact on Satellite Design Requirements	63
5.1.3.1	Structural Loading Requirements	63
5.1.3.2	Structural Vibration Modes	73
5.1.3.3	Attitude Control and Orbit Keeping	79
5.1.4	Impact on Construction Base Requirements	94
5.1.4.1	Radiation Environment	94
5.1.4.2	Occultation/Thermal Cycling Environment	97
5.1.4.3	Collision Probability	104
5.1.5	Transportation System Requirements	104
5.1.5.1	Baseline Transportation System Selection	104
5.1.5.2	Transportation Requirements for LEO and GEO Construction	106
5.1.6	Conclusions and Recommendations	111
5.2	Power Distribution	114
5.2.1	Introduction	114
5.2.2	Baseline Configuration	115
5.2.3	Conducting Structure	117
5.2.3.1	Efficiency and Total Power	117
5.2.3.2	Mass/Efficiency Optimization	117
5.2.4	Central Mast	133
5.2.5	Rotary Joint/Slip Rings	139
5.2.6	Major Study Results	141
5.2.7	Recommendations	142

Table of Contents (Continued)

<u>Section</u>	<u>Title</u>	<u>Page</u>
5.3	Program Plans and Costs	143
5.3.1	Alternate Development Programs and Cost .	144
5.3.2	Technology Development Plans.	161
REFERENCES		185
APPENDIX A - Final Report Briefing		A1
APPENDIX B - Inputs to Econ Inc. for Economic Analysis		B1
BIBLIOGRAPHY		

LIST OF ILLUSTRATIONS

Figure	Title	Page
2-1	Grumman's Role.	3
2-2	Overall Study Flow.	4
3-1	Truss-Type Structure Fabrication/Assembly	9
3-2	Factory-In-Space Concepts	12
3-3	Triads of SPS Program Interactions.	15
3-4	Candidate SPS Construction Scenarios.	20
4-1	Comparison of Concept Descriptions.	22
4-2	Comparison of Efficiency Chains	23
4-3	Comparison of Mass Properties	25
5-1	LEO vs GEO Construction/Assembly Task	27
5-2	Satellite Solar Power Station - Phase II Study Config.	28
5-3	Construction Base	32
5-4	Construction Sequence - Small Construction Base	33
5-5	Construction Sequence - Small Construction Base (Second Pass)	35
5-6	Construction Sequence - Small Construction Base (Third Pass).	36
5-7	Conducting Structure.	37
5-8	Square Mast Support Structure	38
5-9	Antenna Construction Jig.	39
5-10	Rotary Joint.	40
5-11	Rotary Joint Detail	41
5-12	Rotary Drive and Bearing.	43
5-13	Roller Bearing Detail	44
5-14	Construction Sequence - Small Construction Base (10th Bay Stitched)	45
5-15	20-M Beam Fabrication Module.	46
5-16	1-M Beam Maker.	47
5-17	Construction Base Crawler	48
5-18	Switch Assembly	49
5-19	20M Beam Fab Module Apex Assy	51
5-20	Typical Butt Joint Intersection	52
5-21	Selected Joint and Fastener Techniques.	53
5-22	Cable Rigging	54
5-23	Blanket/Reflector Bungee Installation	55
5-24	Construction Sequence - Large Construction Base	56
5-25	Construction Sequence - Large Construction Base	58
5-26	Construction Base Mass Properties and Characteristics	59
5-27	Warehouse Storage Mass vs Construction Time	60
5-28	Construction Base Equipment and Crew Requirements	61
5-29	LEO Construction/Assembly Scenario.	62
5-30	GEO Construction/Assembly Scenario.	64
5-31	SSPS Gravity and Centrifugal Forces	66
5-32	Comparison of Loads Between Small and Large Construction Bases at 200 N-Mi	67

LIST OF ILLUSTRATIONS (Continued)

Figure	Title	Page
5-33	Loads on SSPS During Construction: Variation with Altitude.	68
5-34	Effect of Construction Base Mass on Loads at 200 N Mi . . .	70
5-35	Maximum Member Loads After First Construction Pass.	71
5-36	SSPS Bending Moments, Small Factory 200 N Mi.	72
5-37	Comparison of Vibration Modes With and Without Construction Base	75
5-38	Full SSPS NASTRAN Structural Model With Large Construction Base	76
5-39	One-Bay NASTRAN Structural Model with Small Construction Base	77
5-40	Required Fundamental Structural Frequency vs Orbital Altitude.	78
5-41	Study Matrix.	80
5-42a	Configuration A: Small Factory	81
5-42b	Configuration B: Large Factory	82
5-43	Mass and Body Axis Inertias	83
5-44a	Disturbance Torques: Small Factory	84
5-44b	Disturbance Torques: Large Factory	85
5-45a	Propellant Requirements: LEO Attitude Control During Construction	87
5-45b	Propellant Requirements: LEO Ion Thruster Power.	88
5-46a	Propellant Requirements: GEO Attitude Control During Construction	89
5-46b	Propellant Requirements: GEO Ion Thruster Power.	90
5-47	LEO Ballistic Coefficients ($C_D = 2.0$)	91
5-48	LEO Aerodynamic Drag Force ($C_D = 2.0$)	92
5-49	LEO Orbitkeeping Propellant Requirements.	93
5-50	Attitude Control Orbitkeeping Requirements: Summary Comparison.	95
5-51	Radiation Environment in Space.	96
5-52	Average Biological Rad Doses in GEO	98
5-53	Construction Base Electrical Power Requirements	100
5-54	Structural Temperatures During Occultation.	101
5-55	Solar Look Angle During LEO Construction - Local Vertical Attitude Hold.	102
5-56	Deflections in 20-Meter Beam Due to Thermal Gradients . . .	103
5-57	LEO Collision Probability	105
5-58	Heavy Lift Launch Vehicle	107
5-59	Baseline Cargo Orbital Transfer Vehicle	108
5-60	Baseline Personnel Orbital Transfer Vehicle	109
5-61	Satellite Materials Matrix.	110
5-62	Conclusions - LEO vs GEO Construction Location.	112
5-63	GEO Construction Scenario - Small Construction Base	113
5-64	Comparison of Concept Descriptions.	116

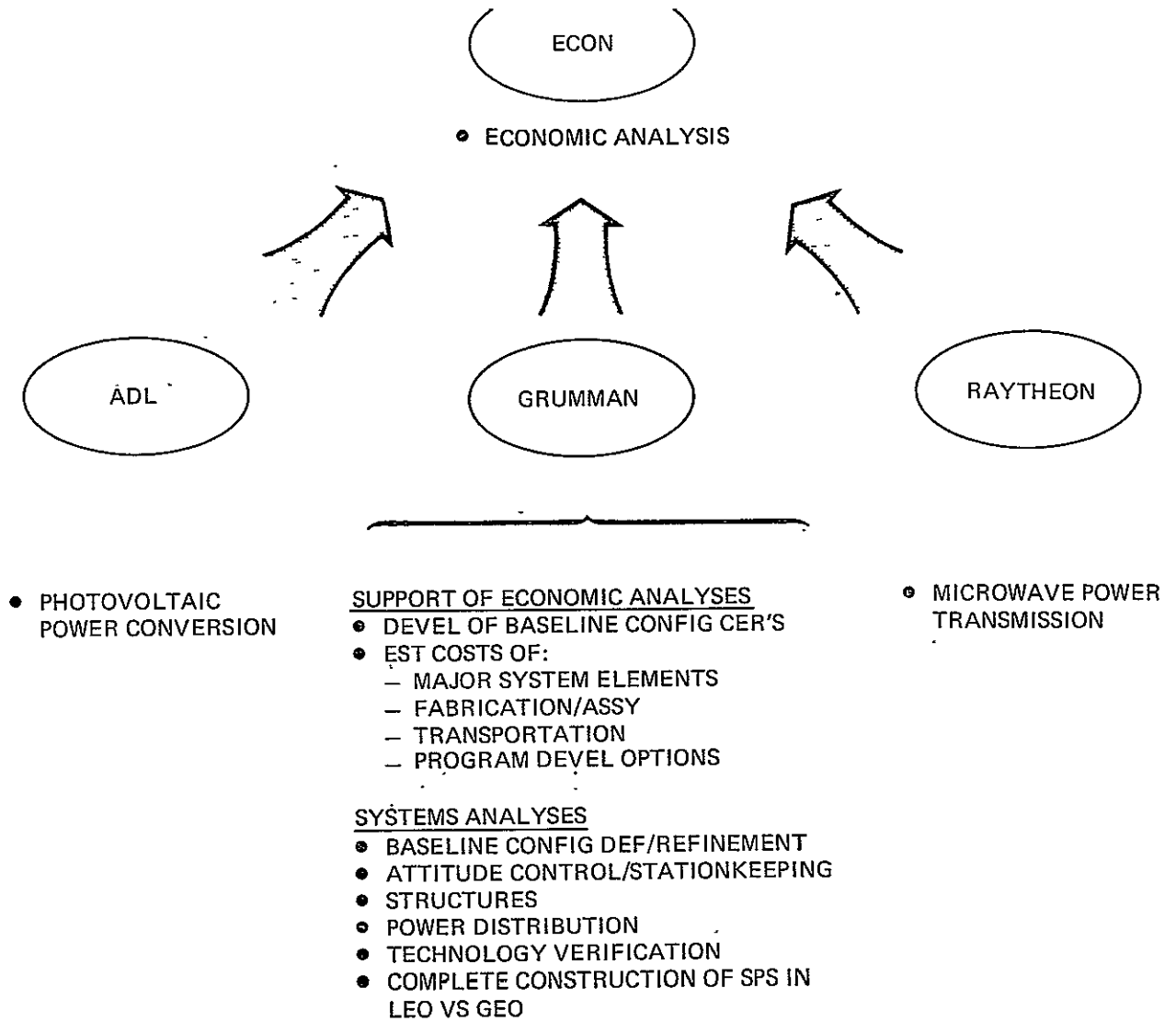
LIST OF ILLUSTRATIONS (Continued)

Figure	Title	Page
5-65	Nominal System Efficiency Chain	118
5-66	Optimized Current Density	120
5-67	Conductor Heating Area Requirements for Optimum Current Density	122
5-68	Thermal Radiation Coupling Model	123
5-69	Conductor Bus Dimensions	124
5-70	Current Density Boundary	125
5-71	Required Conductor Radius	126
5-72	Current Distribution	127
5-73	Solar Array LRU Characteristics	128
5-74	Load in Critical Member	130
5-75	Mass Savings and Power Distribution Efficiency vs Conductor Temperature	131
5-76	System Weights	132
5-77	Power Bus Eclipse Transient Cool-Down	134
5-78	Thermal Stresses in Mast and Conductor	135
5-79	Conducting Structure	136
5-80	Square Mast Support Structure	137
5-81	Rotary Joint Electrical Details	140
5-82	SPS Development Program 4	145
5-83	150 KW LEO Spacecraft Facility: Assembled Configuration	146
5-84	150 KW LEO Spacecraft Facility Launch Mass	147
5-85	150 KW LEO Spacecraft Facility: Assembly Sequence	149
5-86	Shuttle Construction of 150 KW LEO Facility	150
5-87	Program 4 Costs	151
5-88	Space Power Demonstration System - Typical Program Options	152
5-89	Program 4 - Transportation and Assembly Costs for 2 MW Demo Satellite	154
5-90	SPS Development Program 5	155
5-91	150 KW GEO Test Satellite	156
5-92	150 KW GEO Test Satellite Mass	157
5-93	Program 5 Costs	159
5-94	Program 5 - Transportation and Assembly Costs for 2 MW Demo Satellite	160
5-95	Near Term Resource Estimates for Key SPS Technology Areas	161
5-96	Microwave Technology Resource Requirements	162
5-97	Microwave Technology Requirements (Sheet 1)	163
5-98	Microwave Technology Requirements (Sheet 2)	164
5-99	Microwave Technology Requirements (Sheet 3)	165
5-100	Microwave Technology Requirements (Sheet 4)	166
5-101	Large Solar Array Technology Resource Requirements	167
5-102	Large Solar Array Technology Improvement (Sheet 1)	168
5-103	Large Solar Array Technology Improvement (Sheet 2)	169

LIST OF ILLUSTRATIONS (Continued)

Figure	Title	Page
5-104	Resource Requirements for Solar Blanket Verification Testing	170
5-105	Space Environment Implications.	171
5-106	Solar Cell/Solar Blanket Test Program (Sheet 1)	172
5-107	Solar Cell/Solar Blanket Test Program (Sheet 2)	173
5-108	Key Solar Cell/Solar Blanket Detail Test Objectives and Requirements (Sheet 1).	174
5-109	Key Solar Cell/Solar Blanket Detail Test Objectives and Requirements (Sheet 2).	175
5-110	Key Solar Cell/Solar Blanket Detail Test Objectives and Requirements (Sheet 3).	177
5-111	Structural Technology Resource Requirements	178
5-112	Assembly and Operations - Verification/Demonstration of Manned and Remote Assembly Rates	179
5-113	Test Program for Verification/Demonstration of Manned and Remote Assembly Rates (Sheet 1)	180
5-114	Test Program for Verification/Demonstration of Manned and Remote Assembly Rates (Sheet 2)	181
5-115	Test Program for Verification/Demonstration of Manned and Remote Assembly Rates (Sheet 3)	182
5-116	Test Program for Verification/Demonstration of Manned and Remote Assembly Rates (Sheet 4)	183

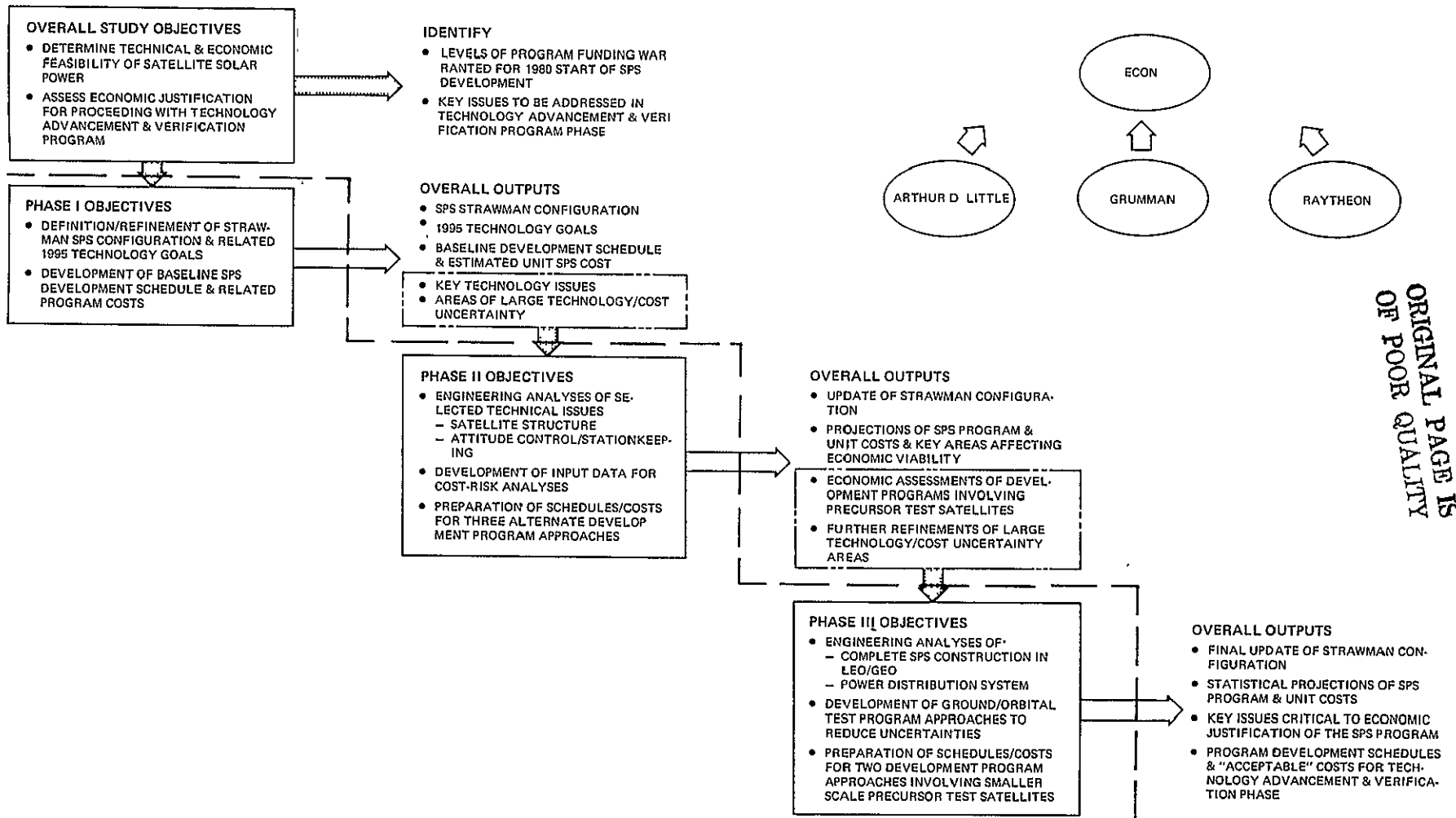
PRECEDING PAGE BLANK NOT FILMED



A-66

Fig. 2-1 Grumman's Role

PRECEDING PAGE BLANK NOT



ORIGINAL PAGE IS
OF POOR QUALITY

Fig. 2-2 Overall Study Flow

the assumption that all SPS technology goals projected for the 1995 time frame were achieved.

As a consequence of the Phase I studies, key issues were surfaced which were critical to the technical and economic assessment of a crystal-silicon 5-GW SPS, and which warranted further engineering analysis to reduce their levels of uncertainty.

Phase II: An objective of this phase was to conduct engineering analyses of selected technical issues surfaced during Phase I. These involved the following subjects:

- The satellite's structure and its ability to withstand applied loads during LEO operations, during transport from LEO to GEO, and during on-orbit operations at GEO
- Loads and deflections induced by thermal effects as the SPS enters and exits earth shadowing at GEO
- Overall attitude control/stationkeeping requirements (thrust actuation and propellant) for maintaining an SPS within allowable drift tolerances for constellations of as many as 120 satellites evenly spaced over the continental United States.

An additional objective of this phase was to support the development and application of ECON's cost-risk analysis methodology to further assess the economic feasibility of the crystal-silicon 5-GW SPS. In this economic assessment, SPS costs are presented in terms of probability distributions, as a function of achieving various levels of technology. To support this activity, relationships were developed to express the size and mass of SPS systems, subsystems, orbital construction equipment, and transportation system requirements. These relationships, together with subsystem performance projections, were expressed in the form of worst, most likely, and best values, and used to establish probability density functions within ECON's cost-risk analysis.

A final objective of this phase was to support assessments of economic justifications of alternative SPS program development plans, and the implications of using LEO and GEO test satellites in the overall SPS development plan. Three program development plans were developed, containing none, one, or two test satellites ranging in power outputs between 15 - 1000 MW. These test satellites were assumed to operate in LEO and/or GEO and were precursors to the deployment of a 5-GW prototype SPS. Overall program costs were estimated for each program plan, together with estimates of the percentage reduction in technology uncertainties contributed by the alternative test satellites. These were provided to ECON for application within a decision tree analysis. This analysis identified the expected net economic value of each program development approach, and thus provided a measure of the economics of buying information via the various test satellite approaches.

The results of studies conducted during this phase, identified key areas greatly affecting SPS unit cost distributions, and their respective sensitivity to the overall economic feasibility of the program. Additionally, the negative expected economic values of the large test satellite development programs suggested investigation of smaller test satellite precursor approaches.

Phase III: Study objectives during this phase were focused on engineering analyses that would further reduce the uncertainty in key SPS cost drivers, and upon technology issues that were critical to evaluations of SPS technical feasibility. These included:

- Analysis of construction concepts for building a complete crystal-silicon 5-GW SPS in LEO or GEO, and development of related cost estimates for constructing and assembling this large structure in space
- Analysis of the power distribution system, and development of design concepts for a central mast conducting structure compatible with electrical, thermal, and structural loadings
- Development of ground/orbital test program approaches that would reduce the uncertainties associated with key SPS cost drivers. Approaches were developed addressing: (1) rate of manned and unmanned construction and assembly, (2) solar cell efficiency, and (3) specific mass and cost of the solar blanket
- Development of two alternate program development plans, and related cost estimates, using smaller test satellites in LEO and/or GEO as precursors to the development of a prototype 5-GW SPS system.

Results of this study phase continue to support the technical feasibility of the strawman crystal-silicon 5-GW SPS concept and its chances for economic viability. They further confirm the economic merits of smaller-scale test satellites as precursor development toward full-scale SPS systems. Grumman's overall findings and conclusions from the subject study, and recommendations for further efforts, are summarized in the following section.

3. SUMMARY OF ENGINEERING ANALYSES

This section summarizes the overall results of engineering analyses conducted during the initial and extension phases of this study. As discussed in Section 2.0, Grumman's participation in this study was directed towards two major objectives, namely:

- The support of SSPS economic analyses by providing related programmatic and system cost information for the orbital system elements
- The conduct of selected system analyses of the baseline 5 GW crystal silicon configuration to establish technical feasibility and provide substantive engineering information for use in the economic studies.

The major technical findings and conclusions, as established through these studies, are expressed herein within the framework of Subprogram Areas established by the NASA's Satellite Power Team, and are subsequently followed by Grumman's study recommendations. The final briefing for this study also provided a further expansion of the study's findings and conclusions, and is presented in Appendix A for convenient reader reference.

The scope of this study, although addressing a specific baseline configuration, has also provided results which are applicable to Satellite Power Systems in general. These results are highlighted herein with the following notation (✓).

3.1 Major Findings and Conclusions

Systems Definition

- ✓• The complete assembly of an operational SPS in low earth orbit (LEO) followed by transport to geosynchronous earth orbit (GEO) does not appear technically desirable, but the mix of GEO versus LEO construction activity remains to be resolved. An important issue, therein, is the influence of high productivity factory-type construction operations on the SPS configuration concept, since compatible requirements must be imposed on an SPS and its Factory (ies)-in-space.
- The 5-GW crystal-silicon photovoltaic SPS configuration baselined for this study and having a concentration ratio of two (2) is a workable system, as no unsolvable engineering problems have been uncovered to date

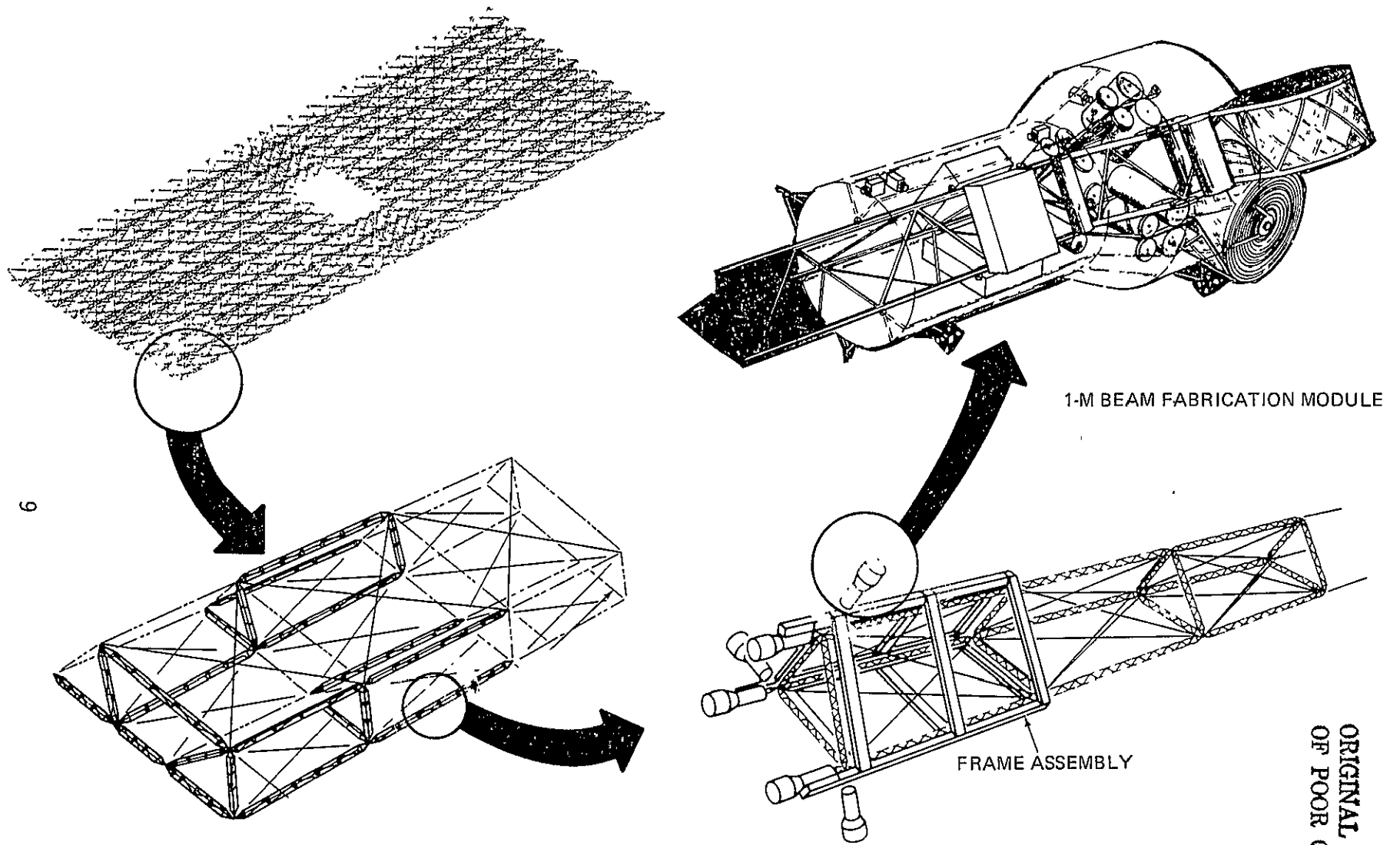
- Applying most likely values of technology projections for the 1995 time frame, system efficiency (exclusive of solar conversion) is 58.3%, and thus requires a solar array output of 8.57 GW to achieve 5-GW at ground output.
- A deterministic estimate of mass-on-orbit of the 5-GW crystal-silicon photovoltaic SPS baseline configuration is 27×10^6 Kg

Microwave Energy Technology

- ✓ • Maintenance of surface flatness tolerances of a microwave (MW) antenna favors the use of composites as basic antenna structures
- ✓ • Pointing control requirements of 1 arc-min can be accommodated for the MW antenna.

Space Structures

- ✓ • Truss-type structural configurations are feasible, can satisfy SPS needs for low mass and structural stiffness, and represent about 20% of total system mass
- ✓ • Truss-type structures, characteristic of the photovoltaic SPS configurations examined, are conducive to employing automated structural fabrication/assembly techniques in orbit to improve productivity of construction processes in space (see Figure 3-1)
- ✓ • Very large area low mass structures configured for operation in space:
 - are controllable during operational on-orbit conditions at LEO or GEO, and during construction in GEO while joined to a construction facility
 - could encounter higher-than-operational structural loading during construction in LEO depending on the in-orbit construction concept
 - should be transported from LEO to GEO by electric (low acceleration) propulsion systems
 - will face size limitations in LEO due to space debris collision considerations
- Aluminum structural materials appear to be viable candidates for solar array primary structure and current - carrying functions
- During occultation or eclipse periods, thermally-induced deflections in a solar array configuration having a central mast (backbone) are tolerable both structurally and deflection-wise.



9

1-M BEAM FABRICATION MODULE

FRAME ASSEMBLY

ORIGINAL PAGE IS
OF POOR QUALITY

Fig. 3-1 Truss-Type Structure Fabrication/Assembly

Power Distribution

- ✓● A rotary joint comprised of slip rings and brushes is a feasible concept for transmitting electric power across the power system/antenna interface
- ✓● Both distributed or central mast power distribution approaches are acceptable, but the distributed approach offers simplifications in construction/assembly
- Minimum overall system mass is achieved with a power distribution efficiency of 94% for a 5-GW crystal-silicon photovoltaic system operating at 40 Kv.

Attitude Control and Stationkeeping

- ✓● Solar array pointing control of $\pm 1^\circ$ concurrent with microwave antenna pointing control of ± 1 arc-min is achievable at GEO operational conditions
- ✓● A truss-type structural configuration with a 10:1 structural-to-control frequency relationship provides acceptable structure/control system stability
- ✓● High performance, low thrust electric propulsion is necessary for attitude control and stationkeeping
- ✓● Based on a 3-month construction period, attitude control propellant needs for:
 - Construction/assembly of a complete SPS in LEO represent about 10% of total SPS mass, as compared to less than 0.1% at GEO
 - Fabrication of subassemblies of an SPS in LEO would appear reasonable, but maximum practical sizes/masses need to be determined
 - Negating air drag effected in LEO are insignificant.
- ✓● Control/structural dynamic interactions occur in LEO between very large minimum weight structures and their construction facility which could lead to SPS mass penalties
- Annual propellant quantities of about 93,000 kg. are needed for a 5-GW crystal-silicon photovoltaic SPS, to satisfy attitude control/stationkeeping requirements while operating within a 120-satellite constellation system serving the US. This propellant quantity, over a thirty year period, represents about 10% of the total mass of a single SPS satellite.

Transportation

- ✓● To minimize transportation costs, large volume/low density structures associated with photovoltaic SPS concepts require automated on-orbit construction
- ✓● Transportation of large solar array subassemblies or a complete SPS satellite from LEO to GEO:
 - via chemical propulsion, would impose structural mass penalties of 100 to 400% on large area, low mass structures, and thus requires low thrust electric propulsion.

Operations

- ✓● Construction/assembly in orbit of truss-type photovoltaic SPS concepts are technically feasible. Acceptable approaches are:
 - construction of major subassembly modules in LEO, with transport to GEO by low acceleration OTV's, and
 - construction/assembly of the complete SPS in GEO
- ✓● Factory-in-Space concepts (Figure 3-2) for fabrication and assembly of SPS-type systems will involve:
 - factory type assembly line operations in the space environment, optimized for high productivity
 - crew work stations and mobility aids located at key spacial intervals, with astro-workers accommodated in a shirt-sleeve environment
 - internal transportation systems for moving people and equipment
 - a base management organization and heirachy, and
 - supporting facilities including warehousing, cafeteria, recreational, medical, living, etc
- Representative staffing of a Factory-in-Space, at peak activity levels, for producing a complete 5-GW crystal-silicon, photovoltaic SPS in LEO or GEO at a construction rate of 4/year is estimated at:

Base Management	45
Factory Workers	430*
Supporting Personnel (medics, warehousing, cafeteria, etc.)	225
Total	700

*Approximately 100 person-years of direct labor are required to construct one 5-GW SPS

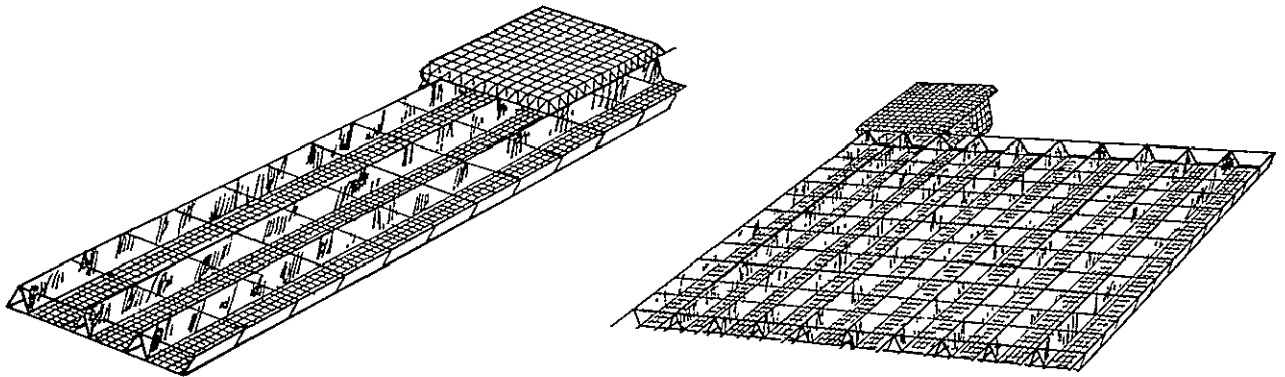
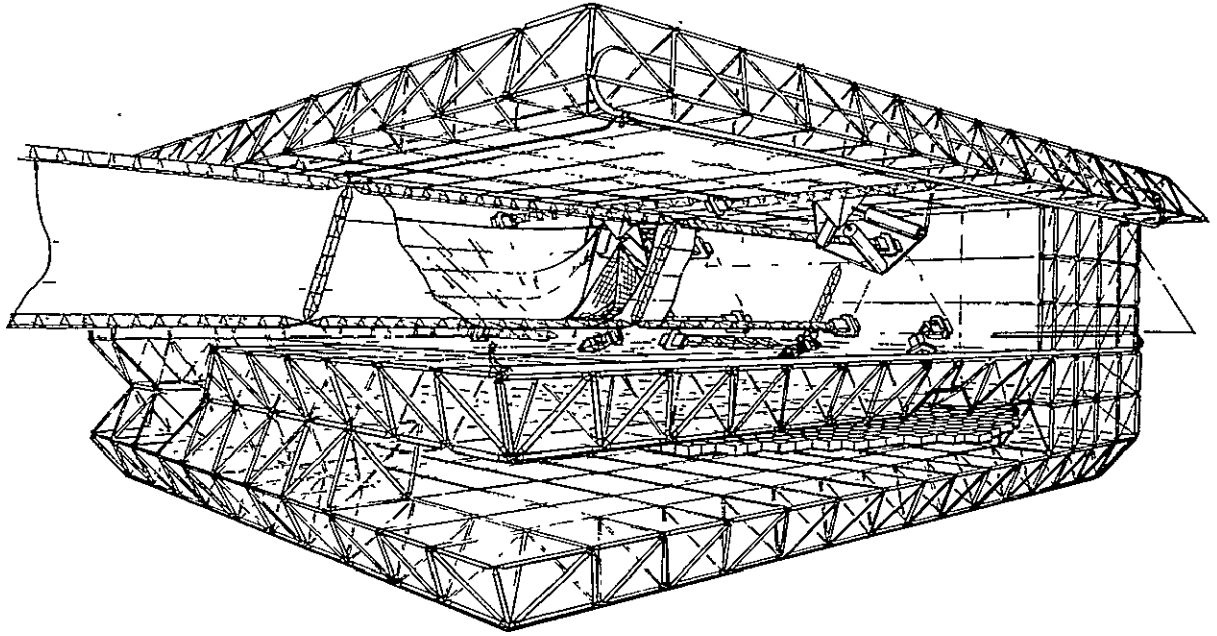


Fig. 3-2 Factory-in-Space Concepts

- ✓ ● SPS components and subassemblies apparently suited to on-orbit and/or earth fabrication and their potential for automated construction and assembly are:

ELEMENT	EARTH FABRICATION	ON-ORBIT FAB	ASSY	ON-ORBIT AUTOMATION POTENTIAL
SOLAR ARRAY ● STRUCTURE ● BLANKETS & REFLECTORS	X	X	X	HIGH HIGH
MICROWAVE ANTENNA ● STRUCTURE ● COMPONENTS	X	X	X	HIGH LOW
PWR DISTRIB SYS ● STRUCTURE ● COMPONENTS	X	X	X	MODERATE/HIGH MODERATE
CONTROL SYS ● COMPONENTS	X		X	LOW
ROTARY JOINT ● STRUCTURE ● COMPONENTS	X	X	X	HIGH LOW

- ✓ ● A high degree of automation is envisioned for solar array construction/assembly, but comparable automation of the complete microwave antenna system appears uncertain
- ✓ ● The microwave antenna system, rotary joint, and close-proximity portions of the power distribution system:
 - involve complex factory operations with large personnel complements and
 - because of their denser mass characteristics and smaller projected areas, are less susceptible to space debris collision problems.

This suggests that construction of these elements be confined to LEO, and that construction of solar array subassemblies be also considered for LEO, in preference to complete construction of an array at GEO.

Technology Verification

- ✓ ● Ground and space-based development/demonstration activities are necessary to provide sufficient technical confidence to commit to development of an operational 5-GW SPS. Program development options can be formulated which: (1) utilize existing or planned transportation elements, and (2) provide necessary decision-making information at key programmatic decision points.

3.2 Recommendations

Dynamic interactions occur between major SPS program elements which will have a significant influence upon system-level decisions. As illustrated in Figure 3-3, triads of interactions exist for major phases of an SPS program: Commercial Operations, Manufacturing and Construction, and Precursor Activities. The triads are interactive amongst themselves and also provide inputs to the other program phases. The SPS Manufacturing and Construction phase, for example, is the basis for establishing SPS-related requirements for a precursor construction base, while both Commercial Operations and Manufacturing/Construction Phases provide requirements for SPS Technology Verification.

The attainment of an economical programmatic approach, therefore, must consider the interactive nature of the major program elements, and tradeoff analyses amongst the elements is necessary. Within this framework of the interactive nature of the SPS program, further studies are recommended to resolve major system issues, and to provide a better understanding of major SPS options. The following areas are recommended.

CONFIGURATION DEVELOPMENT

DEFINITION OF GENERIC THIN-FILM PHOTOVOLTAIC SPS CONFIGURATIONS WITH FLEXIBILITY TO ACCEPT TECHNOLOGY IMPROVEMENTS



Recent developments in CdS thin-film technology, coupled with ERDA-sponsored R&D related to thin-film photovoltaic materials (e.g. polycrystalline silicon, gallium arsenide, indium phosphide), suggest that cost and efficiency breakthroughs may be forthcoming in the thin-film photovoltaic area. ERDA's goal, for example, is that by FY'86, the feasibility of achieving a \$100 to \$300 per peak KWE array price goal would be demonstrated for these devices. This sponsored R&D over the next ten years could also surface thin film materials with high radiation resistance (a very desirable characteristic for an SPS program), and allow considerable simplification in SPS solar array structures, by effectively using non-concentrating solar-energy conversion approaches. In anticipation of these developments, it would be desirable to establish a generic thin-film SPS configuration which would be sufficiently flexible (in its design approach) to accommodate future improvements in thin-film technology and other system technology developments.

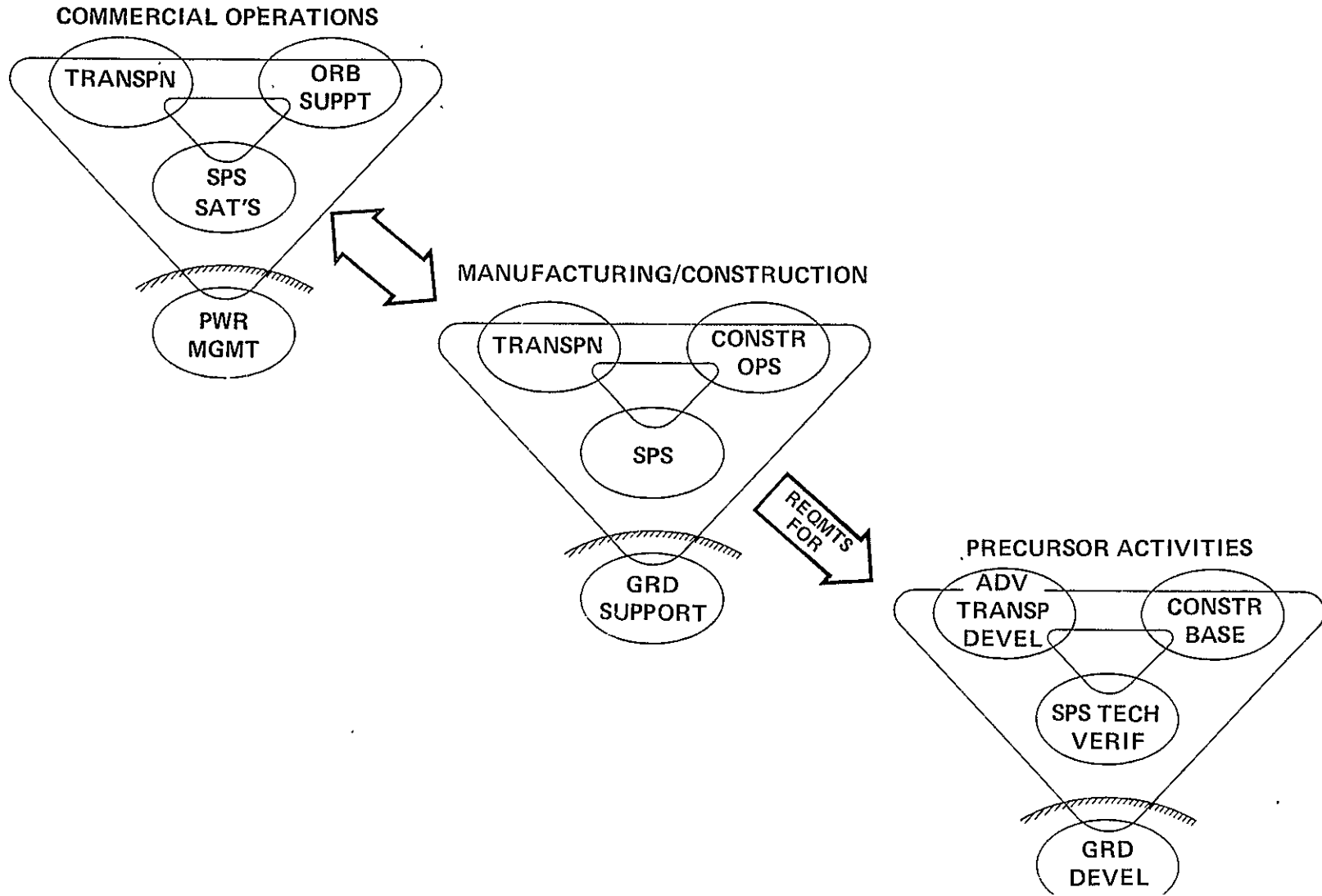


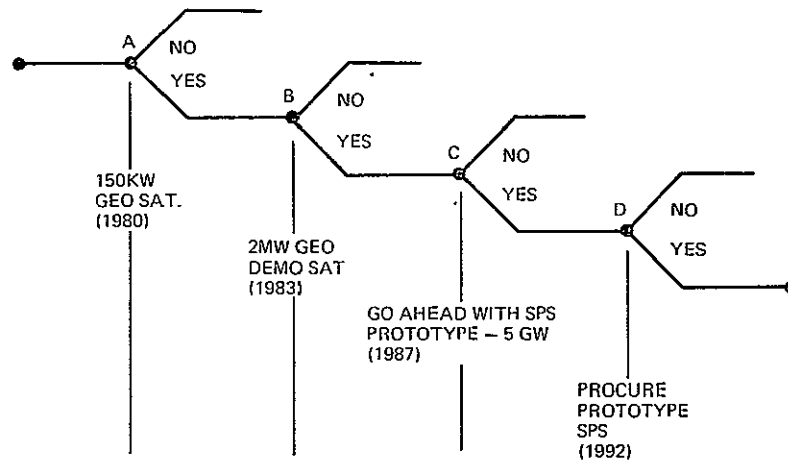
Fig. 3-3 Triads of SPS Program Interactions

SPS TECHNOLOGY VERIFICATION

DEVELOP/EVALUATE PROGRAM OPTIONS WITHIN THE FUNDING RANGES SUGGESTING POSITIVE "EXPECTED NET PRESENT" VALUES FOR AN SPS PROGRAM (E.G., ≈ \$3.0B - \$3.5B FOR GROUND/ORBITAL DEVEL)

Positive SPS program "Expected net present values" resulted from small-scale test satellite program options (Programs 4 and 5) examined in this study. Positive values indicate that a decision to undertake an early program phase is economically justified. The program options examined cost between \$3.0-3.5B for a direct SPS-related technology verification effort, prior to commitment to a large scale 5-GW SPS system. These technology verification programmatic approaches, however, should only be viewed as benchmarks representative of program funding levels that could be economically acceptable. Other programmatic options should be developed within these general funding ranges, which might also represent acceptable economic programs.

TECHNOLOGY TARGETS VIA DECISION TREE ANALYSIS



SPACE MFG FEASIBILITY	20%	50%	70%	90%
SOLAR ARRAY PERFORMANCE	40%	70%	85%	90%
SOLAR ARRAY COSTS	20%	50%	90%	100%
RFI AVOIDANCE	20%	40%	80%	100%
MW TRANSMISSION PERFORMANCE	20%	40%	70%	90%
ADV TRANSPORTATION DEVELOPMENT	20%	50%	70%	100%

TYPICAL
REDUCTIONS
IN
TECHNOLOGY
UNCERTAINTIES

DETERMINE DESIRABLE RANGES OF UNCERTAINTIES
MAXIMIZING NET EXPECTED PROGRAM VALUES

The funding level sensitivity of technology verification program options to an SPS program's expected net present values, should also be established. Within this context, the rapidity of reducing technology uncertainties should also be examined (e.g. how soon must we have all the answers?). The decision tree analysis affords a useful tool to examine the economic merits of reducing technical uncertainties as a function of time. As shown in the above illustration, the economically acceptable small-scale test satellite approaches, developed within this study, reflected progressive reductions in technology uncertainties at various phases of the overall program. The extent to which reductions in technology uncertainties are necessary to maximize expected program values, and their associated funding levels, should be identified. This will assure that realistic technology targets compatible with an economic SPS program are available, and within which acceptable technology verification programs can be structured.

TECHNOLOGY DEVELOPMENT

ESTABLISH PROBABLE RANGES OF PERFORMANCE REQUIREMENTS ASSOCIATED WITH LOW THRUST ELECTRIC PROPULSION SYSTEMS TO FOCUS & ACCELERATE SUPPORTIVE R & D

- GEO ATTITUDE CONTROL/STATIONKEEPING
- LEO → GEO ORBIT TRANSFER OF LARGE SUBASSEMBLIES

Previous phases of this study have identified technology development needs for:

- Solar Array Technology
- Microwave Power Technology
- Large Space Structures (including manufacturing, assembly, maintenance and control)

Transportation issues have also been addressed, and it is clear that electric propulsion systems will be needed for both attitude control/stationkeeping and payload transfer from LEO to GEO. It is appropriate, therefore, that SPS-related technology developments in the electric propulsion area be expanded. Toward that end, a more in-depth understanding of the probable ranges of performance requirements and technical issues associated with low thrust electric propulsion systems is needed. This will focus and accelerate supportive ground-based research and development efforts. Considerations should include:

- attitude control/stationkeeping at GEO operational conditions for a minimal 30 year SPS lifetime, and
- LEO-to-GEO orbit transfer of large subassemblies (e.g. Microwave antenna and rotary joint) and masses that could range from 6-7 million Kg to the complete mass of an SPS.

MANUFACTURING AND CONSTRUCTION

- CONTINUE DEVELOPMENT OF "BEAM MACHINES" FOR FABRICATION OF ALUMINUM/ COMPOSITE TRUSS-TYPE STRUCTURES IN SPACE
- DEFINE/ASSESS APPROACHES FOR AUTOMATING CONSTRUCTION/ASSEMBLY OF THE MW ANTENNA SYSTEM A COMMON SPS ELEMENT
- EVALUATE ALTERNATE ROTARY JOINT APPROACHES & IN-ORBIT PRODUCIBILITY POTENTIALS . . . & DEFINE TECHNIQUES FOR AUTOMATING CONSTRUCTION/ASSEMBLY
- CONDUCT PARAMETRIC ANALYSES OF SPS MANUFACTURING & CONSTRUCTION OPTIONS TO IDENTIFY APPROACHES OPTIMIZING PRODUCTIVITY IN-ORBIT & MINIMIZING OVERALL CONSTRUCTION COSTS TO SERVE AS THE BASIS FOR ESTABLISHING REQUIREMENTS FOR PRECURSOR CONSTRUCTION BASE OPERATIONS & ADVANCED PROPULSION SYSTEMS DEVELOPMENT

Studies should be conducted to identify desirable SPS manufacturing/construction approaches, to serve as the basis for establishing productivity verification requirements and demonstrations of space manufacturing feasibility in precursor SPS programs. These efforts should initially address major elements of an SPS (microwave antenna assembly and rotary joint), and then final assembly of the complete satellite. Varying degrees of on-orbit automation should be examined, within the context of alternate LEO/GEO construction scenarios (see Fig. 3-4). From these, the interrelated impacts of construction operations in space, extent of ground fabrication/assembly, LEO-to-GEO transportation options, and SPS configuration approaches should be appropriately surfaced for conducting parametric trade analyses.

19/20

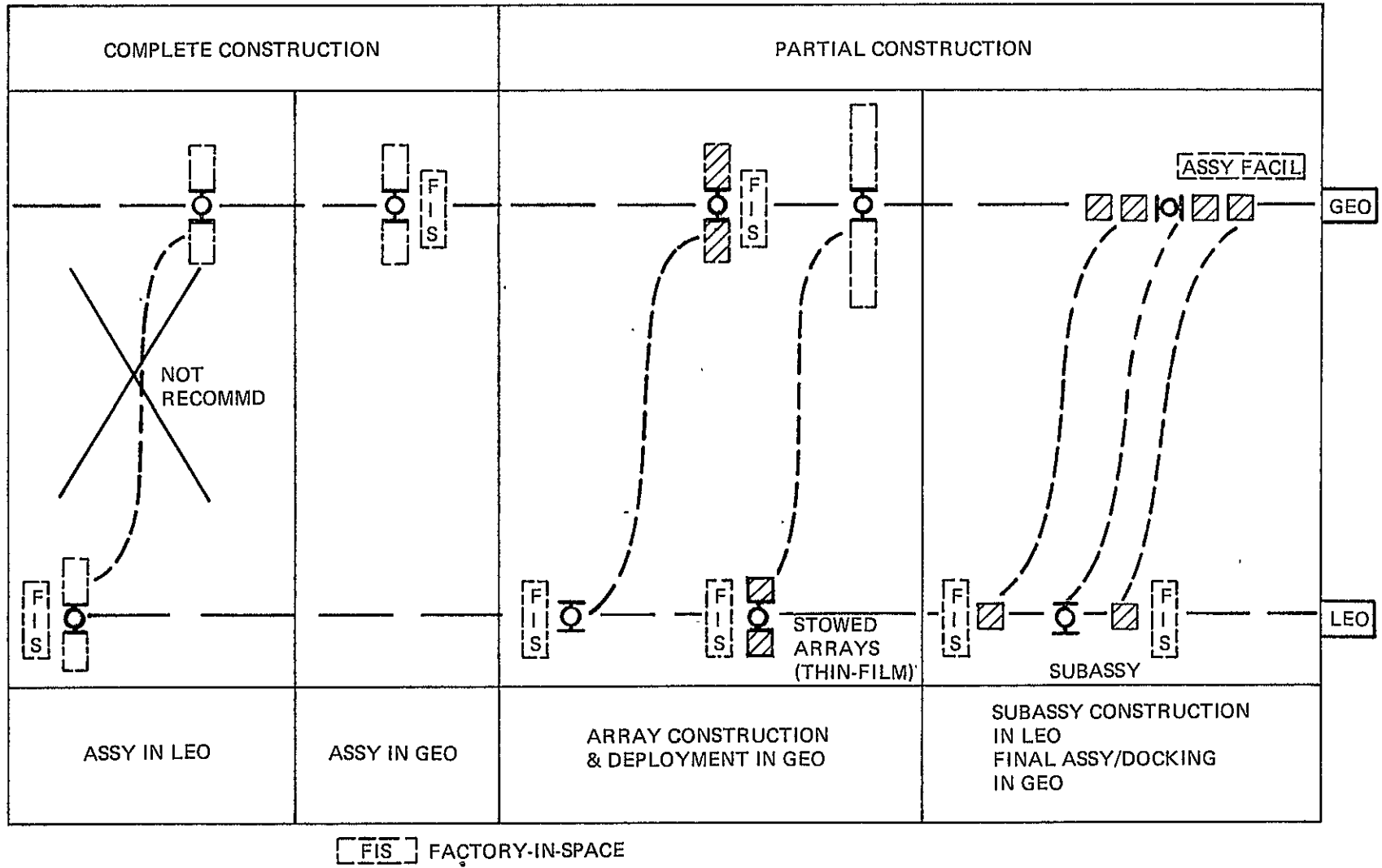


Fig. 3-4 Candidate SPS Construction Scenarios

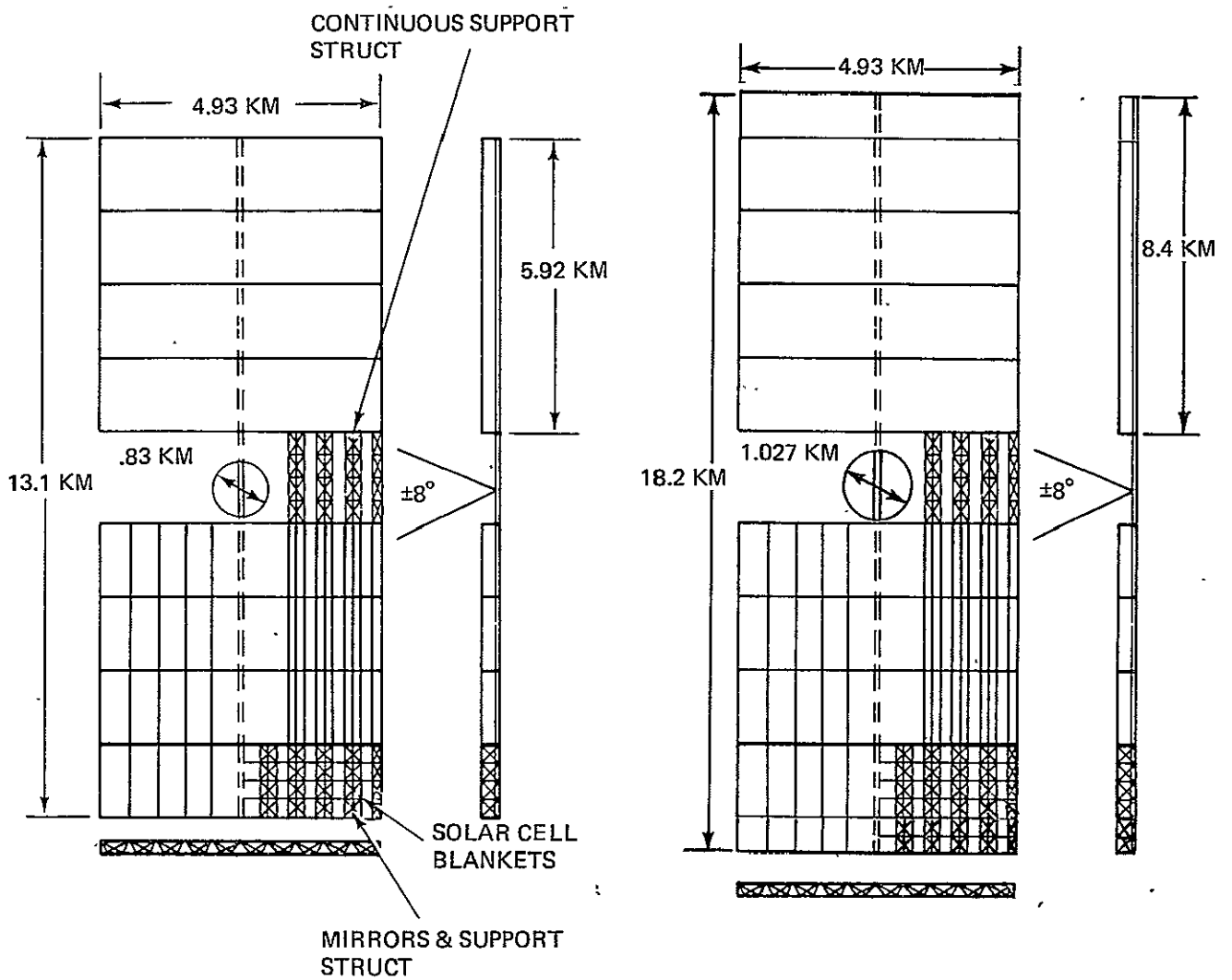
4. UPDATING THE BASELINE CONFIGURATION

As a result of trade-off and preliminary concept selection studies performed during Phase I of this study, a baseline configuration, representative of the 1995 orbital system, was evolved and its associated technology goals defined (Ref. 1). This configuration served as a basis from which credible cost data could be estimated for use in the deterministic economic analysis. This section summarizes the current status of the strawman configuration as it has evolved through the various phases of the engineering studies.

Figure 4-1 shows the characteristics of the strawman SPS configuration, as defined at the end of the Phase I studies, and at the study's conclusion. The configuration consists of two large aluminum structure solar array collectors, using silicon crystal photovoltaic cells with a concentration factor of two. The arrays are connected by a carry-through structure made of dielectric material. The microwave antenna is located on the centerline between the arrays, and is attached to a central mast which extends the full length of the satellite. The central mast serves as the main power transmission bus, interfacing with the antenna through a rotary joint. This enables the antenna to rotate 360 degrees in azimuth (east-west) and ± 8 degrees in elevation (north-south).

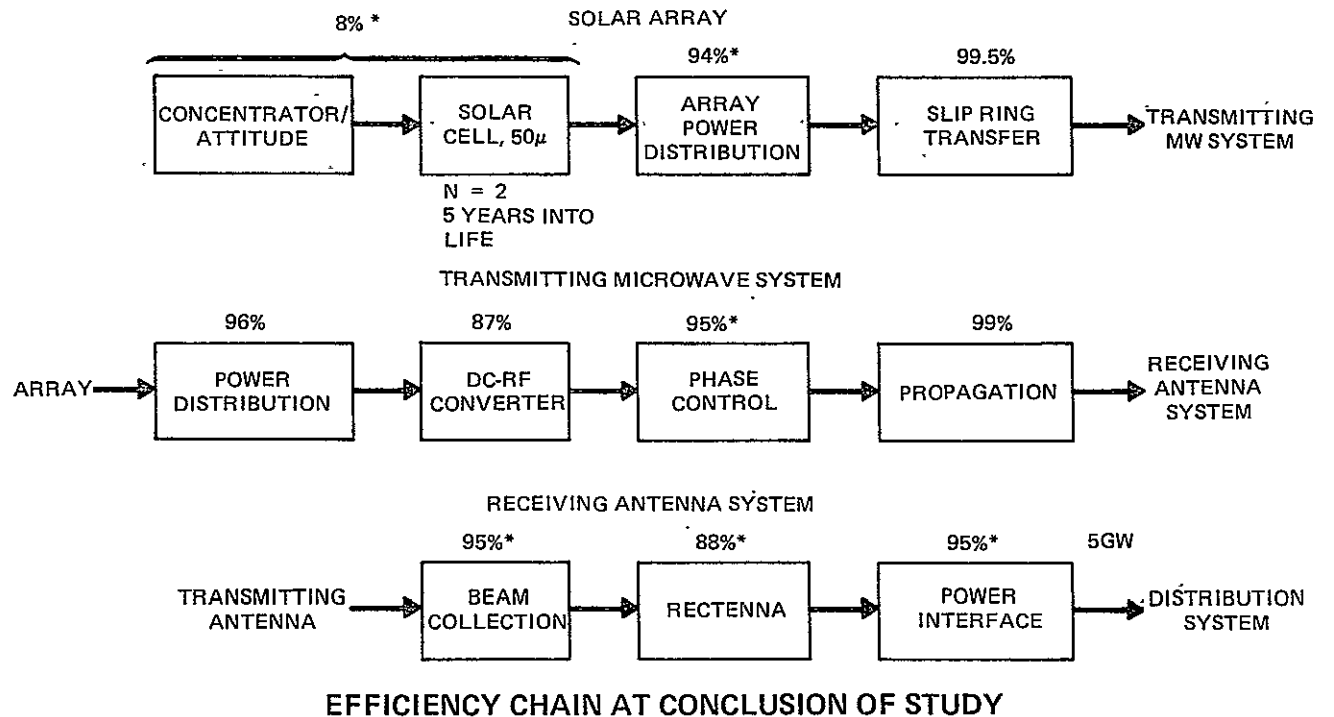
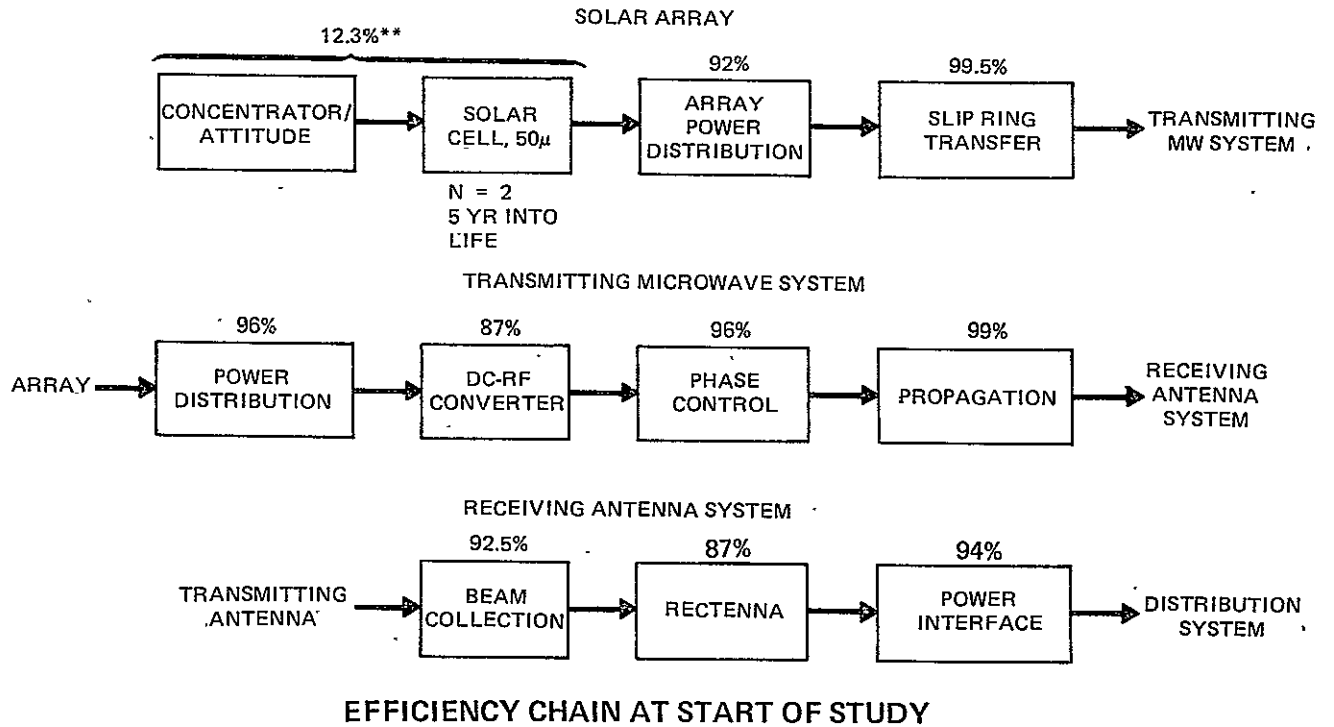
Changes in the strawman configuration resulted from two major factors: (a) solar cell performance updates and (b) microwave antenna performance improvements. These modifications surfaced during the Phase II and III studies.

The most significant factor impacting the update of the baseline configuration was the efficiency projected for the performance of the solar array in the 1995 time frame. In the Phase I studies, projections for lightweight silicon-crystal solar cells were obtained from early Spectrolab data (Ref. 2). This data projected operating efficiencies for cells employing band pass filters to reflect the ultraviolet portion of the solar spectrum (0.37-1.01 μ bandpass), at 13.7% based on a concentration factor of 2. This projection considered a GEO radiation fluence of $\Phi = 10^{15}$ e/cm² (1MEV), representative of values at the end of 5 years into life. A projected efficiency of 90% for concentration/attitude control variations was also assumed. These factors resulted in an overall solar array efficiency projection of 12.3%. (Ref: Fig. 4-2).



CHARACTERISTICS.	END OF PHASE I	END OF STUDY
● POWER	5000 MW	5000 MW
● MASS	18.1×10^6 KG	27.2×10^6 KG
● SIZE	13.1 X 4.9 KM	18.2 X 4.9 KM
● ORBIT	GEOSYNCHRONOUS	GEOSYNCHRONOUS
● LIFE	30 YR	30 YR
● OPERATING FREQ	2.45 GHz	2.45 GHz
● DC-TO-DC EFFIC	55%	58%
● SOLAR CONV EFFIC	12.3%	8.0%

Fig. 4-1 Comparison of Concept Descriptions



* REPRESENT MOST LIKELY VALUES OF TECHNOLOGY PROJECTIONS FOR THE 1995 TIME FRAME AS ESTABLISHED THROUGH PHASE II & III STUDIES
 ** REPRESENT MOST OPTIMISTIC TECHNOLOGY PROJECTIONS AS ESTABLISHED IN PHASE I STUDIES.

Fig. 4-2 Comparison of Efficiency Chains

During the Phase III studies, ADL developed a refined computer model to estimate the performance of solar cells. The model accounts for cell degradation resulting from temperature effects, solar intensity, angle of incidence, radiation degradation, and other factors. Since economic analyses conducted in subsequent phases were approached on a statistical basis, rather than the earlier deterministic basis, performance data was compiled for each subsystem representing "best", "worst", and "most likely" values. "Most likely" values correspond to a 1σ value, whereas "best" and "worst" values correspond to 90% and 10% values in typical cumulative density functions. To input ADL's computer model, data projected by ERDA for performance of a 1985 silicon cell was used as the "most likely" value for the SPS operational time frame. This data assumed that lightweight silicon solar cells could achieve an efficiency of 16% (beginning of life AMO, 26°C) at a concentration of one. Using this data in the computer model, ADL identified an overall efficiency for the solar array of 9.2%, at a concentration factor of 2, beginning of life. This resulted in an overall solar array efficiency of approximately 8% at the end of 5 years into life (Fig. 4-2). The increase in solar array size resulting from these assumptions required the array to be lengthened by approximately 2.5 km.

The second factor contributing to overall size-growth of the satellite relates to the microwave antenna. Recent studies by Raytheon conclude that microwave transmission characteristics should be based on a 10 db taper rather than the 5 db taper specified in earlier Phase I studies. This refinement reduces power densities in the sidelobes to very low levels ($<0.2 \text{ mw/cm}^2$) but increases the diameter of the transmitting antenna to 1.026 Km. The baseline configuration and dielectric structure was adjusted accordingly.

Fig. 4-3 summarizes the strawman SPS mass properties at the start of the study, at completion of the Phase I, and at the study's conclusion. The largest increase in mass is attributed to growth in solar array size (approximately 50%). This reflects the now-projected 16% efficiency for silicon crystal solar cells. Also reflected is the resultant mass growth of the central power distribution mast. (Ref. Fig. 5-7). Other mass increases as shown for the microwave transmitting antenna, reflect structure and wave guide mass growth resulting from the increase in diameter to 1.026 Km.

SUBSYS/COMP	SSPS MASS PROP. AT START OF STUDY		SSPS MASS PROPERTIES RESULTING FROM STUDY			
	5 GW; 1-km DIA ANTENNA		AT END OF PHASE I STUDY 5 GW; 0.83 KM ANTENNA		AT END OF PHASE III STUDY 5 GW; 1.027-KM ANTENNA	
	Kg X 10 ⁶	LBM X 10 ⁶	Kg X 10 ⁶	LBM X 10 ⁶	Kg X 10 ⁶	LBM X 10 ⁶
SOLAR ARRAY	(9.57)	(21.1)	(12.30)	(27.29)	(18.5)	(40.8)
• BLANKETS	6.11	13.47	7.83	17.25	11.12	24.52
• CONCENTRATORS	0.93	2.05	1.23	2.71	1.74	3.84
• NONCONDUCTING STRUCT	1.73	3.81	2.33	5.14	3.21	7.08
• BUSES, SWITCHES	0.23	0.51	0.27	0.59	.27	.60
• MAST	0.57	1.26	0.64	1.37	2.16	4.76
MW ANTENNA	(1.89)	(4.16)	(5.55)	(12.22)	(6.79)	(14.96)
• MW TUBES	0.63	1.39	2.33	5.13	2.24	4.94
• POWER DISTRIB	0.03	0.07	0.54	1.19	.30	.65
• PHASE CONTROL ELECT	0.28	0.61	0.13	0.29	.13	.28
• WAVEGUIDES	0.70	1.54	2.31	5.09	3.61	7.96
• STRUCT	0.25	0.55	0.14	0.31	.37	.81
• CONTOUR CONTROL	-	-	0.10	0.22	.15	.33
ROTARY JOINT			(0.17)	(0.37)	(.17)	(.37)
• MECHANISM	-	-	0.066	0.14	.066	.14
• STRUCT	-	-	0.106	0.23	.106	.23
CONTROL SYSTEM	(.02)	(.04)	(0.036)	(.079)	(1.74)	(3.84)
• ACTUATORS			0.012	0.026	.107	.236
• PROPELLANT/YR			0.024	0.053	.067	.148
TOTAL SYSTEM	11.48	25.30	18.06	39.75	27.2	59.96
MAJOR CHANGES IN CONFIGURATION:						
• REFINED ESTIMATE OF ANTENNA WT FROM MPTS STUDIES NAS 3-17835						
• REFINED ESTIMATE OF MICROWAVE EFFIC CHAIN AND INCREASES POWER SOURCE SIZE						

ORIGINAL PAGE IS
OF POOR QUALITY

Fig. 4-3 Comparison of Mass Properties

5. PHASE III ENGINEERING STUDIES

5.1 Analysis of LEO and GEO Construction/Assembly Approach

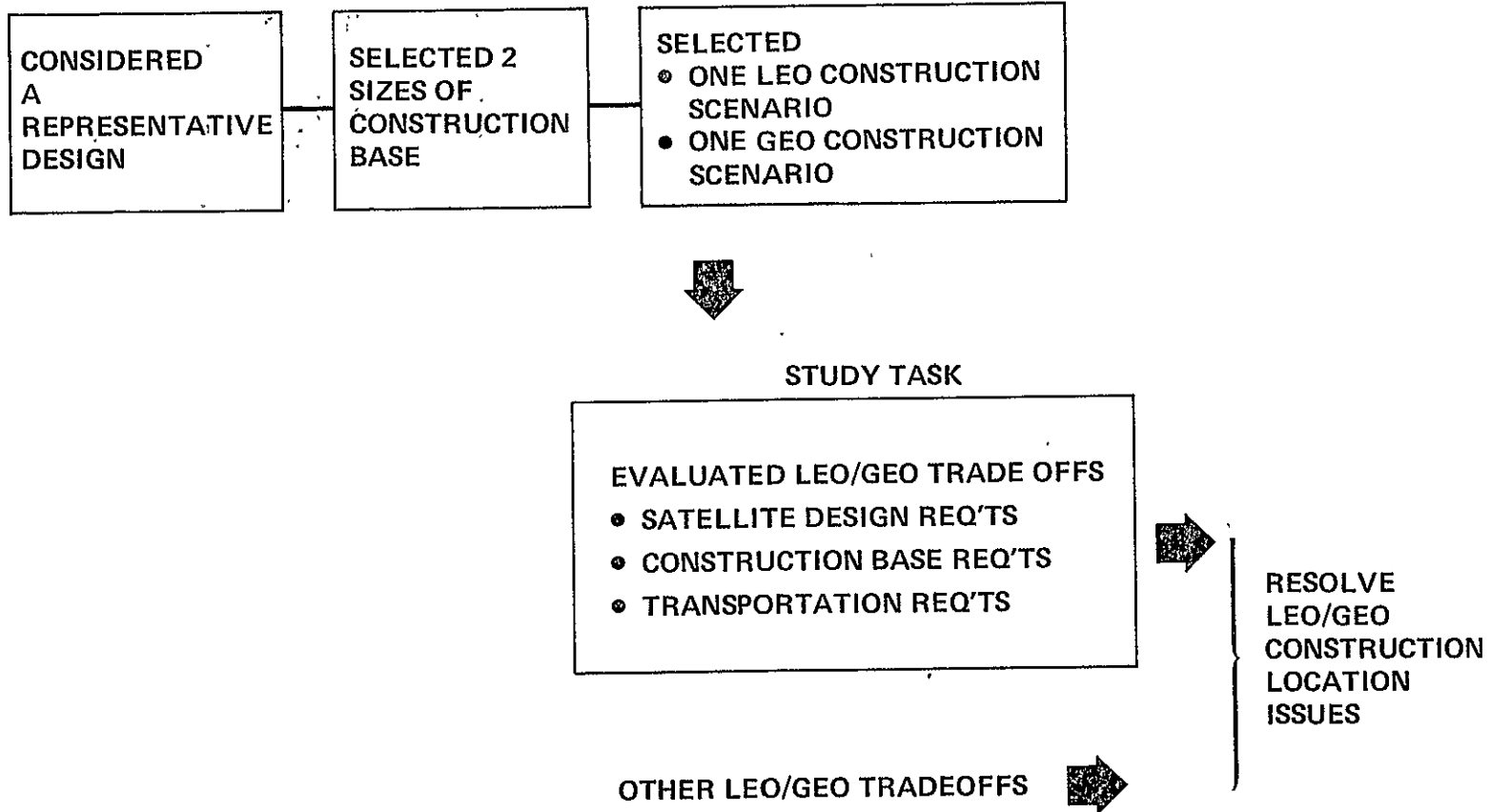
Engineering and economic analyses conducted during the Phase I and II studies indicated a very sensitive factor related to overall SPS program implementation costs, namely, the uncertainties associated with fabrication and assembly of large structures in space. Within these earlier analyses, the SPS was assumed to be constructed totally in LEO, and transported to GEO using advanced electric propulsion systems.

To better understand both the technical and economic impact of SPS construction on overall technology requirements, studies were conducted during Phase III to assess the merits of both LEO and GEO construction. The study approach used to conduct this effort is depicted in Fig. 5-1.

The baseline configuration, consisting of the 5-GW crystal silicon truss type design with a concentration ratio of 2, was used as the basis for analysis. Fig. 5-2 shows the overall dimensions of the satellite. Although configurations utilizing other photovoltaic materials and associated concentration factors are viable configurations to be considered, the study focused on this singular configuration because it was considered to be at the greatest point of maturity.

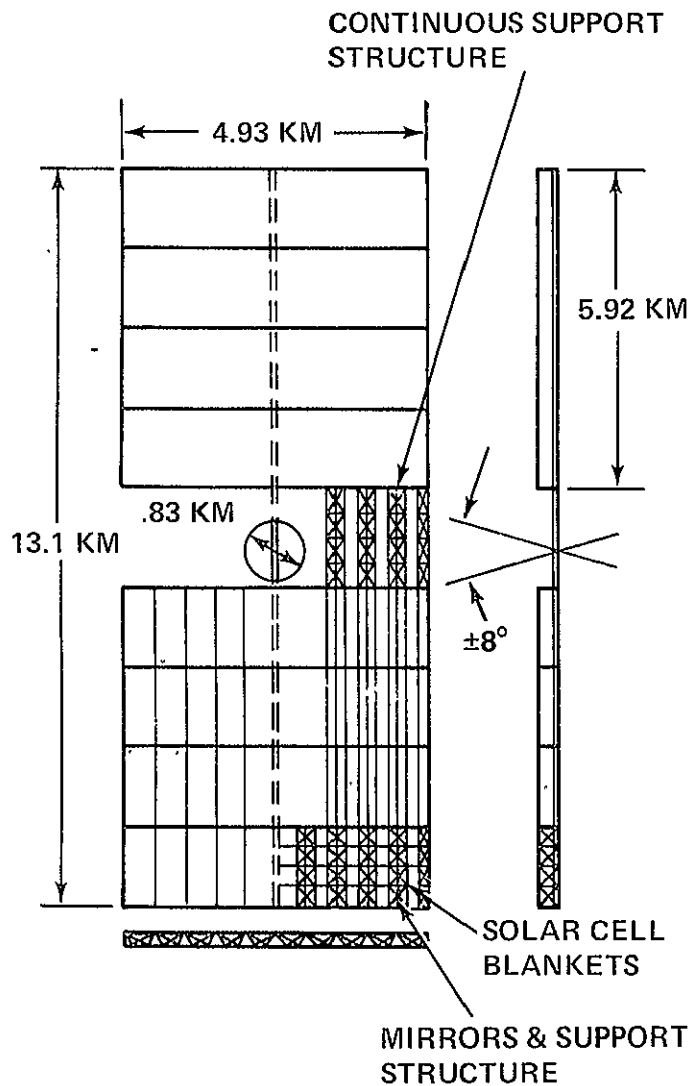
Two construction base concepts were developed, representative of those considered to span the range of potential construction base sizes. Construction base variables considered included the rate at which the integrated satellite structure/solar array was fabricated, and the number of troughs or bays that could be fabricated simultaneously. For both of these concepts, work station functions and locations were identified, numbers of construction personnel were estimated, equipments required in the construction process were established, and an overall construction base layout developed. These concepts considered a production rate of as high as 6 satellites per year. Two construction scenarios were defined, one based on complete construction in GEO, the other in LEO. Although it is clear that a wide assortment of construction scenarios could fall within these two selected scenarios, the two basic scenarios selected provided valuable insight into the extent of the in-orbit construction problem.

• STUDY GROUND RULES



27

Fig. 5-1 Leo vs Geo Construction/Assembly Task



- CONCEPT DESCRIPTION

COLLECTS SOLAR ENERGY USING PHOTOVOLTAIC CONVERTERS & TRANSMITS POWER TO EARTH AS MICROWAVE ENERGY. THE MICROWAVE ENERGY IS RECTIFIED TO DC POWER AT THE GROUND RECEIVING STATION

- CHARACTERISTICS

- POWER	5000 MW
- WEIGHT	18.1×10^6 KG
- SIZE	13.1 X 4.9 KM
- ORBIT	GEOSYNCHRONOUS
- LIFE	30 YR
- OPERATING FREQ	2.45 GHZ
- DC-TO-DC EFFIC	58%
- SOLAR ARRAY EFFIC	11.3%

Fig. 5-2 Satellite Solar Power Station - Phase II Study Configuration

This aspect of the study, consequently, addressed three major issues - the impact of construction location on:

- Construction base requirements
- Satellite design requirements
- Transportation system requirements.

Having surfaced these impacts, data commensurate with both the SPS and construction base costs were estimated and used in the SPS economic analysis. The overall conclusions from this portion of the study follow:

A. Key Satellite Design Requirements

- Satellite Structural Loading Requirements

At LEO, structural loads imposed on a satellite under construction, while attached to the construction base, are influential in establishing satellite structural design requirements. The loads result from tension forces and bending moments induced by center-of-mass offsets between the satellite and construction base. Reducing the mass of the construction base, and/or minimizing the center-of-mass off-sets between the satellite and construction base during all phases of construction, will minimize structural loading. At GEO, the structural loads resulting from center-of-mass off-sets is not a factor in establishing satellite structural design requirements.

- Structural Stiffness Requirements

The structural frequencies of the satellite are significantly reduced when attached to the construction base. Moreover, the modes are no longer pure bending and torsion, but rather, combined bending and torsion, because of the center-of-mass off-sets. This may have an impact on satellite structural stiffness requirements, particularly for LEO construction, where higher frequency control forcing functions are required. Applying control forces at the construction base has less of an effect on exciting the structure than on-orbit operational conditions, but requires significantly more propellant, because of the reduced moment arms.

- Control System Requirements

Maintaining local vertical attitude hold orientation during construction requires significantly more control system propellant for LEO construction than GEO. Results showed that approximately 2.8×10^6 Kg of propellant are required per

satellite build at LEO, as compared with $30-60 \times 10^3$ Kg at GEO (considering use of ion propulsion thrusters). Maintaining inertially fixed orientations during construction will require more propellant than local vertical attitude hold requirements. Propellant requirements for counteracting air drag at LEO are not excessive, approximately 10,000 Kg.

B. Construction Base Requirements

• Electrical Power Requirements (EPS)

Construction base electrical power requirements and resulting mass penalties for powering control system ion thrusters are significantly greater for construction of a complete SPS at LEO versus construction in GEO. Power requirements for construction at LEO are reasonable for subassembly fabrication, but as the satellite reaches full scale development, power needs are prohibitive. Power requirements of up to 350 MW are required at LEO for controlling the completed satellite while attached to the construction base. This penalty is further magnified by battery storage requirements needed to accommodate periods of earth occultation of the construction base. Mass penalties for other power requirements, such as power needs for construction base equipments and house-keeping functions, are not significantly influential for LEO construction.

• Thermal Effects Due To Earth Occultation At Leo

Solar incident angle variations on satellite construction are larger and with higher frequencies at LEO than GEO. Assuming that local vertical attitude hold orientations are specified during construction, the solar look angles at LEO vary seasonally relative to the construction base. This takes place through elevation angles of $\pm 45^\circ$ with orbital period azimuth angle variations of 360 degrees. At GEO, for the same attitude conditions, elevation angles are reduced to ± 23.5 degrees. This may be significant in reducing solar thermal gradients resulting during construction, caused by high frequency orbital solar incident angle variations.

• Collision Probability At LEO

Reference data shows that a collision probability of as high as 10 collisions per month may be expected during LEO construction at 500 KM.

- Radiation Shielding Requirements

Adequate shielding in crew work station and habitability modules can be provided for 90-day stay times at GEO without significant mass penalties.

C. Transportation System Requirements

Transportation system requirements for construction at LEO were found to be significantly less than that required for GEO. This is based upon assuming transport modes for LEO construction involving chemical propulsion to low earth orbit followed by ion transport to GEO as compared to all chemical transport to GEO for the GEO construction modes. A total of 85 HLLV flights were required for LEO construction, 74 of these for transporting the satellite materials to the LEO construction base. This compared with 213 required for GEO construction, 74 flights to transport satellite materials and 139 for transporting COTV's and their propellant to a low earth orbit depot.

An HLLV fleet size of 7-10 vehicles would be required to meet the launch rates of LEO construction, as compared with 19-27 for GEO construction. In addition, with all chemical transport, GEO construction requires 78 COTV flights and 20 POTV flights per satellite build.

5.1.1 Construction Base Concepts

To evaluate the impact of construction location on construction base requirements, generalized construction scenarios were developed for the fabrication and assembly of the 5 GW crystal silicon baseline configuration. These construction scenarios defined a typical construction concept, in which a truss-type structure is fabricated and assembled using automated beam makers.

Two sizes of construction base, both employing the "typewriter carriage" concept, were developed for this study. Fig. 5-3 is an artist's rendition of the construction base design. Shown in this concept are two working floor areas, the top floor used for fabricating the solar array structure and installing the blankets and concentrators, . . .and the lower floor, used for constructing the microwave antenna. Readily visible are the rollers used for storing and unfurling the solar cell blankets and concentrators which attach to the structure, and the 20-meter beam makers located in the proper geometric location, to fabricate the structure.

A small size construction base was configured to produce a completed satellite with six passes thru the construction facility. Figure 5-4 shows the construction of the first trough as it emerges from the construction base during the first pass. The entire length of the first trough is fabricated during this operation. Also shown in the

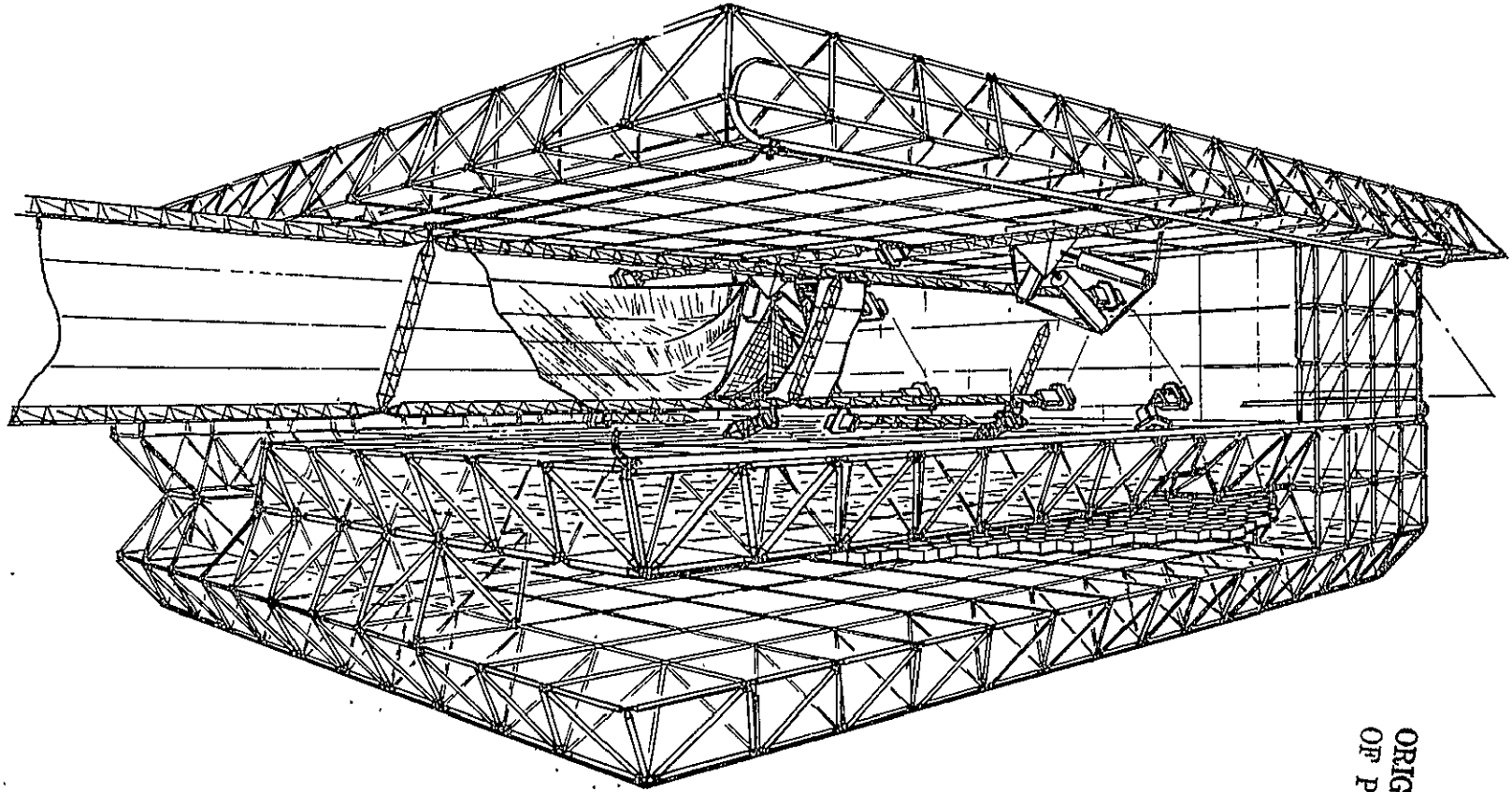


Fig. 5-3 Construction Base

ORIGINAL PAGE IS
OF POOR QUALITY

• 1ST BAY CONSTRUCTION

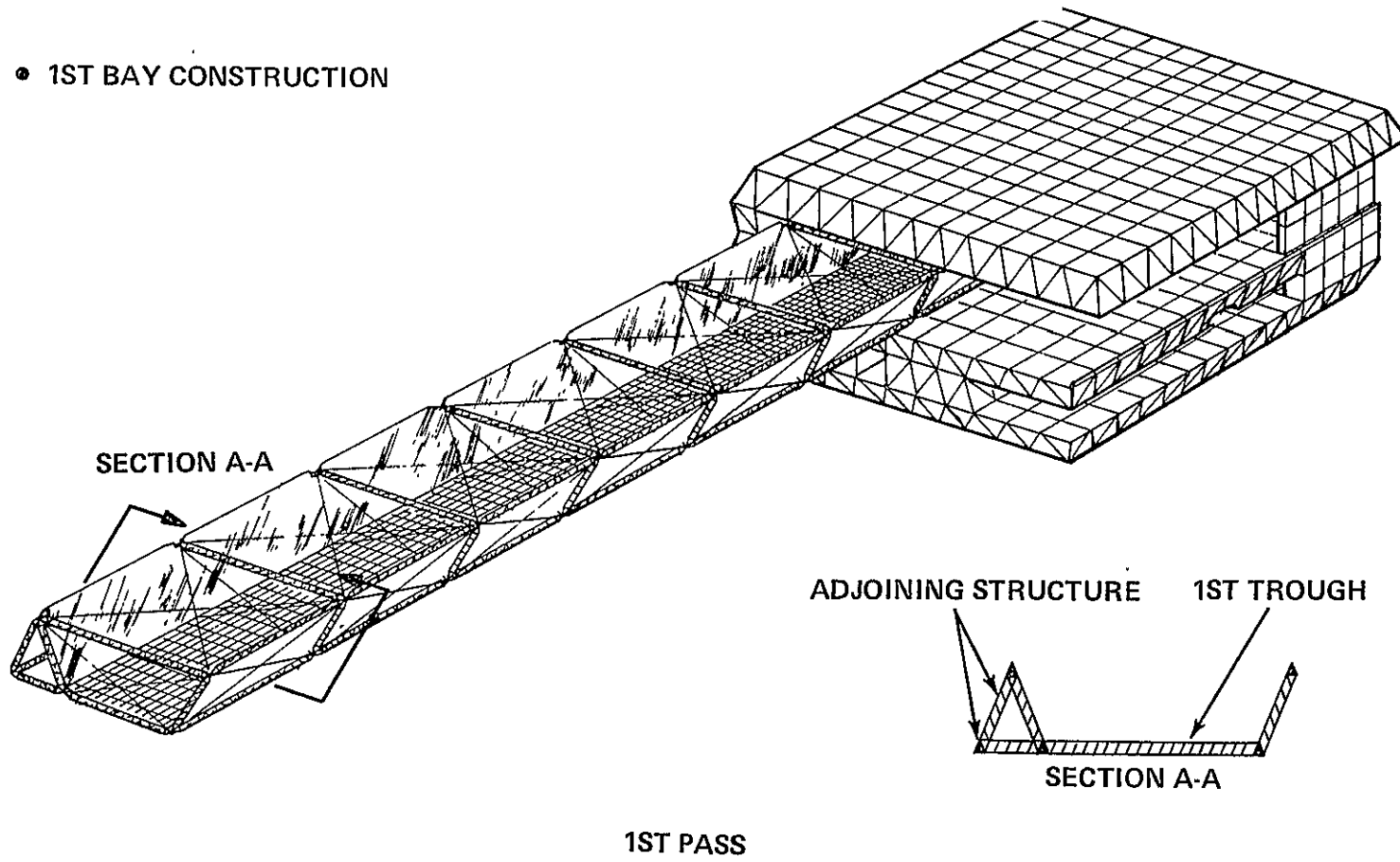


Fig. 5-4 Construction Sequence - Small Construction Base

figure is the cross-section of the trough produced, with the adjoining structural section that holds the concentrator of the next trough. The adjoining structure produced during the first pass is used to stitch the next trough to the completed trough during the subsequent pass.

Figures 5-5 and 5-6 depict the construction sequence during the second and third passes thru the construction base. Fig. 5-5 shows the second trough being stitched to the completed first trough, while the fabrication and assembly of the third trough is performed. Similarly, Figure 5-6 shows the third pass thru the construction base, wherein the fourth trough is stitched to the already completed portion of the satellite, and the fifth trough is manufactured and joined. During the third pass, the central mast, which is fabricated in a dedicated area of the construction base, is installed to the completed half of the satellite.

Figures 5-7 and 5-8 depict the general arrangement of the central mast design that was developed during the Power Distribution System Analysis task of Phase III of this study. The central mast consists of 24 aluminum conductor tubes, configured into an 80-meter-square pattern, and connected by support structure sections spaced 493 meters apart. The support structure is built up from 20-meter beams made of dielectric material. To provide further bending stability within the 493-meter spans, a series of frames is placed around the aluminum conductor tube sections spaced approximately 20 meters apart. The frames are also made up of dielectric material. S-glass, with an "addition polyimide" resin system of Hexcel F-178, was selected as the baseline dielectric material.

During the fourth pass thru the construction base (i.e. stitching the sixth and constructing the seventh troughs), the microwave antenna is joined to the satellite. The antenna, together with the rotary joint assembly, is constructed on the lower floor of the construction base, and moved into proper position for connecting to the central mast assembly. Figure 5-9 shows the construction jig, and the fabrication technique used to construct the antenna subarray structure. The beams are constructed using 1-meter beam makers, and transported to the fabrication jig, where they are placed into the construction jig and assembled into subarrays. This construction process is taking place while the solar arrays are being fabricated. The completed antenna is joined with the satellite during the proper assembly point in the construction sequence.

Figure 5-10 depicts the overall rotary joint design developed during the Phase III studies, to permit a full 360-degree antenna rotation in azimuth, and $\pm 8^\circ$ rotation in elevation. The inner and outer race support structure is assembled using 1-meter beams as shown in the detail view of Figure 5-11. The inner race is comprised of 11.78 M circular sections, prefabricated on the ground, and supported by 1-meter beam structure attached to the central mast bulkheads.

- 2ND BAY STITCHED
- 3RD BAY CONSTRUCTED

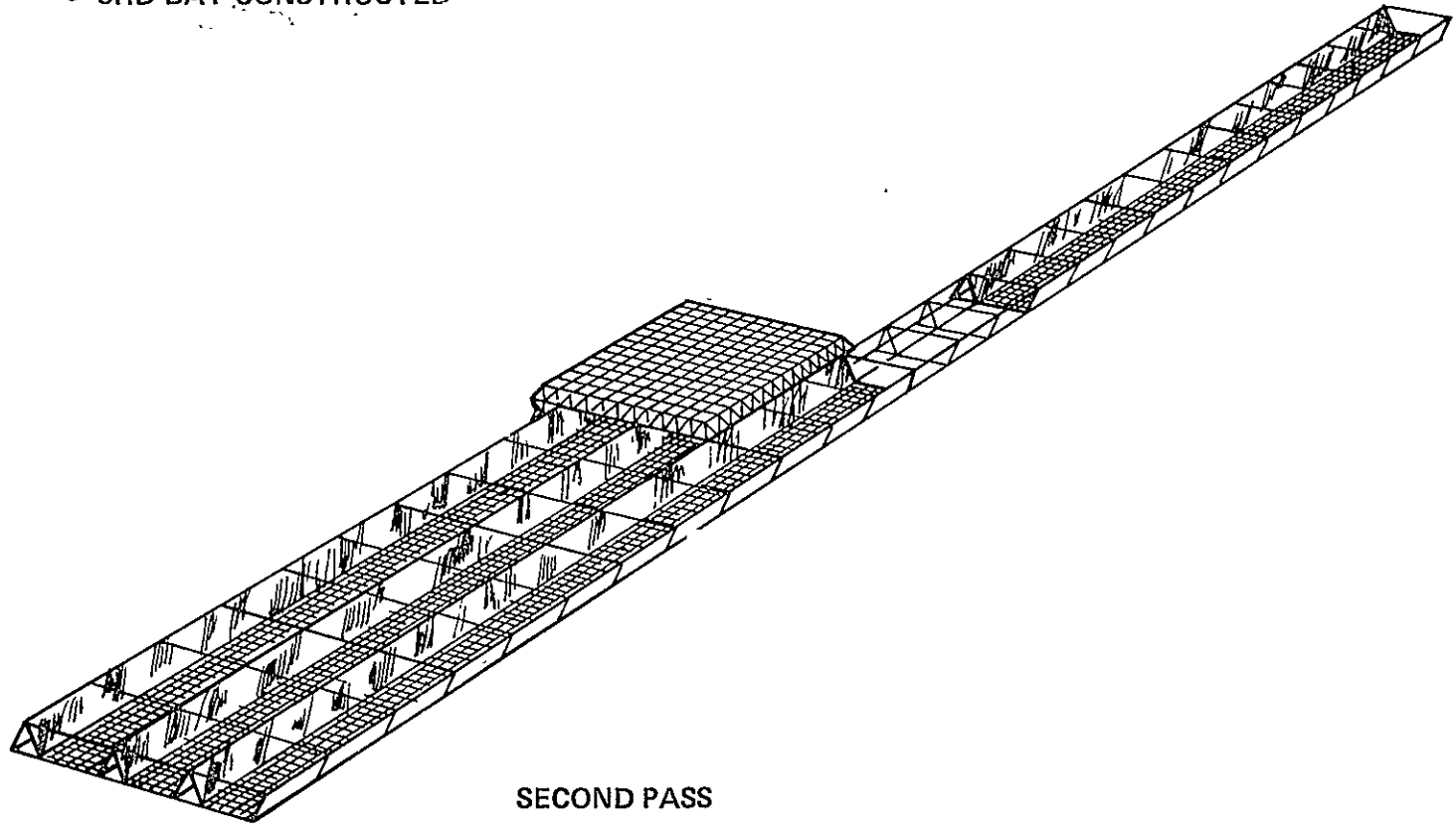
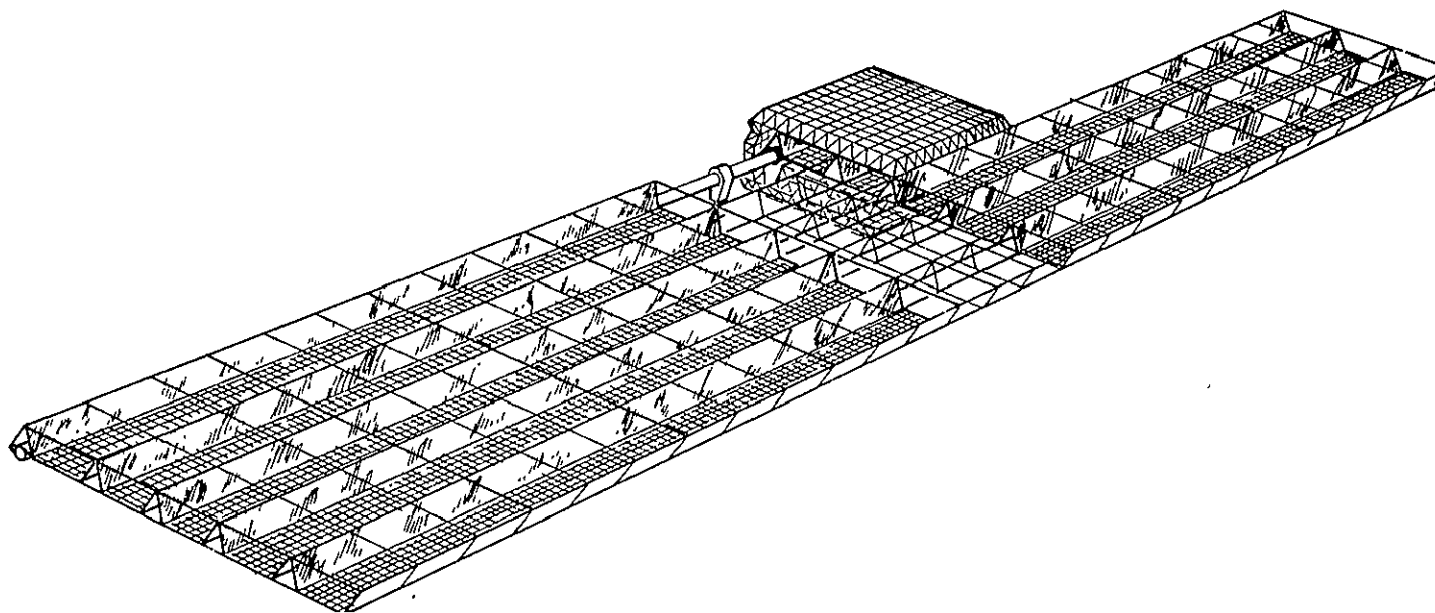


Fig. 5-5 Construction Sequence - Small Construction Base

- 4TH BAY STITCHED
- 5TH BAY CONSTRUCTED
- MPTS ANTENNA ATTACHED



36

THIRD PASS

Fig. 5-6 Construction Sequence - Small Construction Base

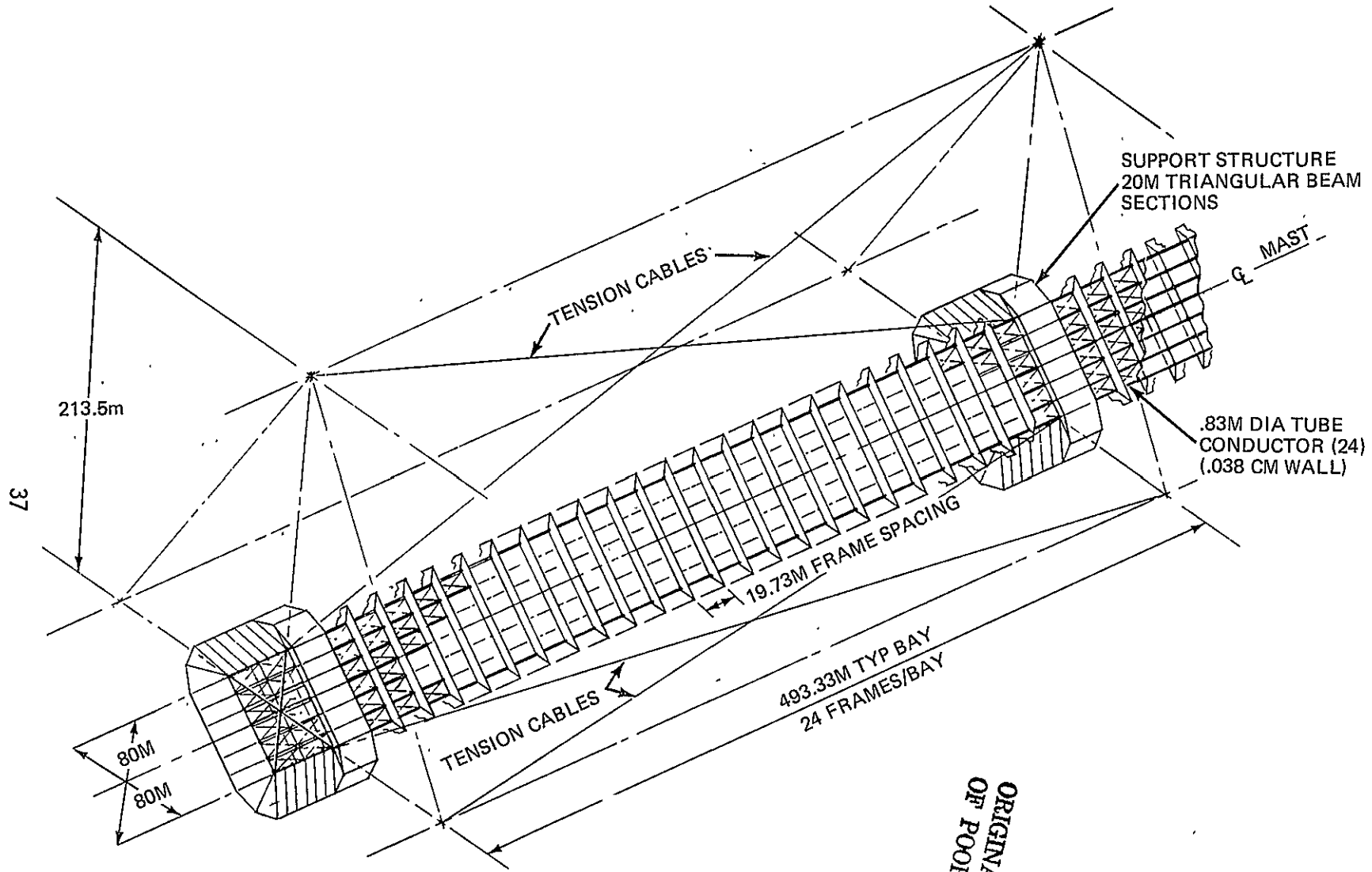


Fig. 5-7 Conducting Structure

ORIGINAL PAGE IS
OF POOR QUALITY

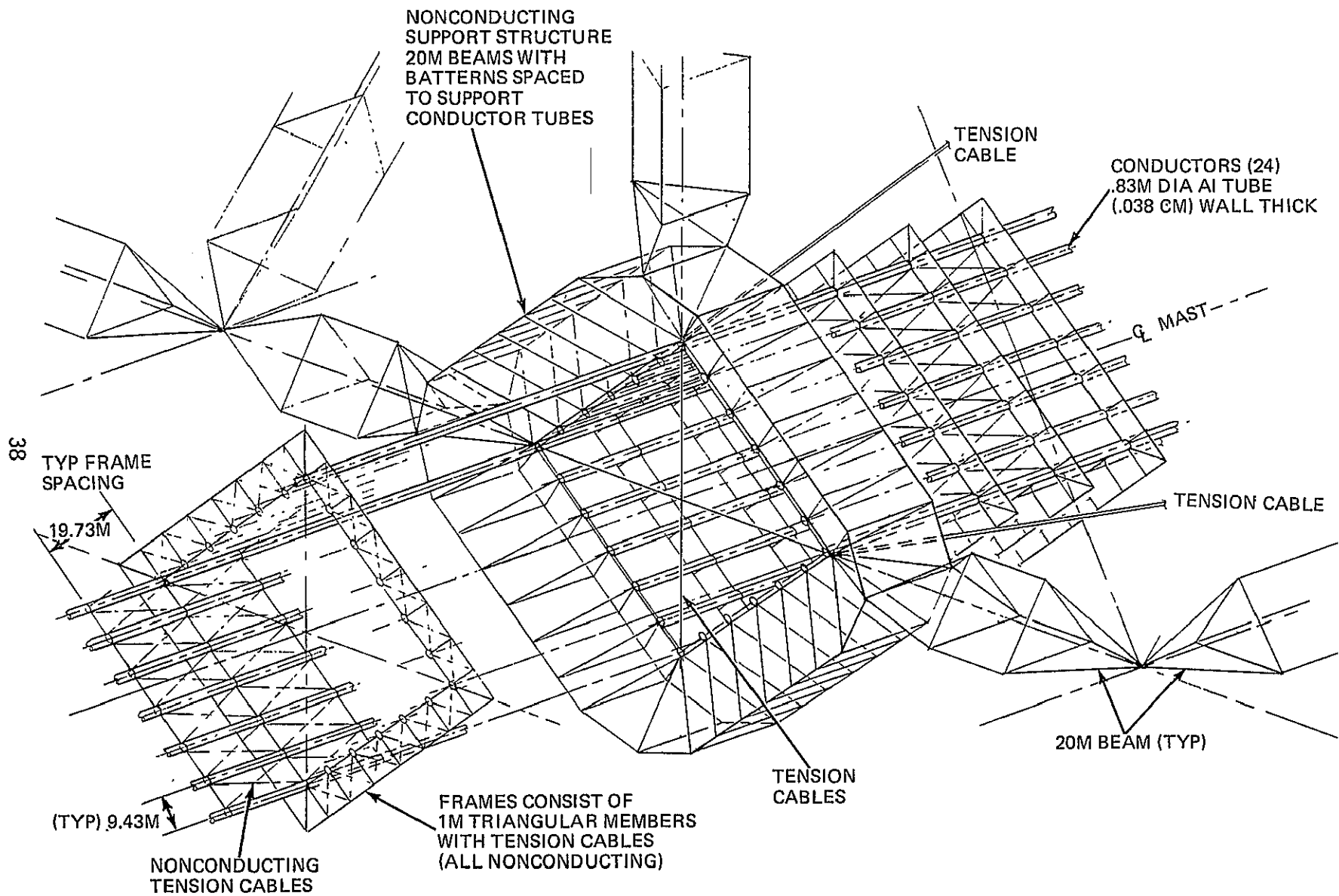
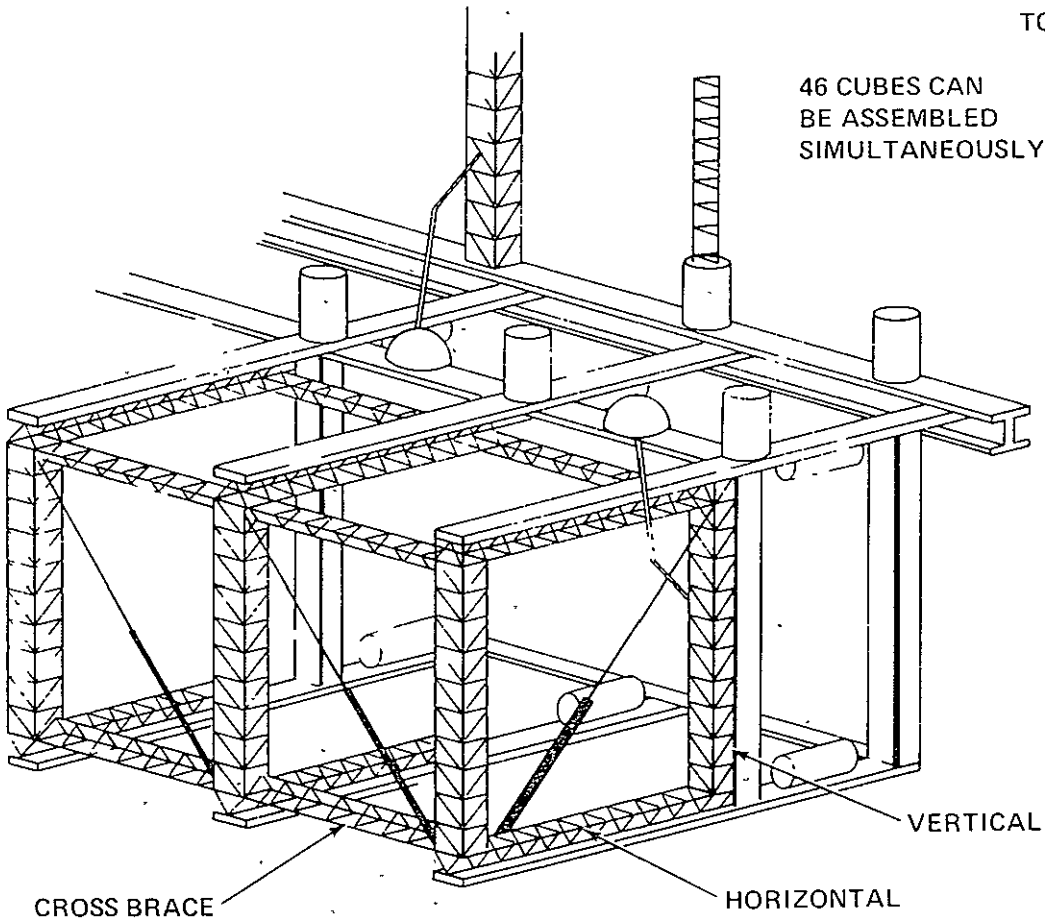


Fig. 5-8 Square Mast Support Structure

ESTIMATED TIME

STEP	TIME
I. INSTALL HORIZONTALS	23 MIN
II. INSTALL VERTICALS	42 MIN
III. INSTALL CROSS BRACE	16 MIN
TOTAL	81 MIN

46 CUBES CAN
BE ASSEMBLED
SIMULTANEOUSLY



REF (NAS 9-14916)

Fig. 5-9 Antenna Construction Jig -

ORIGINAL PAGE IS
OF POOR QUALITY

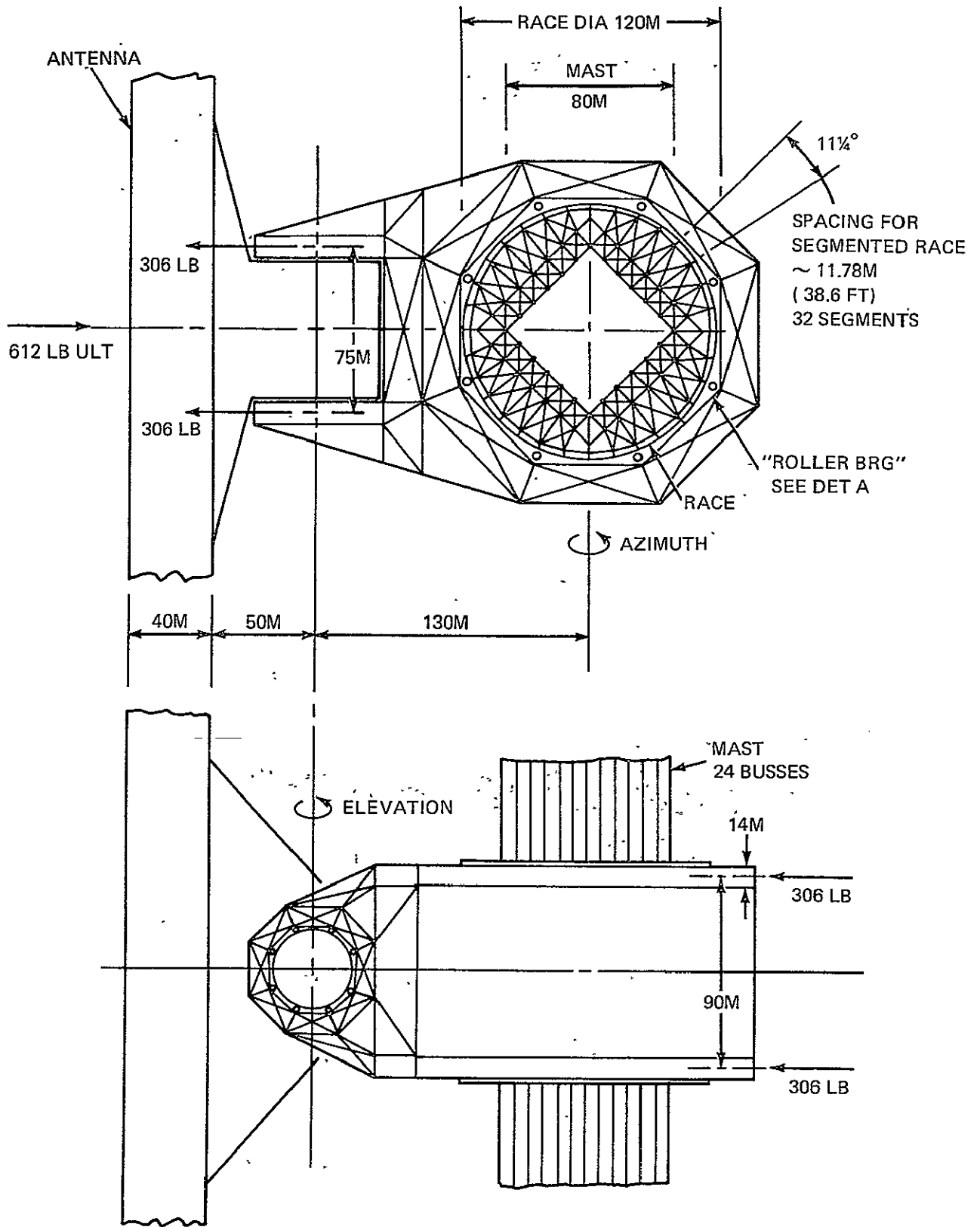
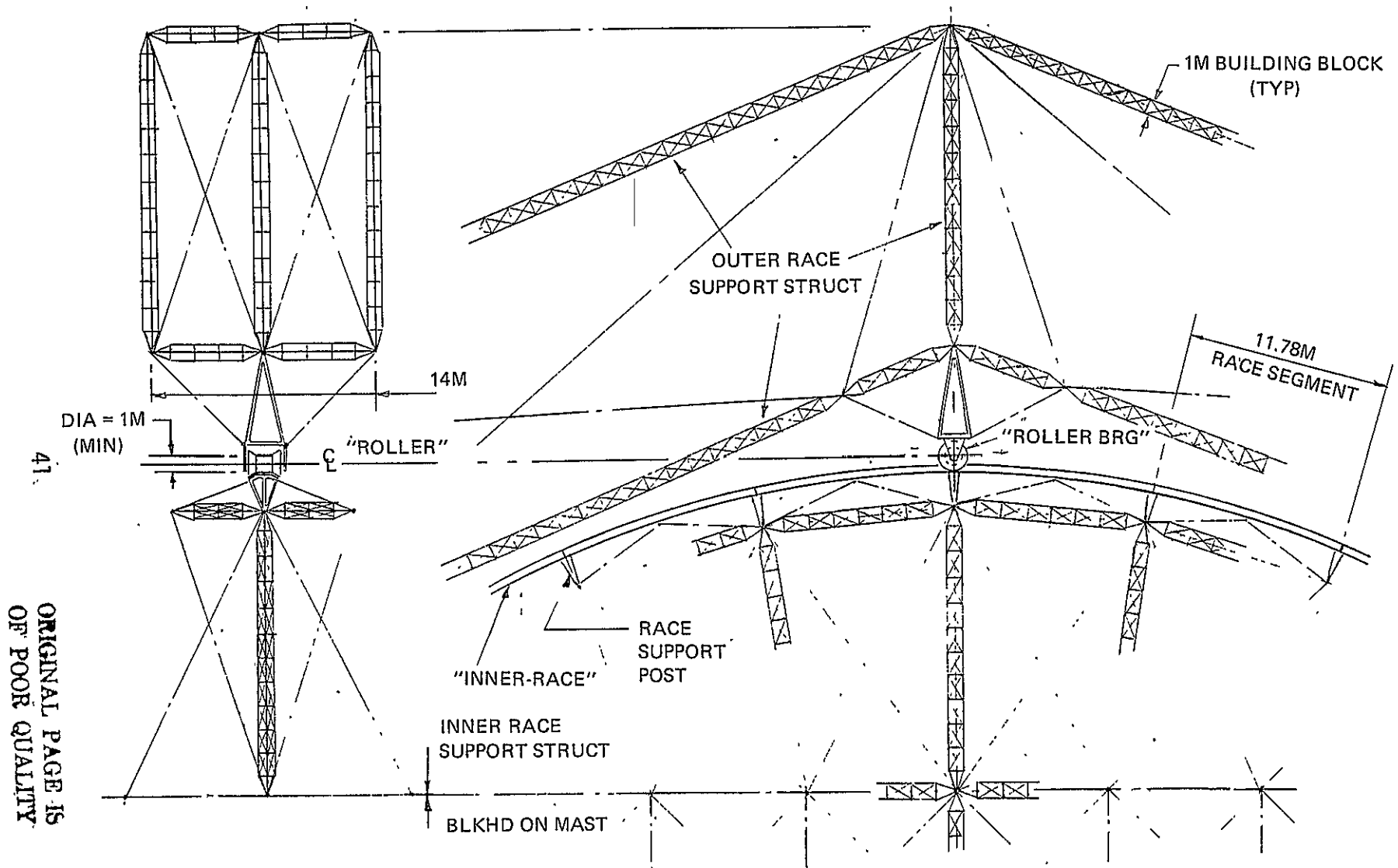


Fig. 5-10 Rotary Joint



41

ORIGINAL PAGE IS
OF POOR QUALITY

Fig. 5-11 Rotary Joint Detail

The outer race support structure is comprised of octagonal frame sections, also made of 1-meter beams, which support rollers used to drive the antenna rotation. The rollers are made into a concave shape, and ride along the race structure shaped to mate with the roller, as shown in Figure 5-12. The race is an extruded aluminum track, contoured to provide stiffness, and permit both radial and lateral loads to be applied as encountered during orbit transfer and stationkeeping. Conventional bearings are used to transmit roller loads to the supporting structure. Drive motors, attached to the roller axis of rotation, power the overall antenna motion in the azimuth direction. Figure 5-13 shows a detailed view of the roller and the order of magnitude of potential loads expected. The overall 1-meter diameter roller rotates at an average rate of 5 rev/hr, experiencing a total of 1.3 million revolutions during the 30 year life. These requirements are well within present conventional bearing designs. Roller hub designs, also shown in Fig. 5-13, are assumed prefabricated on the ground. Silicon coatings are used to reduce overall friction wear.

After completing construction and assembly of the sixth and seventh troughs, which includes the installation of the central mast and microwave antenna assemblies, the procedure is repeated thru a 5th and 6th pass, to complete construction of the entire satellite. The 6th pass is used to stitch the tenth trough of the satellite. Fig. 5-14 depicts the completed satellite, attached to the construction base, at completion of the 6th pass. Assuming an average speed of fabrication and assembly thru the construction base of 2 ft/min, the satellite is constructed over a 3 month-period. The average rate of 2 ft/min was selected from the NASA/MSFC Space Fabrication Techniques Study (NAS8-31876), where it was specified that the average speed of production of a 1-meter truss beam may be as high as 5 ft/min.

Fig. 5-15 shows the typical 20-meter beam fabricator used within the construction base, which consists of six 1-meter beam makers positioned onto a frame assembly. A detailed view of a 1-meter beam maker is shown in Fig. 5-16. Pre-cut sheet stock is transported to orbit on rolls, and loaded into the 1-meter beam maker. The raw stock is passed thru rollers used to form the sides of a triangular beam structure, which are then spot welded to form an integrated beam.

The completed satellite structure is carried thru the construction base during each pass, using a crawler assembly as shown in Fig. 5-17. The motion of the crawler assembly is representative of a "type-writer carriage" operation, wherein the completed structure is carried thru construction base from start to end, indexed outward, and returned to its original starting position. The completed parts of the satellite are never released from the construction base until the satellite is totally constructed and readied for transport to geosynchronous orbit. The tracks of the crawler assembly are equipped with switch assemblies, allowing the crawler to operate on either lateral tracks, during the indexing, or longitudinal tracks during the fabrication. The switch assembly is depicted in Fig. 5-18.

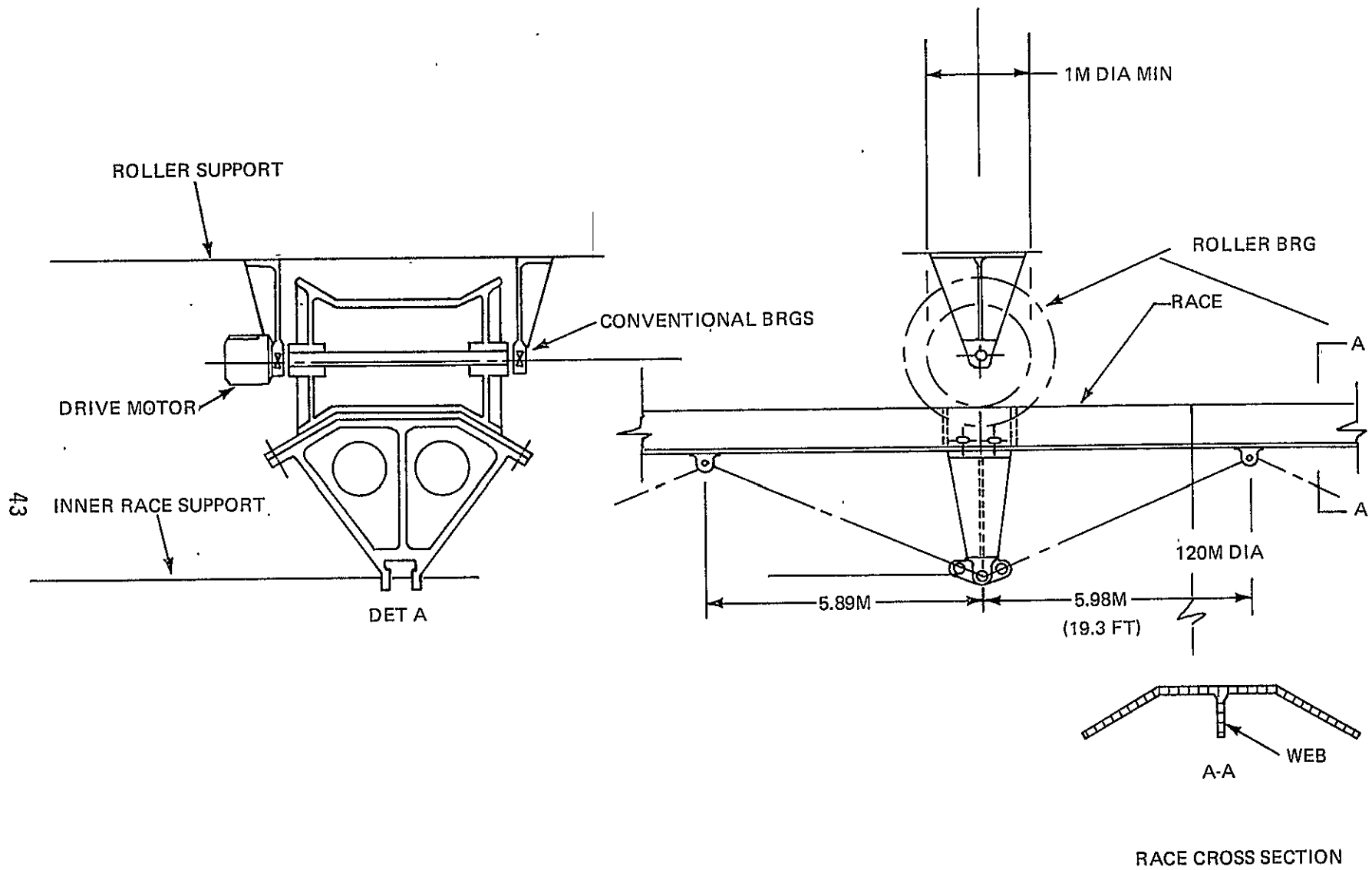


Fig. 5-12 Rotary Drive and Bearing

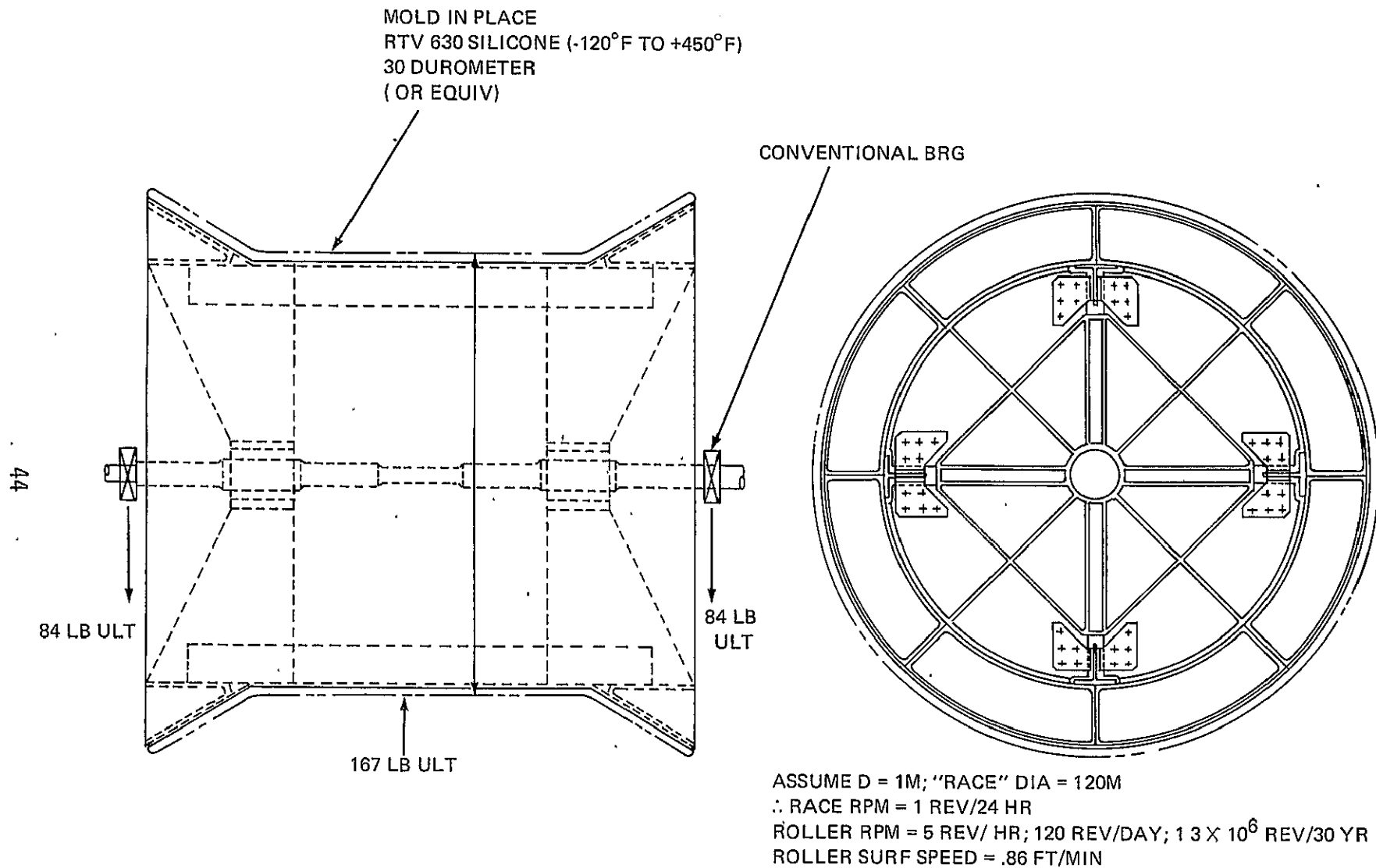
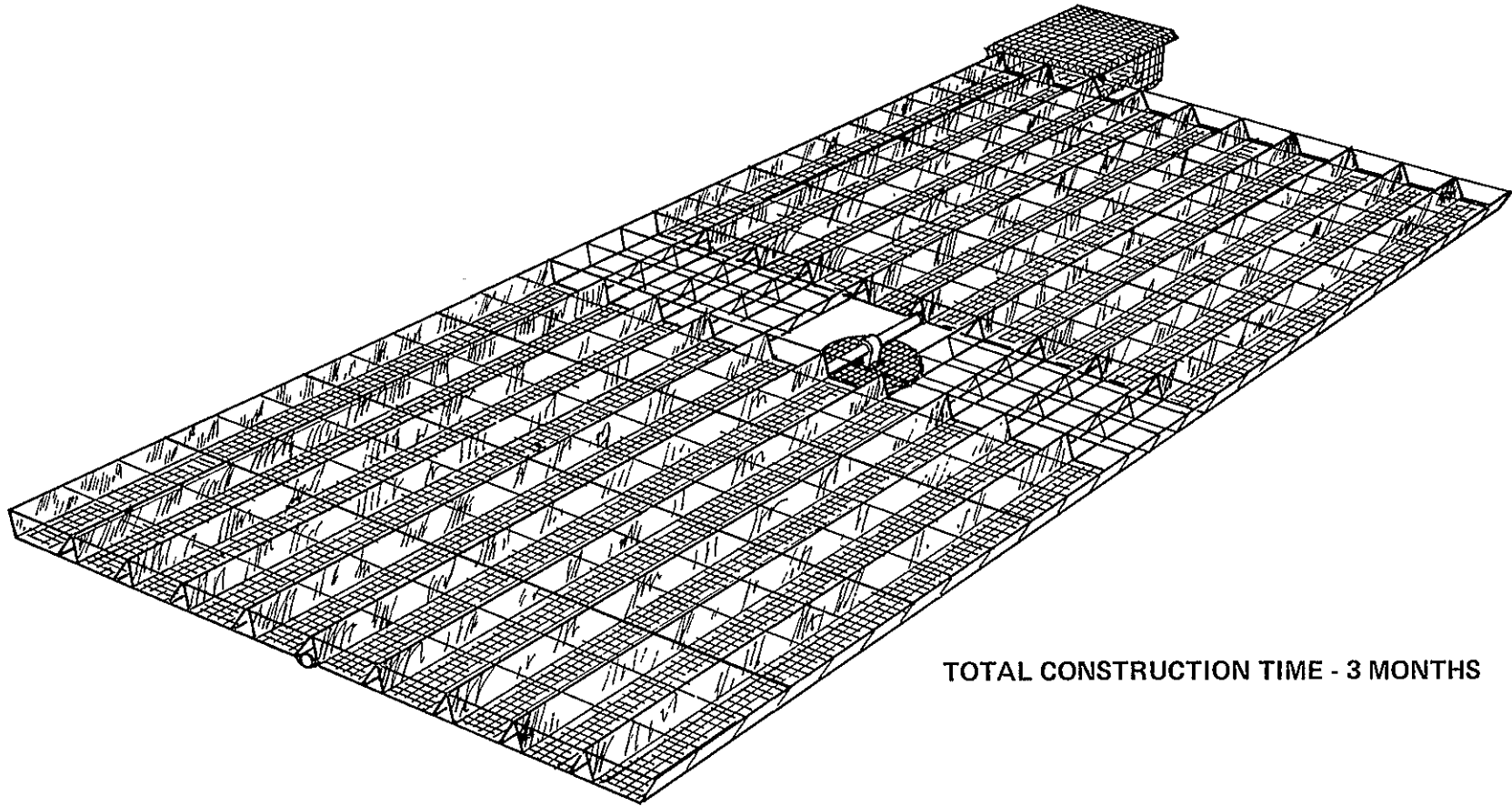


Fig. 5-13 Roller Bearing Detail

• 10TH BAY STITCHED

45



TOTAL CONSTRUCTION TIME - 3 MONTHS

Fig. 5-14 Construction Sequence - Small Construction Base

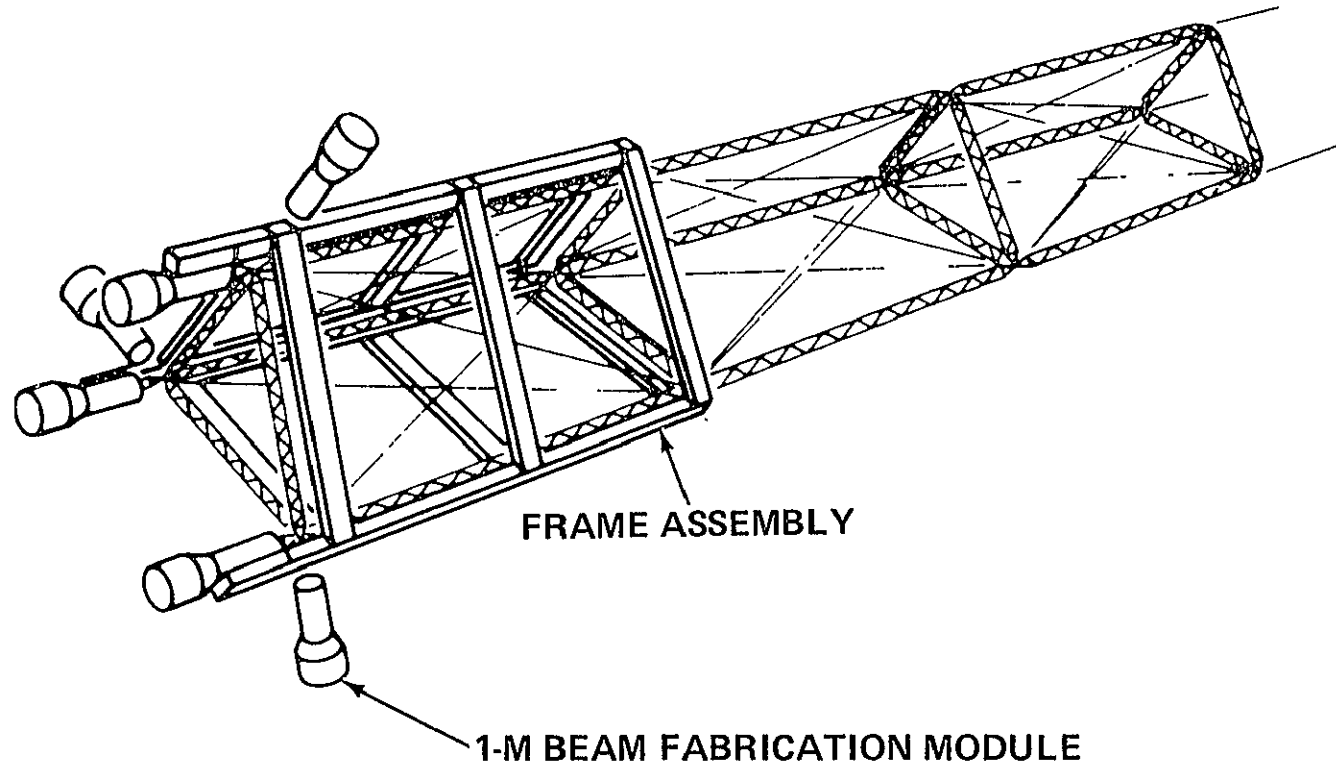


Fig. 5-15 20-M Beam Fabrication Module

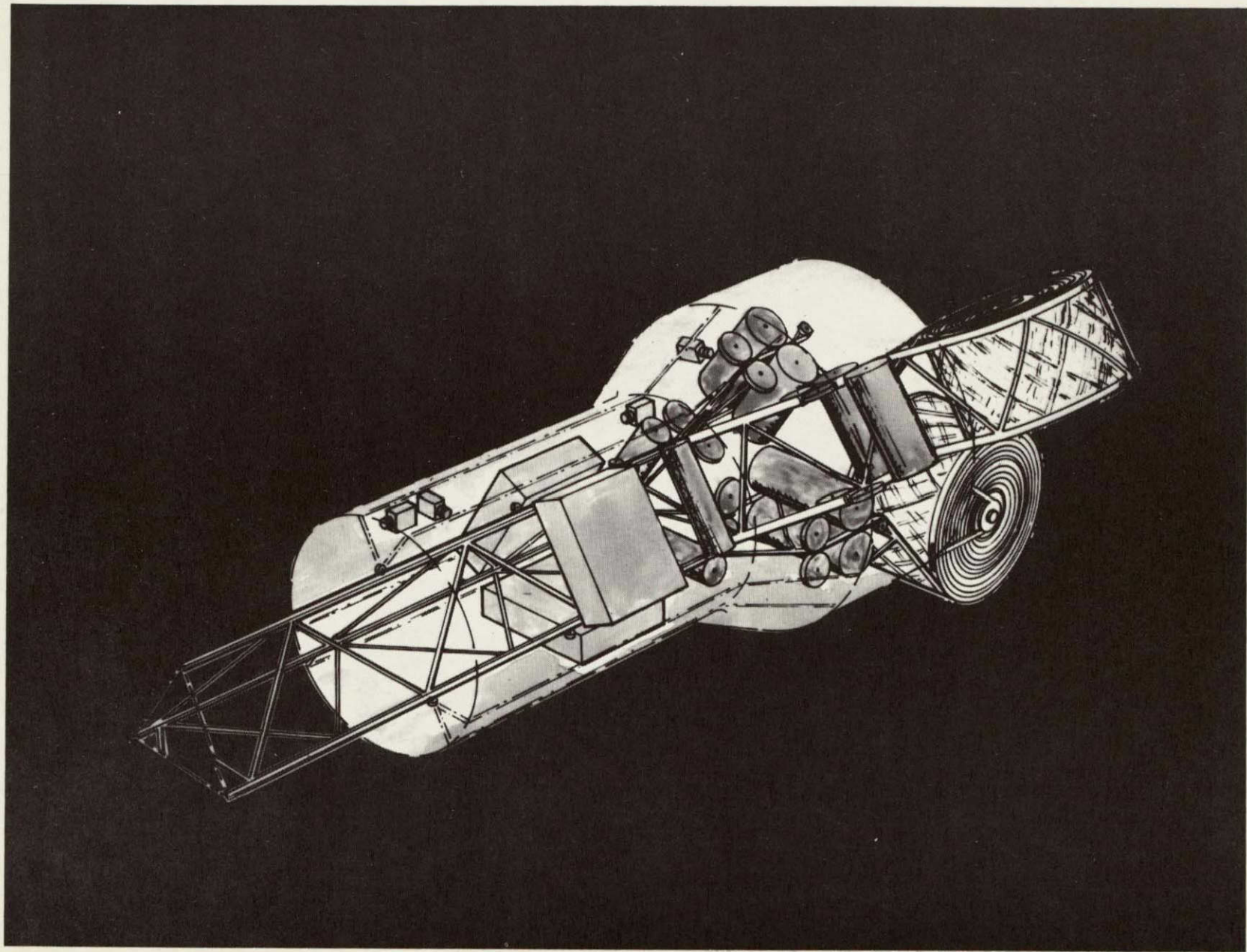


Fig. 5-16 1-Meter Beam Maker

ORIGINAL PAGE IS
OF POOR QUALITY

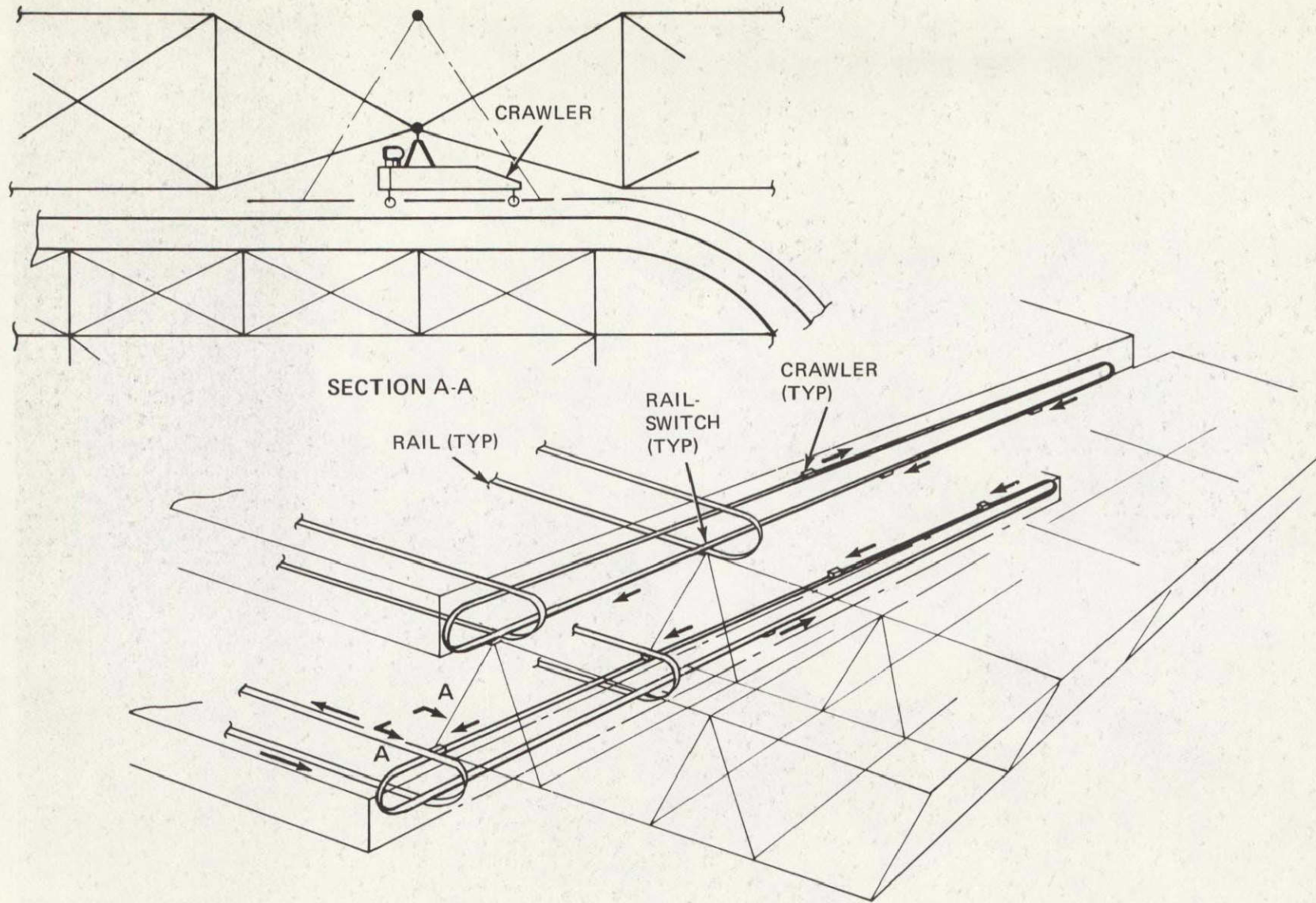


Fig. 5-17 Construction Base Crawler

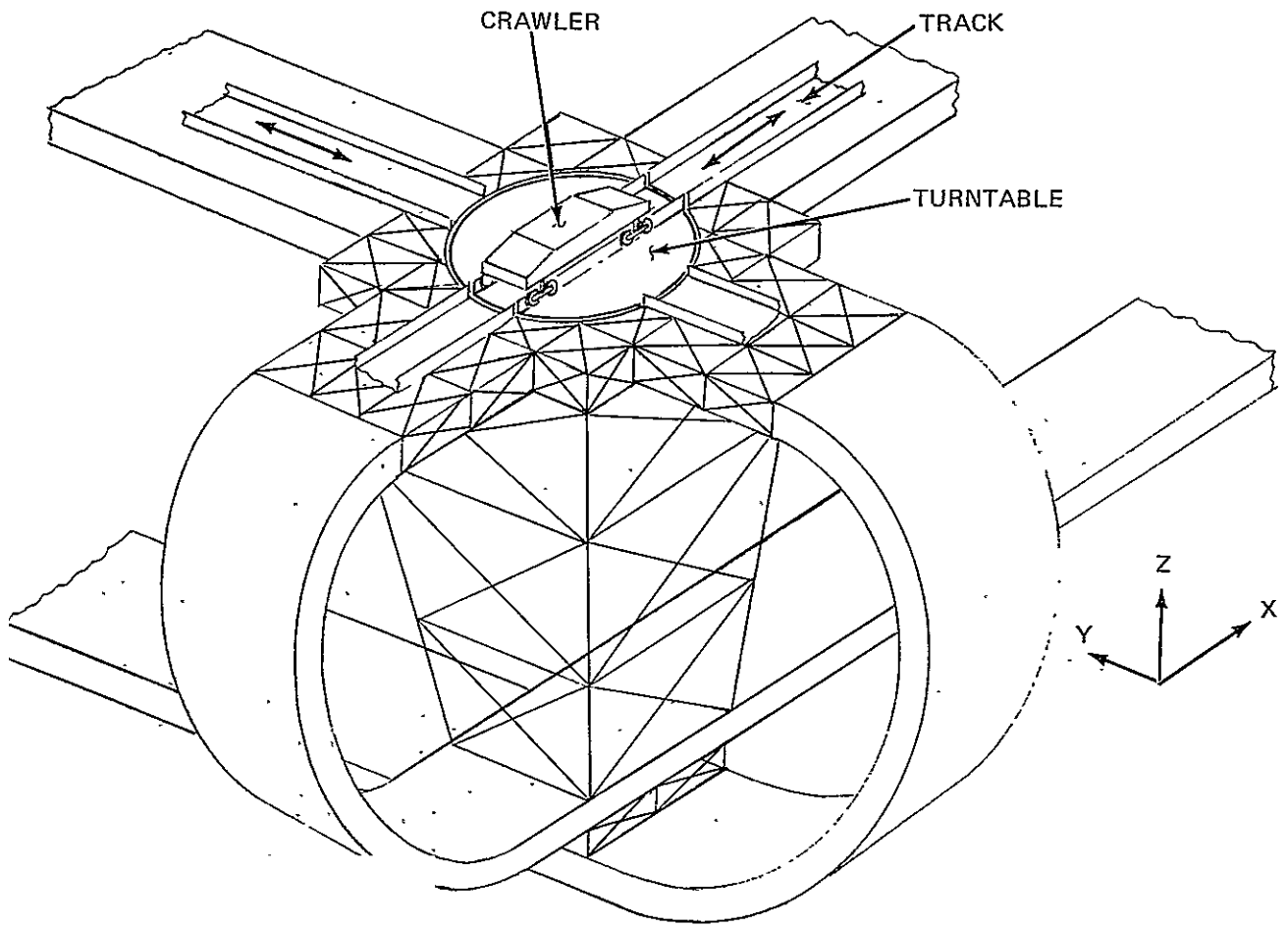


Fig. 5-18 Switch Assembly

Typical fabrication and assembly operations performed during the construction of the satellite troughs are shown in Figs. 5-19 thru 5-23. Fig. 5-19 depicts the fabrication technique, in which apex assemblies, used to terminate 20-meter beams that connect to other 20-meter beams, are made. One-meter beams are pivoted to a common point of connection using swing arms, where end fittings joining the three 1-meter beams to a 20-meter beam end fitting are installed. Construction personnel, located in crew modules at points where these fittings are installed, perform these operations. Fig. 5-20 depicts a typical butt joint assembly wherein four 20-meter beams are joined. The butt joint was selected as the baseline joint assembly technique from data derived in the NASA/JSC Orbital Construction Demonstration Study (NAS9-14916). In that study (see Fig. 5-21), the centroidal butt joint assembly was recommended over other joint techniques, because it provided better alignment for transferring loads axially from member to member. Furthermore, it facilitated the time required to construct the joints thru better crew accessibility.

Fig. 5-22 shows the manner in which cables are rigged within the major truss frames. Cables, stored on rolls, are transported to opposite structural joints using a drive pulley system, and connected at one end. As the structure is moved along the assembly line, it unrolls the cables to the lengths required for connection at the diagonally opposite end. Crew personnel located at these work stations cut and connect those opposite ends.

Solar cell blankets and reflectors are stored in a similar manner. Rolls of solar cell blankets, measuring 246.5 meters in width (i.e. the width of each of the troughs) are folded into a flattened "W" form, and rolled up on rollers for transport to orbit. This concept is illustrated in Fig. 5-23. The folded configuration allows rolls of solar blankets to fit within the 62-meter HLLV payload bay. Prefabricated within the ends of the solar cell blankets are "curtain rods", used for connecting the blankets to the structure. As the structural frames are fabricated in the assembly line operation, the solar blankets are unfurled and connected to the 1-meter beams with bungees. Installing the bungees approximately every 9 meters provides the forces required to keep the solar blankets taut thru the range of solar blanket temperature variations.

To better understand the impact of construction base configurations on LEO and GEO construction, an alternate construction base design was developed. The alternate concept was to use similar construction techniques described for the small construction base, but sized to produce a completed satellite using only two passes thru the construction base. Fig. 5-24 shows half the satellite (5 troughs) being constructed during the first pass. The central mast, which is fabricated in sections in designated parts of the construction base, is installed

51

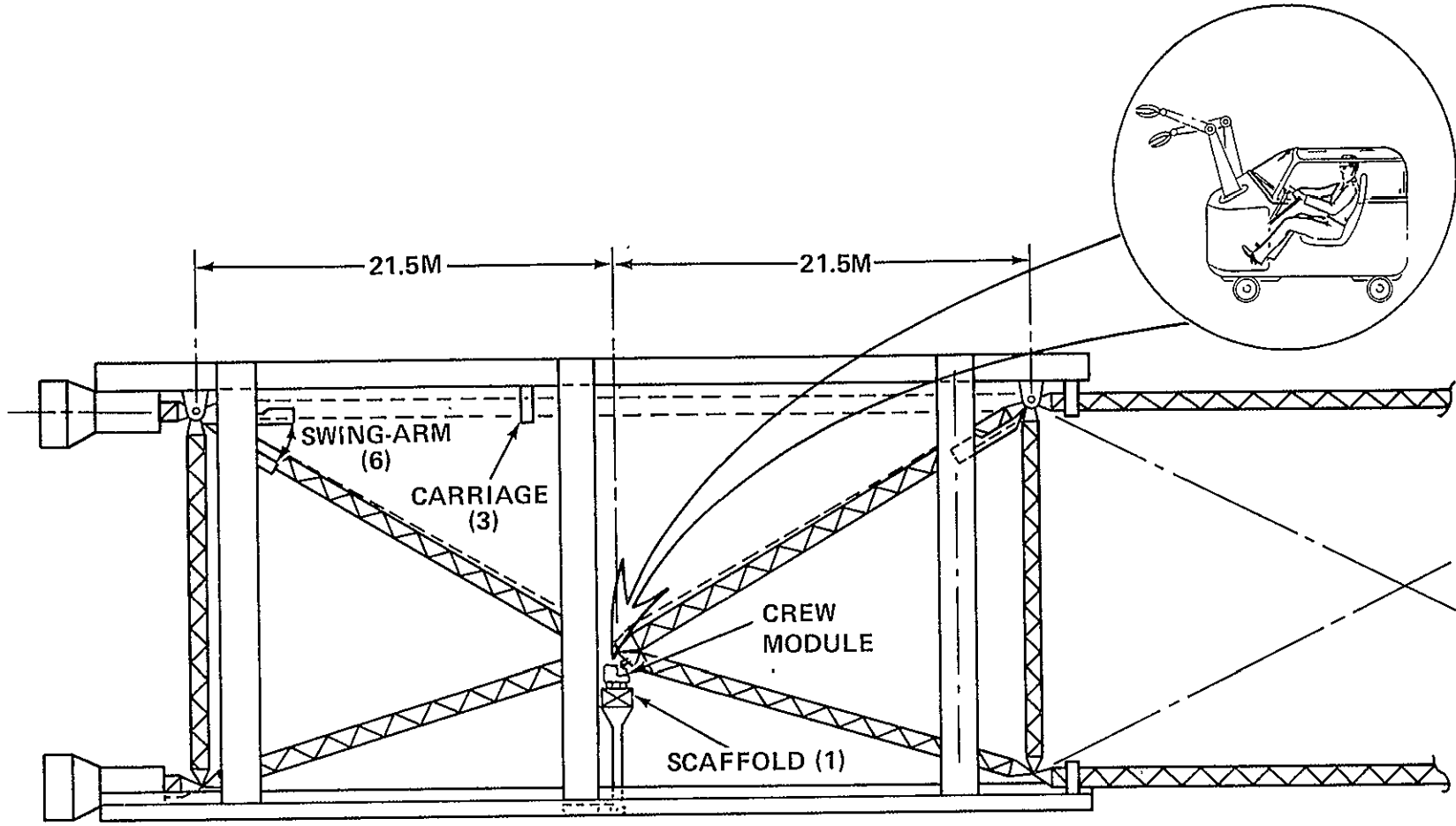


Fig. 5-19 20-M Beam Fab Module Apex Assy

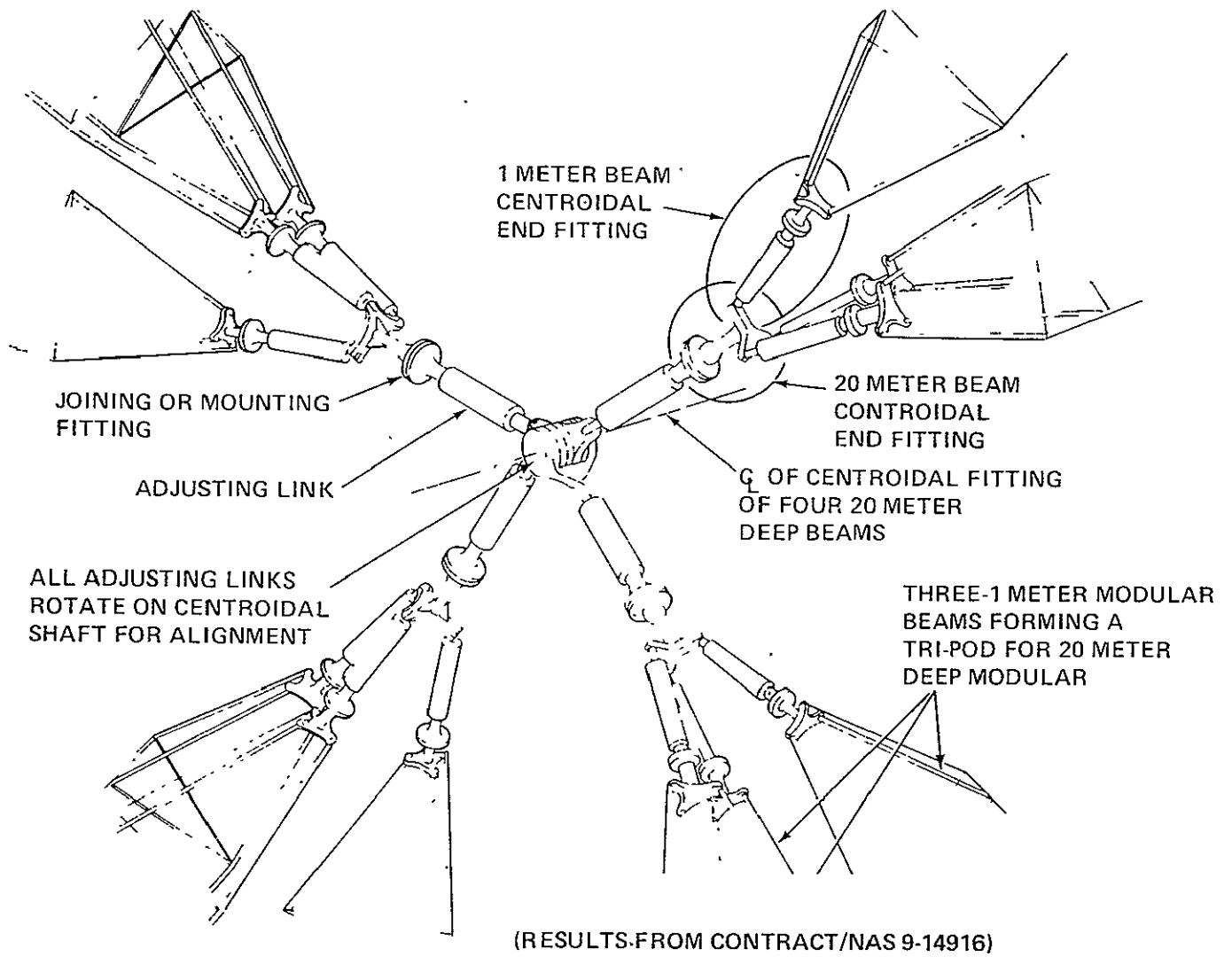


Fig. 5-20 Typical Butt Joint (Centroidal) Intersection of Four 20-Meter Deep Beams

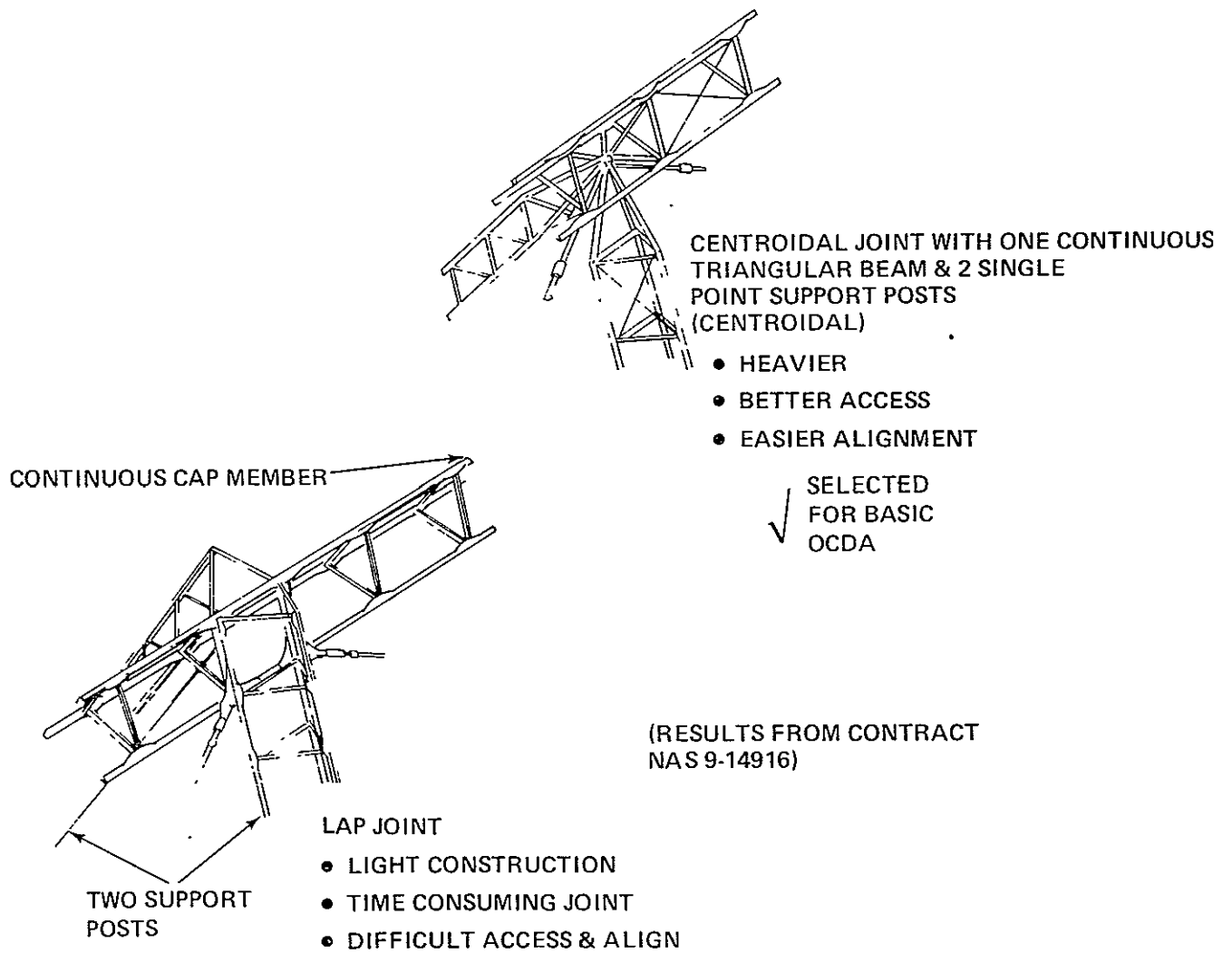


Fig. 5-21 Selected Joint and Fastener Techniques

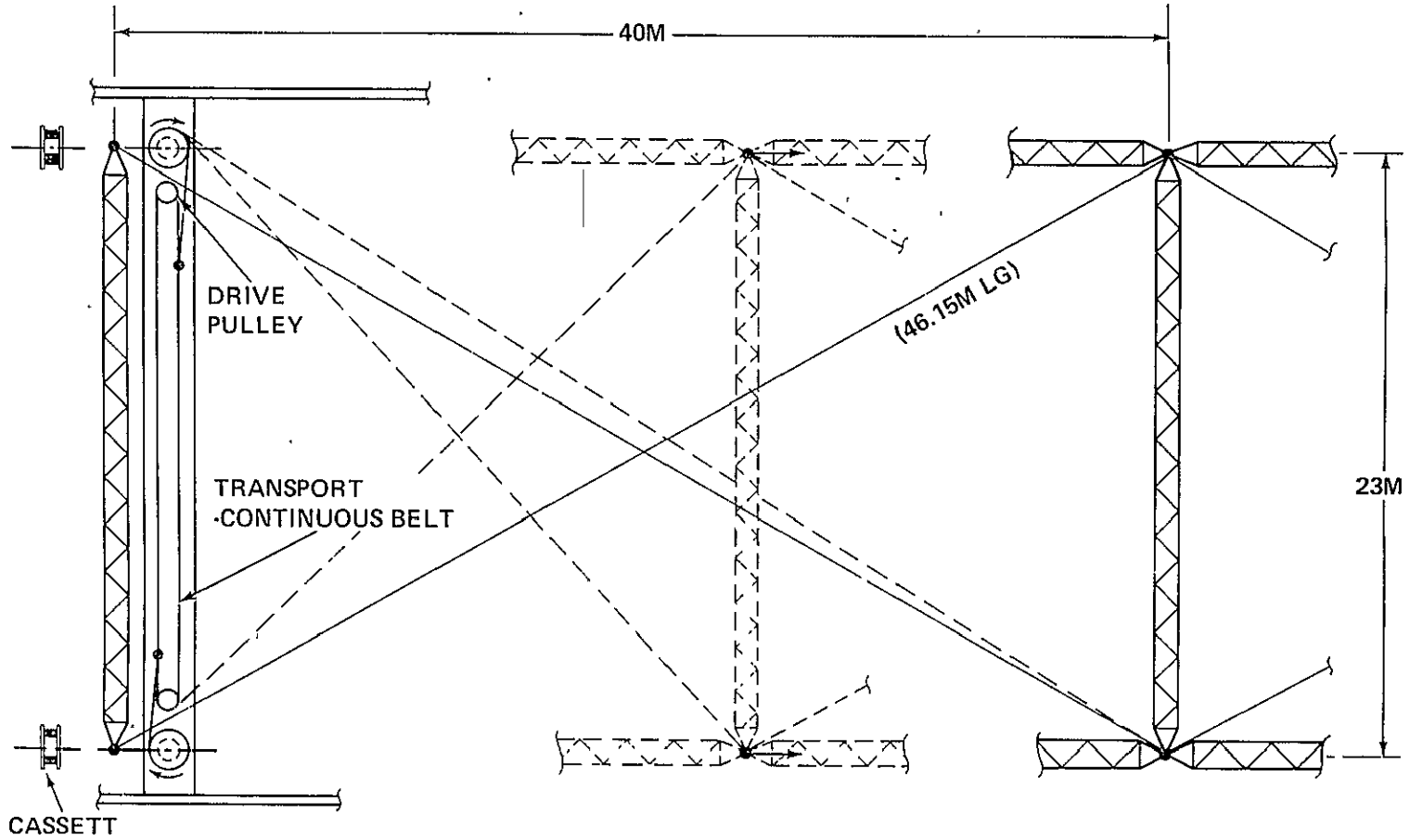


Fig. 5-22 Cable Rigging

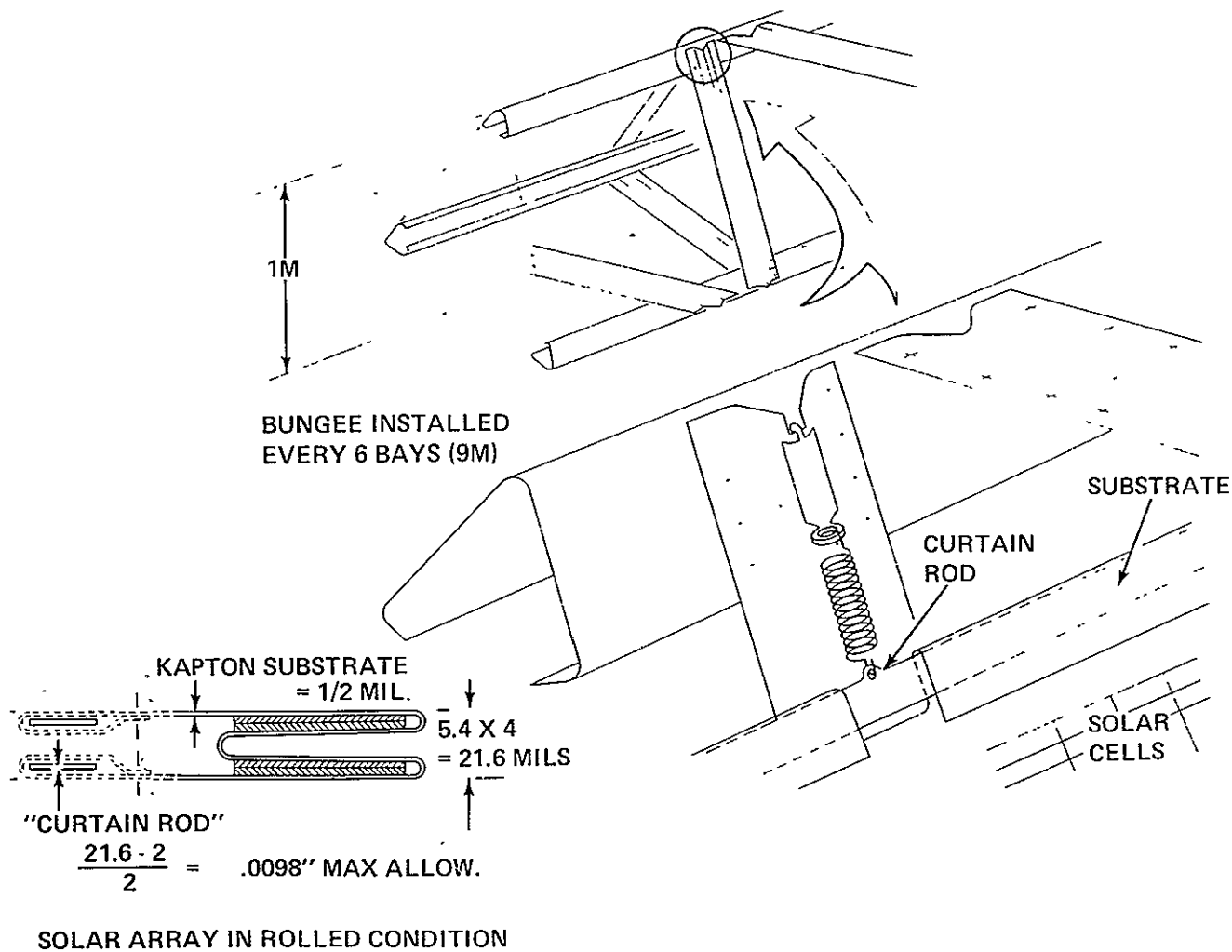


Fig. 5-23 Blanket/Reflector Bungee Installation

ORIGINAL PAGE IS
OF POOR QUALITY

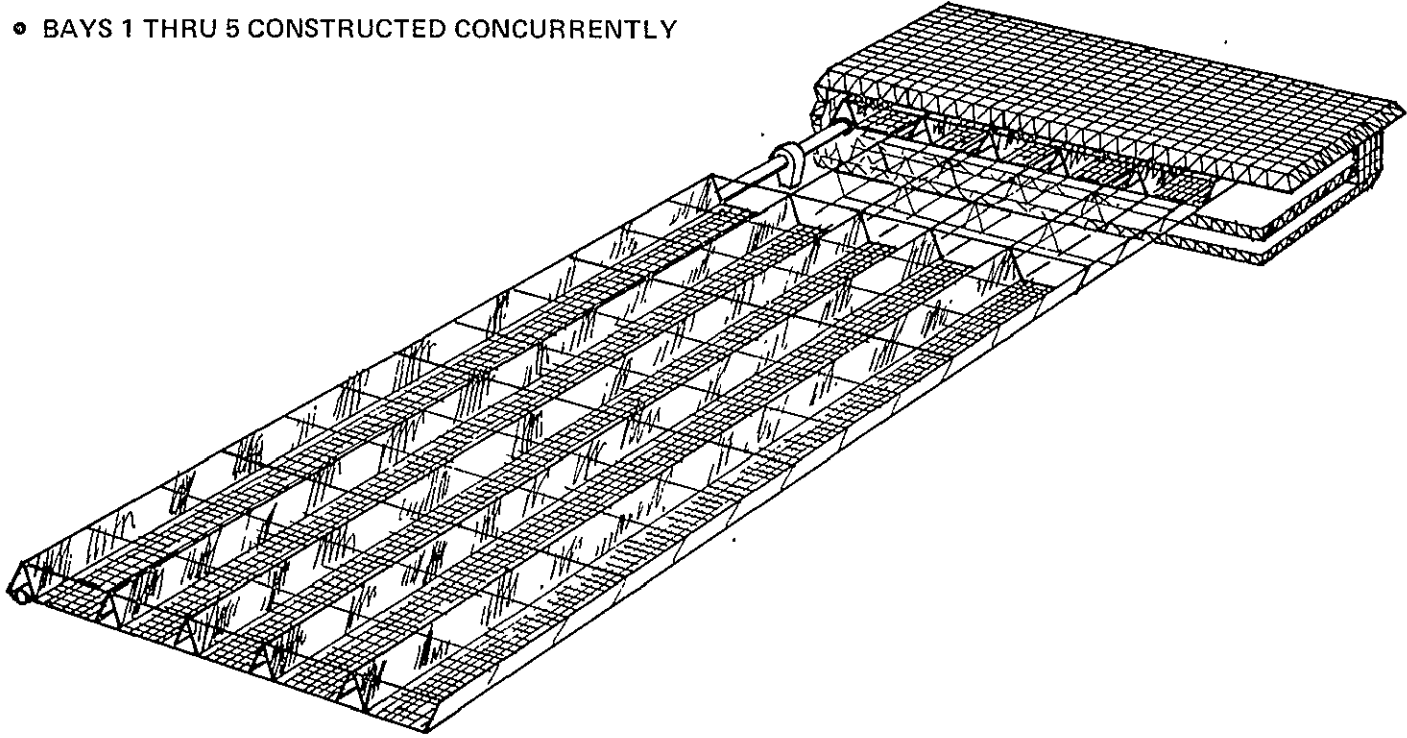


Fig. 5-24 Construction Sequence - Large Construction Base

on this pass. The average rate of production was assumed at 1 ft/min. Figure 5-25 shows the completed satellite at the end of the second pass. The MW antenna and rotary joint, fabricated on the lower floor, are moved into position, and attached to the central mast midway thru the second pass.

Summarized in Fig. 5-26 are the dimensions, mass properties, and production characteristics for both the small and large construction bases. Note that the 1.5 KM depth of the construction base permits it to remain connected to the completed portion of the satellite by at least two 493-M length sections at all times. The mass properties data shown include an average amount of materials accumulated in warehouse storage, during the satellite construction period. These data was derived using information shown in Figure 5-27, which gives a time history of materials in storage based on a transportation delivery schedule averaged over the period of construction of each satellite. This schedule is phased to provide an initial four week build-up. The average mass in storage may be reduced to less than half these amounts by shortening the initial material delivery phasing to less than two weeks.

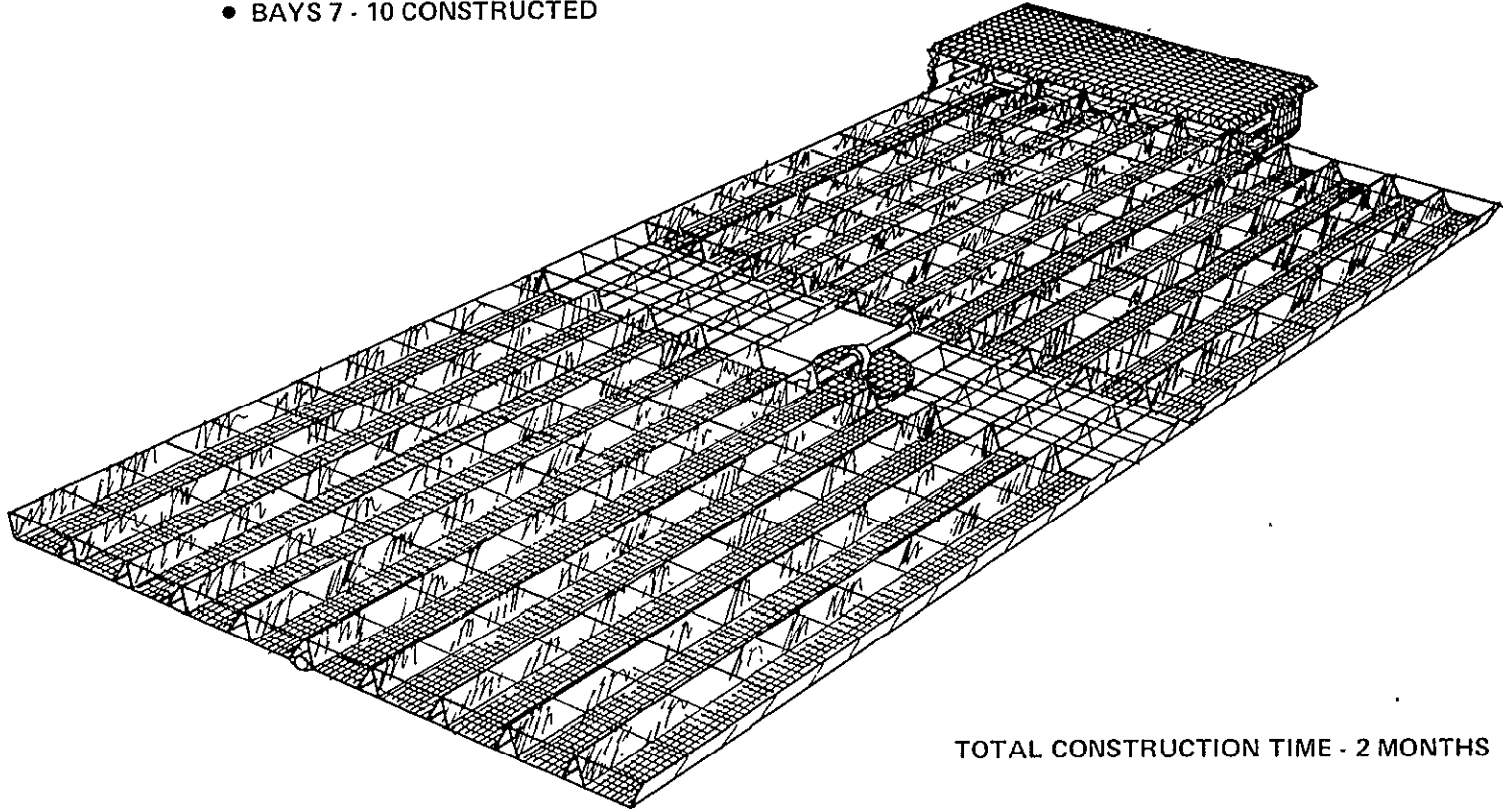
The crew size required to support a 24-hour construction operation, for each of the construction bases, is summarized in Fig. 5-28. A total of 108 work stations for the small construction base and 293 for the large construction base require personnel attendance to either monitor automated functions, or perform light duty construction tasks. Four crews, each working 8-hr. work days, and rotated on a 6-day on, 2-day off schedule, are needed to provide 24-hour construction coverage. Another complement of personnel is needed for management and supporting services. This brings the total crew size to approximately 700 and 1900 people required during peak production activities, for small and large construction bases, respectively.

5.1.2 Construction/Assembly Transportation Scenarios

Two scenarios were formulated and evaluated with respect to fabrication, assembly and placement of the baseline 5-GW silicon crystal configuration. The scenarios considered: (1) complete construction of the satellite in LEO and, (2) complete construction in GEO. These two scenarios, although not representative of the complete spectrum of alternatives, identified key issues related to LEO and GEO construction. Furthermore, they allowed extrapolation into a wide assortment of mixed LEO/GEO scenarios.

Figure 5-29 depicts the LEO construction scenario. It consists of placement of a construction base in low earth orbit (i.e. $i = 28.5^\circ$, $h = 500$ Km), equipped with construction equipment, materials warehouse storage areas, crew habitability modules, and all supporting facilities. Heavy Lift Launch Vehicles (HLLV), carrying satellite

- BAY 6 STITCHED
- BAYS 7 - 10 CONSTRUCTED



TOTAL CONSTRUCTION TIME - 2 MONTHS

Fig. 5-25 Construction Sequence - Large Construction Base

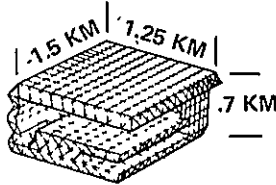
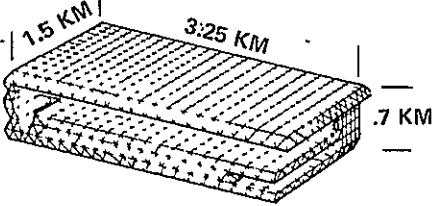
CONFIGURATION		
	SMALL CONST. BASE	LARGE CONST. BASE
	MASS (KG)	MASS (KG)
<ul style="list-style-type: none"> • STRUCTURE • HABITAT • EQUIPMENTS, POWER COND, BATTERIES ETC • AVG. MATERIALS IN STORAGE 	<p>1.58 X 10⁶</p> <p>.5 X 10⁶</p> <p>.67 X 10⁶</p> <p>9.25 X 10⁶</p>	<p>3.93 X 10⁶</p> <p>1.25 X 10⁶</p> <p>1.32 X 10⁶</p> <p>8.0 X 10⁶</p>
TOTAL	12.0 X 10 ⁶	13.5 X 10 ⁶
AVG RATE OF PRODUCTION	2 FT/MIN	1 FT/MIN
NO SATELLITES PRODUCED PER YEAR	4	6

Fig. 5-26 Construction Base Mass Properties and Characteristics

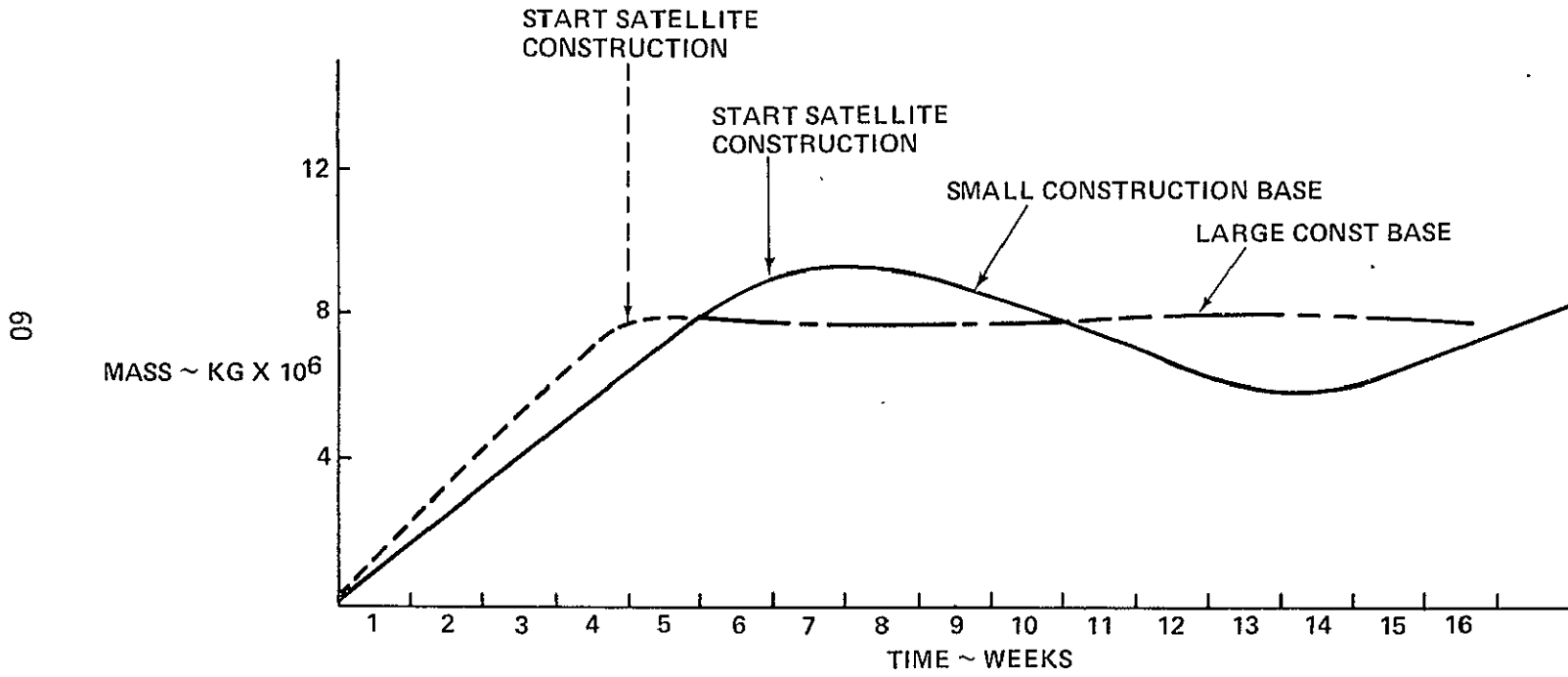
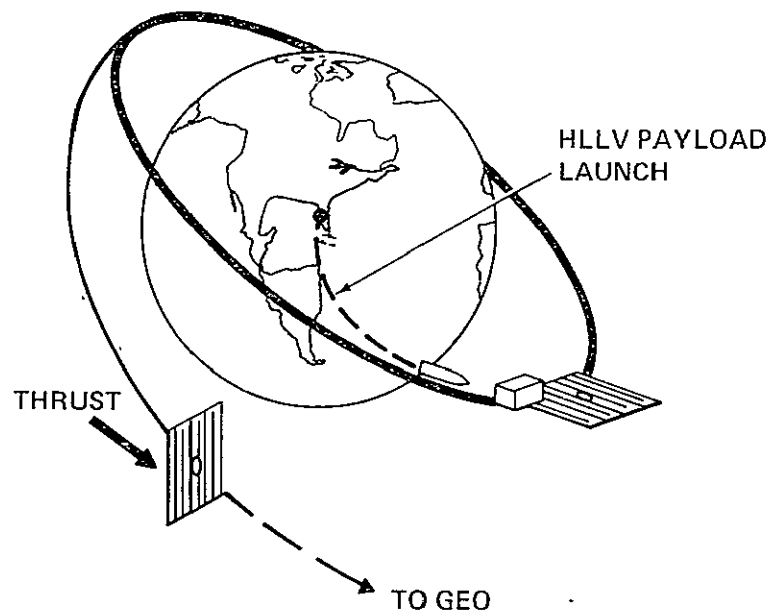


Fig. 5-27 Warehouse Storage Mass Vs Construction Time

	SMALL BASE		LARGE BASE	
	NO. OF SYSTEMS	CREW SIZE	NO. OF SYSTEMS	CREW SIZE
• 20M FABRICATION MODULE MANIPULATORS	16	48	48	144
• CABLE ATTACHMENT ASSEMBLY	10		30	
• SOLAR BLANKET DRIVE MECHANISM – ATTACHMENT ASSEMBLY	–	20		60
• CONCENTRATOR DRIVE MECHANISM – ATTACHMENT ASSEMBLY	2		6	
• CABLE RIGGING MECHANISM	4	4	12	12
• CABLE PRETENSION MECHANISM	4		12	
• CRAWLER	8	8	24	24
• CENTRAL MAST ASSEMBLER MANIPULATORS	10		30	
• ANTENNA FABRICATION	8	8	20	20
	1	4	1	4
	1	4	1	4
	2		2	
		12		24
TOTAL CREW PER SHIFT		108		293
TOTAL CREW BASED ON 4 SHIFTS 6 DAYS ON, 2 DAYS OFF _____		432		1172
60% ADD PERSONNEL FOR MGMT CONTROL CENTER, WAREHOUSE, MEDICS FOOD SERVICE, ETC _____		260		703
TOTAL CONSTRUCTION BASE PERSONNEL AT PEAK ACTIVITY _____		692		1875

Fig. 5-28 Construction Base Equipment and Crew Requirements



- HLLV DELIVERS MATERIALS TO CONSTRUCTION BASE IN LEO
- SATELLITE CONSTRUCTED TOTALLY AT ALT $\approx 500\text{KM}$, $i = 28.5^\circ$
- ASSEMBLED SSPS TRANSFERRED TO GEO USING ADVANCED ION OTV

Fig. 5-29 LEO Construction/Assembly Scenario

construction materials, and launched from Cape Kennedy, rendezvous with the construction base. The HLLV is returned to the launch site, where it is recovered and readied for subsequent reuse. At completion of satellite construction, low-thrust electric type propulsion systems, also brought to orbit using the HLLV, are mated with the satellite and used to transfer it to geosynchronous orbit. Power requirements of the propulsion stage are supplied by partial deployment of SPS solar blankets, requiring 20% deployment. The remaining 80% of the solar blankets are stowed during transport and deployed at GEO.

The GEO construction/assembly scenario used for this study, is depicted in Fig. 5-30. A depot, placed in LEO ($i = 28.5^\circ$; $h = 500$ km) serves as a staging area for delivering materials and personnel from earth launch to GEO. An HLLV carries materials and OTV propellant from earth to the depot, where they are integrated with a cargo orbit transfer vehicle (COTV). At the proper orbit phasing points, the COTV initiates a Hohman transfer/plane change maneuver, to rendezvous and dock with the construction base in GEO. Materials are transferred to the construction base, and at the proper phasing, the COTV is returned to the low orbit depot where it is refueled and readied for subsequent cargo transfer flights to GEO.

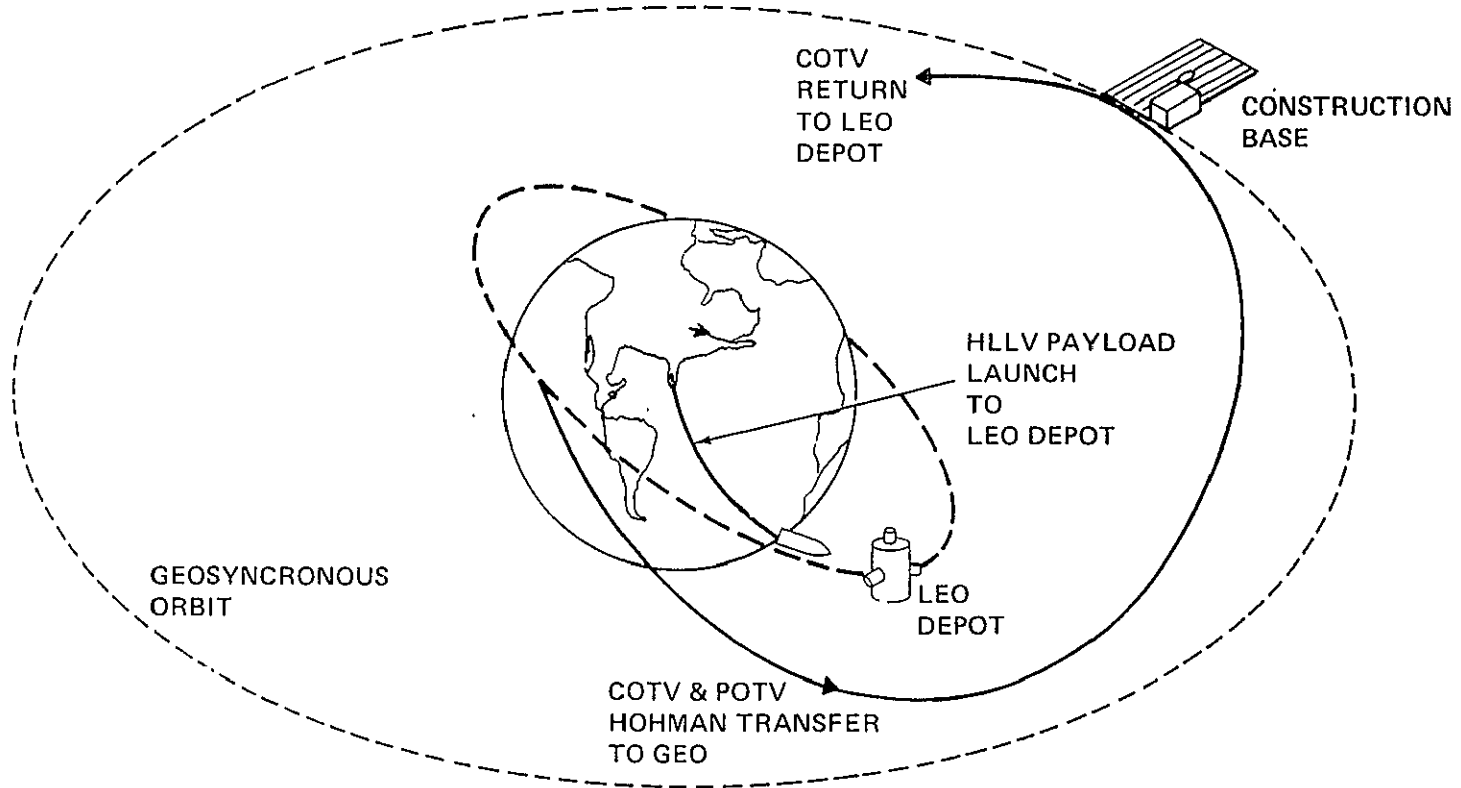
Personnel are transferred to GEO and returned, using a similar scenario. Shuttle-type vehicles are used to launch a crew of personnel to the low earth orbit depot, where Personnel Orbit Transfer Vehicles (POTV) carry the crew to the geosynchronous construction base. The POTV's return the crew to the LEO depot, and are readied for subsequent reuse.

5.1.3 Impact on Satellite Design Requirements

Using the generalized LEO and GEO construction concepts, construction and assembly scenarios were developed, and analyses performed to evaluate the impact of construction location on the baseline 5 GW crystal silicon satellite's design requirements. Design areas considered were satellite structural loads imposed during construction, overall satellite structural stiffness requirements, and attitude control requirements while attached to the construction base.

5.1.3.1 Structural Loading Requirements

Previous studies (Ref. 3) have shown that loads imposed on the baseline satellite design, while operational in GEO, were not significant drivers in establishing structural design requirements. Loads imposed at GEO, due to both gravity gradient effects and structural excitation, were several orders of magnitude less than baseline design limits. These studies have also shown that loads resulting during low orbit operations, while not attached to the construction base, and due to gravity gradient and aerodynamic loading, were within acceptable levels.



- HLLV DELIVERS MATERIALS TO LEO DEPOT
- COTV DELIVERS MATERIALS FROM LEO DEPOT TO GEO CONSTRUCTION BASE
- SATELLITE CONSTRUCTED TOTALLY AT GEO

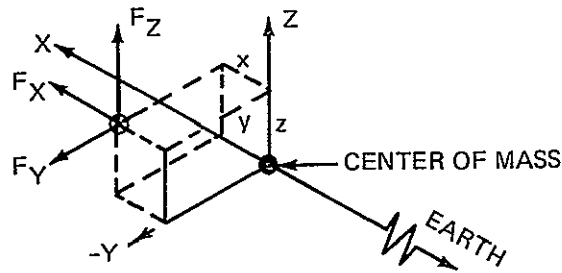
Fig. 5-30 GEO Construction/Assembly Scenario

A factor determined to be significant in establishing structural design requirements were the loads resulting from applied forces used to transfer the completed satellite from low earth orbit to GEO. Consequently, thrusting acceleration limits, commensurate with LEO-to-GEO transfer times of not less than 170 days, were established as viable satellite transfer scenarios for the baseline SPS design.

In addressing the structural loads on the satellite during construction, and while joined to the construction base, it was identified that these loads can be more severe than those resulting during operational phases of the SPS mission. These increased loadings were attributed to three factors, as illustrated in Fig. 5-31. They are the increased gravity gradient loads resulting from the larger mass concentrations of the construction base, the decrease in the structural strength of the satellite while only partially constructed, and the large center-of-mass off-set resulting from combined satellite/construction base geometry. The overall earth/satellite orientations used in the analyses are also shown. The preferred selected orientation places the longitudinal axis along the local vertical, and the thin edge into the windstream. These orientations were selected to minimize the gravity gradient effects and aerodynamic loading.

The most dominant force is the tension load produced during the construction sequence, while the construction base is joined at one corner of the satellite. A bending moment (M_7) is produced by this force because of the lateral offset of the construction base, relative to the overall center of mass. Rotating the joined satellite and construction base to an alternate orientation (i.e. with the principal axis aligned with the local vertical as shown in Fig. 5-31), does not alleviate these loads, but increases the projected area with respect to the windstream.

Figures 5-32 and 5-33 summarize the tension loads and bending moments acting on the baseline satellite structure, during construction at LEO and GEO for both the large and small construction base concepts. As readily noted, the loads incurred during LEO construction, in terms of both tension forces and bending moments, are about two orders of magnitude greater than at GEO. Moreover, it is shown that, at LEO, tension loads are greater for the large factory construction concept, because of the large factory mass (i.e. 13.5×10^6 Kg vs. 12×10^6 Kg or 29.8×10^6 LBS vs. 26.5×10^6 lbs). On the other hand, bending moments are less for the large construction base, because of reduced center-of-mass offsets. The overall impact of combined tension and bending moments, for the large and small construction base concepts, are illustrated in the upper portion of Fig. 5-33, relative to the satellite's allowable combined loads. Allowable loads were estimated for the completed satellite array, using beam theory, but should be verified using a redundant structural analysis. For both large and small construction bases, however, the combined loads on an SPS exceed the



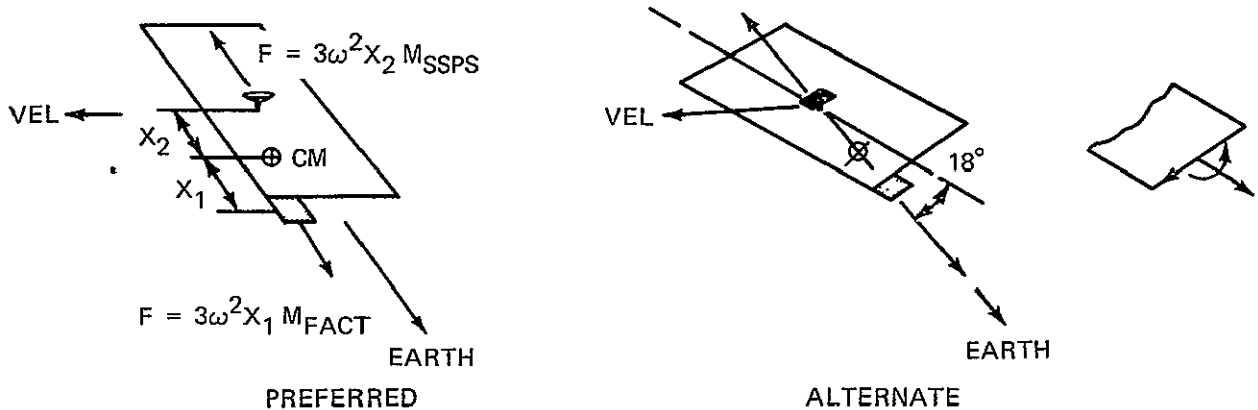
(ASSUMING TRANSLATIONAL AND ROTATIONAL VELOCITIES RELATIVE TO THE CM ARE SMALL)

$$F_X \cong \left[\overbrace{-\omega^2 (R-2x)}^{\text{GRAV}} + \overbrace{\omega^2 (R+x)}^{\text{INERTIAL}} \right] dm = 3\omega^2 x dm$$

$$F_Y \cong \left[\overbrace{-\omega^2 y}^{\text{GRAV}} + \overbrace{\omega^2 y}^{\text{INERTIAL}} \right] dm = 0$$

$$F_Z \cong \left[\overbrace{-\omega^2 z}^{\text{GRAV}} \right] dm$$

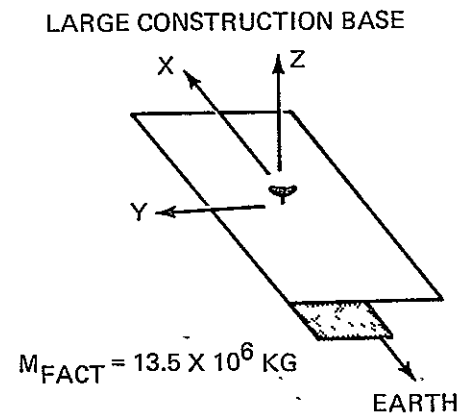
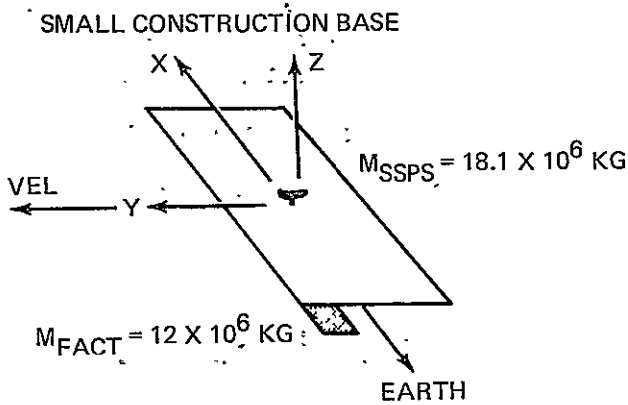
- PREFERRED ORIENTATION IS WITH LONG ARRAY AXIS ALONG LOCAL VERTICAL FOR CONTROL WITH NARROW EDGE INTO WIND TO REDUCE AERODYNAMIC DRAG. ALTERNATE WOULD ALIGN PRINCIPAL AXIS WITH LOCAL VERTICAL



- LOADS ARE CAUSED PRIMARILY BY OFFSET FACTORY MASS
- APPLIED LOADS ARE BALANCED BY ROTATIONAL ACCELERATIONS (INERTIA RELIEF)
- ROTATING ARRAY TO LINE UP MAJOR MASSES WITH LOCAL VERTICAL DOES NOT SIGNIFICANTLY REDUCE LOADS ALONG STRUCTURAL AXES ($V_X = 45,000 \text{ LB (200,000 N)}$, $M_Z = 3.3 \times 10^8 \text{ FT-LB (4.48} \times 10^8 \text{ N-M)}$ SMALL FACT.)

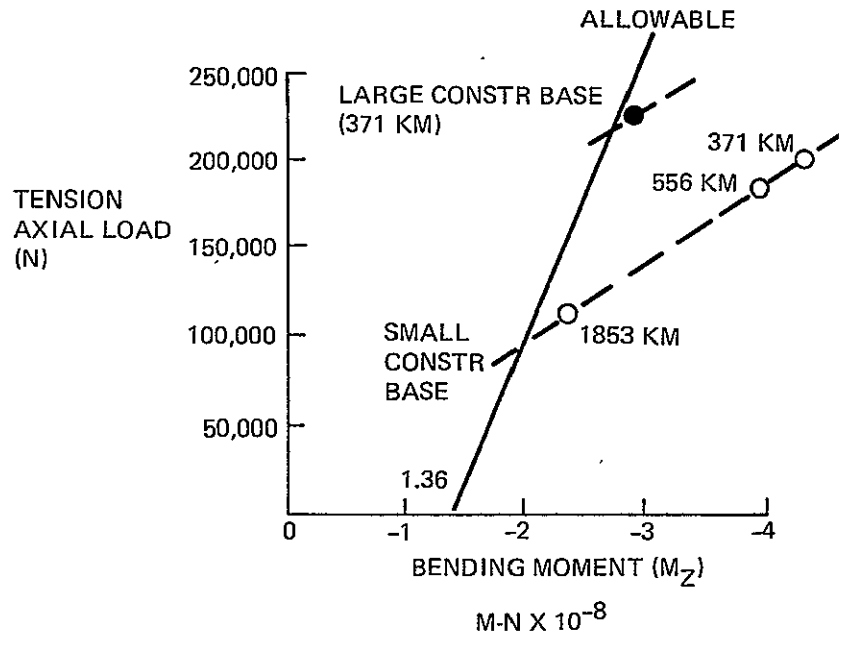
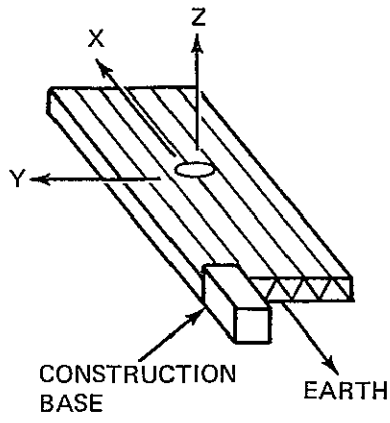
Fig. 5-31 SSPS Gravity and Centrifugal Forces

	WITHOUT AERO DRAG		WITH AERO DRAG	
	LOAD	STATION (M)	LOAD	STATION (M)
V_X (LBF)	50,070	-3096	50,080	-3096
(N)	222,711		222,756	
V_Y (LBF)	-10,840	-3589	-10,810	-3589
(N)	-48,216		-48,083	
V_Z (LBF)	562	-6550	522	-6550
(N)	2500		2322	
M_X (FT-LBF)	1.611×10^6	-315	1.522×10^6	-315
(M-N)	2.186×10^6		2.065×10^6	
M_Y (FT-LBF)	-7.474×10^6	-6550	-6.428×10^6	-6550
(M-N)	-10.142×10^6		-8.723×10^6	
M_Z (FT-LBF)	-3.334×10^8	-6550	-3.335×10^8	-6550
(M-N)	-4.524×10^8		-4.526×10^8	



	WITHOUT AERO DRAG		WITH AERO DRAG	
	LOAD	STATION (M)	LOAD	STATION (M)
V_X (LBF)	54,250	-3096	54,260	-3096
(N)	241,304		241,348	
V_Y (LBF)	-7429	-3589	-7403	-3589
(N)	-33,040		-32,929	
V_Z (LBF)	346	-6550	321	-6550
(N)	1539		1,428	
M_X (FT-LBF)	1.177×10^6	-315	1.084×10^6	-315
(M-N)	1.597×10^6		1.471×10^6	
M_Y (FT-LBF)	5.677×10^6	-315	5.854×10^6	-315
(M-N)	7.704×10^6		7.944×10^6	
M_Z (FT-LBF)	-2.268×10^8	-6550	-2.269×10^8	-6550
(M-N)	-3.078×10^8		-3.079×10^8	

Fig. 5-32 Comparison of Loads Between Small and Large Construction Bases at 200 N MI (322 Km)



MAXIMUM LOADS AT GEOSYNCHRONOUS ORBIT

SMALL FACTORY – FULL ARRAY

	LOAD	STATION (M)
V_X (LBF)	205	-3096
(N)	912	
V_Y (LBF)	44	-3589
(N)	196	
V_Z (LBF)	2	-6550
(N)	8.9	
M_X (FT-LBF)	6587	-315
(M-N)	8939	
M_Y (FT-LBF)	-30,542	-6550
(M-N)	-41,445	
M_Z (FT-LBF)	-1,362,500	-6550
(M-N)	-1,848,913	

LARGE FACTORY – FULL ARRAY

	LOAD	STATION (M)
V_X (LBF)	222	-3096
(N)	987	
V_Y (LBF)	-30	-3589
(N)	133	
V_Z (LBF)	1.4	-6550
(N)	6.2	
M_X (FT-LBF)	4810	-315
(M-N)	6527	
M_Y (FT-LBF)	23,192	-315
(M-N)	31,472	
M_Z (FT-LBF)	-926,666	6550
(M-N)	-1,257,486	

Fig. 5-33 Loads on SSPS During Construction: Variation With Altitude

allowable structural loading during LEO construction (ALT = 371 KM). The small construction base results in more excessive loading than the large base. A change in structural loading occurs at higher construction altitudes. To be within allowable structural limits, the small construction base concept should be used at altitudes greater than 2000 KM. The large construction base can be applied, without structural penalty, at an altitude of approximately 400 KM or higher.

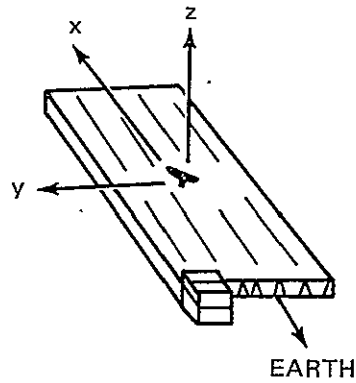
Another factor which affects construction loads acting on the satellite, is the mass of the construction base. Figure 5-34 shows that a reduction in structural loading could result (at an altitude of 322 KM 200 n mi), by reducing the mass of the construction base. The small construction base was assumed at an average mass of 12×10^6 Kg, 9.75×10^6 Kg of which represented satellite materials in storage. By reducing the overall mass in storage to approximately 1.25×10^6 Kg (4×10^6 Kg total construction base mass), the structural loading was reduced to acceptable levels at the LEO construction altitude. The impact of materials storage mass requirements on transportation traffic models and fleet size requirements should be further evaluated.

Maximum internal member loads were investigated during the early construction passes of the construction base, to determine the compatibility of structural loading on a partially completed satellite structure. Fig. 5-35 shows the loads resulting at completion of the first pass through the construction base, for both large and small construction base concepts. Recall that the first pass through the construction base produces one trough of the satellite for the small construction base, and 5 troughs for the large construction base.

Also shown in Fig. 5-35 are the internal member loads as the partially completed satellite is shifted outward, prior to being returned for the next pass thru the construction base. As indicated, the loads at that point in the construction sequence (i.e. after the shift), exceed the allowable axial member loads. This occurs because of center-of-mass off-sets resulting between the construction base and the completed portion of the structure.

Other satellite/construction base attitude orientations relative to the earth were examined to determine the impact of structural loading on alternate construction orientations. The results of this analysis is summarized in Fig. 5-36. Alternate orientations considered were:

- The longitudinal axis of the satellite parallel to the velocity vector, with the plane of the array perpendicular to the local vertical
- The longitudinal axis of the array parallel to the velocity vector, with the plane of the array parallel to the local vertical.



CONSTRUCTION BASE MASS WITHOUT MATERIAL STORAGE = 2.75×10^6 KG

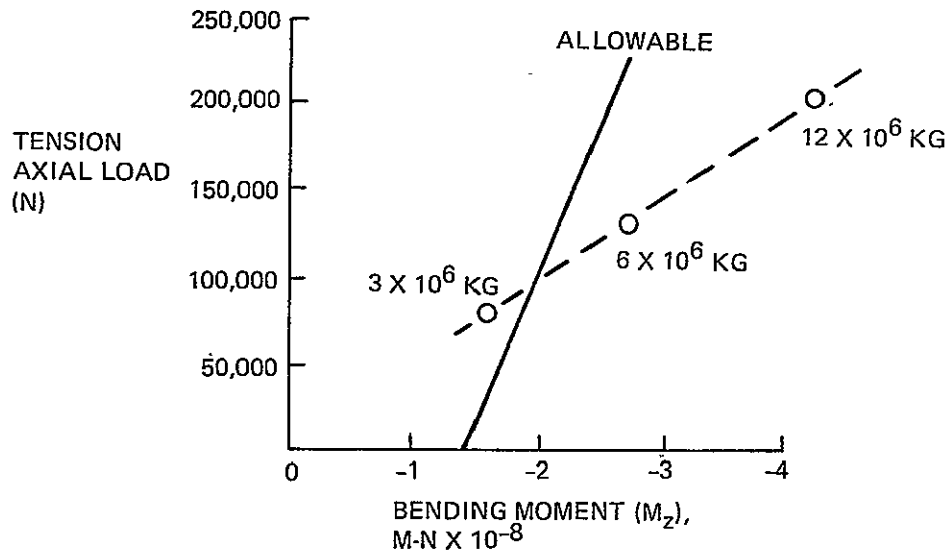
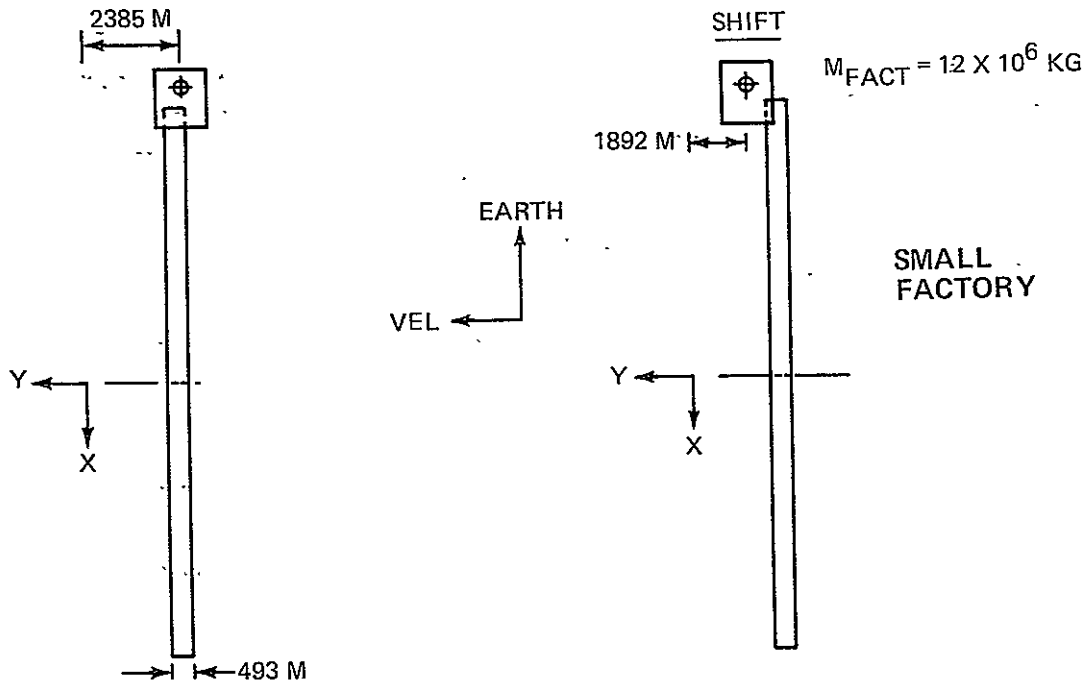


Fig. 5-34 Effect of Construction Base Mass on Loads at 200 N MI (322 Km)

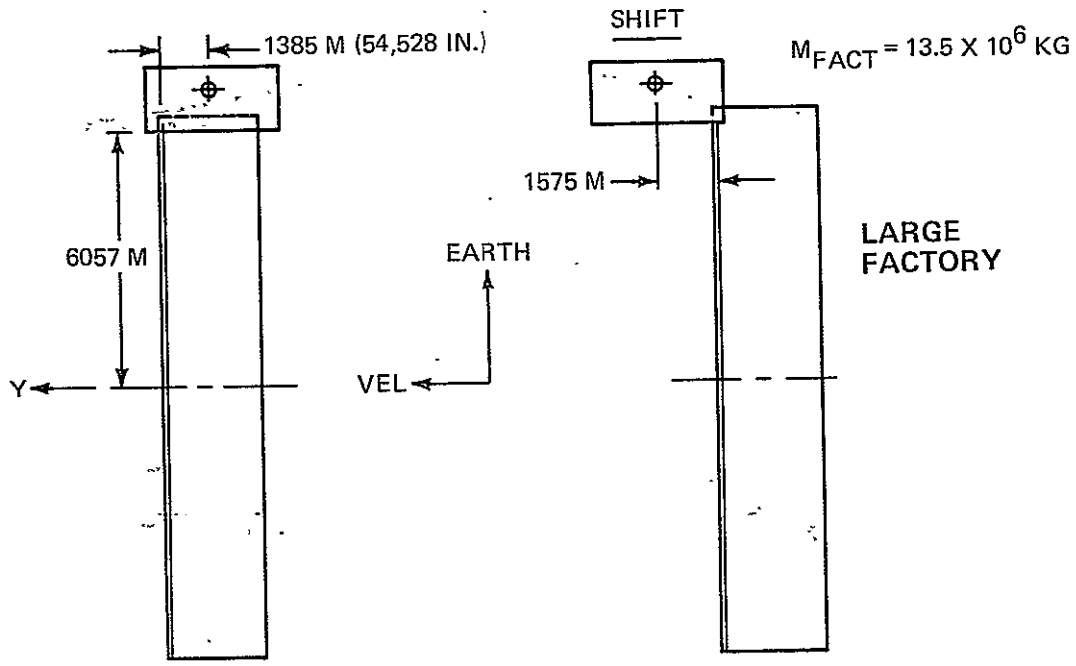


MAXIMUM MEMBER LOAD

- COMPR = -930 LBF (-4137 N)
- TENSION = 4027 LBF (17,912 N)

MAXIMUM MEMBER LOAD

- COMPR* = -1763 LBF (-7842 N)
- TENSION = 3446 LBF (15,328 N)



MAXIMUM MEMBER LOADS

- COMPR = -652 LBF (-2900 N)
- TENSION = 3808 LBF (16,938 N)

MAXIMUM MEMBER LOADS

- COMPR* = -5752 LBF (-25,585 N)
- TENSION = +3698 LBF (16,413 N)

ALLOWABLE COMPR LOAD = 1221 LBF (5431 N)

Fig. 5-35 Maximum Member Loads After First Construction Pass

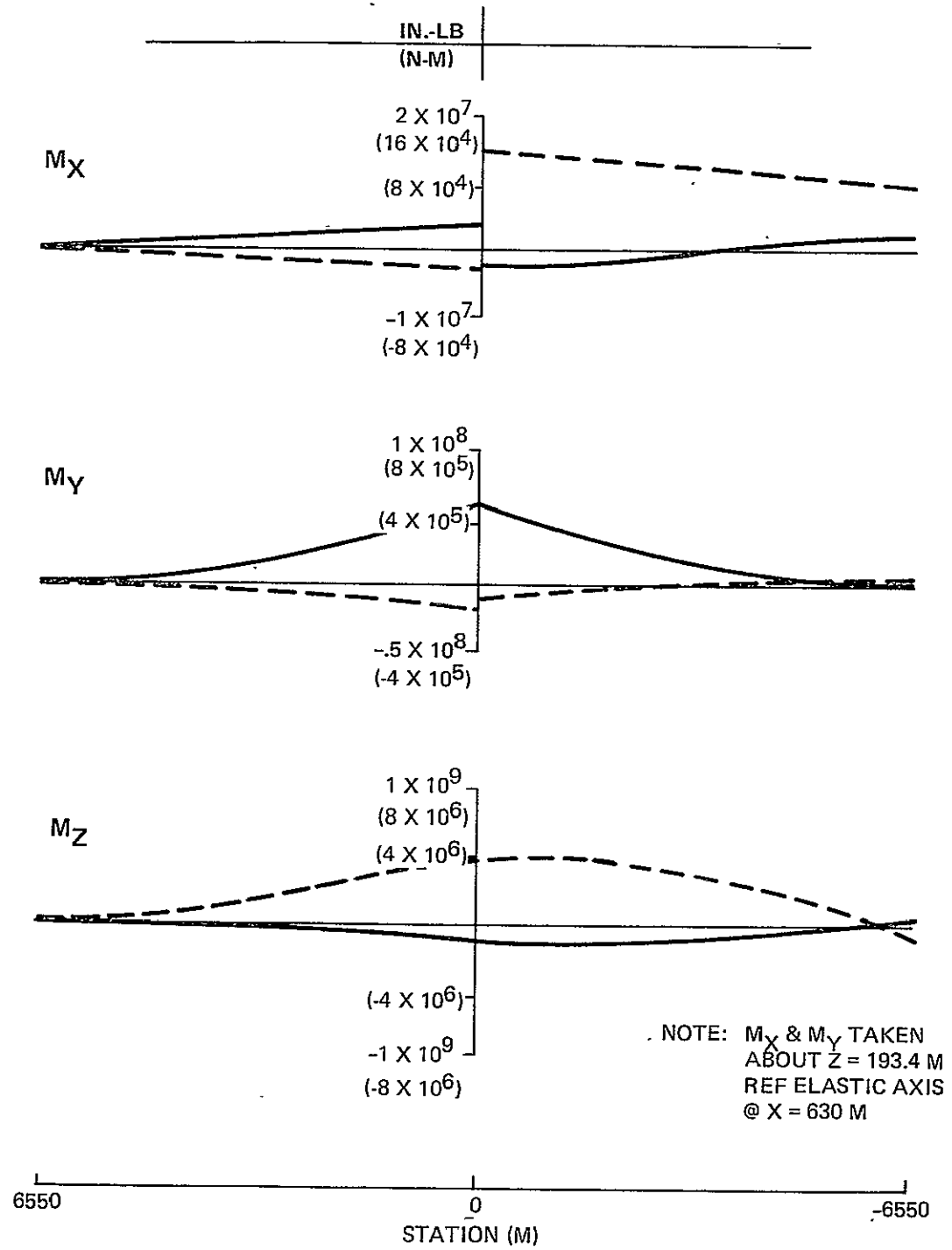
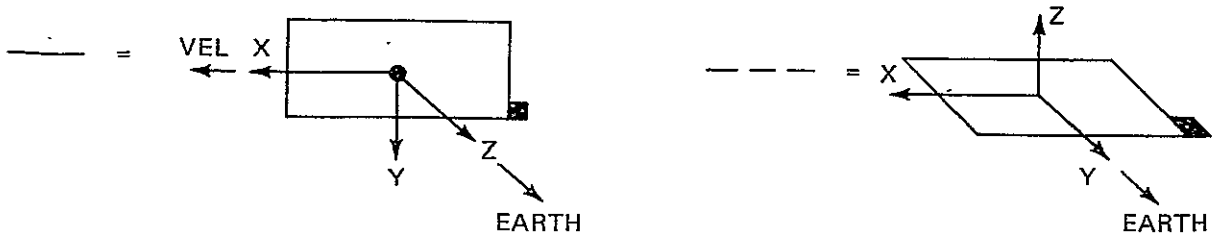


Fig. 5-36 SSPS Bending Moments, Small Factory 200 N MI (322 KM)

These results show that, for both orientations, the bending moments at LEO are reduced to acceptable satellite structural limits. Further reductions can be realized by reducing the construction base mass, and minimizing the center-of-mass offsets between the satellite and construction base. Although these orientations are preferred from a structural loading standpoint, estimates show that additional control system propellant quantities would be required to maintain either of these orientations during the complete construction sequence.

Conclusions

The results of these studies have shown that:

- Depending upon the construction scenario used, structural loading during the construction sequence at LEO can be an influential factor in establishing satellite structural design requirements
- Construction at GEO is not expected to be a major factor in influencing satellite structural design requirements
- Construction of subassembly modules in LEO is feasible, and if appropriately configured, should not impose satellite structural loading beyond that required for operational on-orbit compatibility
- Loads on the satellite structure, during construction, can be reduced by minimizing the mass of the construction base; and decreasing the center-of-mass off-sets between the satellite and construction base
- Further analyses are required to evaluate the dynamic response loads on the satellite as it is released from the construction base.

5.1.3.2 Structural Vibration Modes

During the Phase II studies, a computerized structural model of the baseline satellite configuration was developed. The structure was represented as finite element bar members, and the mass concentrated into node points. Using NASTRAN, modes and frequencies for this model were computed, and used to analyze the structural loading resulting from stationkeeping and attitude control system thruster excitation. The results showed that on-orbit loads resulting from thruster excitation at GEO were small, and that the overall stiffness was acceptable for GEO operations. (Results are presented in Ref. 3).

To evaluate satellite structural stiffness requirements during construction operations, analyses were performed to determine the structural modes and frequencies for the structure, while joined to the construction base. Modes and frequencies were determined for two specific configurations considered to be representative of the range of configurations that may evolve. These were:

- The completed 5 GW baseline configuration, while attached to the large construction base
- The completed first trough of the 5 GW baseline configuration, while joined to the small construction base.

When not joined to the construction base, satellite vibration modes are either symmetric or antisymmetric about the midplane of the structure, and can be identified as bending or torsional modes. When joined to the construction base, symmetry is destroyed and bending and torsional motions are combined.

The results of these analyses are summarized in Fig. 5-37. For the complete SPS, the fundamental frequency drops from 5.26 cycles/hour, to 3.70 cycles/hour, with the base attached. This mode, shown in Figure 5-38, exhibits vertical bending combined with torsion. The fundamental mode for the strip attached to the base occurs at 4.71 cycles/hour, and is shown in Figure 5-39.

An approximation to the permissible range of structural frequencies can be established, by considering that a gravity-gradient-stabilized structure oscillates as a rigid body at approximately $\sqrt{3}$ times the orbital rate. Since it is desirable to design overall satellite structural stiffness with a frequency of about 10 times the rigid body oscillatory frequency, Fig. 5-40 shows that the baseline 5 GW structure while attached to the construction base, satisfies these conditions at a construction altitude greater than about 4000 n mi. Similarly, for the partially constructed satellite, the baseline structural frequency satisfies the conditions at about 2,500 n mi in altitude. This suggests that additional satellite structural stiffness would be required for the construction of large elements in LEO, which imposes an associated mass penalty to the satellite structure.

An alternative is to apply the control thruster firings at the construction base, rather than to the satellite, during the construction sequence, to avoid potential structural excitation. This approach, however, incurs higher attitude control propellant mass penalties, due to the reduced moment arms that result about the combined satellite/construction base center of mass.

The major conclusions resulting from this analysis are:

- Satellite structural stiffness requirements are increased for construction in LEO

ORIGINAL PAGE IS
OF POOR QUALITY

COMPLETE SSPS WITH LARGE CONSTR BASE			COMPLETE SSPS		
MODE	FREQ (CPH)	DESCRIPTION	SYM	ANTI	DESCRIPTION
			FREQ (CPH)	FREQ (CPH)	
1	3.70	1ST BENDING WITH TORSION	5.26	15.65	1ST BENDING
2	8.06	1ST TORSION WITH BENDING	14.14	9.36	1ST TORSION
3	10.37	2ND BENDING WITH TORSION	28.27	35.05	2ND BENDING
4	13.84	2ND TORSION WITH BENDING	28.78	19.93	2ND TORSION
5	15.65	1ST IN-PLANE BENDING	18.91	29.30	1ST IN-PLANE BENDING
6	16.59	1ST CHORD BENDING	32.21	30.83	1ST CHORD BENDING
7	18.64	3RD TORSION	45.24	35.85	3RD TORSION

1 BAY STRIP WITH SMALL CONSTR BASE			1 BAY STRIP	
1	4.71	1ST BENDING	8.08	1ST BENDING
2	6.36	1ST TORSION	11.91	1ST TORSION
3	9.72	1ST LATERAL BENDING WITH TORSION	15.93	1ST LATERAL BENDING WITH TORSION

- STRUCTURAL FREQUENCIES ARE LOWERED WHEN ATTACHED TO CONSTRUCTION BASE
- ROLL MODES (1ST TORSION) ARE LESS EXCITED WHEN APPLYING FORCING FUNCTIONS AT CONSTRUCTION BASE (FACTOR OF 2)

Fig. 5-37 Comparison of Vibration Modes With and Without Construction Base

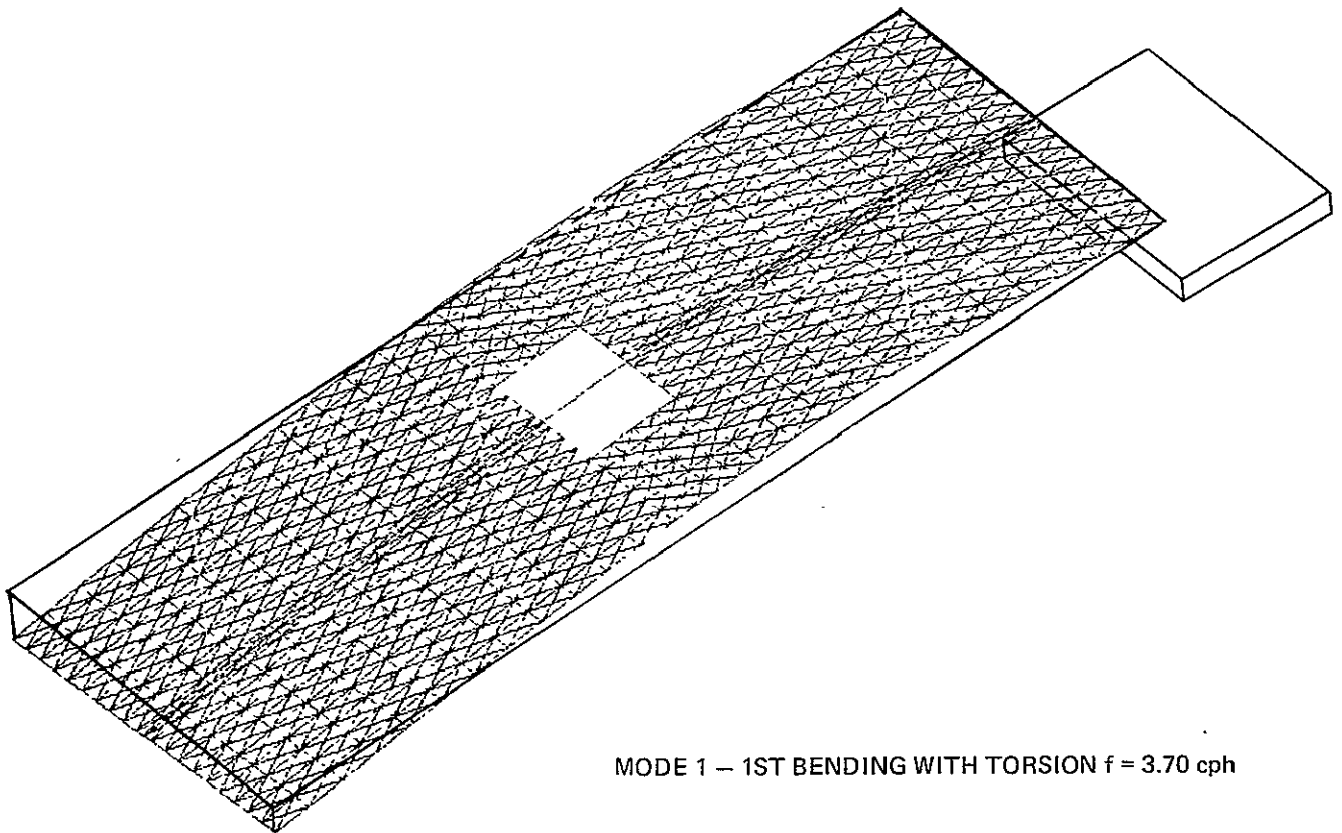


Fig. 5-38 Full SSPS NASTRAN Structural Model With Large Construction Base

ORIGINAL PAGE IS
OF POOR QUALITY

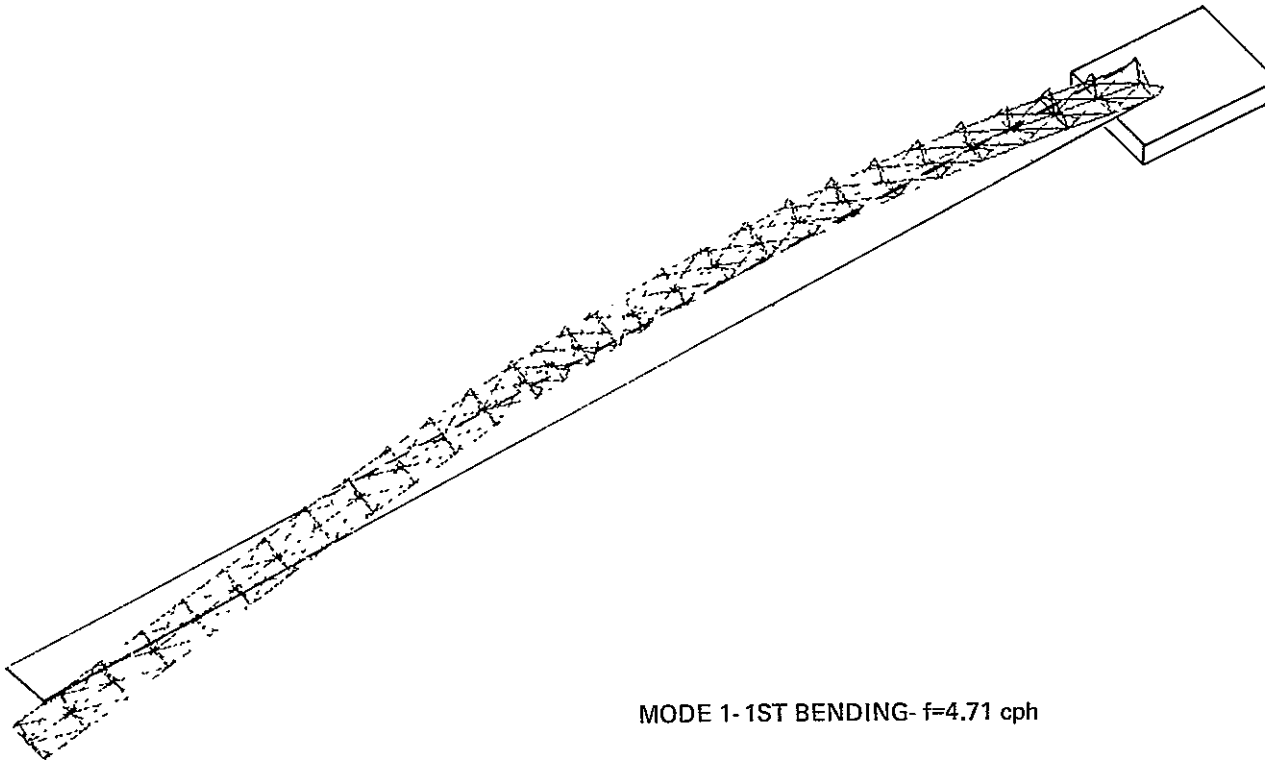


Fig. 5-39 One-Bay NASTRAN Structural Model With Small Construction Base

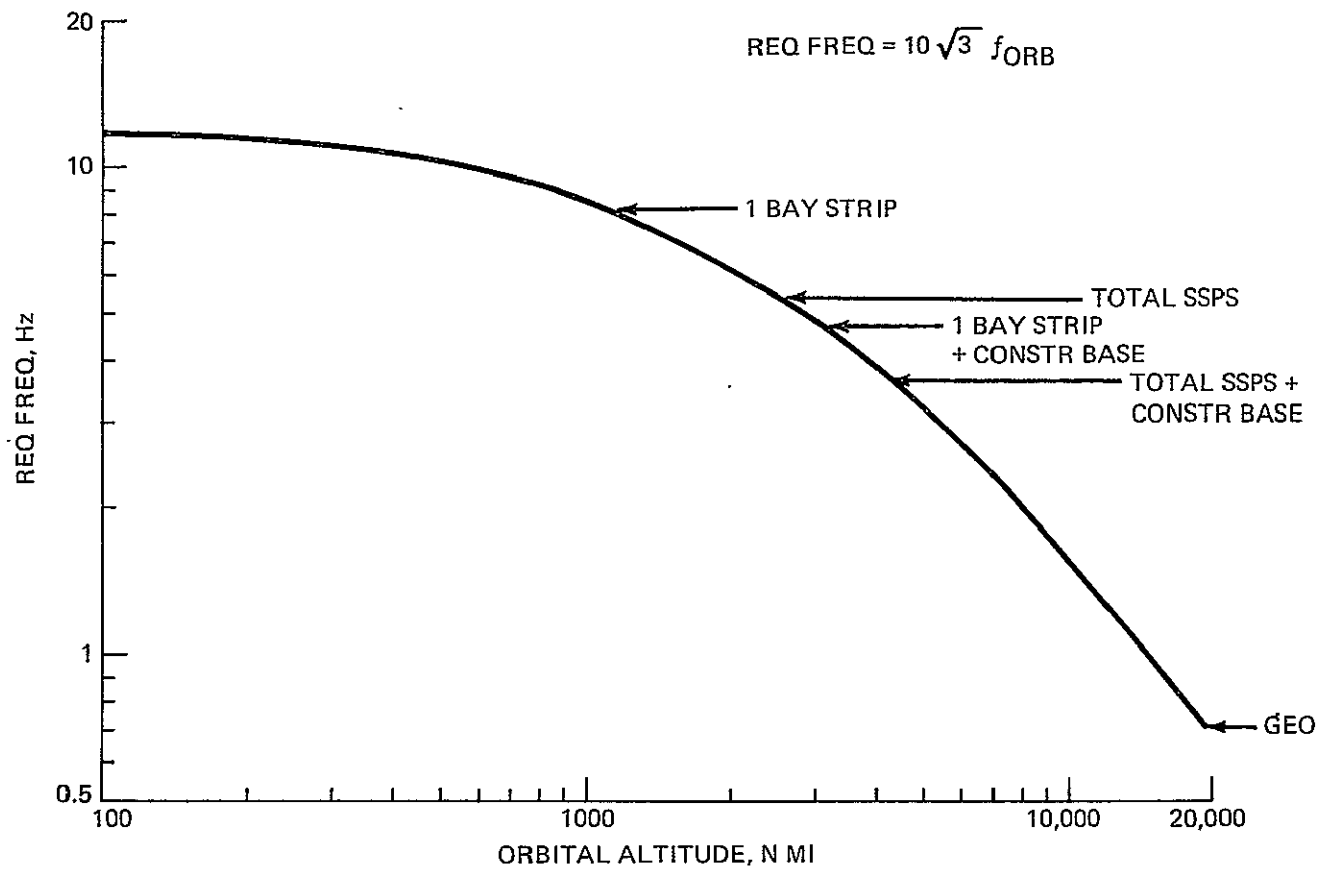


Fig. 5-40 Required Fundamental Structural Frequency vs Orbital Altitude

- LEO construction should be limited to smaller subassembly modules, so as not to place a higher propellant requirement on an assembly than that required for the operational mission.

5.1.3.3 Attitude Control and Orbitkeeping

The attitude control and orbitkeeping requirements for LEO and GEO construction scenarios were analyzed to identify major design impacts to an SPS. The analysis considered changes in configuration geometry during construction, total assembly mass, and mass distribution during various points of construction. A candidate attitude orientation concept was examined for each altitude. The magnitudes of primary environmental effects were estimated, together with propellant requirements for attitude control and orbitkeeping, and the results compared.

A basic requirement during LEO or GEO construction is to maintain satisfactory control during on-orbit operations. Such calculations must include consideration of docking effects, the internal acceleration environment, and the use of a single-axis rotating solar array on the Factory. The maintenance of orbital altitude must also be considered, because of the large area and resulting aerodynamic drag forces at LEO.

The matrix of concepts and scenarios considered is shown in Figure 5-41, including the definition of control and body axes. The following analysis was performed with respect to the conventional control axes, unless otherwise noted. The construction sequence was evaluated at three points for both the large and small factories, as shown in Figure 5-42. The coordinate system center-of-mass locations, and dimensions used in the analysis are also shown in this figure. For both LEO and GEO fabrication, the same attitude orientation was assumed, with the SSPS long axis (X_B) along the local vertical, and the array normal (Z_B), perpendicular to the orbit plane. The propellant estimates which follow are based upon maintaining this orientation within $\pm 5^\circ$.

5.1.3.3.1 Attitude Control Requirements

The mass and moments of inertia for the small and large factory concepts at selected steps in construction, are shown in Figure 5-43. The disturbance torques for various stages of construction, and at selected altitudes, are presented in Figure 5-44. The gravity gradient and aerodynamic torques are given for both the nominal attitude orientation, and a 5-degree offset about the most sensitive control axis.

Aerodynamic torques are based on a C_D of two, characteristic of a flat plate and open gridwork structure. Magnetic torques are based on a typical magnetic density factor of 2 pole-cm per lb. The

CONCEPT	CONSTRUCTION STAGES	ORBITS	DISTURBANCE SOURCES
<ul style="list-style-type: none"> ● SMALL FACTORY ● LARGE FACTORY 	<ul style="list-style-type: none"> ● SINGLE - STRIP ● MIDPOINT (WITH ANTENNA) ● COMPLETE (WITH ANTENNA) 	<ul style="list-style-type: none"> ● LEO: <ul style="list-style-type: none"> - 200 N MI (322 KM) - 300 N MI (556 KM) 	<ul style="list-style-type: none"> ● GRAVITY GRADIENT ● AERODYNAMIC ● MAGNETIC
		<ul style="list-style-type: none"> ● GEO 	<ul style="list-style-type: none"> ● GRAVITY GRADIENT ● SOLAR PRESSURE

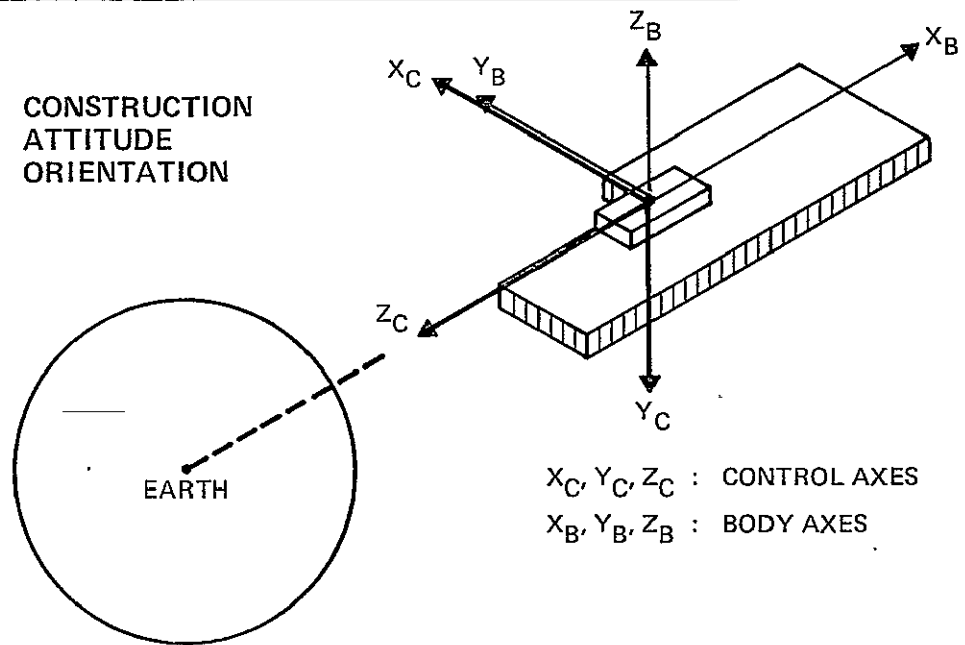
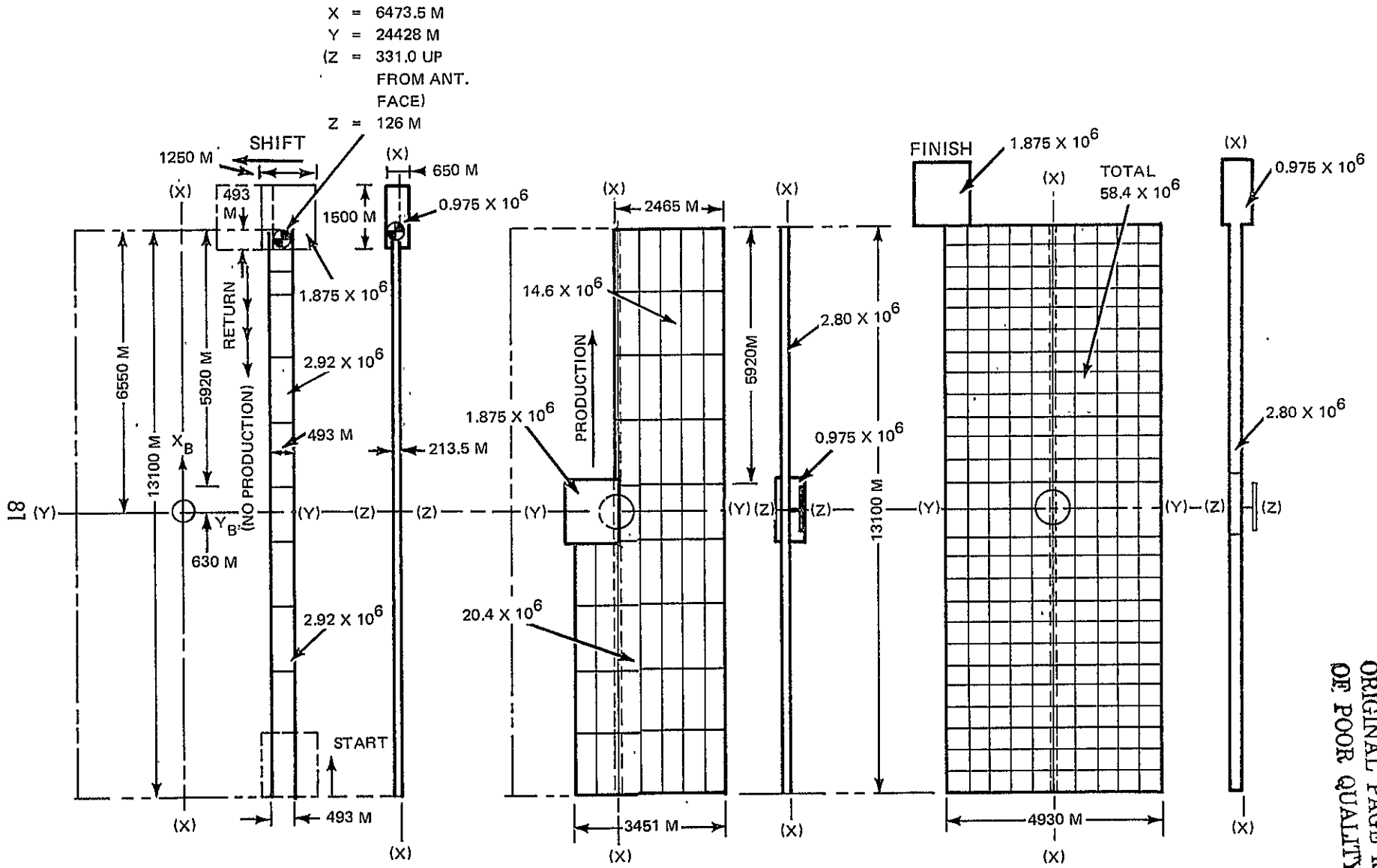


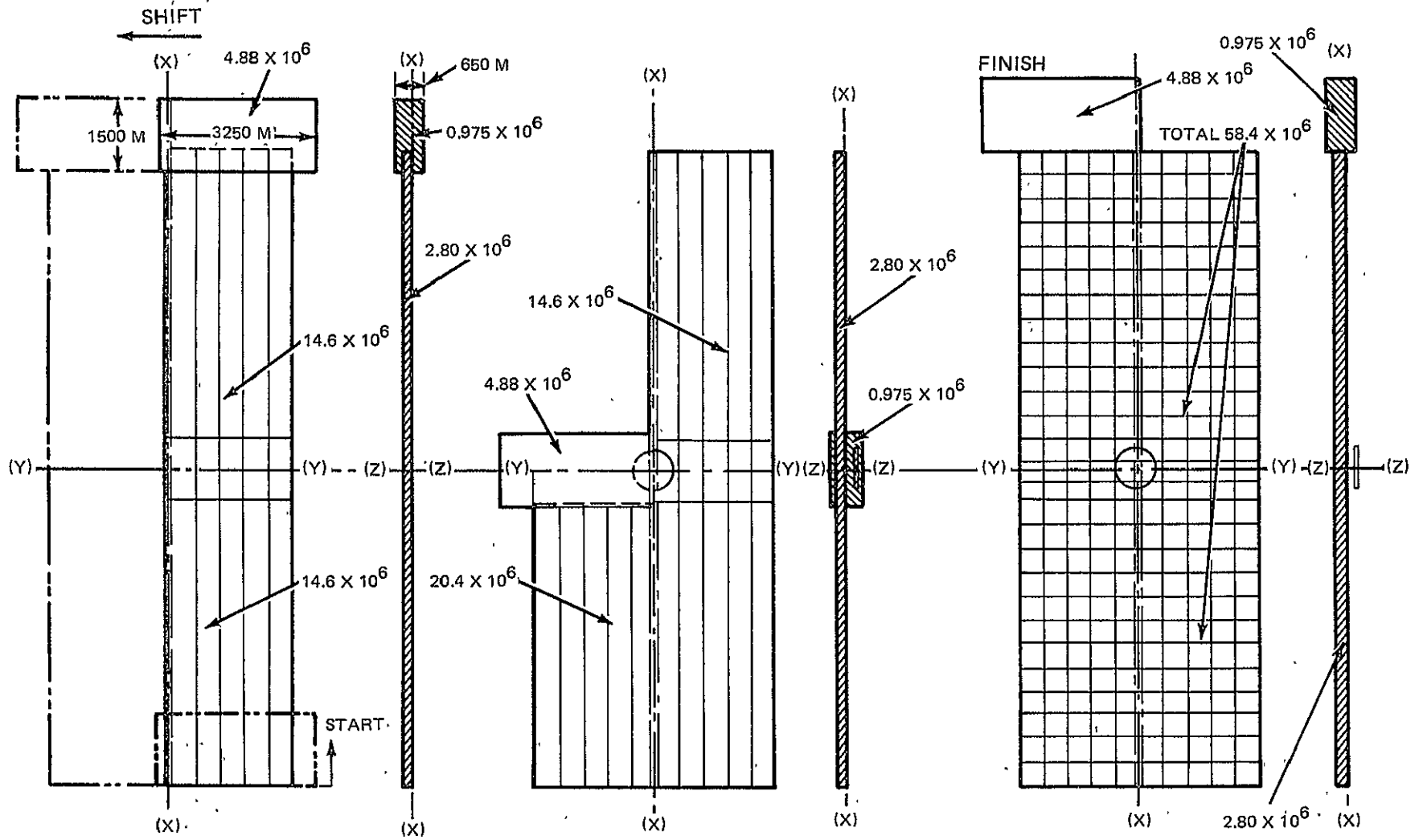
Fig. 5-41 Study Matrix



NOTE: ALL AREAS ARE IN M²

ORIGINAL PAGE IS
OF POOR QUALITY

Fig. 5-42a Configuration A: Small Factory



NOTE: ALL AREAS IN M²

Fig. 5-42b Configuration B: Large Factory

SMALL FACTORY

CONSTR STAGE	MASS 10^6 KG (10^6 LB)	INERTIA, 10^{10} KG-M ² (10^{10} SLUG-FT ²)					
		I_{XX}	I_{YY}	I_{ZZ}	I_{XY}	I_{XZ}	I_{YZ}
SINGLE-STRIP (1A)	13.17 (29.04)	7400 (5459)	7513 (5543)	217.5 (160.5)	5.7 (4.2)	187.9 (138.6)	161.1 (118.8)
MIDPOINT (2A)	22.66 (49.97)	12,420 (9163)	13,870 (10,230)	1670 (1232)	-122.7 (-90.5)	-514.1 (-379.3)	77.0 (56.9)
COMPLETE (3A)	30.06 (66.28)	59,660 (44,010)	66,640 (49,160)	7280 (5371)	-436.7 (-322.2)	-13,620 (-10,050)	1283 (947)

LARGE FACTORY

CONSTR STAGE	MASS, 10^6 KG (10^6 LB)	INERTIA, 10^{10} KG-M ² (10^{10} SLUG-FT ²)					
		I_{XX}	I_{YY}	I_{ZZ}	I_{XY}	I_{XZ}	I_{YZ}
SINGLE-STRIP 4A1	22.46 (49.52)	41,350 (30,510)	42,970 (31,700)	1838 (1356)	-9.2 (-6.8)	854 (630)	714 (530)
MIDPOINT 5A	28.58 (63.02)	14,770 (10,900)	19,230 (14,190)	4743 (3499)	-277 (-204)	115 (85)	91.5 (67.5)
COMPLETE 6A	31.56 (69.59)	62,600 (46,180)	67,700 (49,940)	5470 (4035)	-283 (-209)	-8830 (-6514)	1375 (1014)

Fig 5-43 Mass and Body Axis Inertias

		SOURCE	DISTURBANCE TORQUES, 10^6 M-N (10^6 FT-LB)					
			ESTIMATED MAGNITUDES			TOTAL ($0 = \psi = 0$)		
			T_X	T_Y	T_Z	T_X	T_Y	T_Z
LEO - 370 KM	SINGLE-STRIP	GRAVITY GRAD, 0° (GRAVITY GRAD, 0.5°)	(4.6) (-15.0)	(-5.4) (-21.5)	(0) (0.84)	(5.4)	(-10.2)	(0.8)
		AERODYNAMIC, 0° (AERODYNAMIC, $\psi=5^\circ$)	(0) (0)	(-4.8) (-5.2)	(0) (0)			
		MAGNETIC	(0.8)	(0)	(0.8)			
	MID-POINT	GRAVITY GRAD, 0° (GRAVITY GRAD, 5°)	(2.2) (-30.4)	(14.7) (-9.5)	(0) (-1.5)	(3.6)	(14.7)	(1.5)
		AERODYNAMIC, 0° (AERODYNAMIC, 5°)	(0) (0.49)	(0) (0)	(0.09) (0.63)			
		MAGNETIC	(1.4)	(0)	(1.4)			
	COM-PILETE	GRAVITY GRAD, 0° (GRAVITY GRAD, 5°)	(36.8) (-125.1)	(390.9) (265.2)	(0) (-35.1)	(38.6)	(389.8)	(1.8)
		AERODYNAMIC, 0° (AERODYNAMIC, 5°)	(0) (0)	(-1.11) (-4.99)	(0) (1.32)			
		MAGNETIC	(1.8)	(0)	(1.8)			
LEO - 555 KM	SINGLE-STRIP	GRAVITY GRAD, 0° (GRAVITY GRAD, 5°)	(4.3) (-13.8)	(-5.0) (-19.9)	(0) (0.8)	(5.0)	(-7.2)	(0.7)
		AERODYNAMIC, 0° (AERODYNAMIC, 5°)	(0) (0)	(-2.2) (-24)	(0) (0)			
		MAGNETIC	(0.7)	(0)	(0.7)			
	MID-POINT	GRAVITY GRAD, 0° (GRAVITY GRAD, 5°)	(2.0) (-28.0)	(13.6) (-8.8)	(0) (-1.4)	(3.3)	(13.6)	(1.4)
		AERODYNAMIC, 0° (AERODYNAMIC, 5°)	(0) (0.02)	(0) (0)	(0.09) (0.03)			
		MAGNETIC	(1.3)	(0)	(1.3)			
	COM-PILETE	GRAVITY GRAD, 0° (GRAVITY GRAD, 5°)	(33.9) (-115.3)	(360.4) (244.5)	(0) (-32.4)	(35.6)	(360.3)	(1.7)
		AERODYNAMIC, 0° (AERODYNAMIC, 5°)	(0) (0)	(-0.05) (-0.23)	(0) (0.06)			
		MAGNETIC	(1.7)	(0)	(1.7)			
GEO	SINGLE-STRIP	GRAVITY GRAD, 0° (GRAVITY GRAD, 5°)	(.0190) (-.062)	(-.022) (-.088)	(0) (.0035)	(.019)	(-.022)	(0)
		GRAVITY GRAD, 0° (GRAVITY GRAD, 5°)	(.0091) (-.125)	(.061) (-.039)	(0) (-.006)			
		GRAVITY GRAD, 0° (GRAVITY GRAD, 5°)	(.151) (-.51)	(1.6) (1.09)	(0) (-.144)			

Fig. 5-44a Disturbance Torques: Small Factory

		SOURCE	DISTURBANCE TORQUES, 10 ⁶ M-N (10 ⁶ FT-LB)					
			ESTIMATED MAGNITUDES			TOTAL ($\theta = \psi = 0$)		
			T _X	T _Y	T _Z	T _X	T _Y	T _Z
LEO-370KM	SINGLE-STRIP	GRAVITY GRAD, 0° (GRAVITY GRAD, $\theta = 5^\circ$)	(20.5) (-90.0)	(-24.5) (-113.3)	(0) (3.6)	29.54 (21.8)	29.94 (-22.1)	1.76 (1.3)
		AERODYNAMIC, 0° (AERODYNAMIC, $\psi = 5^\circ$)	(0) (0)	(2.43) (3.89)	(0) (0)			
		MAGNETIC	(1.3)	(0)	(1.3)			
	MIDPOINT	GRAVITY GRAD, 0° (GRAVITY GRAD, $\theta = 5^\circ$)	(2.6) (-35.6)	(-3.3) (-25.1)	(0) (-46)	5.83 (4.3)	4.47 (-3.3)	2.30 (1.7)
		AERODYNAMIC, 0° (AERODYNAMIC, $\psi = 5^\circ$)	(0) (0)	(0) (.2)	(.01) (1.1)			
		MAGNETIC	(1.7)	(0)	(1.7)			
	COMPLETE	GRAVITY GRAD, 0° (GRAVITY GRAD, $\theta = 5^\circ$)	(39.5) (-129.5)	(253.4) (119.5)	(0) (-21.7)	56.10 (41.4)	343.22 (253.3)	2.71 (2.0)
		AERODYNAMIC, 0° (AERODYNAMIC, $\psi = 5^\circ$)	(0) (0)	(-.09) (5.5)	(.07) (0.9)			
		MAGNETIC	(1.9)	(0)	(1.9)			
LEO-559KM	SINGLE-STRIP	GRAVITY GRAD, 0° (GRAVITY GRAD, $\theta = 5^\circ$)	(18.9) (-83.0)	(-22.6) (-104.5)	(0) (3.3)	27.24 (20.1)	30.49 (-22.5)	1.63 (1.2)
		AERODYNAMIC, 0° (AERODYNAMIC, $\psi = 5^\circ$)	(0) (0)	(0.11) (0.18)	(0) (0)			
		MAGNETIC	(1.2)	(0)	(1.2)			
	MIDPOINT	GRAVITY GRAD, 0° (GRAVITY GRAD, $\theta = 5^\circ$)	(2.4) (-32.8)	(-3.0) (-23.2)	(0) (-0.42)	5.42 (4.0)	-4.07 (-3.0)	2.17 (1.6)
		AERODYNAMIC, 0° (AERODYNAMIC, $\psi = 5^\circ$)	(0) (0)	(0) (.009)	(.0006) (.05)			
		MAGNETIC	(1.6)	(0)	(1.6)			
	COMPLETE	GRAVITY GRAD, 0° (GRAVITY GRAD, $\theta = 5^\circ$)	(36.4) (-119.4)	(233.7) (110.2)	(0) (-20.0)	51.63 (38.1)	316.66 (233.7)	2.30 (1.7)
		AERODYNAMIC, 0° (AERODYNAMIC, $\psi = 5^\circ$)	(0) (0)	(.004) (.25)	(.003) (.04)			
		MAGNETIC	(1.7)	(0)	(1.7)			
GEO	SINGLE-STRIP	GRAVITY GRAD, 0° (GRAVITY GRAD, $\theta = 5^\circ$)	(.084) (-.37)	(-.10) (-.46)	(0) (.015)	.114 (0.84)	-.136 (-.10)	0 (0)
	MID-POINT	GRAVITY GRAD, 0° (GRAVITY GRAD, $\theta = 5^\circ$)	(.011) (-.15)	(-.014) (-.10)	(0) (-.002)	.015 (.011)	.019 (-.014)	0 (0)
	COMPLETE	GRAVITY GRAD, 0° (GRAVITY GRAD, $\theta = 5^\circ$)	(.162) (-.53)	(1.04) (.49)	(0) (-.089)	.220 (.162)	1.41 (1.04)	0 (0)

Fig. 5-44b Disturbance Torques: Large Factory

magnetic torque is assumed to be acting in the XY plane, with zero contribution on the Z-axis, because of the low inclination orbit.

The solar pressure disturbance torque was found negligible at LEO altitudes in comparison to other torques. At GEO altitude, this torque is still relatively small and essentially cyclical. Therefore, it is ignored in subsequent propellant computations, because it is assumed that momentum storage devices can satisfactorily meet this requirement.

The total torque values (Figure 5-44), which are the arithmetic sum of the individual sources for each axis (assuming the nominal attitudes), are used in determining propellant requirements. The angular momentum per day per axis for the above torques are presented in Figures 5-45 and 5-46 for LEO and GEO construction locations, respectively. For comparison purposes, construction periods of 3 months and 2 months have been selected for the small and large factory scenarios, respectively, divided into the times per phase shown. (Time is included for checkout after construction, before transfer to final orbit begins.) The corresponding angular momentum per phase, and the estimated available moment arms per phase, permit the calculation of the impulse requirements for each stage of construction.

The estimated propellant requirements for an Isp of 300 sec, corresponding to hydrazine, and 6000 sec for argon ion thrusters, are also shown in Figures 5-45 and 5-46. Note that the ion thrusters require a significant amount of power in LEO as complete assembly of the SPS is attained.

5.1.3.3.2 Orbitkeeping Requirements

Orbitkeeping during construction is only of concern at LEO because of the severe drag environment. The mass, projected aerodynamic areas, and ballistic coefficients for each stage of construction, and for two yaw angles, are presented in Figure 5-47. A drag coefficient of two has been selected as representative of a complex, repetitive open-gridwork structure. The low values of ballistic coefficient for all stages of construction indicate the need for orbit keeping.

The aerodynamic drag forces, as a function of yaw attitude, are shown in Figure 5-48. Assuming a constant counter-thrust to negate the effect of drag, the resulting propellant requirements using hydrazine and ion thrusters are presented in Figure 5-49, and when compared to attitude control requirements, can be considered as negligible.

CONFIG	ALT KM, (N MI)	MOMENTUM PER DAY, 10 ¹² M-N-S (10 ¹² FT-LB-SEC)			DAYS PER PHASE	MOMENT ARMS PER PHASE 10 ³ M (10 ³ FT)			PROPELLANT PER PHASE 10 ⁶ KG (10 ⁶ LB)							
		X	Y	Z		L _X	L _Y	L _Z	I _{SP} = 300 SEC			I _{SP} = 6000 SEC				
									W _X	W _Y	W _Z	W _X	W _Y	W _Z		
SMALL FACTORY	370 (200)	1	.64 (.47)	1.19 (.88)	.09 (.07)	12	13.0 (42.7)	13.0 (42.7)	0.7 (2.3)	.20 (.44)	0.62 (1.37)	0.92 (2.03)	0.017 (.037)	0.031 (.069)	0.05 (.10)	
		2	.42 (.31)	1.72 (1.27)	.18 (.13)	39	6.6 (21.5)	6.6 (21.5)	2.5 (8.2)	0.85 (1.88)	3.48 (7.67)	0.94 (2.07)	0.043 (.094)	0.17 (.38)	0.05 (.10)	
		3	.39 (.29)	4.57 (33.68)	.22 (.16)	39	9.5 (31.2)	9.5 (31.2)	3.5 (11.5)	0.55 (1.21)	63.5 (140.)	0.82 (1.81)	0.027 (.061)	3.18 (7.02)	0.041 (.090)	
	90 TOTAL								TOTAL 71.9 (158.5)			3.61 (7.95)				
	555 (300)	1	.58 (.43)	.84 (.62)	.08 (.06)	12	13.0 (42.7)	13.0 (42.7)	0.7 (2.3)	.30 (.67)	.44 (.97)	0.79 (1.74)	.015 (.033)	.022 (.049)	.039 (.087)	
		2	.39 (.29)	1.6 (1.18)	.16 (.12)	39	6.6 (21.5)	6.6 (21.5)	2.5 (8.2)	0.79 (1.75)	1.71 (3.76)	.87 (1.91)	.040 (.088)	.086 (.19)	.043 (.095)	
		3	4.18 (3.08)	42.2 (31.13)	.20 (.15)	39	9.5 (31.2)	9.5 (31.2)	3.5 (11.5)	5.81 (12.8)	59.0 (130.)	.77 (1.70)	.29 (.64)	2.9 (6.5)	.039 (.085)	
	90 TOTAL								TOTAL 70.4 (155.3)			3.52 (7.77)				
	LARGE FACTORY	370 (200)	4	2.55 (1.88)	2.59 (1.91)	.15 (.11)	20	10.8 (35.4)	10.8 (35.4)	1.1 (3.6)	1.60 (3.53)	1.63 (3.60)	.93 (2.05)	.082 (.18)	.082 (.18)	.045 (.10)
			5	.50 (.37)	.39 (.29)	.20 (.15)	20	6.2 (20.3)	6.2 (20.3)	3.1 (10.1)	.55 (1.21)	.43 (.95)	.45 (.99)	.03 (.06)	.021 (.047)	.022 (.049)
6			4.85 (3.58)	29.7 (21.89)	.23 (.17)	20	9.7 (31.8)	9.7 (31.8)	3.1 (10.2)	3.41 (7.53)	20.8 (45.8)	.50 (1.11)	.17 (.38)	1.04 (2.29)	.025 (.056)	
60 TOTAL								TOTAL 30.3 (66.8)			1.52 (3.34)					
555 (300)		4	2.36 (1.74)	2.63 (1.94)	.14 (.10)	20	10.8 (35.4)	10.8 (35.4)	1.1 (3.6)	1.48 (3.27)	1.66 (3.65)	0.84 (1.86)	.073 (.16)	.082 (.18)	.041 (.09)	
		5	.47 (.35)	.35 (.26)	.19 (.14)	20	6.2 (20.3)	6.2 (20.3)	3.2 (10.1)	.52 (1.15)	.39 (.85)	.42 (.92)	.026 (.057)	.020 (.043)	.021 (.046)	
		6	4.5 (3.29)	27.4 (20.19)	.20 (.15)	20	9.7 (31.8)	9.7 (31.8)	3.1 (10.2)	3.12 (6.87)	19.1 (42.2)	.44 (.98)	.15 (.34)	.95 (2.1)	.022 (.049)	
60 TOTAL								TOTAL 28.0 (61.8)			1.39 (3.07)					

Fig. 5-45a Propellant Requirements: LEO Attitude Control During Construction

	CONFIG	ALT	TORQUE, 10 ⁶ M-N (10 ⁶ FT-LBS)			MOMENT ARMS, KM (10 ³ FT)			THRUST, 10 ³ N (10 ³ LBF)			ION THRUSTER PWR* (10 ³ KW)
			X	Y	Z	L _X	L _Y	L _Z	F _X	F _Y	F _Z	
SMALL FACTORY	1	200	7.3 (5.4)	-13.8 (-10.2)	1.1 (0.8)	13.0 (43)	13.0 (43)	.6 (2)	.58 (.13)	1.1 (.24)	1.8 (.40)	20.6
	2	200	4.9 (3.6)	19.9 (14.7)	2.0 (1.5)	6.4 (21)	6.4 (21)	2 (8)	.76 (.17)	3.1 (.70)	.85 (.19)	28.3
	3	200	52.3 (38.6)	528.6 (389.8)	2.4 (1.8)	9.4 (31)	9.4 (31)	3.4 (11)	5.6 (1.25)	56.0 (12.6)	.76 (.16)	374.1
	1	300	6.8 (5.0)	-9.8 (-7.2)	.9 (.7)	13.0 (43)	13.0 (43)	.6 (2)	.53 (.12)	.76 (.17)	1.6 (.35)	17.1
	2	300	4.5 (3.3)	18.4 (13.6)	1.9 (1.4)	6.4 (21)	6.4 (21)	2 (8)	.71 (.16)	2.9 (.65)	.80 (.18)	26.4
	3	300	48.3 (35.6)	488.6 (360.3)	2.3 (1.7)	9.4 (31)	9.4 (31)	3.4 (11)	5.1 (1.15)	51.6 (11.6)	.67 (.15)	344.4
LARGE FACTORY	4	200	29.6 (21.8)	-30.0 (-22.1)	1.8 (1.3)	11.0 (35)	11.0 (35)	1 (4)	2.6 (.62)	2.8 (.63)	1.5 (.33)	42.2
	5	200	5.8 (4.3)	-4.5 (-3.3)	2.3 (1.7)	6.1 (20)	6.1 (20)	3.0 (10)	.98 (.22)	.76 (.17)	.76 (.17)	15.0
	6	200	56.1 (41.4)	343.5 (253.3)	2.7 (2.0)	9.8 (32)	9.8 (32)	3.0 (10)	5.7 (1.29)	35.2 (7.92)	.89 (.20)	251.2
	4	300	27.3 (20.1)	-30.5 (-22.5)	1.6 (1.2)	11.0 (35)	11.0 (35)	1 (4)	2.5 (.57)	2.8 (.64)	1.3 (.30)	40.3
	5	300	5.4 (4.0)	-4.1 (-3.0)	2.2 (1.6)	6.1 (20)	6.1 (20)	3.0 (10)	.89 (.20)	.67 (.15)	.71 (.16)	13.6
	6	300	51.7 (38.1)	316.9 (233.7)	2.3 (1.7)	9.8 (32)	9.8 (32)	3.0 (10)	5.3 (1.19)	32.5 (7.30)	.76 (.17)	231.2

* 26.7 $\frac{\text{KW}}{\text{LBF}}$

Fig. 5-45b Propellant Requirements - LEO Ion Thruster Power

ORIGINAL PAGE IS
OF POOR QUALITY

CONFIG	ALT, KM (N MI)	MOMENTUM PER DAY 10^{12} M-N-S (10^{12} FT-LB-SEC)			DAYS PER PHASE	MOMENT ARMS PER PHASE 10^3 M (10^3 FT)			PROPELLANT PER PHASE 10^6 KG (10^6 LB)					
		X	Y	Z		L_X	L_Y	L_Z	$I_{SP} = 300$ SEC			$I_{SP} = 6000$ SEC		
									W_X	W_Y	W_Z	W_X	W_Y	W_Z
SMALL FACTORY	↑ GEO ↓	.0022 (.0016)	.0026 (.0019)	(0)	12	13.0 (42.7)	13.0 (42.7)	0.7 (2.3)	.0007 (.0015)	.0008 (.0017)	0 (0)	.00003 (.00007)	.00004 (.00009)	0 (0)
		.0011 (.00079)	.0072 (.0053)	(0)	39	6.6 (21.5)	6.6 (21.5)	2.5 (8.2)	.0022 (.0048)	.004 (.0095)	0 (0)	.00009 (.0002)	.0007 (.0016)	0 (0)
		.018 (.013)	.19 (.138)	(0)	39	9.5 (31.2)	9.5 (31.2)	3.5 (11.5)	.025 (.056)	.26 (.58)	0 (0)	.0012 (.0027)	.0014 (.003)	0 (0)
		90 TOTAL				TOTAL			.29 (.65)			.0035 (.0077)		
LARGE FACTORY	↑ GEO ↓	.0099 (.0073)	.012 (.0086)	(0)	20	10.8 (35.4)	10.8 (35.4)	1.1 (3.6)	.006 (.014)	.007 (.016)	0 (0)	.00032 (.0007)	.00036 (.0008)	0 (0)
		.0013 (.00095)	.0016 (.0012)	(0)	20	6.2 (20.3)	6.2 (20.3)	3.1 (10.1)	.0014 (.003)	.0018 (.004)	0 (0)	.00007 (.00015)	.00009 (.0002)	0 (0)
		.019 (.014)	.12 (.090)	(0)	20	9.7 (31.8)	9.7 (31.8)	3.1 (10.1)	.013 (.029)	.086 (.189)	0 (0)	.00068 (.0015)	.0043 (.0095)	0 (0)
		60 TOTAL				TOTAL			.12 (.26)			.005 (.011)		

Fig. 5-46a Propellant Requirements, GEO Attitude Control During Construction

CONFIG	TORQUES 10 ⁶ N-M(10 ⁶ FT LBS)			MOMENT ARMS KM(10 ³ FT)			THRUST 10 ³ N(10 ³ LBF)			ION* THRUSTER POWER, 10 ³ KW	
	X	Y	Z	L _X	L _Y	L _Z	F _X	F _Y	F _Z		
SMALL FACTORY	1	.026(.019)	-.030(-.022)	0	13(43)	13(43)	.6(2)	.0020(.00044)	.0023(.00051)	0	.025
	2	.012(.0091)	.083(.061)	0	6.4(21)	6.4(21)	2(8)	.0019(.00043)	.013(.0029)	0	.089
	3	.205(.151)	2.2(1.6)	0	9.4(31)	9.4(31)	3.4(11)	.022(.0049)	.23(.052)	0	1.52
LARGE FACTORY	4	.114(.084)	-0.14(-.10)	0	11(35)	11(35)	1(4)	.011(.0024)	.013(.0029)	0	.142
	5	.015(.011)	-.019(-.014)	0	61(20)	61(20)	3.0(10)	.0024(.00055)	.22(.050)	0	1.35
	6	.220(.162)	1.41(1.04)	0	9.8(32)	9.8(32)	3.0(10)	.023(.0051)	.14(.0325)	0	1.00

*26.7 $\frac{KW}{LB FT}$

Fig. 5-46b Propellant Requirements: GEO Ion Thruster Power

CONFIG		MASS LB (KG)	AREA 10^6 FT^2 (10^6 M^2)		$\frac{W_r \text{ LB/FT}^2}{C_D A}$ (KG/M^2)	
			$\psi = 0^\circ$	$\psi = 5^\circ$	$\psi = 0^\circ$	$\psi = 5^\circ$
SMALL FACTORY	1	29.04×10^6 (13.17×10^6)	40.5 (3.76)	47.5 (4.41)	0.359 (1.753)	0.306 (1.494)
	2	49.97×10^6 (22.67×10^6)	40.5	75.1 (6.98)	0.617 (3.013)	0.333 (1.626)
	3	66.28×10^6 (30.06×10^6)	40.5	97.0 (9.01)	0.818 (3.994)	0.342 (1.670)
LARGE FACTORY	4	49.52×10^6 (22.46×10^6)	40.5	58.8 (5.46)	0.611 (2.984)	0.421 (2.056)
	5	63.02×10^6 (28.59×10^6)	40.5	46.0 (4.27)	0.778 (3.799)	0.685 (3.345)
	6	69.59×10^6 (31.57×10^6)	40.5	99.8 (9.27)	0.859 (4.194)	0.349 (1.704)

Fig. 5-47 LEO Ballistic Coefficients ($C_D = 2.0$)



	CONFIG- URATION	MASS, KG X 10 ⁶ (LB X 10 ⁶)	AREA, FT ² X 10 ⁶		DRAG FORCE			
					ALT = 370 KM (200 N MI)		ALT = 555 KM (300 N MI)	
			$\psi = 0$	$\psi = 5^\circ$	$\psi = 0$	$\psi = 5^\circ$	$\psi = 0$	$\psi = 5$
SMALL CONSTR. BASE 	1	13.17 (29.04)	40.5	47.5	1379 N (310 LB)	1610 N (362 LB)	62 N (14 LB)	71 N (16 LB)
	2	22.66 (49.97)	40.5	75.1	1379 N (310 LB)	2550 N (573 LB)	62 N (14 LB)	116 N (26 LB)
	3	30.05 (66.28)	40.5	97.0	1379 N (310 LB)	3290 N (740 LB)	62 N (14 LB)	151 N (34 LB)
LARGE CONSTR. BASE 	4	22.45 (49.5)	40.5	58.8	1379 N (310 LB)	1990 N (448 LB)	62 N (14 LB)	90 N (20 LB)
	5	28.58 (63.02)	40.5	46.0	1379 N (310 LB)	2640 N (594 LB)	62 N (14 LB)	120 N (27 LB)
	6	31.55 (69.59)	40.5	99.8	1379 N (310 LB)	3385 N (761 LB)	62 N (14 LB)	155 N (35 LB)

Fig. 5-48 LEO Aerodynamic Drag Force ($C_D = 2$)

C-2

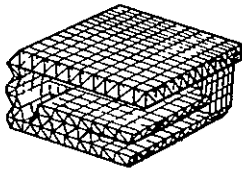
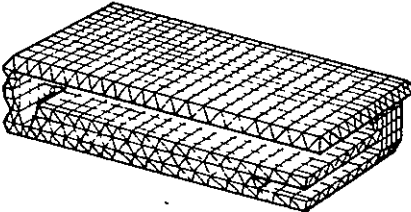
CONFIGURATION	ALT	PROPELLANT REQMTS		POWER REQMTS, KW
		HYDRAZINE (ISP = 300)	ADVANCED ION (ISP = 6000 SEC)	
	370 KM (200 N MI)	3.69 X 10 ⁶ KG (8.15 X 10 ⁶ LBS)	.18 X 10 ⁶ KG (.4 X 10 ⁶ LB)	8277
 BOTH LARGE AND SMALL CONSTRUCTION BASE	555 K (300 N MI)	.16 X 10 ⁶ KG (.36 X 10 ⁶ LBS)	.009 X 10 ⁶ KG (.020 X 10 ⁶ LB)	373 8

Fig. 5-49 Leo Orbitkeeping Propellant Requirements

5.1.3.3.3 LEO vs GEO Comparison

The propellant mass and associated power requirements for LEO and GEO construction are shown in Figure 5-50 for ion thrusters. The attitude control propellant, as a percentage of final configuration (SSPS and factory), is shown as an overall comparison factor. Hydrazine thrusters resulted in an unacceptable mass penalty, twenty times greater than the ion system. LEO construction requires over two orders of magnitude more propellant than GEO, with a significantly increased power requirement as the complete construction is approached. Propellant required to counter drag is not excessive for the higher LEO orbit, but substantial power levels are needed.

Future study areas should include:

- o Partial SSPS construction in LEO, with transfer to GEO for final assembly
- o Optimum control during construction using combined aerodynamics and gravity gradient stabilization with minimum propellant consumption as the objective
- o Momentum storage devices application for rate control during construction
- o Electrical power system weight impacts resulting from ion thrusters in LEO, considering occultation periods.

5.1.4 Impact on Construction Base Requirements

Another factor considered significant in the evaluation of LEO and GEO construction, is the impact of construction location on construction base requirements. Studies were conducted to evaluate several conditions - the effects of the severe radiation environment at GEO, the impact of the differences in the thermal cycling and occultation periods at LEO and GEO, and the collision probability associated with increased orbit debris at lower altitudes. The following sections discuss their impact on construction base requirements.

5.1.4.1 Radiation Environment

The construction base concepts developed for this study require large complements of construction personnel, located in work stations and habitability modules, distributed throughout the construction base. These facilities must provide a shirt sleeve environment, with adequate protection against radiation hazards, during both LEO or GEO construction.

Studies conducted in Ref. (4) indicate that the primary components of the geosynchronous radiation environment are comprised of trapped radiation, galactic cosmic rays, and solar radiation. Fig. 5-51

CONFIG		LEO CONSTRUCTION (300 N MI)				GEO CONSTRUCTION	
		ORBITKEEPING PROPELLANT, 10 ⁶ KG (10 ⁶ LB)	ION THRUSTER POWER, 10 ³ KW	ATTITUDE CONTROL PROPELLANT, 10 ⁶ KG (10 ⁶ LB)	ION THRUSTER POWER, 10 ³ KW	ATTITUDE CONTROL PROPELLANT, 10 ⁶ KG (10 ⁶ LB)	ION THRUSTER POWER, 10 ³ KW
SMALL FACTORY	1	0.0014 (.003)	0.37	0.077 (0.17)	17.1	.0007 (.00016)	.025
	2	0.0039 (.0087)	0.37	0.17 (0.37)	26.4	.00082 (.0018)	.089
	3	0.0039 (.0087)	0.37	3.28 (7.23)	344.4	.0026 (.0057)	1.52
	TOTALS	0.009 (.02)		3.52 (7.77)		.0035 (.0077)	
				~ 12%		~ .01%	
LARGE FACTORY	4	0.003 (.0067)	0.37	0.20 (0.43)	40.3	.00068 (.0015)	.14
	5	0.003 (.0067)	0.37	0.068 (0.15)	13.6	.00016 (.00035)	1.35
	6	0.003 (.0067)	0.37	1.13 (2.49)	231.2	.0050 (.011)	1.00
	TOTALS	0.009 (.02)		1.39 (3.07)		.0059 (.0129)	
				~ 4.5%		~ .02%	

Fig. 5-50 Attitude Control Orbitkeeping Requirements: Summary Comparison

ALT, KM	LEO			GEO
	322	378	50 (SKYLAB)	35,788
ORB INCL, DEG	30	90	50 (SKYLAB)	0
TRAPPED E –	3.5×10^{-3}	0.01	} 0.3	–
BREMSSTRAHLUNG	10-4	2.5×10^{-3}		2.12
TRAPPED PROTONS	0.25	0.17		–
SOLAR FLARE P	0	0.15	0.01	0.60
GALACTIC COSMIC RAYS	4×10^{-4}	0.001	0.001	0.05
TOTAL (REM/DAY)	0.25	0.34	0.31	2.77

NASA PLANNING DOSE FOR 56-DAY SKYLAB MISSION:

- 250 REM TO SKIN
- 25 REM TO BLOOD-FORMING ORGANS

Fig. 5-51 Radiation Environment in Space (Dose Rates (REM/DAY)
Behind 300 Mills of Aluminum (4#/ft²)

shows that daily doses resulting at GEO, behind 4 lb/ft² of aluminum shielding, are about one order of magnitude greater than at LEO. The higher dose rates are due primarily to the higher intensity electron and associated bremsstrahlung environment, and the absence of geomagnetic shielding against solar flare particles and cosmic rays. Consequently, additional shielding material is required at GEO to provide adequate protection.

Figure 5-52 shows the average rem dose resulting at GEO, as a function of shielding thickness. Since, for shield thicknesses greater than typically 250 mils, the dose is primarily from bremsstrahlung, a dramatic dose reduction can be achieved by filtering the bremsstrahlung through a small thickness of tantalum or other high atomic number material. This minimizes the additional mass penalty associated with adequate shielding for the GEO environment.

Construction base mass penalties, for GEO construction, were estimated for both the small and large construction base to be less than 100,000 Kg and 280,000 Kg, respectively. These penalties are not considered significant, relative to the overall mass.

5.1.4.2 Occultation/Thermal Cycling Environment

Effects of the periods of earth occultation between the LEO and GEO construction environment were evaluated to determine their impact on construction base requirements. Two factors were considered. They were (a) the mass penalty associated with providing continuous electrical power during LEO construction, to compensate for the higher frequency of earth occultation of the construction base, and (b), a quantitative assessment of the difference in thermal cycling effects.

During construction in both LEO or GEO, electrical power required for operating the construction base is provided by solar arrays, similar to the SPS solar arrays, extended from the construction base. These arrays are sized to provide power directly to construction base operations, and to charge batteries used to deliver power during periods of eclipse. For GEO construction, eclipse periods have a relatively minor impact, occurring for a period of 72 minutes within a 24-hour period, in the worst case during a few periods in a year. During half of the orbital periods during the solar year, the construction base is in continual sunlight. This differs significantly from the periods of earth occultation experienced in LEO construction, wherein the construction base experiences periods of earth shadow for approximately 30 minutes in each 90 minute orbital period, for most of the solar year. This environment requires storage of power using batteries located in the construction base. Consequently, the solar array power system must be sized to provide power not only for the 60 minutes of construction operations, but additional power required to charge batteries for use during the remaining 30 minutes of the orbit.

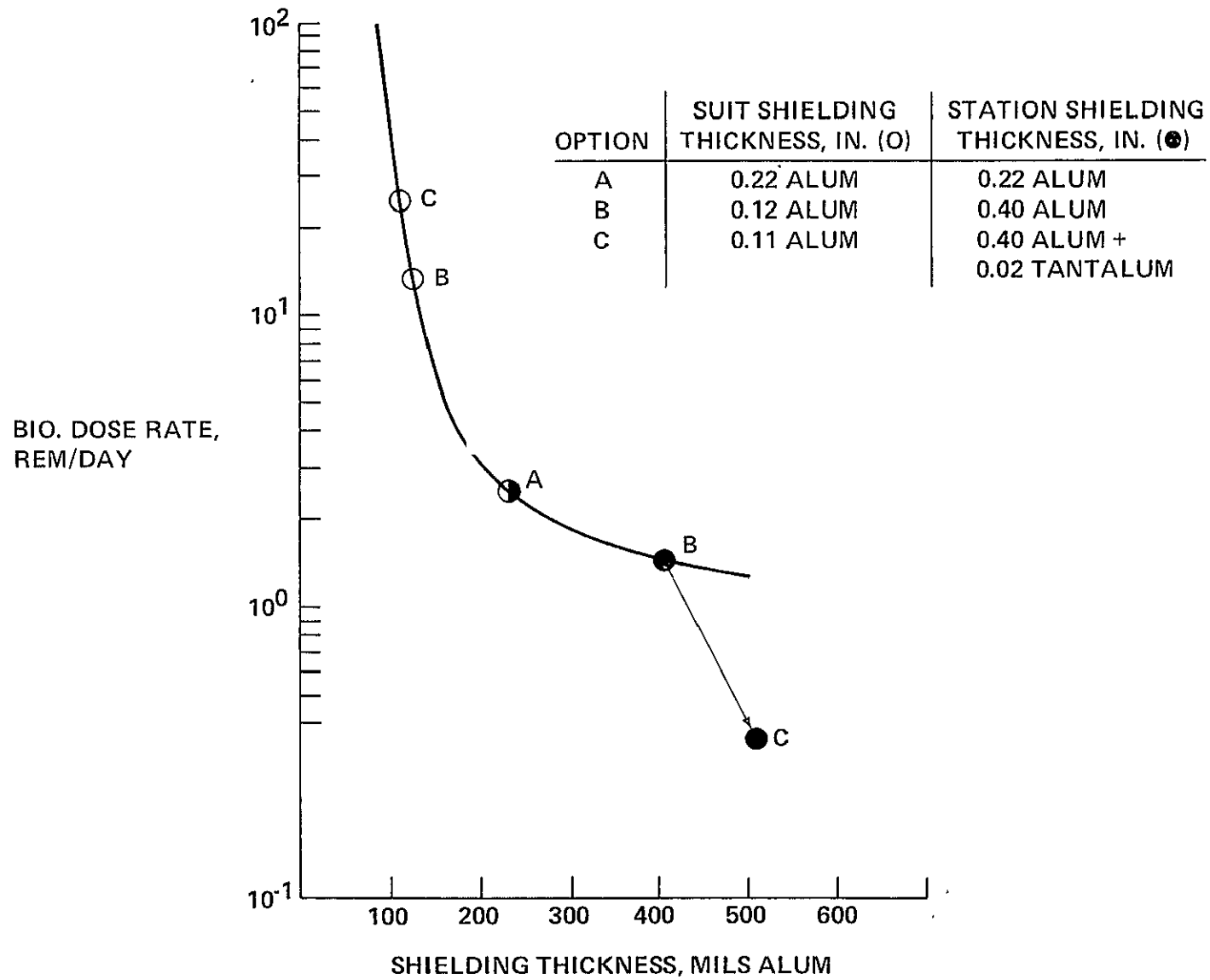


Fig. 5-52 Average Biological Rad Doses in Geo (Trapped Electrons and Bremsstrahlung)

Figure 5-53 shows the solar array power requirements for both the small and large construction base, during LEO and GEO construction. The total power requirements for construction equipment operations in LEO include the additional lighting required for the more frequent eclipse periods. Considering that higher solar incident angles occur in LEO operations, due to the higher orbit inclination ($i = 28.5^\circ$), the LEO construction base requires approximately three times the solar array area of that required at GEO.

This, combined with additional mass associated with battery power storage requirements (assuming the use of nickel hydrogen batteries), requires that mass penalties associated with LEO construction be estimated at 40,000 and 107,000 KGS for the small and large construction base respectively. These penalties are not considered to be significant, relative to the overall mass of the construction base.

Another factor related to differences in occultation times between LEO and GEO construction environment is the frequency of thermal cycling experienced by various elements of the satellite during construction. Figure 5-54, developed during the Phase II study, shows temperature variations experienced during sunlight and earth shadow conditions. Note that major elements of the satellite are at a temperature differential of 100°R during sunlight and are rapidly reduced to a zero differential during occultation. These variations in temperature differences create thermal distortions and misalignments that must be accommodated during construction. The much higher frequency of thermal cycling in LEO construction (16 times per day vs once per day at GEO), serves to accentuate the complexity of LEO construction.

During sunlight operations, the variations in solar look angle, as viewed by the satellite, add further complexity to construction operations in LEO. Figure 5-55 is the solar look angle projected onto a satellite during construction in LEO. Note that, at an inclination of about 28.5° , and assuming a local vertical attitude hold orientation, the solar look angle variation in azimuth is $\pm 180^\circ$ within the 90 minute orbital period. This occurs at seasonal elevation angles, which vary through $+46.5$ degrees over the solar year. Figure 5-56 shows the potential distortions which may occur along a 20 Meter beam of varying lengths in sunlight, due to partial shadowing within the construction base. These conditions are somewhat less pronounced at GEO, where the azimuth variation of $\pm 180^\circ$ occurs over a 24 hour period. Furthermore, because of the zero degree inclination in GEO, the seasonal variation in elevation is limited to $+23.5$ degrees. To eliminate these solar view angle variations, an inertially fixed attitude orientation must be held during construction. This can be accomplished with little burden to the attitude control propellant requirements during GEO construction, but would require, because of the large gravity gradient forces, significant penalties during LEO construction.

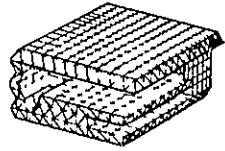
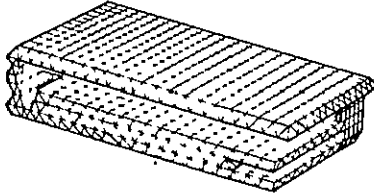
	 SMALL CONSTRUCTION BASE		 LARGE CONSTRUCTION BASE	
	LEO	GEO	LEO	GEO
• TOTAL POWER REQ'TS FOR CONST. EQUIPMENT, COMMUNICATION DATA PROCESSING ETC. (KW)	1,070	955	2,915	2,630
• PWR DISTRIBUTION AND CONDITIONING REQ'TS (11%)	120	105	320	290
• ADDITIONAL PWR REQ'TS IN LEO FOR BATTERY CHG.	1,450		3,950	
TOTAL POWER REQ'TS (KW)	≈ 2,640	1,050	7,185	2,920
• REQ'D SOLAR ARRAY AREA (M ²)	10,840	4,356	29,500	11,980
• REQ'D SOLAR ARRAY TO COMPENSATE FOR SOLAR INCIDENT ANGLE VARIATION (45° – LEO, 23.5° – GEO) – M ²	15,330	4,749	41,719	13,063
• SOLAR ARRAY MASS (.282 KG/M ²) – KG	4,323	1,339	11,764	3,684
• MASS OF BATTERY REQ'TS IN LEO (BASED ON NICKEL HYDROGEN BATTERIES) – KG	37,700	0	99,260	0
MASS OF ELECTRICAL POWER SYSTEM – KG	42,023	1,339	111,024	3,684
PENALTY OF EPS SYSTEM AT LEO – KG	40,684		107,340	

Fig. 5-53 Construction Base Electrical Power Requirements

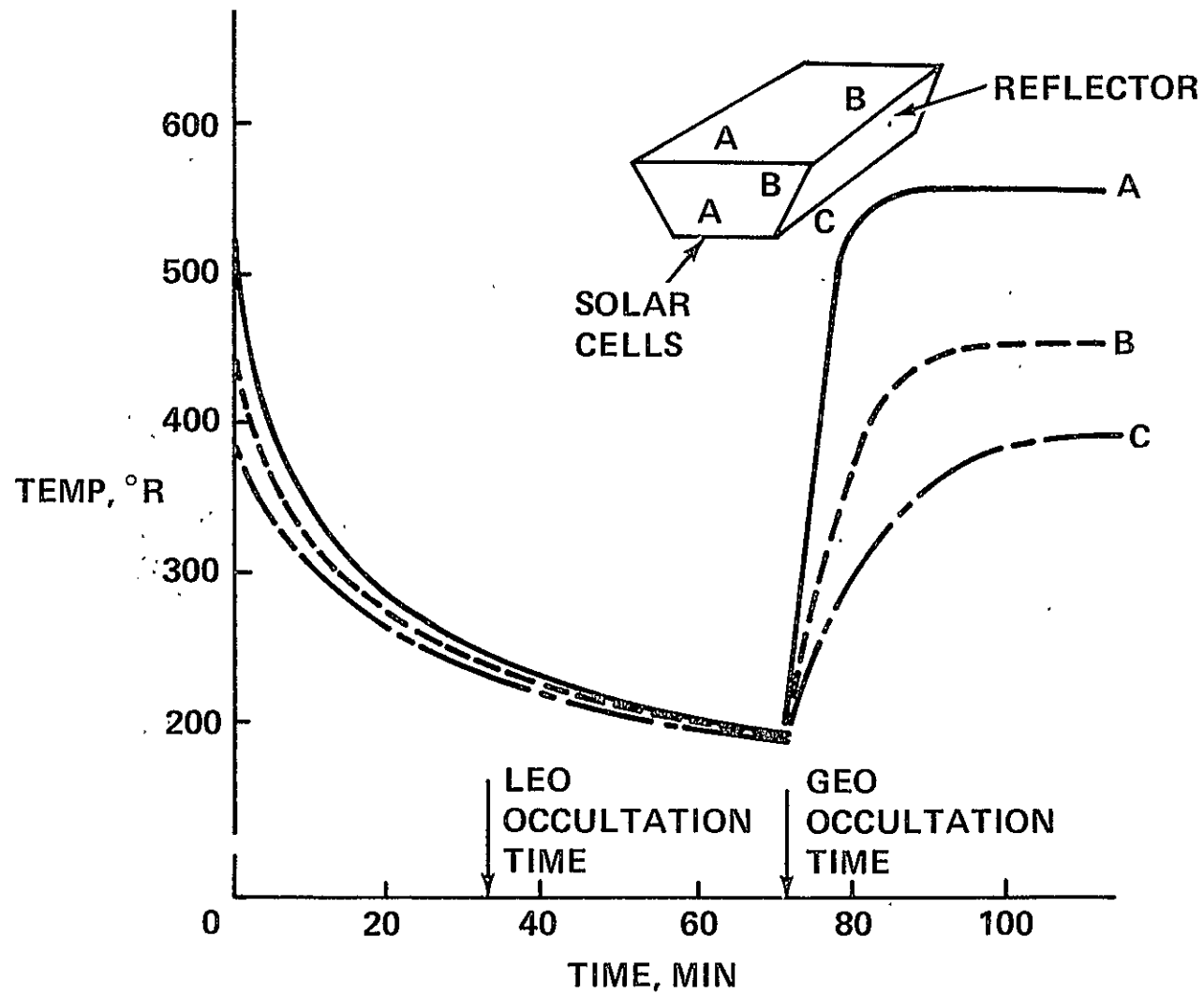


Fig. 5-54 Structural Temperatures During Occultation

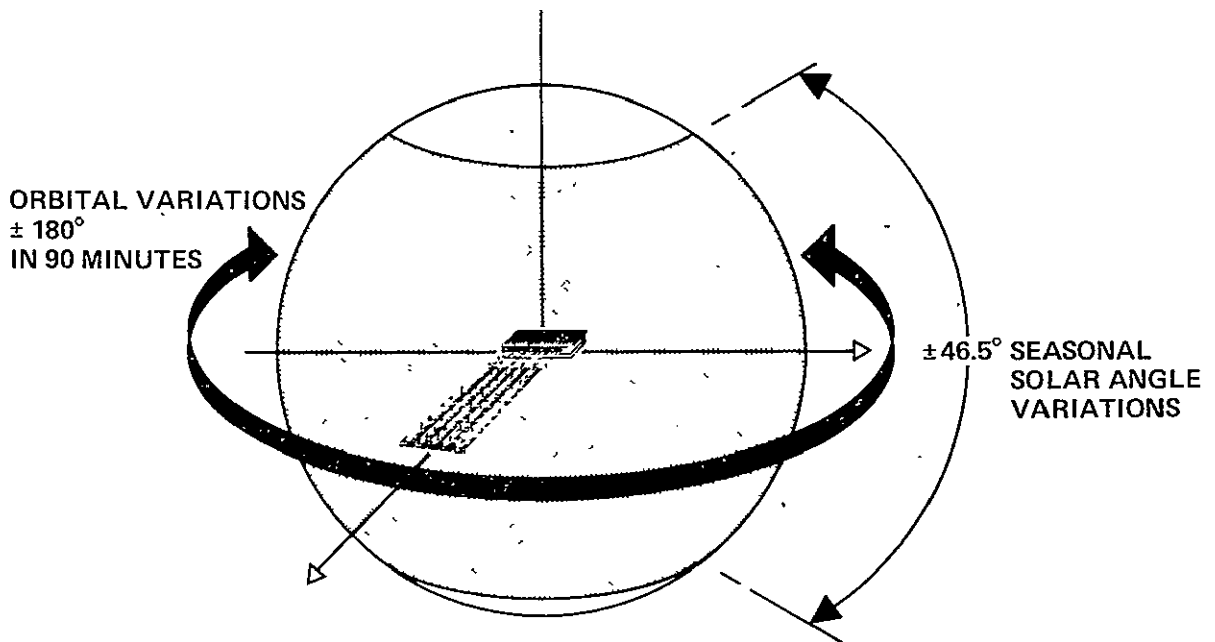


Fig. 5-55 Solar Look Angle During Leo Construction - Local Vertical Attitude Hold

THERMAL GRADIENT $\approx 20^\circ/\text{MIN}$

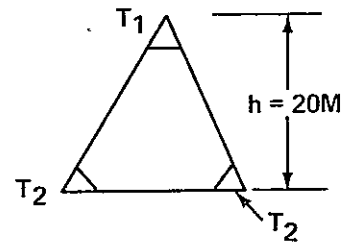
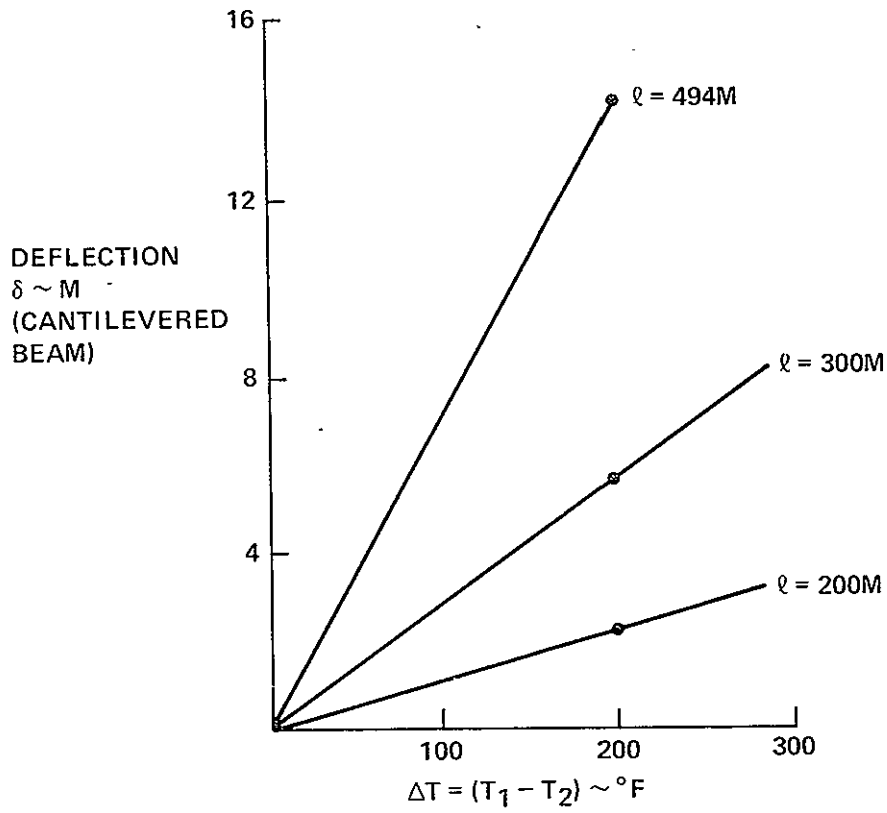


Fig. 5-56 Deflections in 20-Meter Beam Due to Thermal Gradients

5.1.4.3 Collision Probability

Potential hazards and SSPS damage may result from collision with orbital debris, during either the construction phase or while transferring the satellite to geosynchronous altitude. This is a factor which may bear on the selection of SSPS LEO or GEO construction location. Refs. (5) and (6) have developed models, based on the North American Air Defense Command (NORAD) data, that identify the number of objects presently in orbit. These models may be used to estimate the potential collisions that may be expected over a range of orbit altitudes. The results of all these studies show that the collision probability is greatest at altitudes ranging from 500 to 1500 Km. The number of collisions projected, for a satellite with an area of approximately 150 Km², may be as high as several hundred per year, as shown in Figure 5-57. This is in contrast to the GEO construction environment, wherein it is estimated that the collision probability is not more than one over a 30 year period. The potential endangerment to personnel located throughout the construction base, and the complexities involved in repairing damaged satellite components, suggest that LEO construction be limited to smaller area subassemblies and modules.

5.1.5 Transportation System Requirements

Earlier studies have indicated that a major variable influencing overall SPS economic feasibility, are the costs associated with transportation and assembly. Requirements for LEO and GEO construction scenarios were identified within this study, for the construction of the baseline 5-GW silicon crystal configuration, in terms of number of flights, fleet size, and traffic model. Construction scenarios assumed a construction rate of up to 6 satellite builds per year.

5.1.5.1 Baseline Transportation System Selection

Representative transportation system elements were selected from candidate transportation system concepts currently under study. Although substantially more study is required of the most cost-effective transportation modes, suitable to the SSPS, data developed in these early related studies were used for analysis.

Data developed in Ref. 7 has shown that, when considering the delivery of a large mass of payload to orbit (on the order of several hundred million Kgs for the overall SPS program), economics dictate the use of an HLLV-type launch system. Of the vast number of advanced booster systems studied, including two-stage winged vehicles, shuttle growth concepts and two-stage ballistic configurations, the ballistic concepts appeared to offer launch costs of less than \$60/Kg.

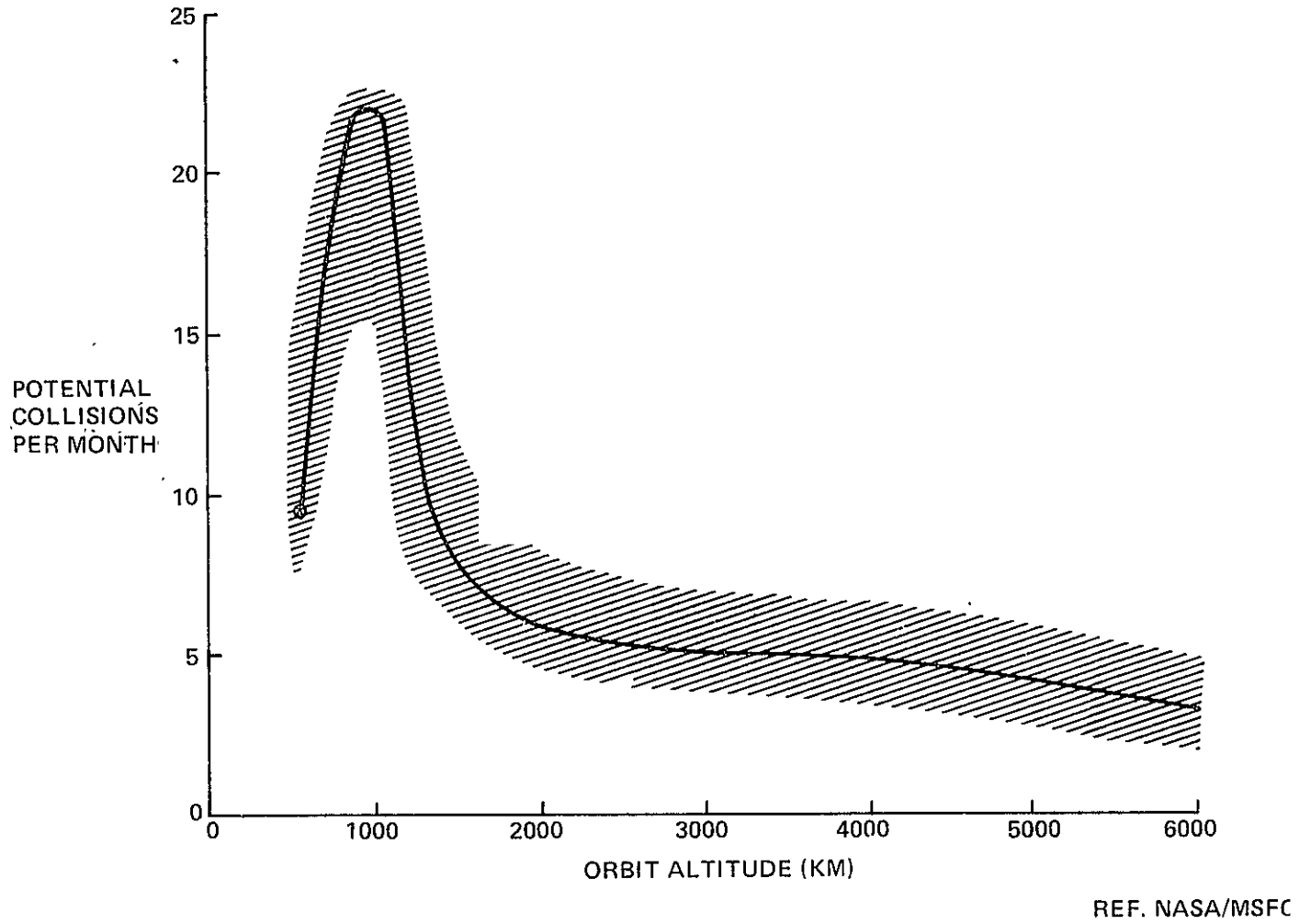


Fig. 5-57 LEO Collision Probability

A two-stage ballistic HLLV, therefore, as shown in Fig. 5-58, was baselined for this study. The vehicle delivers a payload of 265,000 Kg to low earth orbit within a payload bay measuring 62.2-meters long by 16-meters in diameter. This is equivalent to a packaging density of 20 Kg/m³. Both stages are recoverable, with turnaround times of 7.3 days and 5.3 days for the lower and upper stages, respectively. Expected design lifetimes are 300 and 500 reuses, respectively.

For the cargo orbit transfer vehicle baseline selection (i.e. for use in the GEO construction scenario, wherein materials and propellants are transferred from low earth orbit depot to the GEO construction base) a LO₂/LH₂ chemical OTV, as defined in Ref. (7) was chosen. These studies concluded that reusable chemical stages are a viable concept, and may be the least expensive of the options examined. The configuration (Fig. 5-59) exhibits a payload delivery capability to GEO of approximately the same size as the HLLV. In the LEO construction scenario, a solar electric-type propulsion system was baselined for transferring an assembled SPS to geosynchronous orbit.

For the transfer and return of personnel to GEO, a two-stage LO₂/LH₂ system was also selected as the baseline. A crew module, accommodating a crew size of 75, would be transferred from a LEO depot to the GEO construction base in approximately 9 hours. This baseline is illustrated in Fig. 5-60. A shuttle vehicle was assumed used for transfer of crew personnel from earth to a LEO construction base depot.

5.1.5.2 Transportation Requirements for LEO and GEO Construction

Using the LEO and GEO construction concepts developed for both the small and large construction bases, a transportation delivery schedule was developed for transporting materials, propellants, and personnel to each of the construction sites. The schedule addressed day-to-day deliveries required to insure supply of materials necessary for the defined construction sequence. This assumed that the construction base was activated, and fully equipped with all construction equipment and facilities. It is recognized that the construction and placement of the construction base itself is another issue that may impact the selection of construction location. For purposes of this study, however, it was assumed to be a small factor relative to the construction of a 120 satellite constellation.

Fig. 5-61 identifies an assortment of satellite materials that must be transported to the construction base, in a somewhat controlled schedule, to insure that the proper mix of materials is available for construction of the SPS satellite. All materials, with the exception of the microwave antenna subarrays, appear to fall within the

	● HLLV-4	
PAYLOAD BAY	● 16	
	62.2	
P. L.	(599,000)	(265,100 KG)
IOC	EARLY 90's	
TURNAROUND TIME	LOWER	UPPER
	7.3	5.3
	300	500

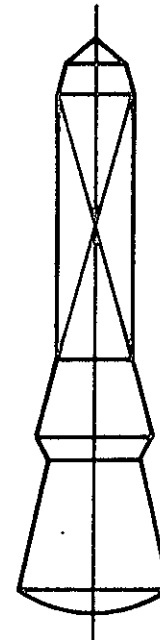
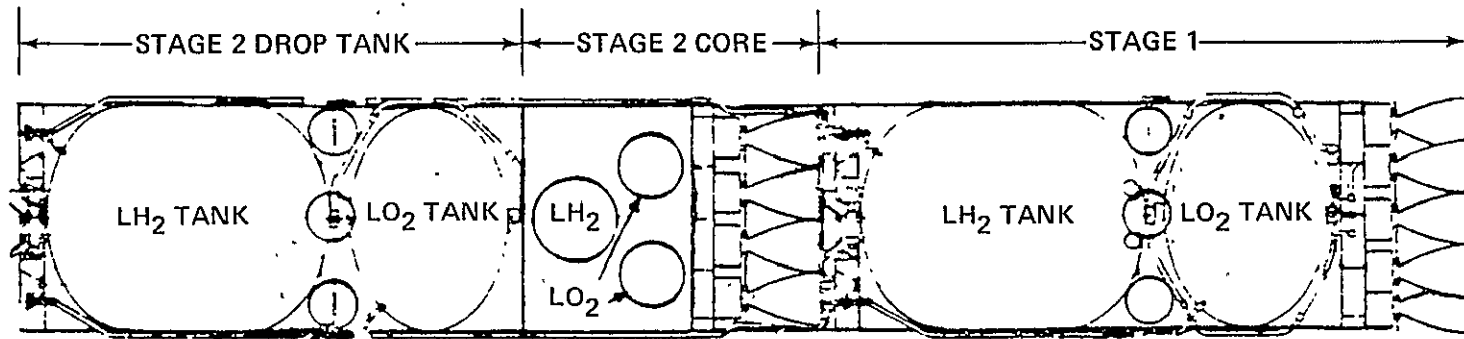


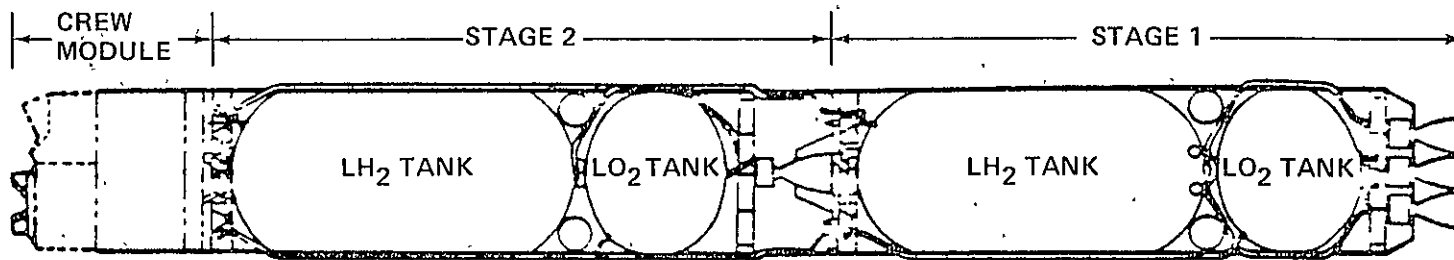
Fig. 5-58 Heavy Lift Launch Vehicle



2-1/2 STAGE LO_2/LH_2
 LIFE: 30 MISSIONS
 PAYLOAD: 250 TONS
 \approx \$10M/FLT

LENGTH: 49 M
 DIAMETER: 8.4 M
 TOTAL WEIGHT: 510 TONS
 PROPELLENT WEIGHT: 475 TONS

Fig. 5-59 Baseline Cargo Orbital Transfer Vehicle



109

COMMON STAGE LO₂/LH₂
 LIFE: 30 MISSIONS
 PAYLOAD: 75 PASSENGERS + 20 TONS (UP)
 75 PASSENGERS (DOWN)
 (2 ND STAGE GEO REFUEL)
 ≈ \$12 M/FLT

LENGTH: 33.28 M
 DIAMETER: 4.42 M
 TOTAL WEIGHT: 123 TONS
 PROPELLANT WEIGHT: 106 TONS
 NUMBER OF ENGINES AT 66 720 NEWTONS EACH:
 STAGE 1: 4 ENGINES
 STAGE 2: 2 ENGINES

Fig. 5-60 Baseline Personnel Orbital Transfer Vehicle (POTV)

SATELLITE	TOTAL MASS PER SATELLITE. KG x 10 ⁶	TOTAL NO OF HLLV FLIGHTS AT 20 KG/M ³ PACKAGING	MASS TRANSPORTED PER FLIGHT (KG) x 10 ³	COMMENTS
• SOLAR ARRAY				
– BLANKETS	7.83	29.6	195	REPRESENTS 1/4 OF LENGTH OF ONE TROUGH
– CONCENTRATORS	1.23	4.7	30.7	ONE COMPLETE SIDE OF ONE TROUGH
– NON-CONDUCTING STRUCTURE	2.33	8.8	233	DIELECTRIC STRUCTURE OF ONE TROUGH
– BUSSES, SWITCHES ETC	.27	1.0	27	MASS PER TROUGH
CENTRAL MAST STRUCTURE	.64	2.4	640	TOTAL MASS
MW ANTENNA	5.55	26 ⁽¹⁾		(1) 4.77 x 10 ⁶ Kg AT 16 KG/M ³ PACKAGING .78 x 10 ⁶ Kg AT 20 KG/M ³ PACKAGING
ROTARY JOINT	.17	.7	170	COMPLETE ROTARY JOINT
CONTROL SYSTEM	.036	.14	3.6	COMPLETE CONTROL SYSTEM
TOTALS	18.06	74		

Fig. 5-61 Satellite Materials Matrix

payload and packaging densities of an HLLV. For example, one-fourth of a solar blanket trough, folded in sections of four, and stored on hollow rollers, could be packaged to fit within HLLV's payload limitations.

Studies conducted for in-orbit fabrication of the microwave antenna, Ref 8, have shown that in-orbit fabrication is very complex, and not a prime candidate for on-orbit construction. It appeared more economical to ground-fabricate the subarray sections, and transport these sections to LEO. This concept, requiring 26 HLLV flights, was therefore selected for constructing the overall microwave antenna.

Figure 5-62 summarizes the total number of flights required for both the LEO and GEO construction of one 5 GW baseline configuration. In both cases, 74 HLLV flights are required for the delivery of satellite materials, with the remaining flights for delivery of COTV and POTV propellant and reusable stages. For the LEO construction scenario, additional HLLV flights are required for transporting the SEPS stage and its propellants to the LEO construction base.

A typical traffic model, for the small construction base concept at GEO, is shown in Figure 5-63. Assuming that one satellite is produced in a period of 12-13 weeks, a monthly HLLV launch rate of 74 flights is required. The large construction base, with one satellite produced in about 8-9 weeks, requires monthly launch rates of more than 100 flights. This is in sharp contrast to LEO construction requirements, which call for launch rates of about 1/3 that required for GEO construction. The results of these studies indicate that GEO construction of SSPS is higher in cost than that required for LEO construction.

5.1.6 Conclusions and Recommendations

Analyses of both LEO and GEO construction scenarios, has surfaced technical findings that are generally applicable to all current concepts of the SPS. These are:

- o The complete construction and assembly of an operational SPS in LEO, followed by transport to GEO, does not appear technically desirable

CONCLUSIONS – LEO VS GEO CONSTRUCTION LOCATION

TRANSPORTATION REQUIREMENTS

– EACH SATELLITE BUILD REQUIRES

LEO CONSTRUCTION

85

0

0

10

1

26-37

7-10

9

NO OF HLLV FLTS

NO OF COTV FLTS

NO OF POTV FLTS

NO OF SHUTTLE FLTS

ADVANCED ION STAGE FLTS

PEAK HLLV LAUNCH RATE PER MONTH

MAXIMUM FLEET SIZE

TIME FROM START OF

CONSTRUCTION TO ON-ORBIT

OPERATION

(SMALL CONST. BASE) – MONTHS

GEO CONSTRUCTION

213

78

20

10

0

74-107

19-27

3

112

Fig. 5-62 Conclusions - LEO vs GEO Construction Location

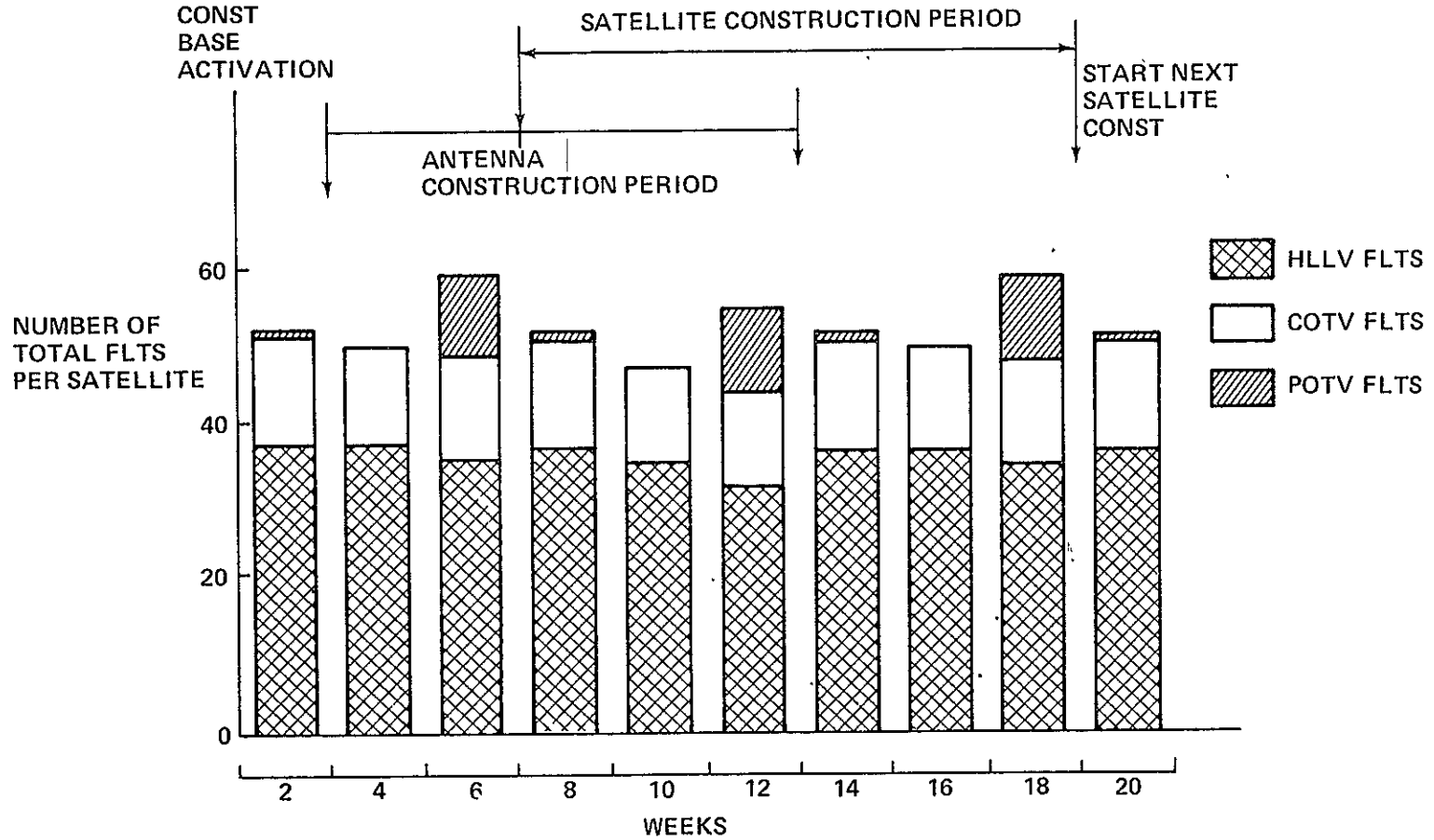


Fig. 5-63 GEO Construction Scenario - Small Construction Base

The principal factors supporting this conclusion are:

- The large size of an 5-10-GW SPS makes it highly susceptible to collision with orbital debris
- The very large dimensions and overall mass distribution of a fully assembled satellite in LEO, subjects it to substantially higher structural loading during construction than that required for operational conditions
- Significant attitude control penalties exist, in terms of both propellant and electrical power requirements, for construction of large scale structures

It appears that construction and assembly of SPS in orbit should be accomplished by construction of sub-assembly modules in LEO, transported to GEO using low acceleration OTV's, and assembled into a fully integrated satellite at GEO. The size and overall design of the subassembly modules is highly dependent, however, upon the specific configuration to be constructed. Studies should focus on satellite configuration concepts, in combination with construction base operations, to insure high producibility in orbit.

5.2 Power Distribution

5.2.1 Introduction

Previous studies (Reference 3) indicated that SPS structural design requirements are heavily influenced by the use of electrical conducting structure, and recommended further analysis to define these effects. The primary objective of this task was to determine the specific design impacts of using SPS structure for electrical power distribution. Detailed electrical, thermal and structural analyses were performed to:

- o Establish mass/efficiency sensitivities of the solar array and structural/power distribution system
- o Define structural design requirements associated with integral power conductors
- o Determine electrical loadings - current/voltage distribution
- o Verify heat rejection capability - establish desired operating temperature
- o Evaluate design requirements for central mast and rotary joint.

5.2.2 Baseline Configuration

The general structural arrangements used for this analysis is shown in Figure 5-64. The main structural frame-work consists of supporting structure for the solar cells and reflectors. Electrical power is distributed via transverse buses and a main transmission bus at the centerline, on the backside of the array. All conducting buses are assumed as an integral part of the structure.

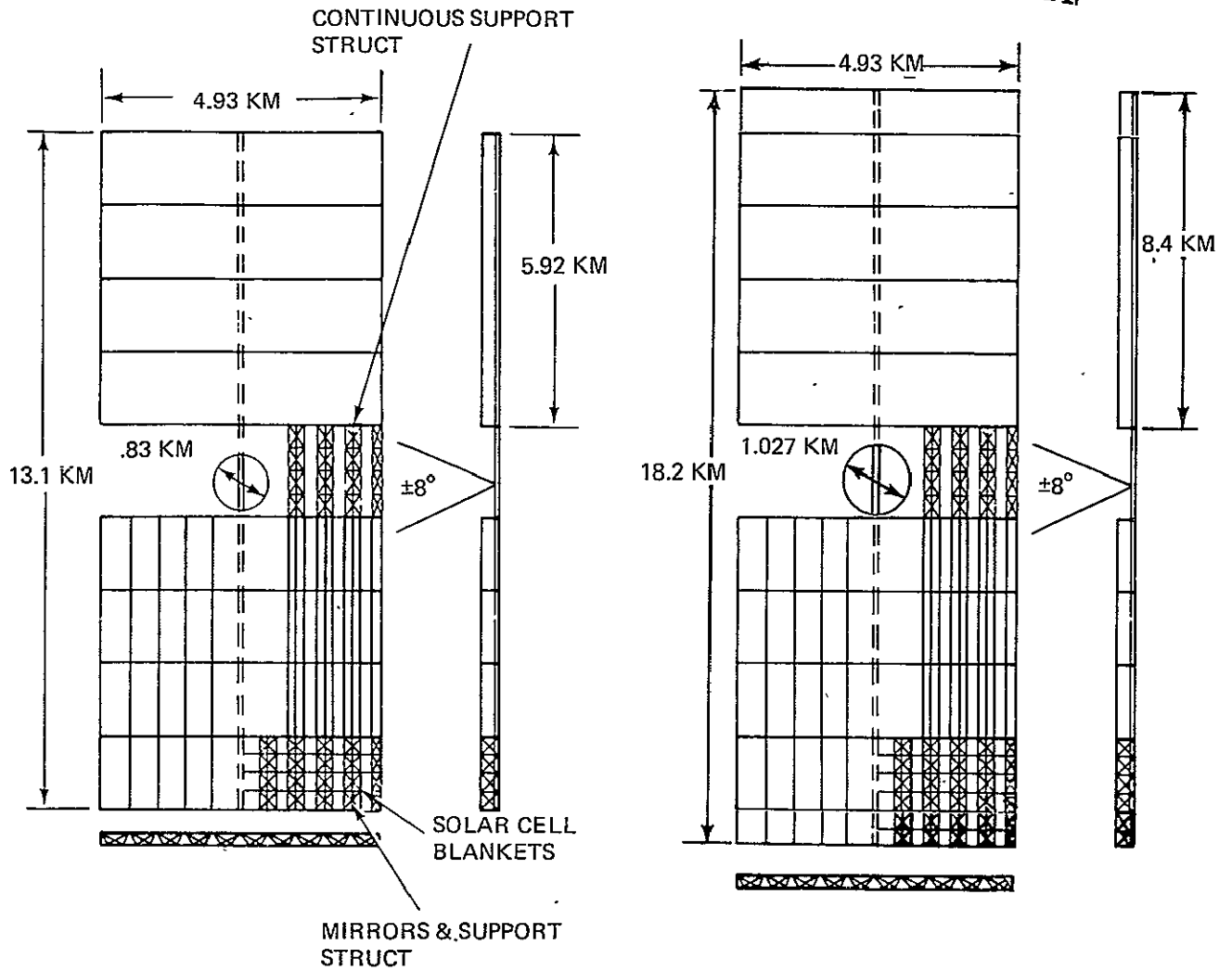
5.2.3 Conducting Structure

The conducting structure was analyzed in detail to establish design requirements, and to define electrical, thermal, and structural design sensitivities associated with a mass-optimum system.

5.2.3.1 Efficiency and Total Power

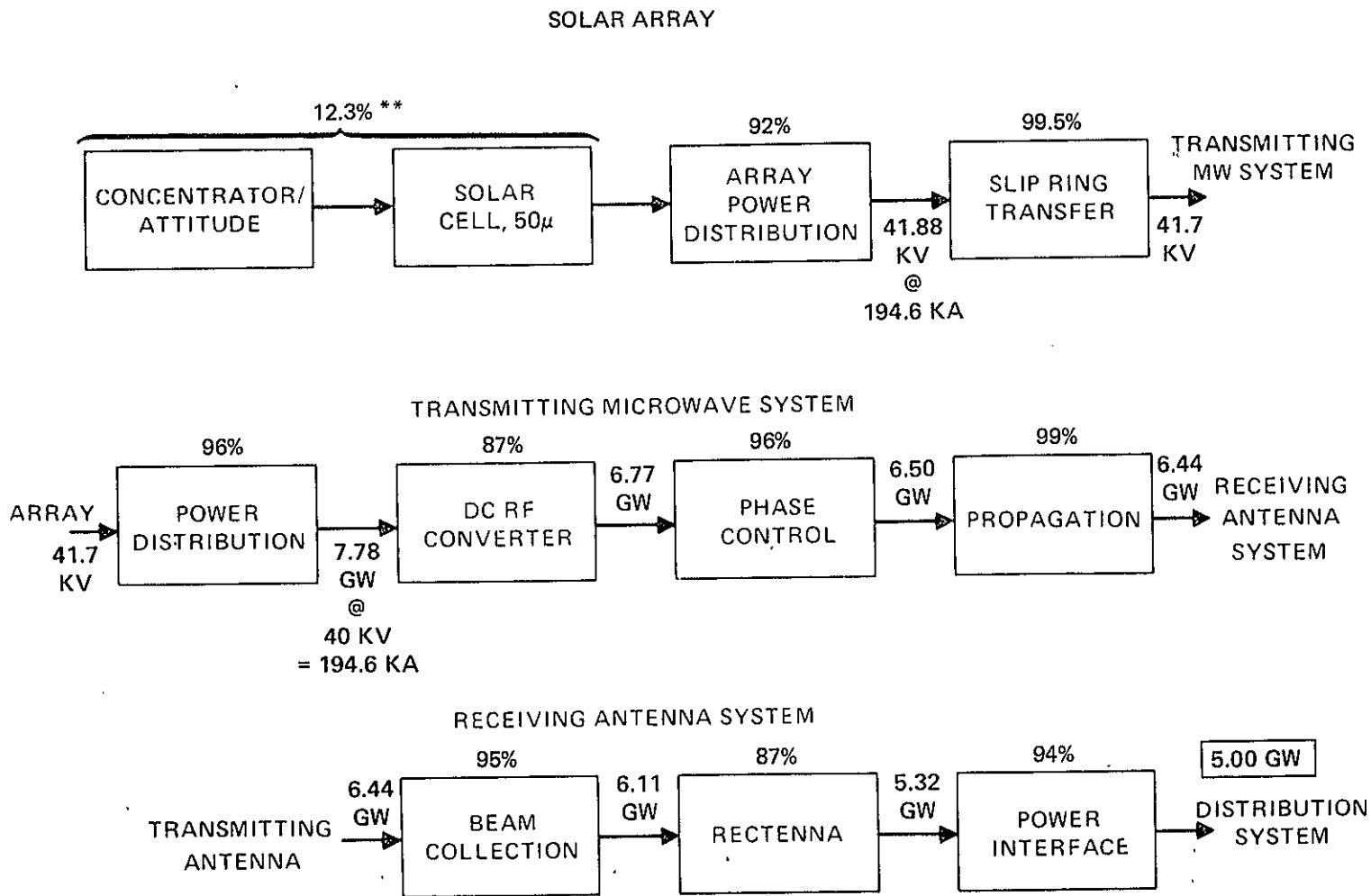
Figure 5-65 shows the efficiency chain for the system as reported in Reference 3. The overall sizing requirement is for 5-GW total output to the terrestrial power distribution system after five years of satellite life. The DC-RF microwave generating devices require an input power of 7.78 GW at 40 KV, thus defining a total microwave generator input current of 194.6 KA. From this point back through the

ORIGINAL PAGE IS
OF POOR QUALITY



CHARACTERISTICS	END OF PHASE I	END OF STUDY
● POWER	5000 MW	5000 MW
● MASS	18.1 X 10 ⁶ KG	27.2 X 10 ⁶ KG
● SIZE	13.1 X 4.9 KM	18.2 X 4.9 KM
● ORBIT	GEOSYNCHRONOUS	GEOSYNCHRONOUS
● LIFE	30 YR	30 YR
● OPERATING FREQ	2.45 GHz	2.45 GHz
● DC-TO-DC EFFIC	55%	58%
● SOLAR CONV EFFIC	12.3%	8.0%

Fig 5-64 Comparison of Concept Descriptions



** REPRESENTS MOST OPTIMISTIC TECHNOLOGY PROJECTIONS AS ESTABLISHED IN PHASE I STUDIES

Fig. 5-65 Nominal System Efficiency Chain

ORIGINAL PAGE IS OF POOR QUALITY

distribution system, all inefficiencies appear as voltage drops, resulting in the requirement to deliver 194.6 KA to the input of the slip ring assembly at 41.88 KV (8.15 GW)

5.2.3.2 Mass/Efficiency Optimization

An optimization analysis was performed to identify mass/efficiency sensitivities, and to define basic design requirements for the conducting structure. As suggested in Reference (3) the optimization of power conductors must consider the trade-off between decreasing conductor mass by reducing cross-sectional area (increasing current density), and making up for the additional distribution loss by increasing the power source output (and weight). An optimum current density ϵ' (A/cm²) is derived, based on density ρ (g/cm³), resistivity σ (ohm-cm), and source incremental mass K (g/watt):

$$\epsilon' = \sqrt{\frac{\rho}{\sigma} \times \frac{1}{K}} \quad (1)$$

Equation (1) modified to include temperature effects, becomes:

$$\epsilon^i = \sqrt{\frac{1}{K} \times \frac{\rho_0}{(1+\beta T)^3} \times \frac{1}{\sigma_0(1+\alpha T)}} \quad (2)$$

In equation (2), T is the conductor temperature in °C, and α and β are the temperature coefficients of resistance and linear expansion, respectively, for density and resistivity referenced to 0°C.

The voltage drop per unit length (ΔV_ℓ) of conductor, at ϵ' is:

$$\begin{aligned} \Delta V_\ell &= \epsilon' \sigma \\ \Delta V_\ell &= \sqrt{\frac{1}{K} \times \frac{\rho_0}{(1+\beta T)^3} \times \sigma_0 (1+\alpha T)} \quad (3) \end{aligned}$$

Assuming aluminum conductors, and a specific solar cell blanket mass of 1 kg/kw, equations (2) and (3) can be linearly approximated over the temperature range of 0-150°C, by:

$$\epsilon' = 977.1 - 1.495 T \text{ (A/cm}^2\text{)} \quad (4)$$

$$\Delta V_{\ell} = .2763 + .0004863 T \text{ (V/M)} \quad (5)$$

Equation (4) and (5) are plotted in Figure 5-66; these curves show the relationship between conductor temperature, voltage drop, and current density, optimized for minimum system mass.

Conductor temperature - A parametric thermal analysis was performed to establish the relations between conductor size, current density and temperature.

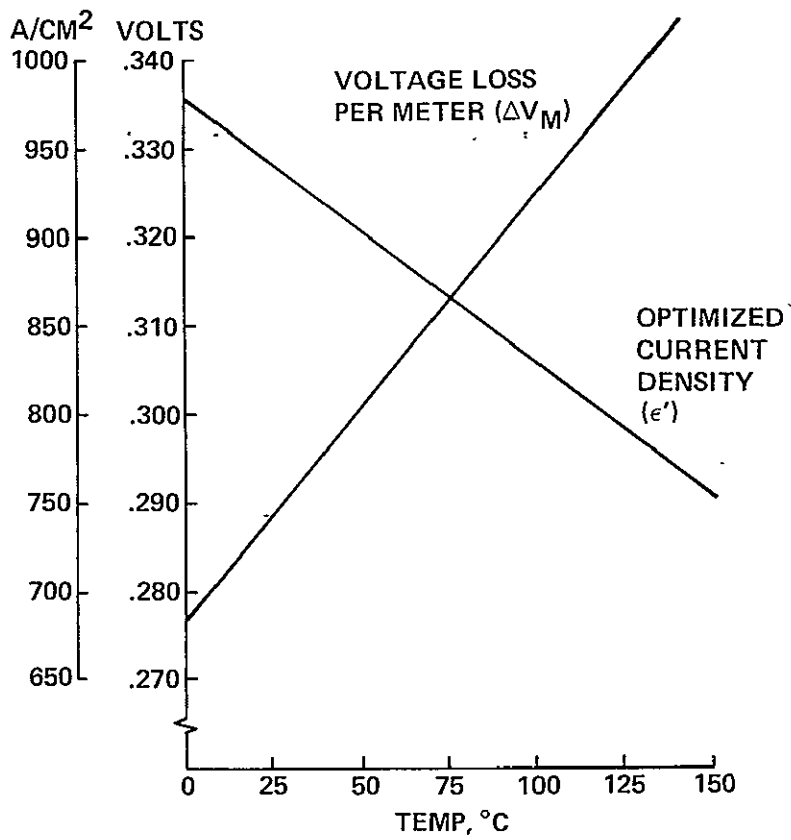


Fig. 5-66 Optimized Current Density

Using optimum current densities/voltage drops from Figure 5-66, incremental heat generation and cross-sectional areas were derived for the anticipated range of conductor currents; these are listed in Figure 5-67.

A geometric/thermal model of the central mast power bus was developed. This, together with the radiation coupling data used for space and reflector back surfaces, is shown in Figure 5-68. A steady reflector temperature of 3°C, based on updated solar array/concentrator analyses, was used.

Conductor dimensions were derived as a function of temperature for the uppermost (No. 1) conductor, and are shown in Figure 5-69. Required surface areas (conductor radii) are computed for each steady state temperature and current density, and required conductor thickness is derived directly from these relationships.

Conductor Size/Thickness

Handling considerations limit the minimum conductor wall thickness to .038 cm (.015 in). Current densities for a .038 cm.-thick conductor are compared to optimum current density values in Figure 5-70. Figures 5-69 and 5-70 indicate that .038 cm.-thick conductors operate at optimum current density at 122°C. Above 122°C, the current density is higher than optimum, meaning that too much additional solar array is required to make up for the conductor losses. Below 122°C, the current density is lower than optimum, but conductors cannot be practically handled if made any thinner. The optimum design point is 122°C at a current density of 795 A/cm². Conductor radius as a function of total conducted current is shown in Figure 5-71 for .038 cm.-thick walls operating at optimum current density.

Current/Voltage Distribution

Based on the optimized current density and voltage drop per meter for 122°C, individual output voltages were calculated for each of the 20 solar array LRU sections in each SPS quadrant and are shown in Figure 5-72. These values were used to compute the weight of all conductors from individual LRU sections (lateral buses) through the central mast to the slip ring assembly. Electrical continuity is achieved through welded joints with conductivity at least as high as that for continuous metal.

Solar Array Utilization Efficiency

Figure 5-73 shows the current and power output characteristics of a solar array LRU, normalized to the peak power point (only the region near the peak power point is shown). The percent spread in plotted LRU voltages from Figure 5-72 is overlaid on the power curve to intersect at equal powers for the high and low voltage units. All others

CURRENT-KA	T = 30°C .002910 V/cm ² 933 Amps/cm ² WATTS/cm		T = 90°C .003202 V/cm ² 843 Amps/cm ² WATTS/cm		T = 150°C .003493 V/cm ² 754 Amps/cm ² WATTS/cm	
	Acs-cm ²	Acs-cm ²	Acs-cm ²	Acs-cm ²	Acs-cm ²	Acs-cm ²
2.4	6.98	2.57	7.68	2.84	8.38	3.18
4.3	12.5	4.61	12.7	5.10	15.0	5.70
8.6	25.0	9.22	27.5	10.2	30.0	11.4
12.9	37.5	13.8	41.3	15.3	45.1	17.1
17.2	50.1	18.4	55.1	20.4	60.1	22.8
24.3	70.7	26.0	77.8	28.8	84.9	32.2

A_{cs} = Cross-sectional area

Figure 5-67 – Conductor Heating, Area Requirement for Optimized Current Density

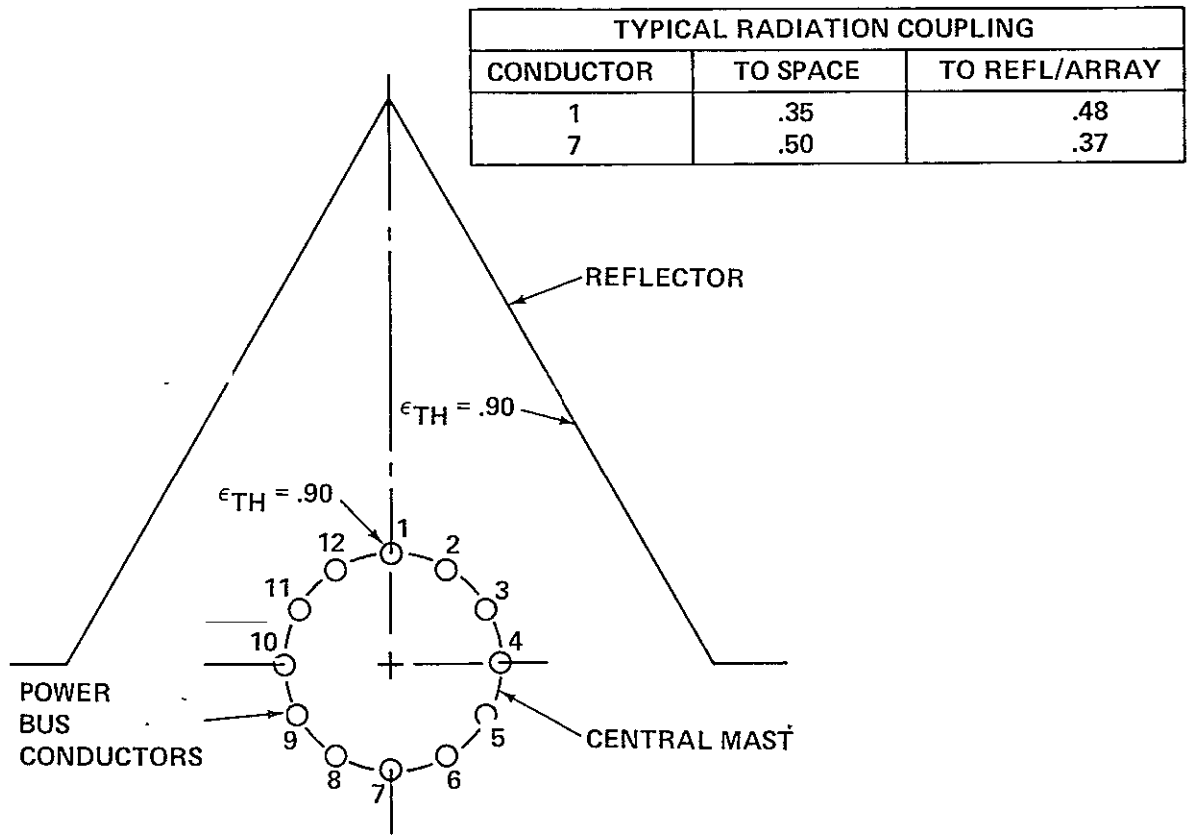


Fig. 5-68 Thermal Radiation Coupling Model

124

• AT OPTIMIZED CURRENT DENSITY

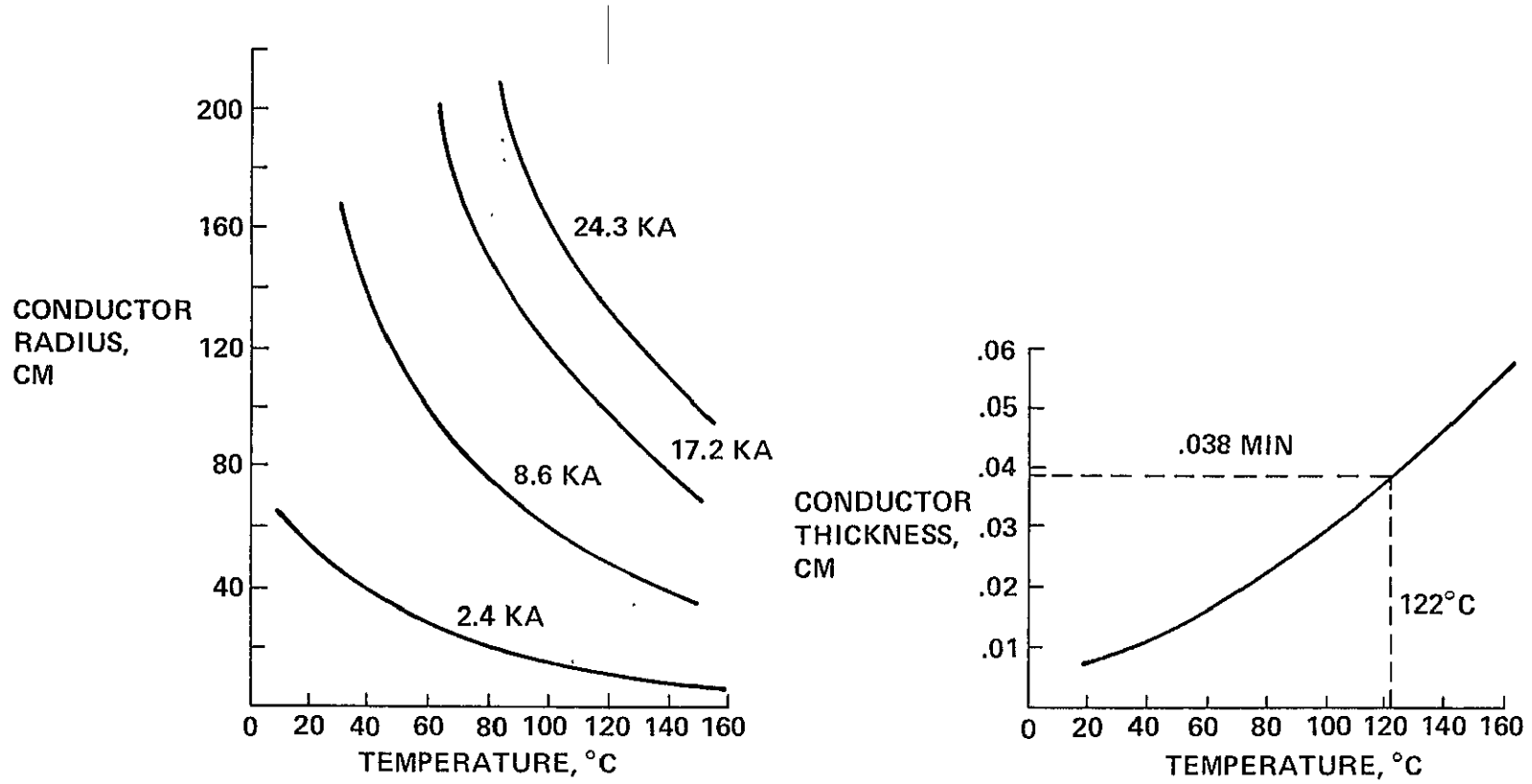


Fig. 5-69 Conductor Dimensions.

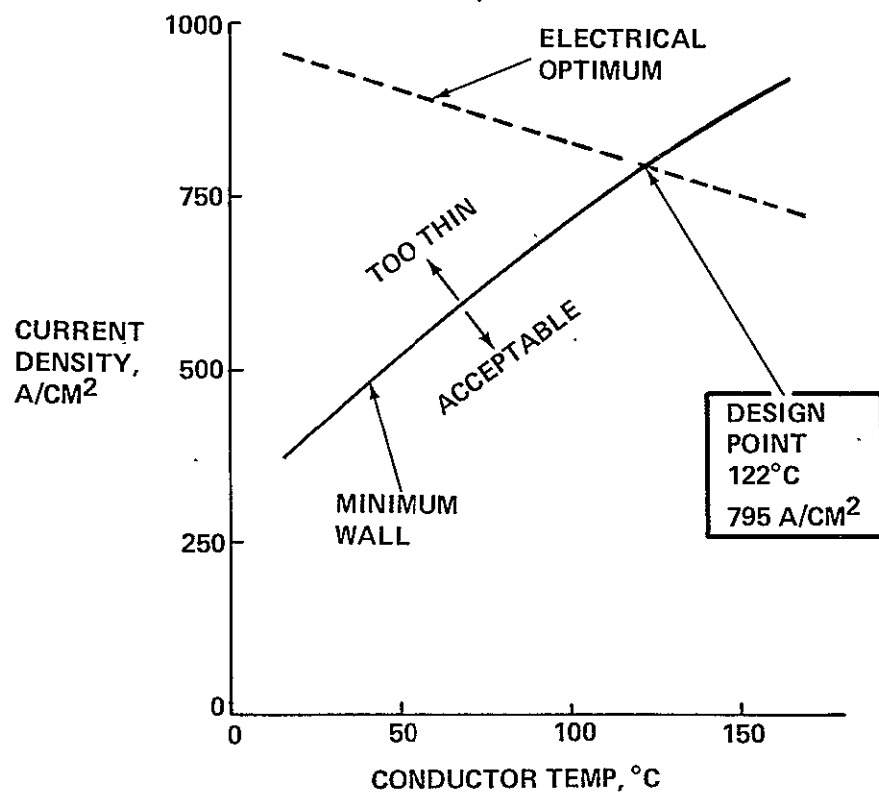


Fig. 5-70 Current Density Boundary

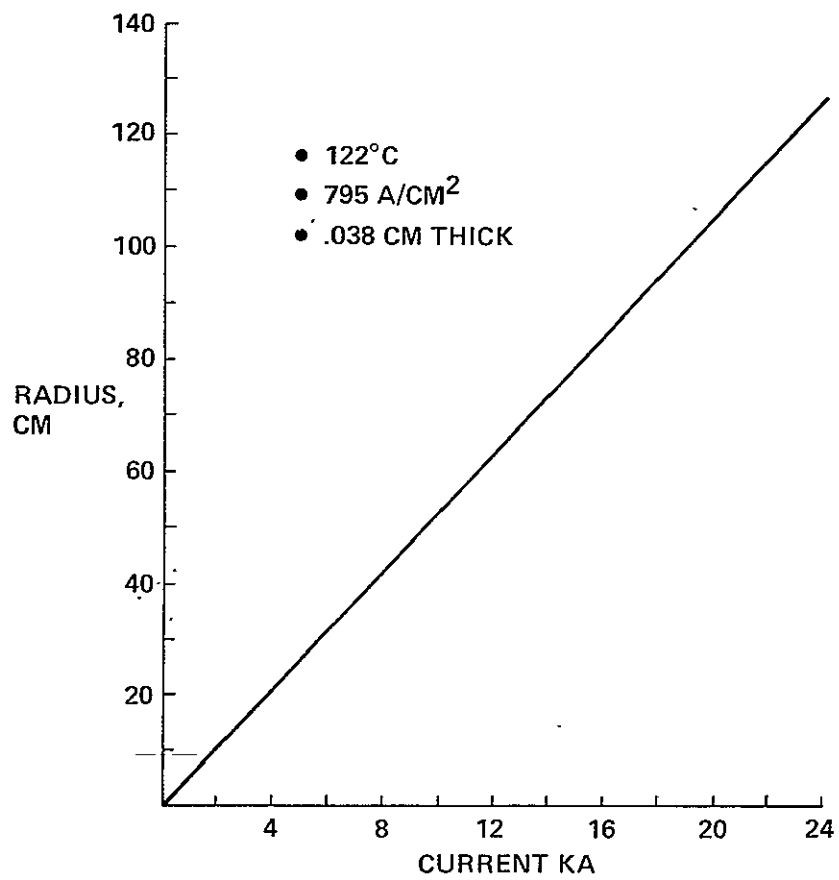


Fig. 5-71 Required Conductor Radius

- CURRENTS IN KILOAMPERES
- LENGTHS IN METERS

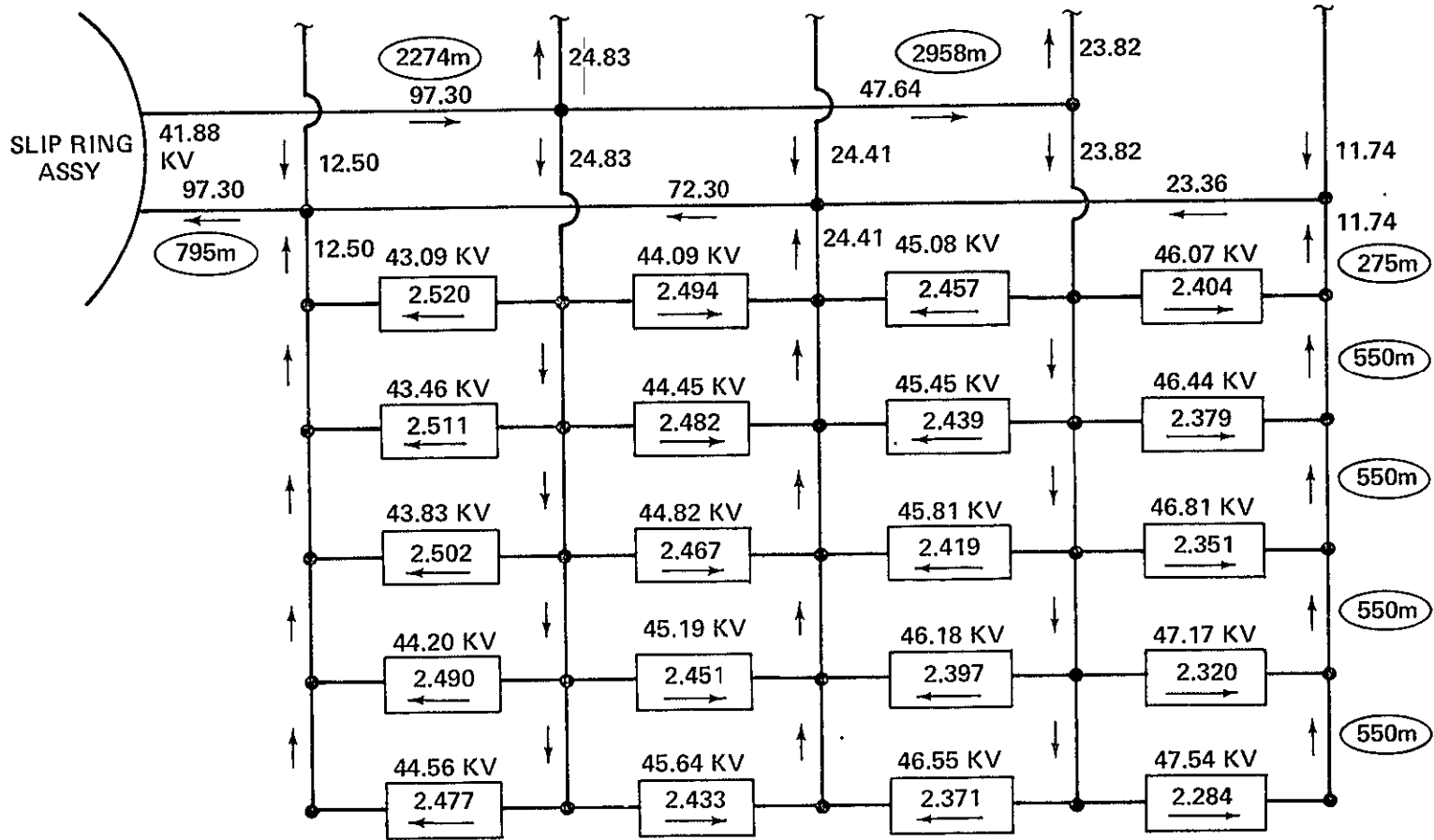


Fig. 5-72 Current Distribution

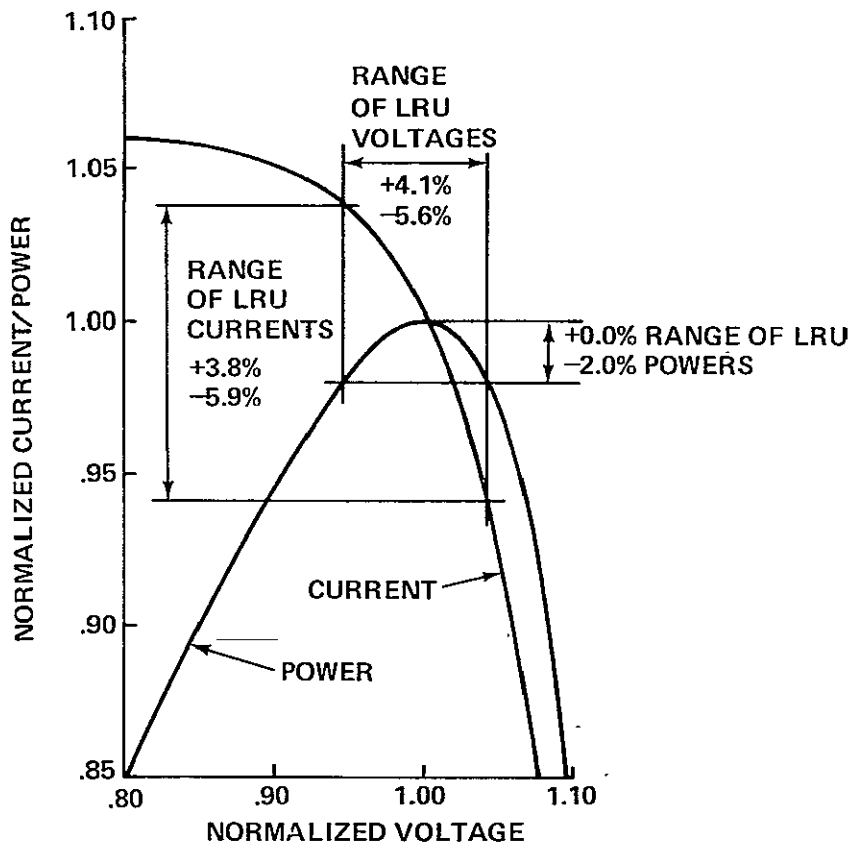


Fig. 5-73 Solar Array LRU Characteristics

operate in between, nearer to the peak power point. All LRU's operate at no worse than 98 percent of peak power, depending on location within the quadrant. Average solar array utilization efficiency is better than 99 percent. The projected overlay on the current curve shows currents varying from -5.9 percent to +3.8 percent of peak power current. Individual LRU output currents were all defined and plotted in Figure 5-72.

Structural Design Effects

Support cables which connect the conducting central mast to the SPS structure must be sized to withstand thermally induced loads which, as reported in Reference 3, were in excess of baseline design values. The finite element model was rerun with different temperatures for the central conductor. The load in the critical cable (member 197) versus central mast temperature is plotted in Figure 5-74. The required area (and weight) for all cables that run in a spanwise (+X) direction was calculated as a function of mast temperature.

Mass/Efficiency Sensitivity

The effect of current density optimization, and the minimum wall thickness constraint, on power conductor/LRU weight is shown in Figure 5-75. The weights shown represent changes to the baseline design reported in Reference 3. Conductor weight includes all lateral bases and central mast conductors.

The trade-off between solar array and conductor weight is obvious from these curves. Minimum system weight results from the optimized design. The minimum wall thickness limit, however, results in non-optimum current densities below 122°C. At the lower temperatures, solar array weight is saved at the expense of additional conductor weight. This, combined with a reduced cable weight penalty, results in a minimum total weight at about 80°C using .038 cm.-thick conductors. The current density for .038 cm.-thick conductors at 80°C is seen from Figure 5-70 to be 640 A/cm².

Array power distribution efficiency improves with decreasing temperature as a result of lower conductor voltage drops. At the minimum weight point, the efficiency is 94 percent, a 2-percent improvement over that reported in Reference 3.

The effect of power transmission weight optimization on total weight is shown in Figure 5-76. Although optimization results in a 300×10^3 Kg saving for the baseline design, the effect on total SPS weight is rather small, with the maximum penalty for off-optimum designs no more than 3-percent of the total weight of the solar array plus conductors.

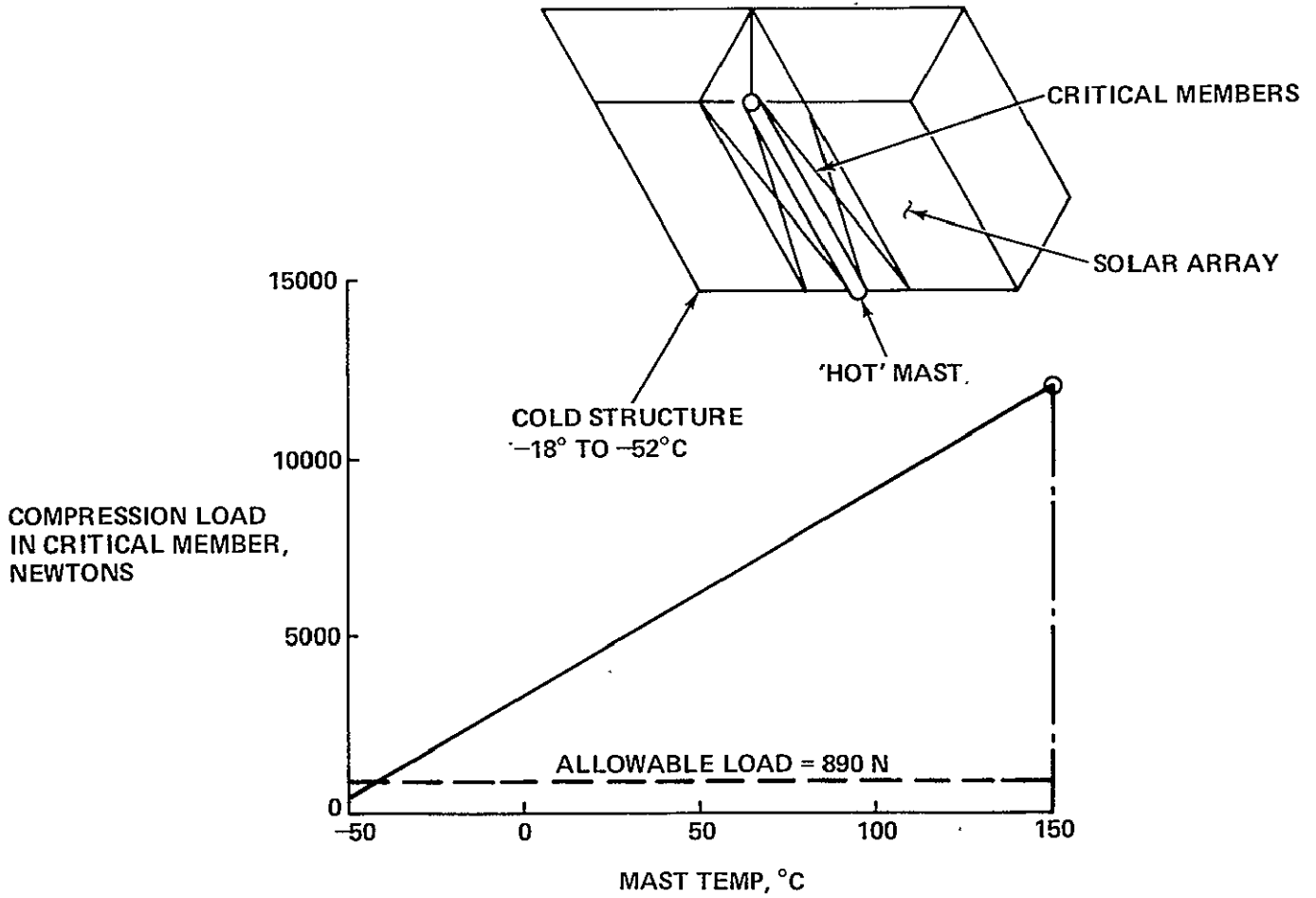


Fig. 5-74 Load in Critical Member

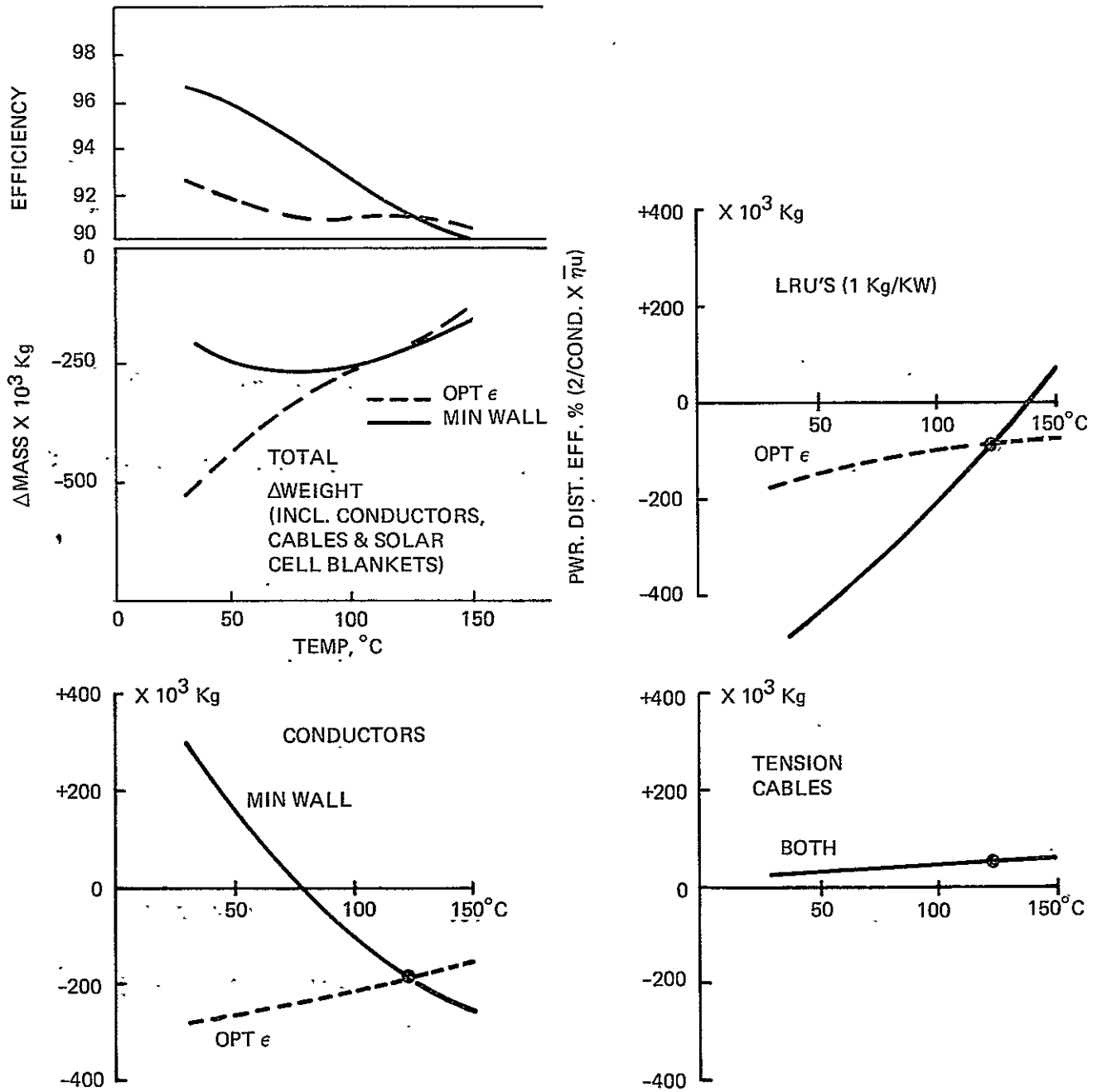


Fig. 5-75 Mass Savings & Power Distribution Efficiency Vs Conductor Temperature

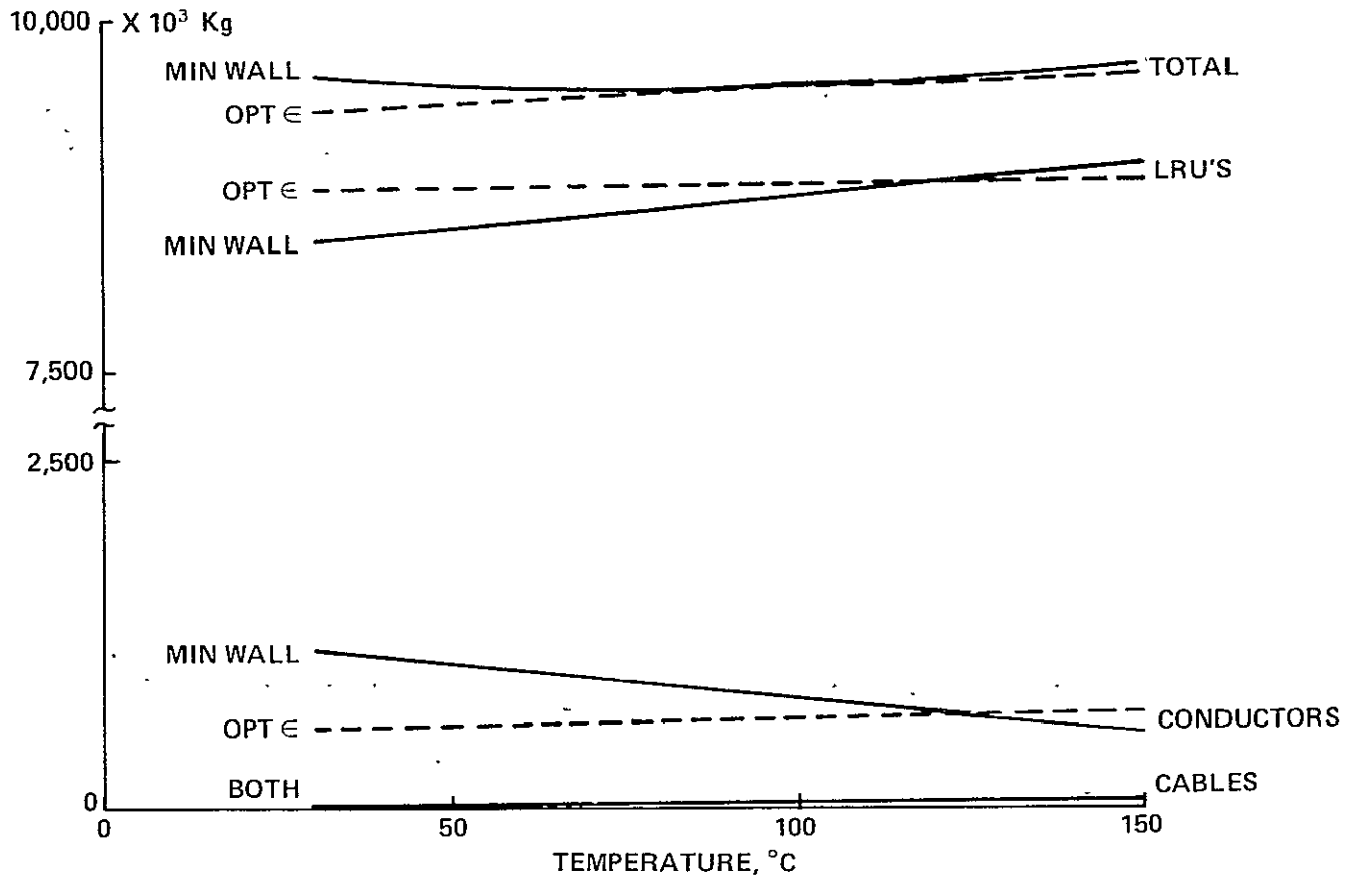


Fig. 5-76 System Weights.

5.2.4 Central Mast

The baseline structural configuration described in Reference 3 was greatly affected by thermally induced internal loads. Longitudinal expansion of the central mast relative to the solar array structure results in loads in excess of any induced by stationkeeping translational maneuvers. Also, more design detail was required to establish mast configuration, structural SSPS attachment, conductor support, fabrication complexity, and weight. Further design and analyses were conducted in this study to refine these areas.

Thermal Analysis

Previous studies assumed that worst-case thermal gradients, resulting in maximum mast deflections, occurred during SSPS entry into earth shadow. An analysis of structure/conductor transient cool-down was conducted to verify these assumptions.

Figure 5-77 shows that the actual temperature gradients between conductors and structure are quite small over a range of initial conductor temperatures from 30°C to 150°C. Even for a non-optimum conductor design, temperature gradients during eclipse are no more than one-third of those for the sunlight condition. Structural design requirements should, therefore, be based on sunlight conditions.

Thermal Stress

The magnitude of the compression stresses induced in the mast due to the thermal load at 122°C is shown in Figure 5-78. The maximum ultimate stress is $68.2 \times 10^6 \text{ N/M}^2$ (9900 lb/in²). As the surface of the conductor serves as a radiator, a means of preventing local instability is to have the conductors made up of multiple tubes. In order to satisfy structural requirements, a total of 24 tubes is required as opposed to the 12 shown in Reference 3. As described in 5.2.3, above, the central mast support cables must be strengthened to account for thermally induced loads. This weight penalty was included in the total weight change analysis depicted in Figures 5-75 and 5-76.

Mast Configuration/Weight

Figures 5-79 and 5-80 show the proposed mast configuration and support frame. The 24 conductors are arranged in a square, enabling the frames to be made up from beam members identical to those used elsewhere on the SPS. The mast is supported at intervals of 493 meters, by 20-meter triangular beam sections which also distribute current from the lateral buses to the central mast at every third station. All primary structural members are identical to those described in Reference 3. Between the main supports, 25 frames are used to stabilize the conductors.

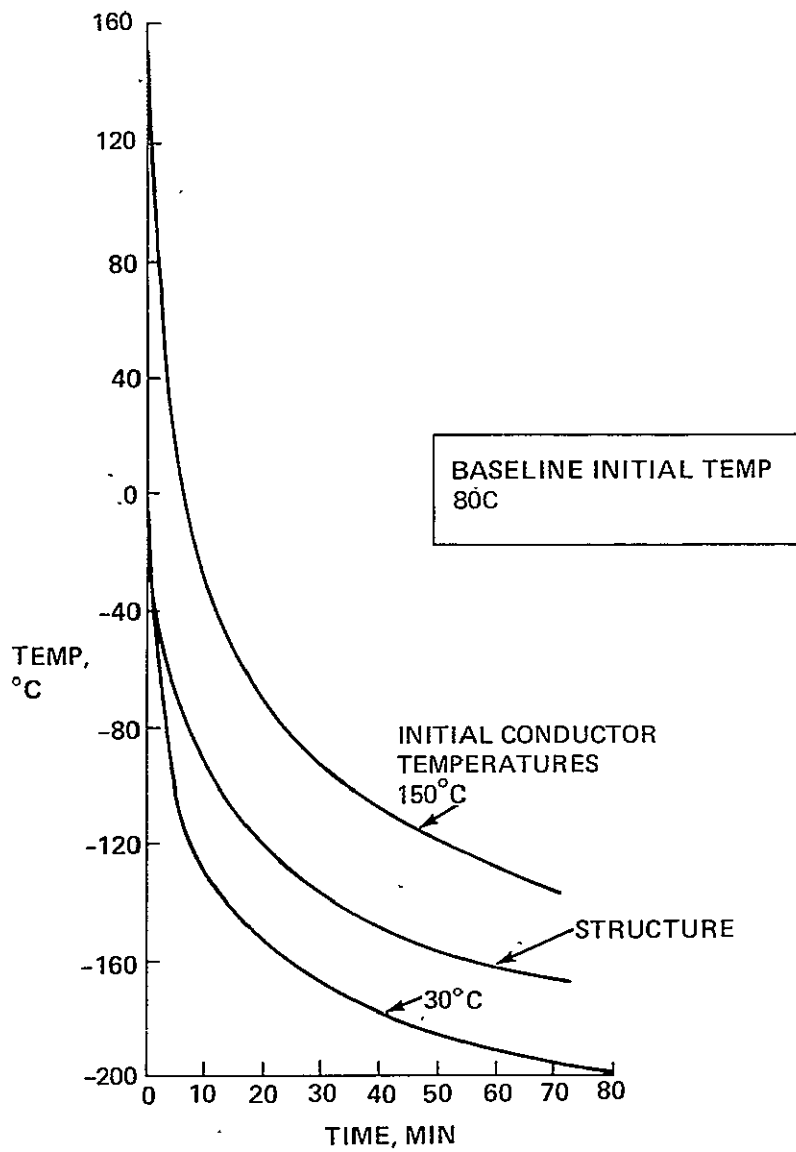
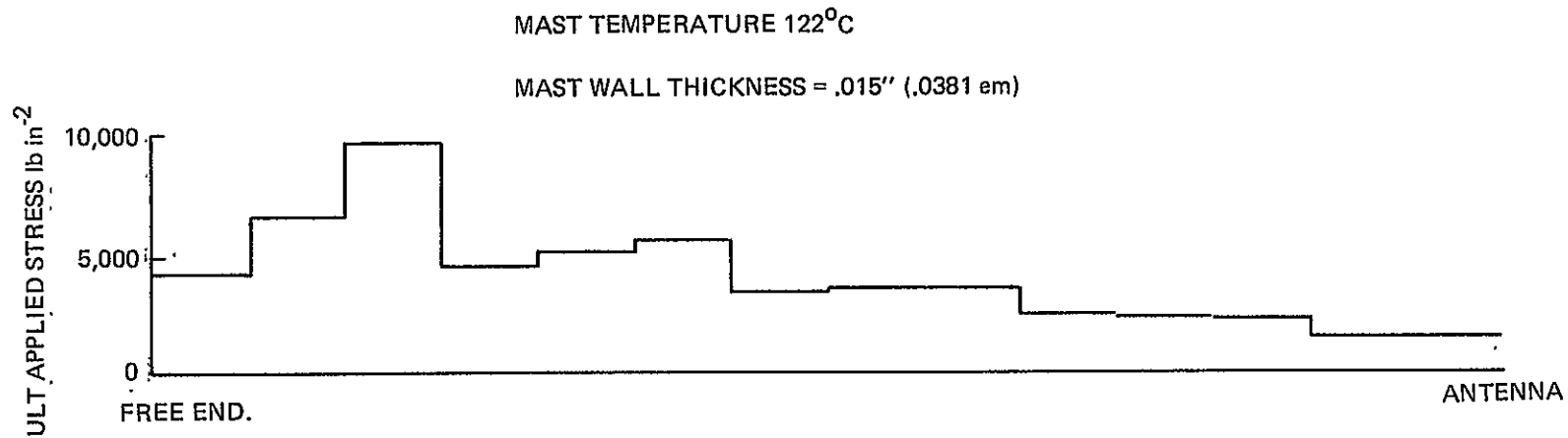


Fig. 5-77 Power Bus Eclipse Transient Cool-Down



135

	BM1	BM2	BM3	BM4	BM6	
AREA M ²	29.9 x 10 ⁻⁴	90.7 x 10 ⁻⁴	153.2 x 10 ⁻⁴	216.9 x 10 ⁻⁴	249 x 10 ⁻⁴	REF. 2
APPLIED fMAX (ULT LB IN ⁻²)	9900	5550	3700	2560	1740	
APPLIED fMAX (ULT N/M ²)	68.2 x 10 ⁶	38.3 x 10 ⁶	25.5 x 10 ⁶	17.6 x 10 ⁶	12 x 10 ⁶	
CURRENT KA	+23.4	23.4 & -47.6	71.9 & -47.6	71.9 & -97.3	97.3 & -97.3	REF. 2
NUMBER OF CONDUCTORS	12	12 12	12 12	12 12	12 12	
ALLOWABLE F LB IN ⁻²	11140	11140 5475	3625 5475	3625 2678	2678 2678	F = .36 t/R
TUBE RAD cm	10.26	10.26 20.88	31.34 20.88	31.54 42.68	42.68 42.68	* R = 5.264 KA REF. 3

ORIGINAL PAGE IS
OF POOR QUALITY

Fig. 5-78 Thermal Stresses in Mast & Conductor

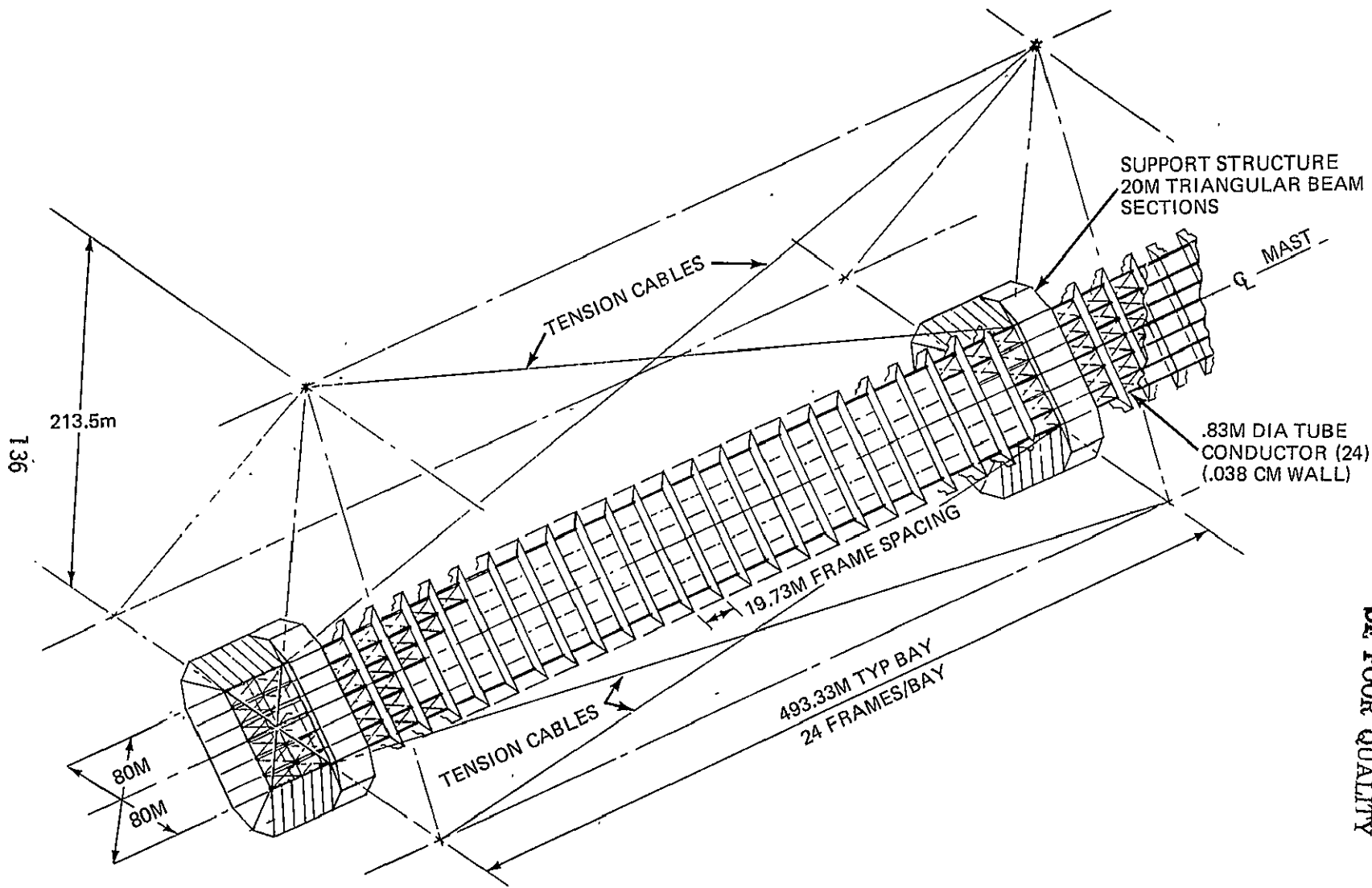


Fig 5-79 Conducting Structure

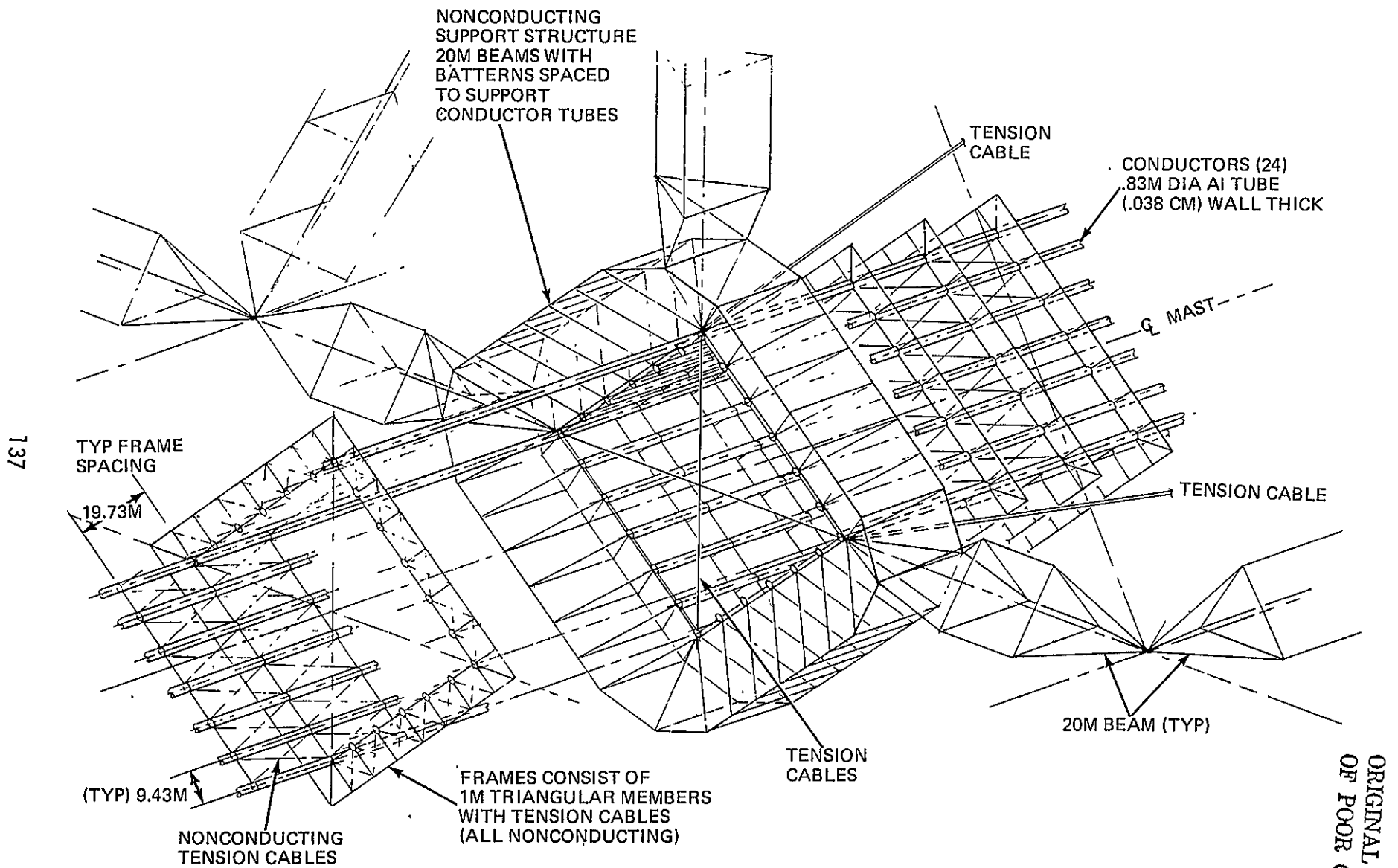


Fig 5-80 Square Mast Support Structure

ORIGINAL PAGE IS
OF POOR QUALITY

These frames are made of 1-meter triangular non-conducting members. The conductors are circular tubes of .038 cm wall thickness. Conductor radii correspond to those shown in Figure 5-71 for the currents indicated in Figure 5-72. The shear connections between the mast and the structure, and between adjacent conductors, are made by non-conducting, pretensioned, diagonal cables.

Major mass elements of the square, central mast structure are listed below.

	<u>LBS</u>	<u>KG</u>
Conductors (Tubes) (A1)	1,131,165	513,096.44
Struct Wires (10M X 20M Panel) (Comp)	300,018	136,088.16
648 Frames (1M X 10M) A1/Comp	1,821,187	826,090.42
26 Supports (20M Beam) (A1)	154,648	70,148.332
Struct Wire (493 M Bays) (A1)	55,559	25,201.562
TOTAL	<u>3,462,577</u>	<u>1,570,625.</u>

A1 - Aluminum

Comp - Composites

The total weight of the central mast is about three times that of the conductors alone. The excess weight evolves from requirements for conductor support/isolation, structural support, and attachment.

Multiple Conductor Options

In addition to a weight penalty, the complex structure required for the central conducting mast concept poses potentially difficult space fabrication problems. This might be resolved by the use of multiple longitudinal main conductors in lieu of a single central mast. Mass estimates were derived for two options of this type and are summarized below.

<u>Configuration</u>	Δ MASS - Kg X 10 ³				
	<u>Support Cables</u>	<u>Conducting Structure</u>	<u>Lateral Buses</u>	<u>Central Conductors</u>	<u>Total</u>
3 Conductors	+74	- 27	0	132	+179
9 Conductors	- 5	-121	-137	209	- 54

Mass for the various conducting elements are compared to those for the Reference 3 baseline with central mast support cables strengthened to accommodate 150°C (non-optimized) conductors. The same non-optimum conductors were assumed for each configuration. Much greater weight improvements will result from optimized conductor design.

Distributing structural/thermal loads over a large number of main conductors should result in lighter, less complex designs compared to the use of a single central conducting mast.

5.2.5 Rotary Joint/Slip Rings

Structural layouts and mechanical details of the rotary joint are described in Section 5.1. A general arrangement is shown in Figure 5-81.

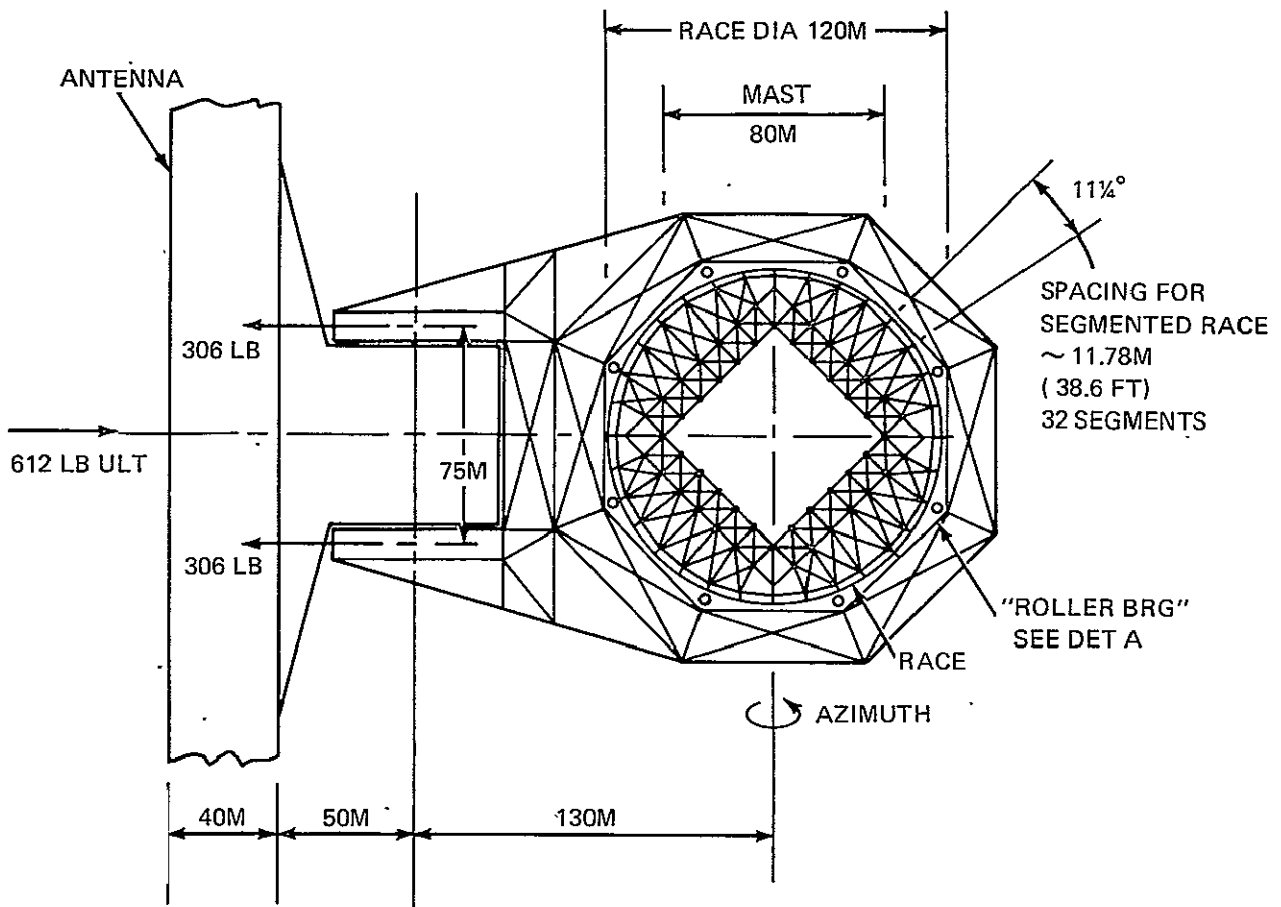
Electrical Design

The rotary joint consists of two groups of slip ring assemblies (one for positive current, one for return) around the central mast. Surrounding this is the rotating microwave antenna assembly, containing brushes fixed to its structure. The brushes slide with the antenna, moving over the slip rings fixed to the mast.

The slip rings are coin silver, while the brushes are a self-lubricating alloy of silver and niobium diselenide (NbSe_2). The very low rotational speed (1 revolution per day) results in a very low brush speed (0.29 cm per minute for an 80M mast diameter). As considered in Reference 3, brush/ring arcing does not appear to be a problem at this low speed. With the addition of an oil vapor lubricant to supplement the solid NbSe_2 in the brushes, and with proper seals and lubricant reservoirs, the estimated life for this type of design is over 100 years.

Each slip ring group contains multiple parallel rings to enhance reliability. With this concept, each group contains five parallel rings, any four of which can carry the full current. For the total current flow of approximately 200 KA, each ring is sized at 50 KA. The fifth ring protects against a single-point failure, and provides maintenance flexibility in which wearing brushes are periodically replaced. Eight brush-mount assemblies, each containing four brushes, are equally spaced around each ring, for a total of 32 brushes per ring.

Use of a large number of rings and brushes distributes brush/ring interface heating. The interface voltage drop is estimated at 0.08V for an interface current density of 7.75 A/cm^2 , generating 0.62 w/cm^2 of heat. Based on four rings carrying 200 KA, each brush will carry 1.5625 KA. Current sizing at 7.75 A/cm^2 yields an area of 202 cm^2 per brush, and heat generation of 125 watts per brush. The heat generated per brush is not extraordinary when compared to the heat generated in the power conductors feeding the brushes. At a current of 1.5625 KA,



GENERAL ELECTRICAL PARAMETERS

- | | |
|--|---|
| <ul style="list-style-type: none"> • 5 SLIP RINGS EACH FOR (+) & (-) CURRENT • 32 BRUSHES PER SLIP RING • ANY 4 SLIP-RINGS CAN CARRY TOTAL CURRENT (~200KA) | <ul style="list-style-type: none"> • MAX VALUE @ 50 KA/RING: <ul style="list-style-type: none"> - 1.563 KA/BRUSH - BRUSH CURRENT DENSITY 7.75A/CM² - HEAT GENERATION 125 WATTS/BRUSH - INTERFACE VOLTAGE DROP < 0.10 VOLT |
|--|---|

Fig. 5-81 Rotary Joint Electrical Details

each meter length of brush feeder will generate 523 watts of heat due to conductor resistance. The low level of extra interface heating is, therefore, not considered to be a problem.

5.2.6 Major Study Findings

Several significant findings have evolved from these refined analyses of the SSPS power distribution system. Although these studies were specific to the baseline configuration described in 5.5.2, most conclusions should apply to solar photovoltaic satellite power systems, in general.

Conducting Structure

- System weight/efficiency optimization must consider power source sizing and structural/thermal design requirements
- Conductor operating temperature has a small effect on total system weight
- Minimum practical wall thickness for tubular aluminum conductors is .038 cm (.015 in)
- Baseline system weight is minimized with .038 cm.-thick conductors operating at 80°C and a current density of 640 A/cm²
- Corresponding array power distribution efficiency is 94 percent, with array utilization efficiency greater than 99 percent under steady state operation
- Strengthening of central mast support cables to account for mast/array thermal gradients results in a small weight penalty.

Central Mast

- Conductor/structure temperature gradients during eclipse cool-down are much smaller than originally assumed. Sunlight conditions represent worst-case structural design requirements
- Detailed design of the central mast becomes quite complex in order to distribute conductor heating/structural loads, and provide conductor support/isolation and array attachment, posing potentially difficult space fabrication problems

- Use of multiple main power buses in lieu of a central conducting mast, promises a lower weight, simpler system.

Rotary Joint/Slip Rings

- The concept of a large rotary joint with multiple redundant slip rings and brushes appears feasible
- Transfer of high currents through multiple rings/brushes should pose no special problems regarding current densities, heating, voltage drop, or operating life.

5.2.7 Recommendations

- Optimization analyses should be expanded to include variable solar array specific weights and alternate structural design approaches
- Electrical/structural/thermal analyses of design options for the power distribution system should be performed, to include:
 - Use of multiple main power buses
 - Non-structural central conductor
 - Non-conducting structure with separate power conductors
- Alternate rotary joint/slip ring concepts should be developed, including multiple redundant brush contact and liquid metal slip rings
- The in-space fabrication complexity of alternate conductor arrangements and rotary joint designs should be assessed.

5.3 Program Planning Analyses

Earlier program plans which were developed in this study, indicated that the use of large scale test satellites, prior to full scale system deployment, were not economically favored. The methodology used to evaluate these plans was based on a decision tree analysis, wherein the net expected value of each program plan was determined. The measure of acceptability of a program plan was measured by the magnitude of its expected value; the "best plan" being that which maximizes the positive expected value.

Using the methodology developed in these earlier studies, efforts were initiated to evaluate the economic viability of two other alternate development programs. Both employed a 150-KW test satellite in the 1983 time frame, and a 2-MW test satellite in the 1986 time frame. These test satellite approaches were intended to provide data/information necessary for SSPS technology verification. Differences within these alternate programs related to the operating orbit altitude of the 150-KW test satellites, and the extent of early microwave antenna testing. The principal findings obtained from these studies are:

- o An overall SSPS Technology Verification Program, with direct expenditures of about \$3.0 to \$3.5 Billion could provide the ability to exercise the SPS concept as a major source of our country's energy for the late 1990's time frame
- o The use of small-scale test satellites (150-KW to 2-MW range) does not require the development of high cost transportation elements (HLLV) for their deployment. This approach postpones the development of these systems, until sufficient technical confidence relative to an overall full-scale SSPS development is obtained
- o Early, small-scale test satellites would principally address microwave power transmission issues, to provide a high degree of confidence in the operation of a subsequent large scale system. Analyses indicate that early test satellites are favored at geosynchronous altitude
- o The use of small-scale test satellites during the technology verification phase can apparently provide sufficient technical depth from which a decision to proceed with a large-scale prototype can be made.

In another earlier related study, analyses were conducted to evaluate both unit production cost, and risk associated with the production of a baseline 5-GW crystal silicon SSPS. A statistical model, which considered effects of more than 150 parameters, showed that both the SSPS cost and risk were principally sensitive to a small number of parameters (Ref. 9). These included the uncertainties in cost of the rate of manned and remote assembly, solar cell efficiency, and the specific mass

of the solar array blankets. Consequently, an effort was initiated to define the ground development programs and costs that would provide a measure of the uncertainties in these areas. The program plans and costs are presented herein.

5.3.1 Alternate Development Programs and Costs

As a result of earlier analysis, which indicated that large-scale test satellites were not economically favored, two alternate SSPS programs, utilizing smaller-scale satellites in the technology verification phase, were formulated and evaluated.

Fig. 5-82 shows the first of the two alternate overall SSPS programs considered. The program was patterned after one formulated by the NASA/MSFC in-house studies (ref. 10). In this program, a satellite designed to provide 150-KW of power continuously, in low earth orbit, would be deployed in the 1983 time frame. This activity would be preceded by a ground development program, focusing on key technology areas as summarized in Section 5.3.2. A series of Shuttle sortie missions was also planned in the early 1980 time frame, for purposes of addressing man's capability to construct large structures in the space environment.

The 150-KW continuous power satellite in LEO consisted of twin solar array panels. These were joined through supporting structure, and measured 154 meters in length, as shown in Fig. 5-83. Details of this configuration were developed during a six week NASA/MSFC in-house study, summarized in Ref. 11. For convenience of the reader, figures from this study were extracted and included herein. The solar arrays were designed using a 0.7-meter beam structure, fabricated in orbit via shuttle sortie missions. The baseline solar cells were advanced silicon of approximately .020 cm thick, with fused silica cover shades for LEO radiation protection. Overall efficiency was assumed at 14.0% AMO, with an expected degradation of approximately 11.1% over the first 5 yrs. of life. A flat solar array (concentration = 1) was selected, to minimize complexities with on-orbit construction.

Sub-module switching concepts were designed into the solar array panels, to provide parallel operation of all modules at 125-, 250-, or 500-volt outputs. Two parallel modules of the blanket can be put in series with two others, to yield a blanket output of 1000 volts, or all four modules selected to produce 2000 volts. External switching was also provided, to allow additional blankets to be put in series, for outputs of up to 20 KV.

An energy storage system was included to provide continuous power during periods of earth occultation. Nickel Cadmium batteries were baselined for this purpose.

Construction and assembly of the 150-KW test satellite was developed with the use of 2 Shuttle sortie missions, employing an assembly jig, a beam forming machine, and a two-segment pallet. Fig. 5-84 lists

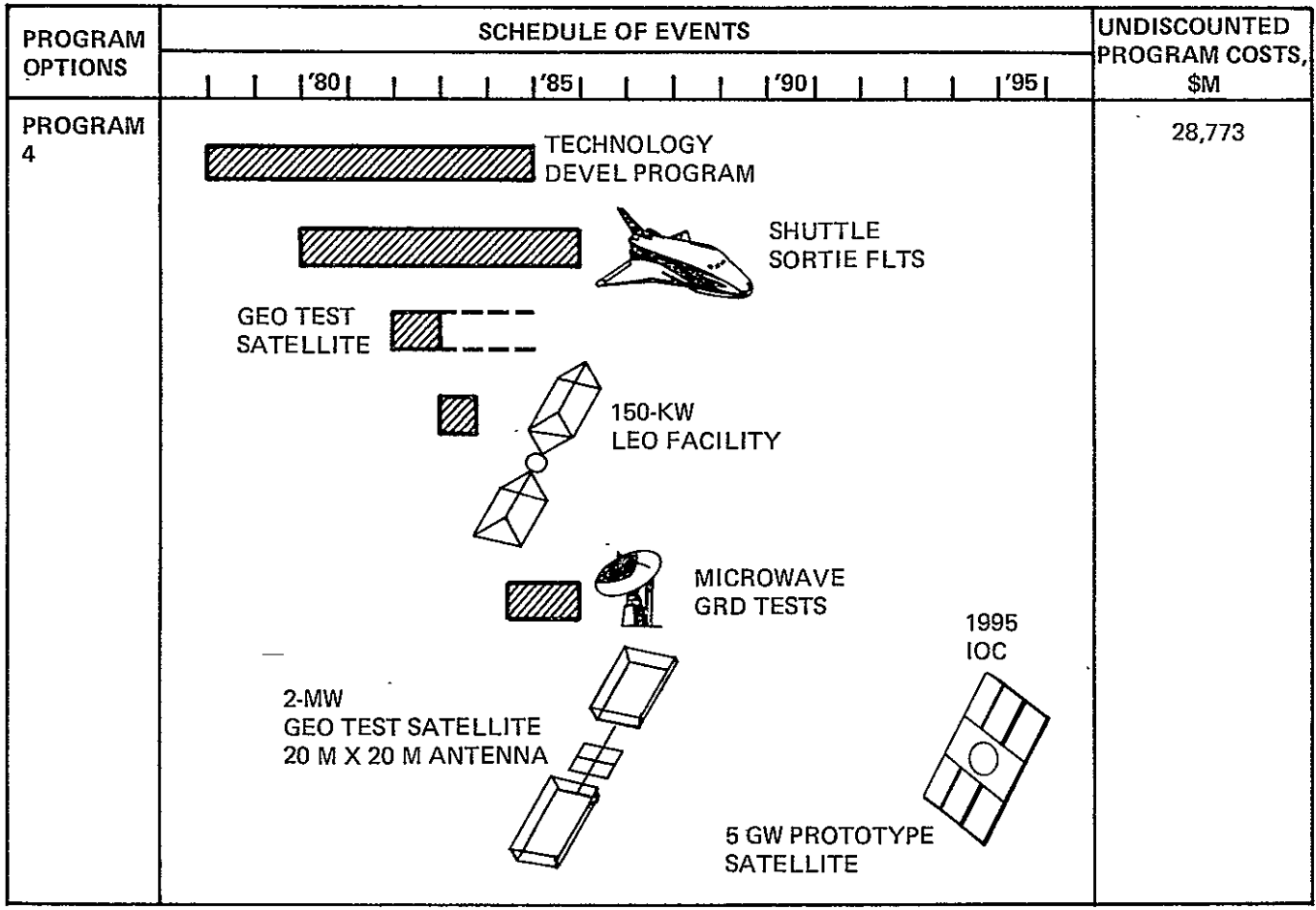
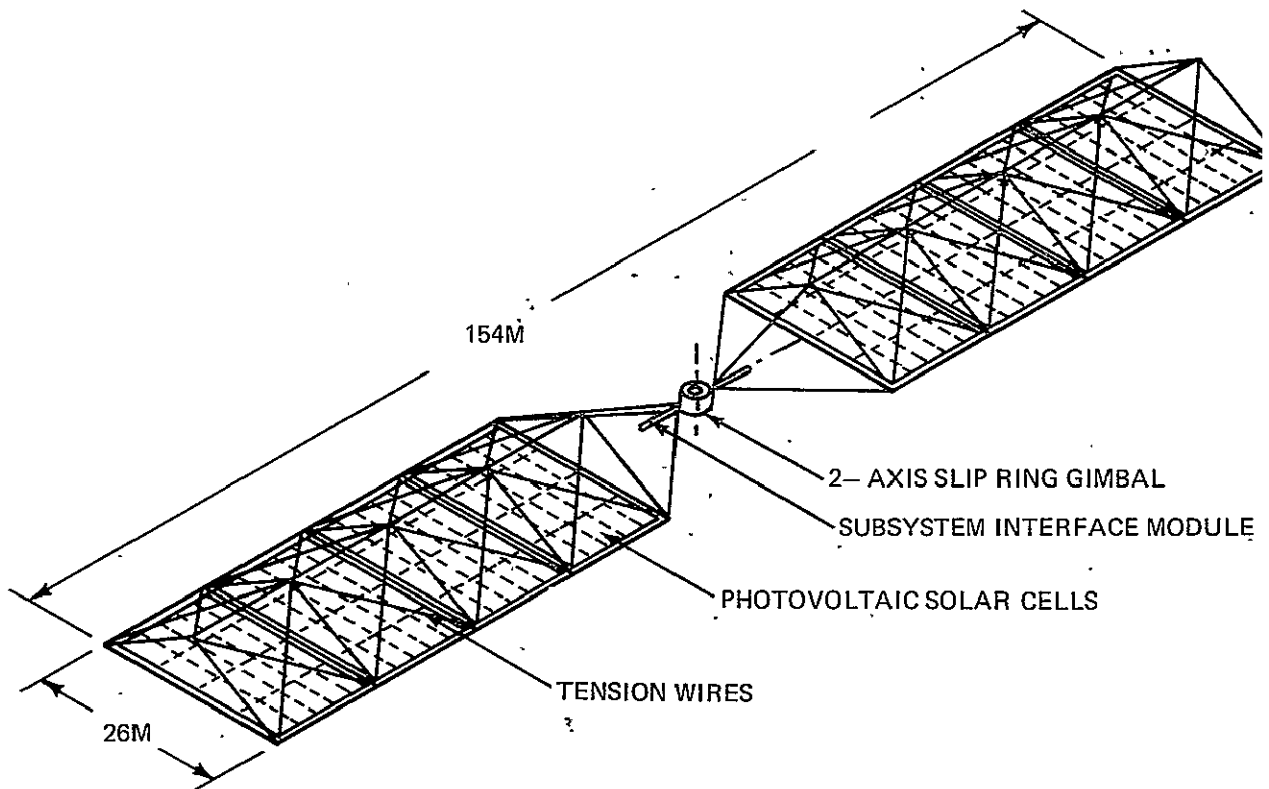


Fig 5-82 SPS Development Program 4



REF NASA/MSFC

Fig 5-83 150-Kw LEO Spacecraft Facility: Assembled Configuration

	FIRST FLIGHT-KG	SECOND FLIGHT-KG
SOLAR ARRAY	3157	2881
• SOLAR BLANKETS	(1436)	(1436)
• STRUCTURE	(506)	(506)
• POWER DISTRIBUTION	(495)	(495)
• PROPULSION SYSTEM	(340)	(203)
• PROPELLANT/YEAR	(380)	(241)
SUBSYSTEMS MODULE	3368-7888	4754-9274
• STRUCTURE	(500)	(500)
• DATA MANAGEMENT	(59)	(4)
• COMMUNICATIONS	(59)	—
• ROTARY	—	(1500)
• POWER COND & DIST	(750-1750)	(750-1750)
• ENERGY STORAGE: FUEL CELL/FLYWHEEL/ BATTERY	(2000-5520)	(2000-5520)
BEAM MACHINE	3200	3200
ASSEMBLY JIG	4500	
PALLET	1300	1300
ADDL MANIPULATOR	340	340
TOTAL	15865-20385	12475-16995

REF: NASA/MSFC

Fig 5-84 150-Kw LEO Spacecraft Facility Launch Mass

the materials and subsystem mass carried to orbit in each of the two Shuttle flights. The SPS assembly fixture is made up of 16 telescoping astro mast booms deployed from the Shuttle bay. The fixture is also equipped with a conveyor system to move sections of the satellite as the fabrication is completed. Fig. 5-85 illustrates the assembly sequence in this construction sequence, showing the fabrication process and the "sliding" of these sections as they are completed. Fig. 5-86 depicts the solar array wing completed during the first Shuttle flight. The assembly jig is left with the satellite array structure, while the orbiter returns to the launch site with only the beam forming machine and pallet. A second Shuttle flight docks to the assembly fixture to construct and join the second solar array panel to the first.

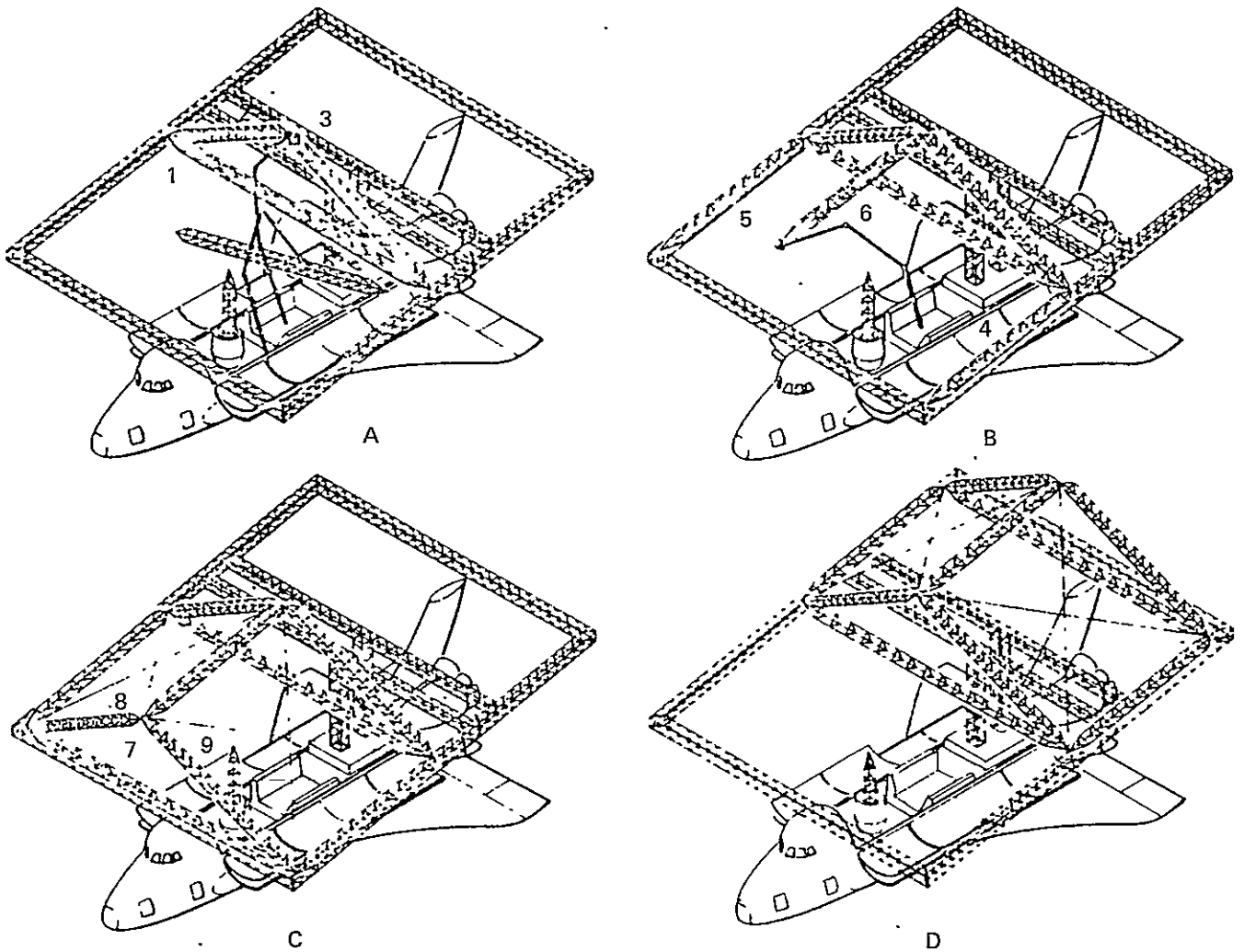
The satellite can be maintained in low earth orbit to analyze and assess several key objectives. These include solar array performance, the structural/control interactions of large structures, the distribution and transfer of high-voltage power through rotary joints, etc. Potential follow-on activities for the satellite include its use for Space Station/construction platforms, and for subsequent in-orbit construction activities. The technical understanding obtained from this test satellite would serve to define configuration concepts for a 2-MW test satellite, to be used to verify integrated SSPS technology.

The 2-MW test satellite facility, placed in geosynchronous orbit, is illustrative of an opportunity to demonstrate end-to-end operation of a scaled SSPS. The satellite is constructed in Low Earth orbit, using construction platforms and then transferred to GEO, using a cryo OTV. The mass of the satellite is estimated at 20,000 Kg.

Attached to the 2-MW satellite is a 20-meter by 20-meter antenna subarray, representative of typical full-scale antenna subarrays. The ground receiving station consists of instrumentation networks configured to measure power densities and phase front control relationships over selected areas of the received ground pattern.

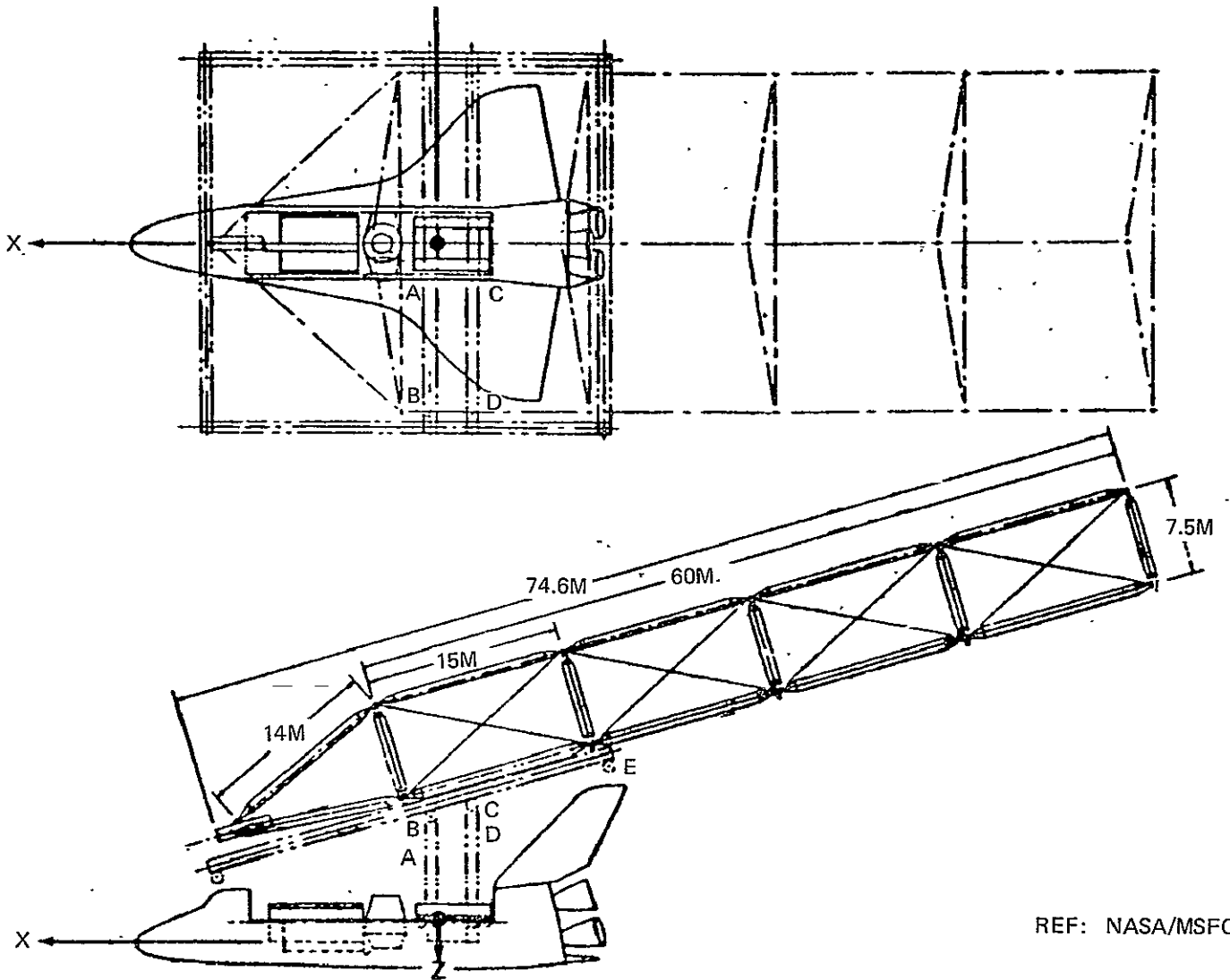
Figure 5-87 summarizes the overall program development costs estimated for Program 4. Fig. 5-88 shows the cost breakdown for developing the 150-KW LEO test satellite, as estimated by NASA/MSFC. DDT&E and unit production costs for the 2-MW facility were estimated using the Koelle Cost Model (Ref. 12). A cost estimating relationship was used, relating total system costs for application satellites, as a function of the percentage of new technology required in its development. For this estimating analysis, the 2-MW facility was assumed to represent a 60% technology complexity factor in the Koelle Cost Model.

Transportation and assembly costs for the 2-MW satellite were estimated as shown in Fig. 5-89. Five Shuttle flights provide the delivery of habitation modules and construction equipments to low earth orbit, for the assembly of a construction facility. Four additional



REF: NASA/ MSFC SPACE POWER
 DEMONSTRATION SYSTEM
 SIX-WEEK STUDY, NOV. 1976

Fig 5-85 150-Kw LEO Spacecraft Facility: Assembly Sequence



REF: NASA/MSFC

Fig 5-86 Shuttle Construction Of 150-KW LEO Facility

		EXPENDITURE PERIOD		
SUPPORTING RESEARCH & TECHNOLOGY PROGRAM	• SOLAR ARRAY	368.9	1978 - 1985	
	• MICROWAVE	70.4		
	• STRUCTURE	39.3		
	TOTAL	478.6		
GEO SATELLITE TEST PROGRAM	55	1982		
MICROWAVE GROUND HEATING TESTS & FACILITIES	80	1983 - 1987		
SHUTTLE SORTIE FLTS	598.9	1980 - 1985		
TOTAL	733.9			
	DDT&E	UNIT PROD	ASSEMBLY OPS	
150-KW CONTINUOUS PWR SYSTEM IN LEO	110*	20*	48	
2MW FACILITY (20 M X 20 M MICROWAVE ANT.)				
• SOLAR ARRAY	166	52		
• ANTENNA INTERFACE	61	8		
• TRANSMITTING ANTENNA	260	156		
• RECEIVING ANTENNA		7		
SUBTOTAL	487	223		
MANAGEMENT, S&I (40%)	194.8	89.2	343	
UNCERTAINTIES (20%)	97.2	44.6		
TOTAL	779.2	356.8		
FIRST PROTOTYPE 5GW SYSTEM			\$233/KG	
• SOLAR ARRAY	3922	1973		
• ANTENNA INTERFACE	560	170		
• TRANSMITTING ANTENNA	686	1250		
• RECEIVING ANTENNA	1583	3410		
SUBTOTAL	6751	6803		
MANAGEMENT, S&I (40%)	2700.4	2721.2	4217	
UNCERTAINTIES (20%)	1350.2	1360.6		
TOTAL	10801.6	10884.8	4217	
GRAND TOTALS	12903.3	11261.6	4608	\$28,772.9M

Fig 5-87 Program 4 Costs (\$M)

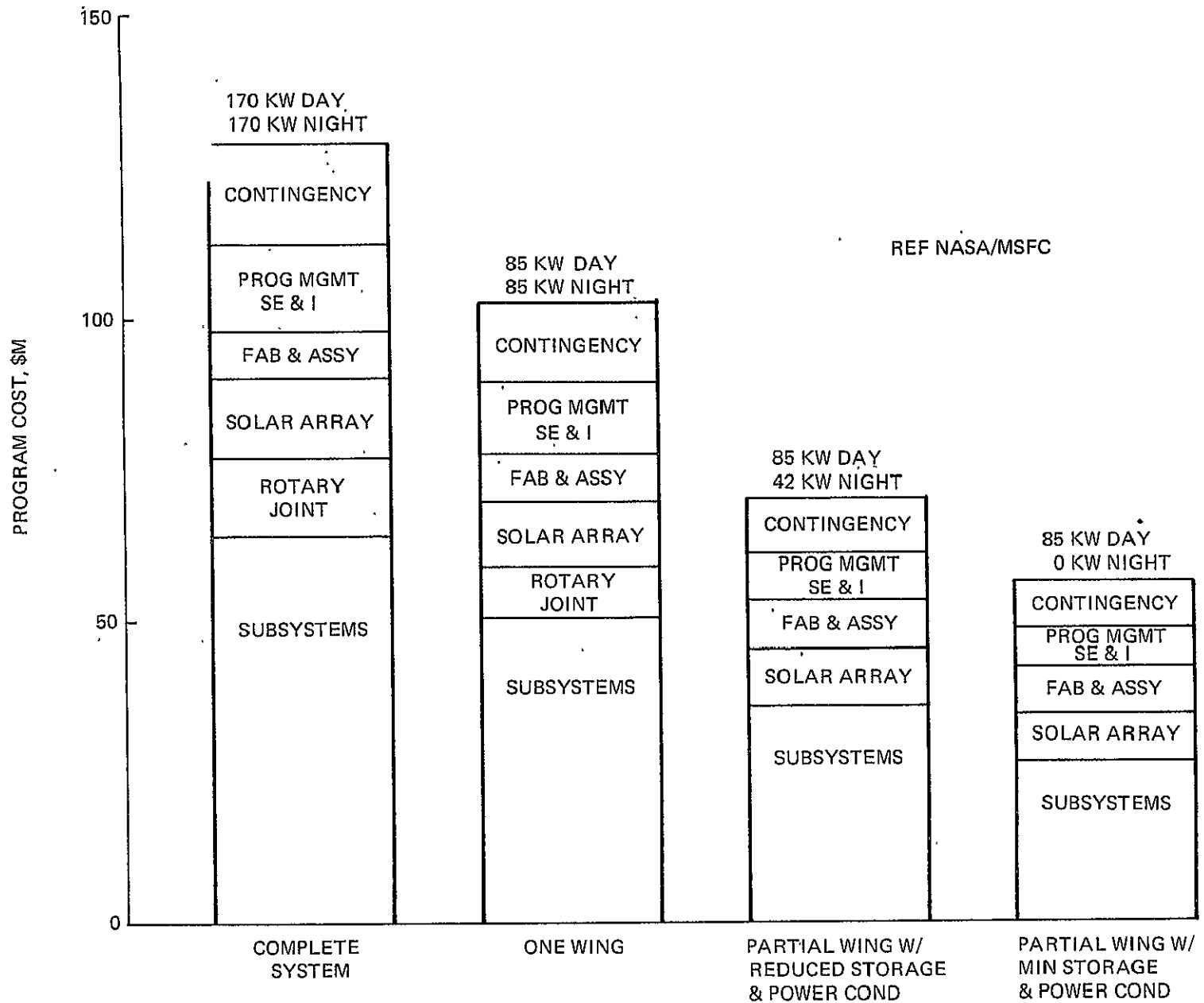


Fig 5-88 Space Power Demonstration System: Typical Program Options

	NO. OF UNITS	EQUIP. COST, \$M	WT TO LEO, KG	NO. OF SHUTTLE FLTS	COST, \$M	
• LEO SPACE STATION	1	50	80	}	50	
• ASSEMBLY EQUIP.						
– PALLET	1	} 16	1			49
– MANIPULATOR	1		4			
– FAB MODULES	3	24	15		} 5	60
– EVA EQUIP	6	9	20			
• MISCELLANEOUS						
• SUPPLY						
– SPACE STATION RE-SUPPLIES			20	}		
– MISCELLANEOUS			3.5			
• CRYO OTV						
– USEFUL PROPELLANT			66	} 3	36	
– STRUCT, PROPELLANT TANKS			11.2			
• MATERIAL			20,000	1	12	
• PERSONNEL					1	
• AMORTIZE L/V					27	
• CREW ROTATION				9	108	
					343	

Fig 5-89 Program 4: Transportation & Assembly Costs for 2-MW Demo Sat. & Preconstr Support (2-Yrs Preconstr, 4 1/2 Months Constr Time)

flights are needed to transport the satellite materials and the cryo-stage and propellants to the LEO construction facility. These are used for transporting the completed satellite to GEO.

The second alternate program considered in this study, Program 5, is shown in Fig. 5-90. The program evolved out of the collective efforts of the study team members, and was designed to improve upon the areas of Program 4 deemed high in risk. As shown, the program is similar to Program 4, with two exceptions. First, the small scale 150-KW test satellite is operated in the GEO environment, and includes a linear microwave antenna. Second, the 2-MW test satellite operated at GEO, includes a large linear antenna in addition to a subarray antenna, to perform a more extensive microwave evaluation and verification. In this scenario, the 2-MW facility represents the major activity for verifying SSPS technology. Therefore, it should be designed with a high degree of operational confidence. This led to the conclusion that early testing of microwave transmission is essential. A key issue is the effects of the interaction of the pilot beam with a heated ionsphere, for phase front control. Addressing this issue early in the technology verification phase, produces the key technical data needed to design the control system, to be demonstrated with the 2-MW test facility. Thus, the 150-KW test satellite, equipped with a 100-meter linear antenna and operating at GEO through a ground-heated ionsphere, provides this data. Raytheon has identified candidate ground system heater concepts that can be considered (Ref. Vol. III). Cost estimates of this facility have been included in the overall program costs.

Other key objectives to be addressed with the 150-KW satellite include evaluation of concentrator surfaces, and their effects on solar cell performance, and the interaction of the magneto plasma on high voltage arcing. A candidate satellite design is illustrated in Figure 5-91. Also shown are the baseline data used for spacecraft sizing. The overall layout was configured for compatibility with the shuttle's construction capability. The satellite's width and depth were maintained within the reach of the manipulator system. Fig. 5-92 lists the satellite's estimated mass. Antenna properties were based on 20 amplitrans for each antenna string, incorporating three strings for operational redundancy.

The 2-MW Satellite facility in Program 5, includes a 1000-m linear antenna and a 20-meter x 20-meter antenna subarray to provide for evaluation of subarray heating characteristics. The linear antenna is intended to substantiate power density distributions on the ground anticipated with an operational SPS system, in a single plane.

Program 5 costs are summarized in Fig. 5-93. DDT&E and unit production costs were also estimated using the Koelle Model. The 150-KW facility was estimated using a 70% technology complexity factor; the 2-MW facility using a 50% factor. As in Program 4, cost estimates for the first prototype were based on data developed during Phase II studies.

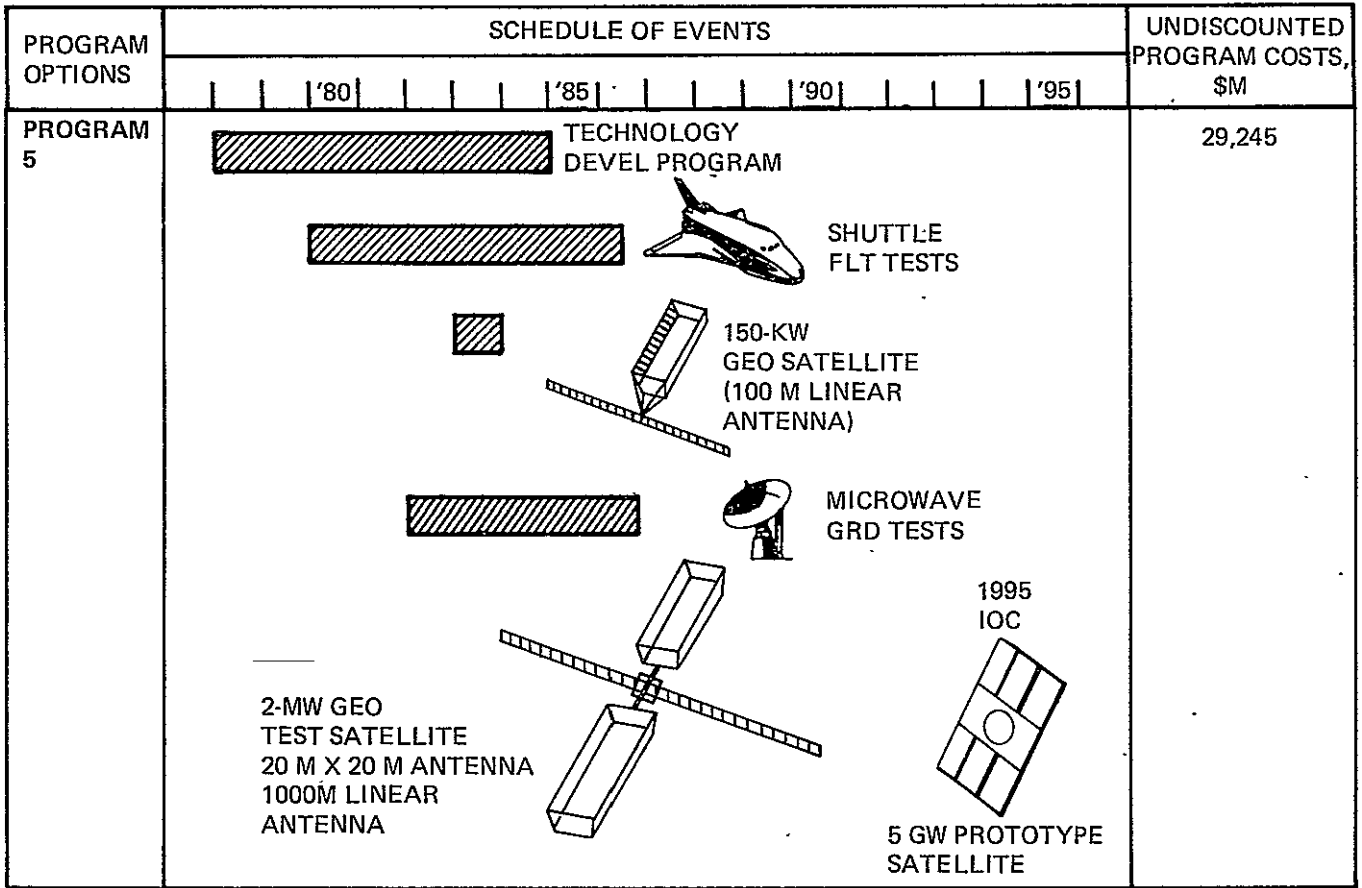


Fig 5-90 Alternate Program Options and Costs

- ASSUMPTIONS
 - DESIGN CONCENTRATION, 1.7
 - EFFECTIVE CONCENTRATION, 1.5
- EFFICIENCY
 - DC-RF CONVERSION, 85%
 - SLIP RING, 98%
 - POWER DISTRIBUTION, 95%
 - SOLAR CELL, 11%

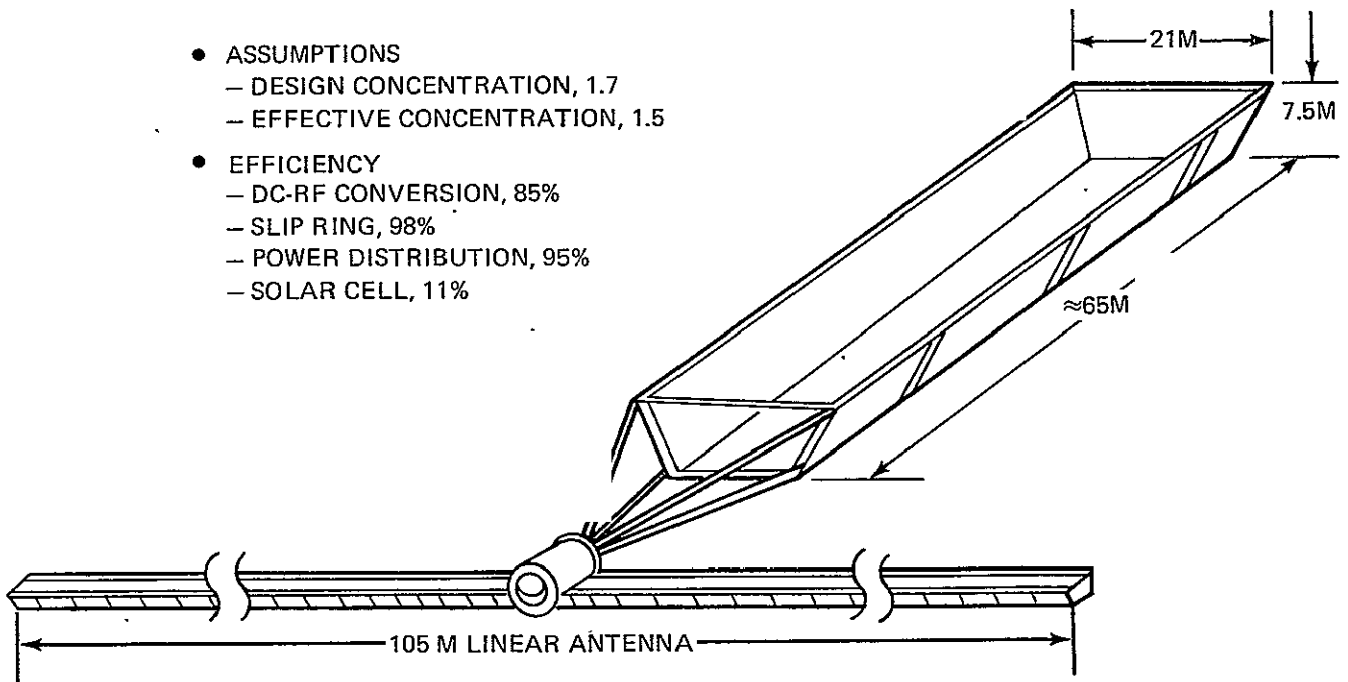


Fig 5-91 150-Kw GEO Test Satellite: Program 5

● SOLAR ARRAY	KG
– SOLAR BLANKETS	1400
– CONCENTRATORS	100
– ROTARY JOINT	1500
– PWR DISTRIBUTION	1000
– PROPULSION SYSTEM.....	350
– PROPELLANT/YR.....	500
● ANTENNA STRUCTURE	
– CONTROL MODULES.....	1100
– AMPLITRONS.....	96
– WAVEGUIDE.....	100
	6150
30% CONTINGENCY	850
	<u>8000</u>

Fig 5-92 150-Kw GEO Test Satellite Mass

ORIGINAL PAGE IS
OF POOR QUALITY

SUPPORTING RESEARCH & TECHNOLOGY PROGRAM				
• SOLAR ARRAY	368.9			
• MICROWAVE	70.4			
• STRUCTURE	<u>39.3</u>			
TOTAL	478.6			
MICROWAVE GROUND HEATING TESTS & FACILITIES	80			
<u>SHUTTLE SORTIE FLTS</u>	<u>598.9</u>			
TOTAL	678.9			
	DDT&E	UNIT PROD	ASSEMBLY OPS	
150KW GEO TEST SATELLITE (105 M LINEAR ANTENNA)				
• SOLAR ARRAY	76	16		
• ANTENNA INTERFACE	17	3		
• TRANSMITTING ANTENNA	28	17	102	
• RECEIVING ANTENNA	<u>-</u>	<u>7</u>	<u>-</u>	
SUBTOTAL	121	43		
MANAGEMENT, S&I (40%)	48.4	17.2		
<u>UNCERTAINTIES (20%)</u>	<u>24.2</u>	<u>8.6</u>	<u>-</u>	
TOTAL	193.6	68.8	102	
2-MW GEO FACILITY (20 M X 20 M SUBARRAY ANTENNA & 1.026 KM LINEAR ANTENNA)				
• SOLAR ARRAY	166	52		
• ANTENNA INTERFACE	111	8		
• TRANSMITTING ANTENNA				
– 1.026 KM LINEAR ANTENNA	28	115	370	
– 20 M X 20 M SUBARRAY	260	156		
• RECEIVING ANTENNA	<u>-</u>	<u>-</u>	<u>-</u>	
SUBTOTAL	565	341		
MANAGEMENT, S&I (40%)	226	136.4		
<u>UNCERTAINTIES (20%)</u>	<u>113</u>	<u>68.2</u>	<u>-</u>	
TOTAL	904	545.6	370	
FIRST PROTOTYPE 5-GW SYSTEM			\$233/KG	
• SOLAR ARRAY	3922	1973		
• ANTENNA INTERFACE	560	170		
• TRANSMITTING ANTENNA	686	1250		
• RECEIVING ANTENNA	<u>1583</u>	<u>3410</u>	<u>-</u>	
SUBTOTAL	6751	6803		
MANAGEMENT, S&I (40%)	2700.4	2721.2	4217	
<u>UNCERTAINTIES (20%)</u>	<u>1350.2</u>	<u>1360.6</u>	<u>-</u>	
TOTAL	10801.6	10884.8	4217	
GRAND TOTALS	13056.7	11499.2	4689	\$29244.9M

Fig 5-93 Program 5 Costs (\$M)

Assembly operations costs for the 150-KW satellite are significantly higher for Program 5. This reflects the cost of an additional Shuttle flight, and two 4-stage IUS flights, needed for transferring the satellite to GEO. Estimated assembly costs of the 2-MW facility are shown in Fig. 5-94.

These cost data, together with estimates of the successive technology improvement resulting from these test satellite operations, were used in the decision tree analysis. The technology improvements expected at the various points in the decision tree are presented in Appendix B. The results of the decision tree analysis, conducted by ECON to evaluate these development programs, are presented in Volume V of this report.

	NO. OF UNITS	EQUIP. COST, \$M	WT TO LEO, 10 ³ KG	NO. OF SHUTTLE FLTS	COST, \$M	
• LEO SPACE STATION	1	50	80	} 5 FLTS	50	
• ASSEMBLY EQUIP.						
– PALLET	1	16	1			49
– MANIPULATOR MANNED	1	16	4			
– FAB MODULES	3	24	15			60
– EVA EQUIP.	6	9	.5			
• MISCELLANEOUS			20			
• SUPPLY						
– SPACE STATION RE-SUPPLIES			20			
– MISCELLANEOUS			3.5			
• CRYO OTV						
– 110,000 KG PROPELLANT						
– 20,000 KG STRUCT & TANKS, ETC.		4	130	5	60	
≈ 5 SHUTTLE FLTS						
• CREW ROTATION & EXPMTS				9	108	
• MATERIAL TRANSPORT			35-45	1	12	
• PERSONNEL					1	
• AMORTIZED L/V					30	
TOTALS					370	

Fig 5-94 Program 5: Transportation & Assembly Costs for 2-MW Demo Sat. & Preconstr Support (2 Yrs Preconstr, 4 1/2 Months Constr Time)

5.3.2 Technology Development Plans

A major factor influencing both the technical and economical success of an overall SPS development program is the near-term technology development and verification program. This is true not only because it involves the earliest program expenditures, which in itself weighs heavily in the economic assessment, but also because it provides the technology base from which early major system design decisions are made. For these reasons, the technology development program, as formulated in the earlier studies, has been updated and is presented herein. The update addressed three specific technology areas, the rate of manned and remote assembly, solar cell efficiency and the specific mass of solar array blankets. Emphasis was placed on defining ground and orbital verification tests which would reduce their level of cost, and performance uncertainties.

A summary of overall near-term resource estimates, for key SPS technology areas, as updated thru this phase of the study, is shown in Fig. 5-95.

TECHNOLOGY AREA	CALENDAR YEAR					
	'77	'78	'79	'80	'81	'82
● Microwave	5.3	8.4	10.05	18.05	16.45	31.9
● Large Solar Array	13.8	16.0	18.8	22.5	24.25	22.75
● Structures	1.9	3.6	11.6	16.35	6.5	1.3
TOTALS:	21.0	28.0	40.45	56.9	47.2	55.95

Fig. 5-95 NEAR TERM RESOURCE ESTIMATES FOR KEY SPS TECHNOLOGY AREAS (M\$)

The updated Microwave Technology Development Program is summarized in Figures 5-96 thru 5-100. A risk rating, using the levels 1 through 5, together with a priority ranking are shown for each of the key issues. Cost estimates reflecting the development of the ground heating facility for heating the ionosphere during the 150 kw test satellite experiments (Reference: Programs 4 and 5) have also been incorporated. This data was supplied thru studies conducted by Raytheon and are further reported in Volume III of this report.

The Large Solar Array Technology Development Program, incorporating a ground/orbital demonstration and verification program, as defined in the Phase III studies, is shown in Fig. 5-101. The program reflects both the basic ERDA areas of development and the development efforts estimated for NASA as related to solar satellites applications. Fig 5-102 and 5-103 list the key issues with their associated ranking and priority.

TASK	Calendar Year									COMMENTS
	77	78	79	80	81	82	83	84	85	
1 ● DC-RF CONVERTERS & FILTERS	.5	.6	.4	.4	.4	.4				
● PHASE CONTROL	.4	.4	.3	.2	.2					
● WAVEGUIDE	.4	.4	.4	.4	.4	.2				
● SWITCH GEAR	.4	.4	.3	.2	.2					
● GROUND TEST (INCLUDE BIO TESTS)	2.4	2.5	2.2	3.3	5.3	7.0				
2 ● ATTITUDE CONTROL	.3	1.0	2.0	2.0	.4	.4				
● POWER TRANSFER	.2	2.0	3.0	6.0	1.0	.4				
3 IONOSPHERE EFFECTS	.4	.8	1.15	5.55	8.55	23.5	4.45	5.25	2.05	NEW HTG FACIL.
4 RADIO FREQUENCY	.3	.3	.3							
TOTAL	5.3	8.4	10.05	18.05	16.45	31.9				

Fig. 5-96 Microwave Technology Resource Requirements (\$ Millions)

ITEM	TECHNOLOGY RISK ASSESSMENT		COMMENTS
	RATING	RANKING	
DC-RF Converters & Filters	4	1	<p>BACKGROUND: Pre-amplifier amplifier & filters convert the high voltage DC power to RF power having low noise and harmonic content. There are at 0.1 to 1.5 million identical devices in one system. This is the highest single contributor to dissipation loss (15 to 19%) with the amplifier contributing 90% of that dissipation. The simplest design concept still results in the most complex mechanical, electrical and thermal set of technology development problems in the system. This combines with requirements for the development of a high production rate at low cost, resulting in reliable operation over a long life. What the noise & harmonic characteristics for the converters are and how they will act in cascade are not known. Filter requirements are to be determined. Ability to develop all the parts, interface them with each other and with the slotted array and operate them with full control and stability constitutes a high development risk and requires the longest lead time in an ambitious development program.</p> <p>TECHNICAL OBJECTIVES: Provide substantial data relating to technical feasibility, efficiency, safety and radio frequency interference.</p>
Materials	4	2	<p>BACKGROUND: Most critical and unusual requirements for materials in this application relate to the presence of the exposed cathodes for the RF generators. In addition, it is desirable that structural thermal strain be small so that distortions over the large dimensions are manageable. The waveguide distortions must be small to permit efficient phase front formation. The waveguide deployed configuration result in low packaging density so that it is desirable to form the low density configuration on orbit out of material packaged for high density launch. Before meaningful technology development can begin relating to fabrication, manufacture and assembly. It is necessary to determine the applicability of the non-metallic materials in particular as they relate to potential contamination of the open cathodes of the RF generators. Due to the critical interaction of materials with structures, waveguides and RF generators, the materials development risk rating should be a strong 4.</p> <p>TECHNICAL OBJECTIVES: Demonstrate cost effective use of non-metallic in terms of meeting distortion free waveguide and minimum impact on open cathodes performance.</p>
Phase Control Subsystems	4	3	<p>BACKGROUND: Phase front control subsystems projected scatter losses (2 to 6%) are second only to the microwave array losses (19 to 25%) in the microwave power transmission efficiency chain. The uncertainty associated with limiting losses to this value is significant. Phase control, being essential to beam pointing as well as focusing, must be shown to be reliable for power user and safety purposes. Risk rating should then be a strong 4.</p> <p>TECHNICAL OBJECTIVES: Demonstrate phase control steady state accuracy subject to error contributions of DC-RF converters and high power radio frequency environment.</p>

ORIGINAL PAGE IS
OF POOR QUALITY

Fig 5-97 Microwave Technology Requirements, Sheet 1 of 4

ITEM	TECHNOLOGY RISK ASSESSMENT		COMMENTS
	RATING	RANKING	
Waveguide	4	4	<p>BACKGROUND: Slotted waveguides interface with the RF generators in a high temperature environment. They must distribute the power and emit it uniformly with low losses. They represent a large % of the weight and are conceived to be of .020" wall thickness in aluminum or possibly non metallic composite layups with metallic coating. The ability to manufacture, fabricate and assemble such waveguides is not certain. To provide proper interfacing with RF generators, to limit distortion so as to operate satisfactorily as a subarray of slotted waveguides, and to do so within estimated cost and schedule constitutes high development risk. Risk rating should therefore be a strong 4+; however, significant materials technology development and selection must precede in depth technology investigations.</p> <p>TECHNICAL OBJECTIVES: Demonstrate capability of mass producing light weight, distortion free waveguides that can efficiently operate in a harsh thermal environment.</p>
Biological	4	5	<p>BACKGROUND: The CW microwave frequency and power densities to be investigated are rather well established. Effects to be anticipated in the sites yet to be selected are functions of ambient condition and the file forms peculiar to the region and those that are in transit. Most certainly areas like the desert southwest of the U S would be leading contenders so that effects on plants and animals should be investigated. Detailed investigations building on these conducted for more general purposes must be conducted to assure complete understanding of long term and transient effects and to provide the basis for securing national and international agreement on frequency allocations, intensities and exposure limits. Development risk rating should be 4.</p> <p>TECHNICAL OBJECTIVES: Demonstrate safety of microwave frequency and power densities being considered for SSPS use.</p>
Attitude Control	4	6	<p>BACKGROUND: Control of antenna pointing conceived to be accomplished by mechanical action between the antenna and main mast as well as between the ends of the main mast and the solar array primary structure in the vicinity of the slip rings. These are very large members, of light weight construction, having to transmit unprecedented power across the relative motion interfaces, to operate in the space environment, with high reliability and safety, at low cost, packaged for high density earth launch, deployed or assembled in space, for a very long time with limited operations and maintenance attention. The actuators to establish the motion, the moving joints and the moving or flexing conductors are the largest and most complex machinery employed in the photovoltaic powered station and will be the subject of most critical operations and maintenance analyses in order to design the machinery to be essentially maintenance-free. Nevertheless it must be designed to permit maintenance under most adverse conditions of damage and environment. Development risk rating should be 4.</p> <p>TECHNICAL OBJECTIVES: Demonstrate the accuracy and life potential of the microwave mechanical pointing system.</p>

Fig 5-98 Microwave Technology Requirements, Sheet 2 of 4

ORIGINAL PAGE IS
OF POOR QUALITY

ITEM	TECHNOLOGY RISK ASSESSMENT		COMMENTS
	RATING	RANKING	
Ionosphere	4	7	<p>BACKGROUND: Effects of the ionosphere on the phase control link are not known definitively, however existing data and analysis indicate that they are probably insignificantly small at the frequencies and power densities being considered. The effects on the ionosphere induced by the microwave power beam are believed to be small. However, from the point of view of other users of the ionosphere and its participation in natural processes there may yet be limits imposed on the power density. The theoretical approaches to doing this are known but the limits that may, yet be imposed are unknown. Development risk rating should be 4.</p> <p>TECHNICAL OBJECTIVES: Measure effects of microwave radiation on the ionosphere and determine social impact.</p>
Power Transfer	4	8	<p>BACKGROUND: The electrical power transfer function, at this large size and power level across flexing and rotating joints, cannot be separated from the mechanical and attitude control functions entirely. Although the technology for performing the functions is basically known, the large scale will present significant new problems. Development risk rating should be 4.</p> <p>TECHNICAL OBJECTIVES: Select power best power transfer design for SSPS and demonstrate performance.</p>
Switch Gear	4	9	<p>BACKGROUND: Switch gear had been conceived assuming multiple brushes from high voltage DC source transferred power to a single slip ring. Extraordinarily high currents in the switch gear resulted and would be the subject of a high risk (4+) technology development program. Decision has now been made to make the multiple brushes feed multiple sliprings, bringing the individual switch gear currents close to the region where the basic technology is known and the major advances would be in packaging for space operations. Risk rating should then be 4. Some aspects of the packaging technology having to do largely with size are not known, which leads to a risk rating of 4.</p> <p>TECHNICAL OBJECTIVES: Develop and demonstrate switch gear including protective elements for spaceborne applications.</p>

Fig 5-99 Microwave Technology Requirements, Sheet 3 of 4

ITEM	TECHNOLOGY RISK ASSESSMENT		COMMENTS
	RATING	RANKING	
Radio Frequency	4	10	<p>BACKGROUND: Radio frequency and bandwidth allocation is normally a long process involving national and international technology and socio-economic considerations. It will take 2 to 4 years of DC-RF converters' and filters' technology development to mature the concept and make available meaningful data. Convincing the national and international community involved that gigawatts of power beamed from space at an allocated frequency with a specified narrow bandwidth will not in fact result in significant interference requires a positive approach that is yet to be defined. When it is shown convincingly that power from space would (a) be a significant answer to the national and international future power needs and (b) permit frequency allocation and bandwidth to be defined without significant interference outside the band; then securing high priority for frequency allocation will be a normal process. The appropriate risk rating is 4.</p> <p>TECHNICAL OBJECTIVES: Investigate radio frequency interference and allocate band to SSPS that would have minimum impact on other users, particularly Radio Astronomy.</p>

Fig 5-100 Microwave Technology Requirements, Sheet 4 of 4

TASK		77	78	79	80	81	82	83	84	85	COMMENT	
SOLAR CELL/BLANKET TECHNOLOGY IMPROVEMENT(1)		TECHNOLOGY ←				→ PROOF OF CONCEPT						
	1. REDUCE RAW MATERIAL PROCESS COST	0.8 (0.1)	1 (0.2)	1.5 (0.3)	2 (0.5)	← (1) →		50				AUGMENT INDUSTRY/ERDA EFFORT
	2. REDUCE CRYSTAL GROWTH PROCESS	2.5 (0.5)	4 (1.0)	3.5 (1.0)	5 (2.0)	← (3) →		30				AUGMENT INDUSTRY/ERDA EFFORT
	3. BLANKET PROCESS	2.5 (2.5)	2.5 (2.5)	3 (3)	4 (4)	5 (5)	← (3) →		80			NASA SUPPORT SPACE-BASED BLANKET PROCESS DEVELOPMENT
	4. PERFORMANCE IMPROVEMENT	4 (4)	4.5 (4.5)	5 (5)	5 (5)	5 (5)	5 (5)	5 (5)	5 (5)	5 (5)	5	NASA SUPPORT SPACE-BASED BLANKET IMPROVEMENT
	5. ALTERNATE PHOTOVOLTAIC DEVICES	3 (3)	3 (3)	3 (3)	4 (3)	5 (5)	5 (5)	5 (5)	5 (5)	5 (5)	5	NASA SUPPORT SPACE-BASED ALTERNATES
	SUBTOTAL: ERDA NASA	12.8 (10.1)	15 (11.2)	16 (12.3)	20 (14.5)	← (16.25) →		225 (12.25)			→ (11.75)	
TECH VERIF'N	6. BLANKET TEST PROGRAM(2)	3.7	4.8	6.5	8.0	8.0	10.5	12.0	14.0	17.0		
	NASA TOTALS	13.8	16.0	18.8	22.5	24.25	22.75	23.75	25.75	17.0		

Fig 5-101 Large Solar Array Technology Resource Requirements \$M

ITEM	TECHNOLOGY RISK ASSESSMENT		COMMENTS
	RATING	RANKING	
1. Raw Material Process	3	4	<p>BACKGROUND: The initial process in fabricating solar blankets requires three energy intensive high temperature cycles. A single step process could result in savings of 3 to 5 over the \$60/kg to \$80/kg price paid today. Trichlorosilane used in the process is a large contributor to both energy use and cost. Alternates to this process should be pursued. Presently, Dow Corporation is researching more economical goals for producing semiconductor grade silicon. Dow is actively investigating 20 promising chemical reactions with the goal to reduce the cost to \$10/kg.</p> <p>TECHNOLOGY OBJECTIVES: Achieve a 3 to 5 reduction in cost for bringing raw material to semiconductor grade silicon.</p>
2. Crystal Growth	2	5	<p>BACKGROUND: Three approaches to single-crystal growth being pursued today are: 1) Czochralski; 2) WEB and 3) EFG. The Czochralski method is characterized by large amounts of waste materials and is projected to achieve at most a factor of 2 savings in cost. WEB process could be scaled up in crystal growth speed and geometry with the potential of achieving a factor of 5 reduction in cost. The EFG process shows the promise for the most significant cost reductions (a factor of 10 to 100). The major problems are to find die materials that can withstand the temperatures of the process and you maintain the efficiency of the solar cell produced. The current process work being performed by TYCO fabricates a silicon ribbon 100 μ thick approaching the 50 μ SSPS requirement.</p> <p>TECHNOLOGY OBJECTIVES: Develop the EFG process to the point where 50 μ silicon ribbon can be produced with 100% crystal and cell yield. WEB process should be continued as a program backup.</p>
3. Blanket Processes	4	2	<p>BACKGROUND: Current methods for fabricating solar blankets is a slow, mostly hand-made process. A continuous process is indicated. An automated process that includes function formation, installs contacts, performs etching, etc. is basically an engineering problem. A pilot plant and verification program is needed.</p> <p>TECHNOLOGY OBJECTIVES: Formulate alternate concepts for blanket processing and demonstrate most promising techniques.</p>
4. Packaging	3	5	<p>BACKGROUND: The requirement for 30 year life in a space environment suggests that improvements in cell encapsulation would be required. Materials technology that improves the thermal and radiation resistance of the cell must be developed and included in the overall automated fabrication of the blanket.</p> <p>TECHNOLOGY OBJECTIVES: Develop new materials that improve cell efficiency and radiation resistance. Incorporate advanced encapsulation approach into the continuous cell fabrication process.</p>

Fig. 5-102 Large Solar Array Technology Requirements, Sheet 1 of 2

ITEM	TECHNOLOGY RISK ASSESSMENT		COMMENTS
	RATING	RANKING	
5. Solar Cell Performance Improvement	4	1	<p>BACKGROUND: Current industry space qualified solar cells can achieve beginning of life conversion efficiencies of 12 to 14%. A program that strives to improve these efficiency levels to 18 to 20% (AMO) is required. This goal can be achieved through increases in fill factor, short-circuit current, and open-circuit voltage. It would be desirable to decrease resistivity of the bulk silicon to 0.01 ohm-cm. Lower resistivity gives higher open-circuit voltage. Increased short-circuit current could be achieved by antireflective coatings that match across the cell spectrum. The major issue is to achieve these efficiency improvements in a mass produced light-weight solar cell blanket.</p> <p>TECHNOLOGY OBJECTIVES: Improve solar cell conversion efficiency to 19% (AMO) and maintain this efficiency in a mass produced light-weight solar cell blanket.</p>
6. Alternate Photovoltaic Devices	4	3	<p>BACKGROUND: Investigations into alternate photovoltaic conversion devices are showing a great deal of promise. Of particular interest is the Gallium Arsenide Al GaAs/GaAs heterojunction cell. These devices shown high performance at concentration (12% AMO at a concentration ratio of 300). An active research and proof of concept program on alternate devices to the silicon cell should be pursued.</p> <p>TECHNOLOGY OBJECTIVES: To identify and develop at least one new photovoltaic conversion device that can serve as an alternate to the silicon.</p>

Fig 5-103 Large Solar Array Technology Requirements, Sheet 2 of 2

A summary of the expenditures related to the Solar Blanket ground/orbital verification issues, as developed in Phase III studies, is presented in Fig 5-104.

VERIFICATION	77	78	79	80	81	82	83	84	85
● SOLAR CELLS & COVERS	2	3	3	3	3	3	4	5	5
● SOLAR ARRAY COMPONENT MODULES & BLANKETS	1	1	2	4	4	6	6	6	8
● PLASMA INTER-ACTIVE POWER LOSS	.5	.5	1	1	1	1.5	2	3	4
● SPACECRAFT CHARGING	.2	.3	.5						
	3.7	4.8	6.5	8.0	8.0	10.5	12.0	14.0	17.0

NOTE: SHUTTLE LAUNCHES NOT INCLUDED

A-11

Fig. 5-104 Resource Requirements for Solar Blanket Verification Testing (\$M)

Figures 5-105, 5-106 and 5-107 identify the LEO and GEO environments considered in defining where test/demonstrations are performed. In addition, SPS, because of its size, interacts with the environment at GEO and in effect, creates a unique environment which must be considered in solar array blanket design.

A summary of the test/demonstrations required for each solar cell and solar blanket technology issue is shown in Figure 5-108 and 5-109. Potential ground and piggyback experiments, Shuttle-LEO construction platform flights and GEO demonstrations are identified.

LEO (190 N MI ALT)

- TEMPERATURE VARIATION (SUN/DARK – 60/40%)
- RADIATION: UV & PARTICLE IN VAN ALLEN BELTS
- HIGH VOLTAGE/PLASMA INTERACTION DURING SUNLIGHT PORTION OF THE ORBIT
- METEOROIDS
- VACUUM PRESS. (10^{-9} TO 10^{-10} TORR)
- IONOSPHERE MODIFICATION BY MICROWAVE ILLUMINATION AND/OR PROPELLANT EFFECTS

GEO

- TEMP VARIATION THERMAL CYCLING FROM $+88^{\circ}\text{C}$ TO -190°C TEMP RATE OF CHANGE IMMEDIATELY AFTER ECLIPSE: (60°C TO 200°C /MINUTE)
- RADIATION
 - UV
 - CHARGED PARTICLES IN VAN ALLEN BELT *
 - SOLAR FLARES
- HIGH VOLTAGE/PLASMA INTERACTION (PLASMA SHEATH THICKNESS ABOVE 10^4M)
- LARGE BODY CHARGING DUE TO MAGNETIC SUBSTORMS
- METEOROIDS

*IN GEO ONLY

ENVIRONMENT UNIQUE TO SPS

- POSSIBLE TRAPPING OF CHARGED PARTICLES DUE TO LARGE MAGNETIC FIELDS WHICH COULD BE PRODUCED BY THE SPS PDS. THEREFORE, THE PDS CIRCUIT MUST BE DESIGNED TO MINIMIZE THE MAGNETIC MOMENTS
- DIFFERENTIAL CHARGING AT 20 KV TO 80 KV DURING SUBSTORMS

THE FOLLOWING SEQUENCE OF EVENTS ACCOUNTS FOR THE ANOMALOUS BEHAVIOR OF SPACECRAFT DURING THE SUBSTORM

1. IMMERSION OF A SPACECRAFT IN A SUBSTORM PLASMA
2. DIFFERENTIAL CHARGING OF COMPONENT PARTS OF THE SPACECRAFT
3. GENERATION OF A VACUUM ARC WHEN THE VOLTAGE STRESS LEVEL EXCEEDS THE BREAK-DOWN POTENTIAL OF THE MATERIAL
4. IRRADIATION OF SPACECRAFT COMPONENTS BY THE ELECTRO-MAGNETIC INTERFERENCE (EMI) WAVES ASSOCIATED WITH THE VACUUM ARC
5. INDUCTION INTO ONBOARD ELECTRONIC CIRCUITRY OF A TRANSIENT PULSE OF SUFFICIENT MAGNITUDE TO ACTIVATE THE CIRCUIT OR BURN OUT SOME OF ITS COMPONENTS.

IN ORDER TO PREVENT THE SPS CATASTROPHIC FAILURE, CLOSE ELECTROSTATIC CLEANLINESS IS REQUIRED.

- INTERFACE WITH AMPLITRONS
- POSSIBLE INTERFACE WITH X-RAY GENERATING KLYSTRONS (IN CASE KLYSTRONS OR MIXTURE WILL BE USED)
- STRUCTURAL FLATNESS REQMT FOR SOLAR BLANKET & ANTENNA SUBARRAYS
- INTERFACE WITH OUTGASSING STRUCTURES (COMPOSITE MATERIALS, DIELECTRIC, SLIP RING MATERIALS, ETC.)
- THERMAL (I^2R) STRAIN DYNAMICS OF PDS AT STARTUP & SHUTDOWN
- THERMAL SHIELDING OR BLOCKAGE OF DC-RF CONVERTERS WASTE HEAT DISSIPATING RADIATORS
- SENSITIVE EQUIP. MUST BE SHIELDED OR ENCAPSULATED TO ASSURE NO ADVERSE EFFECTS, ETC.

EARLY ENVIRONMENTAL TESTING IN LEO AND GEO WILL BE CRUCIAL TO LARGE SCALE ASSEMBLY OF SPS

Fig 5-105 Space Environment Implications

SYSTEMS/COMPONENTS TECHNOLOGY VERIFICATION TESTS	1977-80 GROUND/PIGGYBACK	1980-85 LEO (SORTIES/ORBITAL CONST. PLATFORM)	1985 & LATER GEO
SOLAR CELLS/COVERS	<ul style="list-style-type: none"> • IMPROVE EFFICIENCY, THERMAL/OPTICAL PROPERTIES • DECREASE & DEGRADATION • TEST/COMPARE ELEC PERF & LIFE OF CANDIDATE CELLS & COVERS 	<ul style="list-style-type: none"> • INVESTIGATE LEO RAD/PLASMA EFFECTS ON SIZE, VOLTAGE, INSULATION, ETC. • METEORITIES • THERMAL CYCLING & RATE OF TEMP CHANGE (°/MIN) 	<ul style="list-style-type: none"> • INVESTIGATE GEO EFFECT ON SOLAR CELL PERFORMANCE: <ul style="list-style-type: none"> - ELEC/THERMAL - RAD: CHARGED PARTICLE/UV ON SOLAR CELLS (Si, GaAs, OTHER ADV TECHNOLOGY CELLS) INTEGRAL FEP OR OTHER SOLAR CELL COVERS • CALIBRATE SOLAR CELL PERFORMANCE FOR STANDARDIZATION USE OF GRD-TESTED CELLS • TEMP MONITORING AND RATE OF TEMP CHG DURING AND AT THE END OF ECLIPSE
SOLAR ARRAY COMPONENT/MODULE	<ul style="list-style-type: none"> • INCREASE STRENGTH/TEMP RAD RESISTANCE (PLASTIC FILM) COVER, SUBSTRATE MATERIALS • DECREASE THICKNESS • IMPROVE REFLECTOR MATERIALS, INTERCONNECTS, BONDING, ETC. • CONTINUE TEST OF ADV TECHNOLOGY SYS • THERMAL EXPANSION BETWEEN BONDED MATERIALS MUST BE CAREFULLY MATCHED 	<ul style="list-style-type: none"> • VERIFICATION TESTS OF SUBSCALE BLANKET ASSY PERFORMANCE • HIGH VOLTAGE/INSULATION • DEMONSTRATE ASSY/CONSTRUCTION OF LARGE SUBSCALE BLANKETS & INTEGRATE WITH STRUCT • DEVELOP INSTRUMENTATION FOR ENVIRONMENTAL SAFETY, STATUS/FAILURE ISOLATION, MONITORING 	<ul style="list-style-type: none"> • TEST SMALL SAMPLES & OPERATING ARRAY PARTS • VERIFY PERF CHARACTERISTICS OF MODULES IN GEO ENVIRONMENT (COMBINED THERMAL CYCLING & PARTICLE & UV RAD, METEORITES) • DETERMINE DEGRADATION AS A FUNCTION OF PARTICLE FLUENCE • DETERMINE ANNEALABILITY OF RADIATION DAMAGE (AS A FUNCTION OF THE TEMP & TIME REQ FOR ANN.) • DEVELOP ANNEALLING TECHNIQUES • PARTICLE RADIATION DAMAGE MONITORING DURING TRANSIT FROM LEO TO GEO
SOLAR ARRAY BLANKET (SOLAR ARRAY/CONCENTRATORS) ASSEMBLY	<ul style="list-style-type: none"> • TEST SMALL MODULES, SUB-ASSEMBLIES • HIGH VOLTAGE/INSULATION/TEMP/ELEC/MECH/CONCENTRATION RATIO-CONFIG TESTS ON SUBSCALE ASSY • VERIFY ATTACHMENT/JOINTS ELEC INTERFACES, WIRE INSULATION, TERMINALS • DETERMINE THE OPTIMUM CONCENTRATION RATIO AS A FUNCTION OF S.C. SEMICOND MATERIAL 	<ul style="list-style-type: none"> • DEMONSTRATE MAINTENANCE & REPAIR CAPABILITY FOR LARGE SUBSCALE SOLAR ARRAY • ATTITUDE CONTROL CAPABILITY OF SUN-POINTING SOLAR ARRAYS & THE EFFECTS OF ATTITUDE CONTROL JET PLUMES ON SOLAR CELL/REFLECTORS AS A FUNCTION OF TEMP & REFLECTANCE • SURFACE FLATNESS OF SOLAR BLANKETS/REFLECTORS MAINTAINABILITY (DETERMINE THE SURFACE FLATNESS RATIO N/D, DOC/DT, DPM/DT) 	<ul style="list-style-type: none"> • DEMONSTRATE MAINTENANCE & REPAIR CAPABILITY OF LARGE (SUBSCALE) SOLAR ARRAY • DEMONSTRATE CONTROLABILITY OF SOLAR ARRAY BLANKET ASSY • DEVELOP AUTOMATIC ONBOARD SENSOR-GUARD FAULT-ISOLATION INSTRUMENTATION: <ul style="list-style-type: none"> - SYS DIAGNOSIS & CONTROL - OVERRIDES AUTOMATIC FUNCTIONS - ALTERNATIVE POWER ROUTING - RAD DAMAGE MONITORING, ETC.

Fig. 5-106 Solar Cell/Solar Blanket Test Program (Sheet 1 of 2)

SYSTEMS/COMPONENTS TECHNOLOGY VERIFICATION TESTS	1977-80 GROUND/PIGGYBACK	1980-85 LEO	1985 & LATER GEO (SMALL PLATFORM)
PLASMA INTERACTIVE POWER LOSS	<ul style="list-style-type: none"> ● INVESTIGATE DESIGN SOLUTIONS BY MATH MODELS <ul style="list-style-type: none"> - DEPRESSED COLLECTOR - BIAS GRID - REDUCING THE OCCURANCE OF DIELECTRIC-TO-METAL ARCS BY MINIMIZING EXPOSED INSULATED SURFACE AREAS - EMI ANALYSIS - POSSIBLE USE OF GROUNDED CONDUCTIVE COATINGS ON SOLAR CELLS & FEP/KAPTON SUBSTRATES ● TEST ASSEMBLIES <ul style="list-style-type: none"> - SOLAR MODULES - INSULATORS - POWER CONDUCTORS - SURFACE BARRIERS 	<ul style="list-style-type: none"> ● TEST INTEGRATED SOLAR ARRAY BLANKET WITH POWER DISTRIBUTION SYS ● MONITOR: ENVIRONMENTAL & THERMAL PERF USING THE FOLLOWING SENSOR TYPES: <ul style="list-style-type: none"> - IONIZATION POTENTIAL - THERMOCOUPLES - TEMP - THERMISTORS - STRESS MEAS - PLASMA MEAS - VOLTAGE/CURRENT MEAS - RAD PARTICLE DETECTORS - MAGNETOMETERS 	<ul style="list-style-type: none"> ● VERIFY MATH MODELS <ul style="list-style-type: none"> - BIAS ARRAYS - DIFFERENT VOLTAGES - LARGE SURFACE CHARGING - ELEC THRUSTERS - PINHOLE ARCS - SPARKING AT NEG VOLTAGE ● MONITOR ENVIRONMENTAL & THERMAL PERF USING THE FOLLOWING SENSOR TYPES: <ul style="list-style-type: none"> - IONIZATION POTENTIAL - THERMOCOUPLES - TEMP - THERMISTORS - STRESS MEAS - PLASMA MEAS - VOLTAGE/CURRENT MEAS - RAD PARTICLE DETECTOR - MAGNETOMETERS ● TESTING MUST BE PERFORMED AT GEO WHERE SPACECRAFT CHARGING OCCURS ● TEST SOLAR ARRAYS, PDS, & SLIP RING ASSEMBLIES <ul style="list-style-type: none"> - MATERIALS - SPACING - EMI - ELECTROSTATIC CLEANLINESS REQMTS UNDER HIGH CURRENT, HIGH VOLTAGE CONDITIONS ● SINCE MAGNETIC SUBSTORM OCCURRENCE IS PREDICTABLE WITH ACCURACY UP TO 1.5 - 3 HR IN ADVANCE <ul style="list-style-type: none"> - DEVELOP INSTRUMENTATION FOR MAGNETIC SUBSTORM MONITORING - DEVELOP AUTOMATIC ON-ARRAY COMPUTER-CONTROLLED SWITCHING FOR VOLTAGE SELECTION & CONTROL - MEASURE THE RANGE OF LEAKAGE CURRENTS
SPACECRAFT ENLARGING	<ul style="list-style-type: none"> ● GRD TESTS (USING SPACE PLASMA SIMULATION FACILITY) ● SCATHA EXPERIMENT ● SPHINXS SATELLITE ● OTHER SATELLITES 	N/A	

ORIGINAL PAGE IS
OF POOR QUALITY

Fig 5-107 Solar Cell/Solar Blanket Test Program (Sheet 2 of 2)

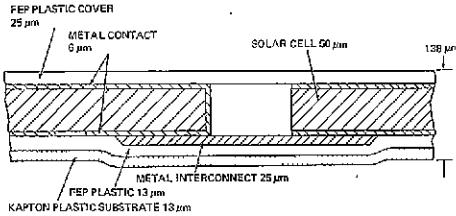
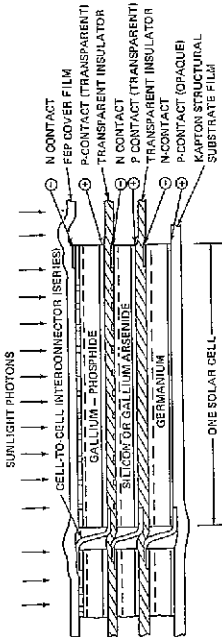
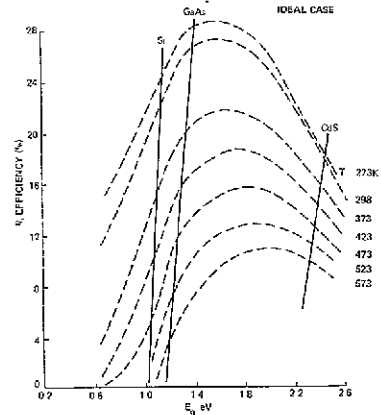
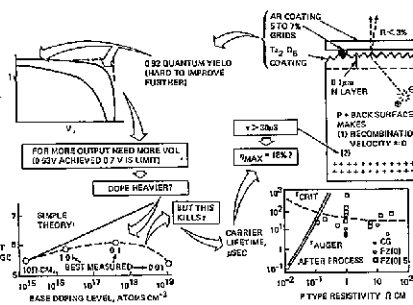
SYSTEM COMPONENTS: SOLAR ARRAY MODULE	DEMO TEST OBJECTIVES AND TEST RATIONALE (GROUND/ORBITAL) DEMO TEST OBJECTIVES:	DEMO REQUIREMENTS	TEST REQUIRED: GROUND TESTS
 <p>SSPS — ADVANCED SOLAR CELL MODULE</p>  <p>MULTIPLE-MATERIAL STACKED CELL CONCEPT</p>	<ul style="list-style-type: none"> DETERMINE SOLAR CELL EFFICIENCY IMPROVEMENT AT EOL AS A FUNCTION OF SOLAR CELL MODULE <ul style="list-style-type: none"> TEMPERATURE BANDPASS FILTERING (SOLAR CELLS/REFLECTORS) CONCENTRATION RATIO EFFECTS: THERMAL SERIES RESISTANCE UV RADIATION CHARGED PARTICLE RADIATION SURFACE FLATNESS RATIO CLOSE MATCH OF THERMAL EXPANSION BETWEEN BONDED MATERIALS, INTERCONNECTS, ETC. NEW (FEBP) ENCAPSULATION TECHNIQUES <ul style="list-style-type: none"> FUNDAMENTAL THEORETICAL PERFORMANCE EFFECTS SEMICONDUCTOR MATERIAL SI, GaAs HETERO-JUNCTION, CdS (MONO-POLYCRYSTALLINE) MULTILAYER, SCHOTTKY BARRIER MFG MODE — RIBBON, CZOCHRALSKY, EPITAXY, VAPOR DEPOSITION, ROLLING, ETC. MATERIAL DEFECTS SCULPTURED SURFACE THICKNESS OF BULK BASE THICKNESS OF UPPER LAYER INFLUENCE ON SPECTRAL RESPONSE & SERIES RESISTANCE GRID SPACING, THICKNESS ANTIREFLECTION COATING TRANSMITTANCE ENHANCEMENT SURFACE PASSIVATION (EL-HOLE RECOMBINATION RETARDATION) PT BACK SURFACE BAND GAP BASE DOPING LEVEL & MATERIALS (ITS INFLUENCE ON BASE RESISTIVITY & MONORITY CARRIER LIFETIME) THERMAL EFFECTS ON MAX POWER, CURRENT, AND VOLTAGE AS A FUNCTION OF TEMPERATURE COEFFICIENT VARIATION: $\frac{1}{P_{MAX}(25^{\circ}C)} \frac{dP_{MAX}}{dt} (\% ^{\circ}C)$ $\frac{1}{I_{SC}(25^{\circ}C)} \frac{dI_{SC}}{dT} (\% ^{\circ}C)$ $\frac{1}{V_{OC}(25^{\circ}C)} \frac{dV_{OC}}{dT} (\% ^{\circ}C)$ 	<p>DEMO REQUIREMENTS</p> <ul style="list-style-type: none"> DETERMINE THE PROPOSED IMPROVEMENTS EFFECTS ON THE THEORETICAL SOLAR CELL EFFICIENCY DETERMINE THE FUNDAMENTAL THEORETICAL LIMITATIONS ON SOLAR CELL PERFORMANCE  <p>THEORETICAL SOLAR CELL EFFICIENCY</p>  <p>FUNDAMENTAL LIMITATIONS</p>	<p>TEST REQUIRED: GROUND TESTS</p> <ul style="list-style-type: none"> DETERMINE THE VARIATIONS OF THE VOLTAGE, CURRENT, & MAX POWER DUE TO: <ul style="list-style-type: none"> TEMPERATURE CHANGES SURFACE WRINKLING DEGRADATION DUE TO PARTICLE RADIATION & UV IMPROVEMENTS OF FUNDAMENTAL THEORETICAL PROPERTIES VARIATION OF TEMPERATURE AS A FUNCTION OF CONCENTRATION RATIO AND GEOMETRY DETERMINE THE OPTIMUM CONCENTRATION FOR SI, AlGaAs-GaAs, & OTHER SEMICONDUCTOR MATERIALS DETERMINE THE THERMAL & OPTICAL PROPERTIES (EMISSIVITY, ABSORPTIVITY, TRANSMISSIVITY, REFLECTIVITY, SPECIFIC HEAT, & THERMAL CONDUCTIVITY) OF THE MODULE MATERIALS AFTER THERMAL CYCLING, UV, VACUUM, & PARTICLE RADIATION THE PRESENT EXPERIMENTS SHOW THAT INTEGRAL 1-MIL FEP COVERS CRACK UNDER THE COMBINED TESTS (TEMP, UV, PARTICLE RAD). DEVELOP A PROCESS OF ENCAPSULATION OF SOLAR CELLS WITH HEAT BONDED TEFLON WITHOUT STRESS PROBLEM DETERMINE THE TRANSMISSIVITY OF THE TANDEM CELL MATERIALS, VOLTAGE MISMATCHES, & OTHER ELECTRICAL CHARACTERISTICS, & TOTAL EFFICIENCY OF SUCH MODULE UNDER THE COMBINED SPACE SIMULATED ENVIRON

Fig 5-108 Key Solar Cell/Solar Blanket Detail Test Objectives and Requirements (Sheet 1 of 3)

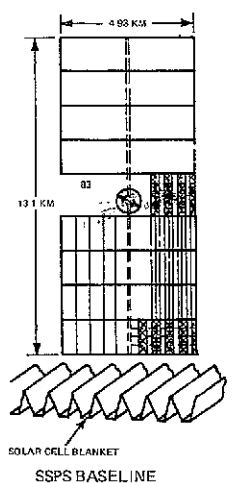
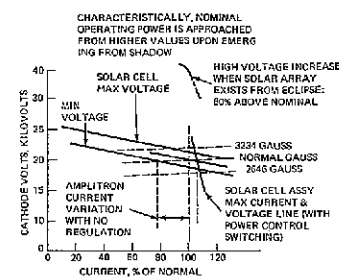
SOLAR BLANKET ASSEMBLY (SOLAR ARRAY/CONCENTRATORS)	DEMO TEST OBJECTIVES	DEMO REQUIREMENTS	TESTING REQUIRED	
			GROUND TESTS	ON-ORBIT TESTS
  <p>PHOTO-VOLTAIC POWER SOURCE CHARACTERISTICS</p>	<ul style="list-style-type: none"> DETERMINE THE EFFICIENCY & PERFORMANCE CHARACTERISTICS OF THE INTEGRATED SOLAR BLANKET ASSEMBLY IN THE SPACE SIMULATED AND LEO/GEO SPACE ENVIRONMENT. INVESTIGATE ENVIRONMENT EFFECTS OF: <ul style="list-style-type: none"> UV PARTICLE RADIATION HIGH VOLTAGE/PLASMA INTERACTION PLASMA EFFECTS ON ARRAY SIZE, VOLTAGE INSULATION, ETC. THERMAL CYCLING METEORITE EROSION OF SOLAR ARRAY/REFLECTORS DEMONSTRATE ASSEMBLY & CONSTRUCTION OF LARGE SUBSCALE BLANKETS & INTEGRATE WITH STRUCTURE DEMONSTRATE MAINTENANCE & REPAIR CAPABILITY OF LARGE SUBSCALE SOLAR ARRAY DEVELOP TEST MONITORING SENSORS VERIFY ATTACHMENT/JOINTS & ELECTRICAL INTERFACES DETERMINE CAPABILITY OF RADIATION DAMAGE ANNEALABILITY TEST INTEGRATED SOLAR ARRAY BLANKET WITH POWER DISTRIBUTION AT HIGH CURRENT & HIGH VOLTAGE DETERMINE THE SPACECRAFT CHARGING EFFECTS ON SOLAR BLANKET ASSEMBLY WITH SPACE ENVIRONMENT ABOVE THREE EARTH RADII (I.E., DURING TRANSFER FROM LEO TO GEO AND AT GEO) 	<ul style="list-style-type: none"> VERIFY THE COMPONENT TECHNOLOGY & PERFORMANCE OF THE INTEGRATED SOLAR BLANKET ASSEMBLY UNDER THE COMBINED ENVIRONMENTAL & SYSTEM-INDUCED CONDITIONS VERIFY THE ESTABLISHED OPTIMUM SYSTEM PERFORMANCE USING MATHEMATICAL MODELS & THE OBTAINABILITY OF THE THEORETICAL EFFICIENCIES OF THE SOLAR CELLS. CERTAIN FACTORS MAY PREVENT OBTAINMENT OF THE PERFORMANCE INDICATED FOR 1985-1990 SOLAR CELLS BECAUSE OF FUNDAMENTAL LIMITATIONS IMPOSED BY SEMICONDUCTOR THEORY VERIFY THE CONTROLLABILITY & SUN POINTING CAPABILITY OF LARGE SOLAR BLANKETS VERIFY THE CAPABILITY OF MINIMIZING THE MAGNETIC MOMENTS IN ORDER TO AVOID POSSIBLE TRAPPING OF CHARGED PARTICLES RESULTING FROM LARGE MAGNETIC FIELDS PRODUCED BY HIGH CURRENTS DETERMINE THE ELECTROSTATIC CLEANLINESS REQUIREMENTS DETERMINE THE HIGH VOLTAGE/PLASMA INTERACTION EFFECTS DEVELOP ON-ARRAY COMPUTER-CONTROLLED SWITCHING FOR VOLTAGE CONTROL DETERMINE THE ELECTROSTATIC CLEANLINESS REQUIREMENTS & DEVELOP THE SHIELDING TECHNIQUES TO PREVENT INDUCTION OF TRANSIENT PULSES INTO ONBOARD ELECTRONIC CIRCUITRY RESULTING IN CIRCUIT ACTIVATION OR COMPONENT BURNOUT 	<p>THE COMBINED ENVIRONMENTAL EFFECTS TEST WILL BE THE SAME AS FOR THE SOLAR CELL MODULE</p> <ul style="list-style-type: none"> SIMULATED SPACE PLASMA ENVIRONMENT TESTS WILL BE CONDUCTED TO DETERMINE THE POWER LOSS DUE TO THE FLOW OF PLASMA COUPLING CURRENTS & ELECTRICAL BREAKDOWN OF MATERIALS AS A RESULT OF OPERATION AT HIGH VOLTAGES IN THE PRESENCE OF PLASMA. TESTS WILL BE DESIGNED TO INVESTIGATE: <ul style="list-style-type: none"> PLASMA COUPLING CURRENTS SPARKING AT NEGATIVE VOLTAGE SURFACE BREAKDOWN OF INSULATORS BULK BREAKDOWN OF DIELECTRICS ELECTRICAL BREAKDOWN DUE TO PINHOLES IN INSULATING MATERIALS CURRENT COLLECTION & ELECTRICAL BREAKDOWN OF SOLAR CELL MODULES ARCING CHARACTERISTICS OF SOLAR BLANKET MATERIALS/ FEP, KAPTON, REFLECTORS EMI THE ELECTROSTATIC REQUIREMENTS METHODS FOR REDUCING POTENTIALLY DEGRADING OR DAMAGING EFFECTS SPACECRAFT CHARGING TESTS IN SIMULATED GEOMAGNETIC SUBSTORM CHARGING CONDITIONS 	<p>THE COMBINED SPACE ENVIRONMENT TESTS WILL BE CONDUCTED AT LEO AND GEO</p> <p>SPACE ENVIRONMENT:</p> <ul style="list-style-type: none"> RADIATION <ul style="list-style-type: none"> UV VAN ALLEN BELTS PARTICLE RADIATION SOLAR FLARE PARTICLES (GEO) HIGH VOLTAGE/PLASMA INTERACTION METEORITES THERMAL CYCLING ELECTRIC THRUSTERS PLUME IMPINGEMENT ON SOLAR BLANKET ASSEMBLY <p>TEST PLATFORMS:</p> <ul style="list-style-type: none"> SHUTTLE CONST. PLATFORM SPACE STATION <p>TESTING MUST BE PERFORMED AT GEO WHERE SPACECRAFT CHARGING OCCURS</p> <p>TEST:</p> <ul style="list-style-type: none"> SUBSCALE SOLAR BLANKET ASSEMBLY UNDER HIGH CURRENT/ HIGH VOLTAGE CONDITIONS <ul style="list-style-type: none"> MATERIALS BIASED ARRAYS DIFFERENT VOLTAGES LARGE SURFACE CHARGE EMI ELECTROSTATIC CLEANLINESS REQUIREMENTS ON-ARRAY VOLTAGE CONTROLABILITY

Fig 5-109 Key Solar Cell/Solar Blanket Detail Test Objectives and Requirements (Sheet 2 of 3)

Test objectives and requirements for key solar cell and solar array system elements are identified in Figure 5-110. As illustrated, one of the prime objectives in development of solar cell efficiency is end-of-life (EOL) efficiency improvements, approaching the theoretical solar cell efficiency limitations. A majority of the demonstrations required to achieve this objective are accomplished in ground tests. Blanket tests for thermal cycling, radiation degradation, blanket wrinkling effect on efficiency, and efficiency degradation rates are considered to be performed in orbit. Degradation effects are readily demonstrable on piggyback flights for GEO missions. These missions would carry cell and cover glass modules of various candidate designs. Large solar array blanket substrates material candidates are ultimately evaluated in Shuttle tests. The final candidates are then evaluated on the 2 MW GEO demonstration satellite.

Structural attachments of concentrator and solar array blankets can be initially evaluated as part of the assembly rate verification program. Further demonstration under actual orbital environments would take place during construction and evaluation of subarrays, using the 2 MW demonstration satellite.

The SPS unique environment causing plasma interactive power loss will be primarily dependent on LEO tests. An integrated and instrumented power distribution and solar array blanket is suggested as the prime test article. The 2-MW demonstration will provide additional data for model verification. Spacecraft charging (SCATHA) effects can only be measured at GEO during a magnetic substorm. The prime source of data will be the SCATHA experiment satellite, which will provide further design and operations guidelines for GEO spacecraft. Final verification will be performed during observation of the 2 MW demonstration flight.

A summary of the Structural Technology Development Program as updated by this phase of the study is shown in Fig 5-111. Verification and demonstration requirements for reducing the uncertainties in manned and remote assembly operations for the baseline configuration have been identified and summarized in Fig 5-112.

Figure 5-113 through 5-116 elaborates on a suggested test and verification program that will develop the data necessary to estimate the assembly rates of major SPS elements. Assembly operations identified are for those areas which require the significant portion of SPS construction time and represent repetitive tasks. Thus, the assembly operations verification program encompasses the following SPS assembly tasks:

- 1M Truss Fabrication
- 1M Truss end fitting fabrication and installation

DEMO TEST OBJECTIVES	
SWITCHGEAR & POWER CONDITIONING	DETERMINE THE COMPOSITE ENVIRONMENTAL/FUNCTIONAL EFFECTS ON MATERIALS, INSULATION UNDER THE HIGH VOLTAGE, & HIGH POWER CONDITIONS. DETERMINE OUTGASSING PRODUCTS, VOLTAGE GRADIENTS, TEMPERATURE LIMITATIONS IMPOSED ON MATERIALS BY THE NATURAL & INDUCED ENVIRONMENTS
POWER CONDUCTORS (CONDUCTORS, INSULATORS, CONNECTORS, ETC.)	<ul style="list-style-type: none"> ● DETERMINE THE MATERIALS COMPATIBILITY WITH THE ELECTRICAL, STRUCTURAL, THERMAL REQUIREMENTS; HIGH VOLTAGE EFFECTS (ARCING, THERMAL EMI); THERMAL STRAIN IN THE CONDUCTORS WHEN CURRENT FLOW IS INITIATED & TERMINATED ● DEMONSTRATE SPACE HANDLING & ELECTRICAL CONNECTION TECHNIQUES
ROTARY JOINT	<ul style="list-style-type: none"> ● SELECT MATERIALS/PARTS BRUSHES/RINGS, CONDUCTORS/JOINTS, BEARINGS/SHAFTS, INSULATORS, ETC. & TEST IT UNDER COMPOSITE ENVIRONMENTS (SPACE/SYSTEM INDUCED - FUNCTIONAL) ● DETERMINE THE HIGH VOLTAGE EFFECTS WEAR/DEGRADATION, TORQUE/FRICTION STARTUP/SHUTDOWN, NOISE, CHECKS, REPAIR/ MAINTENANCE, & OUTGASSING PRODUCTS

Fig 5-110 Key Solar Cell/Solar Blanket Detail Test Objectives and Requirements (Sheet 3 of 3)

TASK	77	78	79	80	81	82	83	84	85	
1. STRUCTURE • CONFIGURATION • STRUCTURAL & CONTROL ANALYSIS • THERMAL • STRUCTURAL ELEMENT DESIGN & FABRICATION	PRELIMINARY DESIGN				DESIGN DEMO SATELLITES & SORTIE PAYLOADS					
	.5	.5	1.0	1.0						
	.3	.7	1.0	1.6						
	.3	.7	1.0	1.0						
	.7	1.0	2.0	3.5						
2. ASSEMBLY & OPERATIONS	.1	.7	6.6	9.25	6.5	1.3	1.5	2.5	5.5	
TOTAL	1.9	3.6	11.6	16.35	6.5	1.3	1.5	2.5	5.5	

Fig 5-111 Structural Technology Resource Requirements

VERIFICATION	77	78	79	80	81	82	83	84	85	86	87	88	89
● 1-M TRUSS FAB RATE	.1	.2		.3	1.0					*			
● 1-M JOINT FAB & INSTL RATES			.1	.2	.5	.3				*			
● 1-M TRUSS JOINING RATES		.5	6	8	2					*			
● 20-M & 493-M LONG STRUCT MODULE ASSEMBLY TIMES			.5	.75	2.5	.5	.5	1.0	1.5	4.0*			
● FUNCTIONAL EQUIP. ASSEMBLY RATES					.5	.5	1.0	1.5	4.0	*			
	.1	.7	6.6	9.25	6.5	1.3	1.5	2.5	5.5	4.0			

Fig 5-112 Assembly & Operations Verif'n/Demo of Manned/Remote Assy Rates. . .

VERIFICATION TEST OBJECTIVE	77	78	79	80	81	82	83	84	85	TEST APPROACH - DESCRIPTION
VERIFICATION OF BASIC TRUSS FABRICATION										
VERIF OF BASIC 1-M TRUSS DSGN & ALLOWABLE FAB TOLERANCES	☐									GRD TEST OF CONVENTIONALLY FAB BEAM & JOINTS
VERIF OF FAB MACHINE DSGN & RATES OF TRUSS FAB		☐								GRD DEVEL TESTS IN SUPPORT OF MACHINE DSGN
VERIF OF STRUCT INTEG OF MACHINE-FAB TRUSS JOINTS FOR REPEATIBILITY, & TOLERANCES		☐								X-RAY, PULL TESTS, THERMAL TESTS, & ALIGNMENT MEAS OF MACHINE FAB JOINTS IN GRD TESTS
VERIF STRUCT INTEG & CHAR. OF TRUSSES MACHINE-FAB AT ORBITAL PROD. RATES		☐								GRD ALIGN. MEAS COMPR TESTS, SHEAR STRENGTH TESTS AT AMB & ELEV TEMP
VERIF STRUCT DYNAMIC CHAR. & POTENTIAL ON ORBIT FAB ATTITUDE CONTROL PROB INDUCED BY LONG TRUSSES		☐								GRD VIBRATION SURVEY OF 40-M TRUSS TO ESTAB FUNDAMENTAL MODES & FREQ
VERIF FAB MACHINE RANGE OF PROD. RATES & ORBITAL ENVIR EFFECTS ON: • FEASIBILITY • TRUSS FAB RATE • GROSS ALIGN. • LENGTH CONTROL						☐				SHUTTLE SORTIE FLT OF FAB MACHINE, MEAS PROD. RATES & TRUSS ALIGN. ONE SHARED SHUTTLE FLT
VERIF STRUCT INTEG & QUALITY OF ON-ORBIT FAB TRUSSES						☐				RETURN 1-3M SECTIONS FOR GRD JOINT X-RAY, PULL TESTS & CAP COMPR TESTS. RETURNED FROM SHUTTLE SORTIE FOR FEAS TESTS
VERIF STRUCT STIFFNESS AND DAMPING OF 40M LONG 1M TRUSS TO ESTAB CONTROL REQMTS & VERIFY ANALYTICAL MODELS						☐				ON-ORBIT CANTILEVERED VIBRATION TEST OF 1M x 40M LONG TRUSS
VERIF ABILITY TO CONSTRUCT 1-M TRUSSES 40-M LONG WITHIN REQ SPS FLATNESS & TORSIONAL ALIGNMENT TOLERANCES, AT PLANNED CONSTR RATES WITH ANTICIPATED SHUTTLE MANEUVER LOADS & ORB TEMP ENVIRON						☐				SHUTTLE - CONSTRUCTION PLATFORM MISSION USING OPTICAL TECHNIQUES TO MEAS ALIGN- & OCDA OR SHUTTLE RCS TO SIM GEO INPUT LOADS. USE HOT PART OF ORBIT TO SIM GEO THERMAL ENVIR
VERIF STRUCT STRENGTH OF ON-ORBIT FAB BEAMS						☐				SHUTTLE - PLATFORM - USE CABLE-JACK-SWIVEL PLATE TO PULL COMPR TEST
VERIF RECOVERY FROM OFF-NOMINAL BEAM FAB CONDITIONS						☐				DEMONSTRATE TRUSS REPAIR AND/OR GUILLOTINE TECHNIQUES TO ESTAB RECOVERY TIMES
1-M TRUSS END FITTING FAB & INSTL										
VERIF BASIC JOINT ERECT OR FAB APPROACHES			☐							GRD TESTING TO EVAL BASIC APPROACHES TO FAB OF END FITTINGS BY INTEGRATION OF APPROACHES WITH DEVEL TRUSS FAB MACHINE & ESTAB EFFECT OF ALTERNATES ON TRUSS PROD. RATE

Fig 5-113 Test Program for Verification/Demonstration of Manned and Remote Assembly Rates (Sheet 1 of 4)

VERIFICATION TEST OBJECTIVE	77	78	79	80	81	82	83	84	85	TEST APPROACH – DESCRIPTION
VERIF OF STRUCT QUALITY OF END FITTING INSTL			■	□						GRD PULL TESTS & ALIGN. VERIF OF INSTALLED JOINTS
VERIF ALLOWABLE ALIGN. TOLERANCES			■	□						GRD COMPR TESTS OF A 2-M LENGTH TRUSS WITH END FITTINGS INSTALLED AT VARIOUS ALIGN. MISMATCHES
VERIF OF END FITTING ERECT & INSTL UNDER ANTICIPATED CONSTRUCT. ENVIRON TO ESTAB TIMES & INTEGRITY AT INSTL RATES					■	□				<ul style="list-style-type: none"> • SHUTTLE SORTIE FLT TO DEMONSTRATE END FITTING INSTALL TIMES & ALIGN CAPABILITY WHILE SIM EXPECTED CONSTR INPUT LOADS • RETURN OF END SECTIONS TO GRD & RUN COMPR TESTS TO VERIFY ATTACH. INTEGRITY
1-M TRUSS JOINING										
VERIF BASIC FORCES REQ TO MATE TRUSS JOINTS FOR NOMINAL & OFF-NOMINAL MATES			■	□						GRD TESTS MEAS JOINT MATE FORCES UNDER FULL RANGE OF NOMINAL & OFF-NOMINAL MATING ANGLES WITH END FITTINGS ON 1-M LENGTHS OR SIM TRUSSES
VERIF RETENTION FORCES OF MATED JOINTS			■	□						GRD TENSION TESTS OF END FITTINGS MOUNTED ON 1-M LENGTHS OR SIM TRUSSES MATED WITH MAX & MIN FORCES & NOMINAL & OFF-NOMINAL ALIGN.
VERIF PLANNED JOINT QUALITY CONTROL TECHNIQUE			■	□						GRD TEST TO ESTAB A RELIABLE INDICATION OF HARD MATE OF TRUSS JOINTS AS THEY ARE ASSEMBLED
VERIF CAPABILITY OF HANDLING & JOINING TRUSSES OF 20 TO 40M LENGTH			■	□						ESTAB A GRD SIM FACILITY USING EITHER NEUTRAL BOUYANCY OR INFLATABLE STRUCT TO SERVE AS TEST & TRAINING FACILITY. MANNED & REMOTE MANIPULATORS & CONSTR EQUIP WILL BE USED OR SIMULATED. TESTS TO VERIFY HANDLING & JOINING OF 20 TO 40M TRUSSES INCLUDING:
		■			■	□				<ul style="list-style-type: none"> • USING REMOTE MANIPULATORS TO HANDLE & MATE 40-M LONG TRUSSES FOR TRANSFER & JOINING. MEASURE RATE & INERTIA LOADS USING EITHER NEUTRAL BOUYANCY OR INFLATABLE STRUCT • USING NEUTRAL BOUYANCY TECHNIQUES MEAS MATING FORCE REQMTS OF TWO, THREE, & FOUR BEAM JOINTS • PERFORM JOINING OPS WITH VARIED TRUSS LENGTHS & EVAL POTENTIAL FOR JOINING RATE IMPROVEMENT • SIMULATE JOINT MOTIONS ANTICIPATED DURING CONSTR & VERIFY ABILITY TO JOIN • SIMUL POTENTIAL REMOTE ASSY TIME DELAYS & VERIF ABILITY TO CONTROL JOINT ASSY
			■							
			■							
				■	□					
				■	□					

Fig. 5-114 Test Program for Verification/Demonstration of Manned and Remote Assembly Rates (Sheet 2 of 4)

VERIFICATION TEST OBJECTIVE	77	78	79	80	81	82	83	85	86	TEST APPROACH - DESCRIPTION
STRUCTURAL MODULE ASS'Y (20 & 493-M)										
VERIFY CABLE ATTACH. & TENSIONING TECHNIQUES FOR 20-M STRUCT MODULES		■	□		■					USING SECTIONS OF 1-M BEAMS WITH PLANNED CABLE ATTACH. POINTS, RUN END TENSION LOAD TESTS TO DEMO STRUCT STRENGTH DEMO & EVAL AUTO VS MANIP VS OTHER ALTERNATIVE APPROACHES TO CABLE INSTL & TENSIONING ON THE GRD USING NEUTRAL BOUYANCY TEST FACILITY
VERIFY 20-M STRUCT MODULE FAB APPROACH		■			■	■				GRD DEMO OF 20-M STRUCT MODULE FAB USING INFLATABLE TRUSSES IN SIM FACILITY. INCLUDE ALL PROCED & CONSTR EQUIP. TO DEMO CABLE INSTL, TENSIONING, JOINT MAKEUP, & TRUSS HANDLING
VERIFY FREE TRUSS HANDLING & JOINING UNDER INERTIAL LOADS ANTICIPATED DURING CONSTR BY FAB OF 20-M BEAM (20-M HIGH X 40-M LONG)					■			■		SHUTTLE - PLATFORM-USING 2 MW DEMO SAT. CONSTR BASE FAB A 20-M STRUC BAY USING RCS TO SIM INERTIAL LOADS KEY DEMO TO INCLUDE: <ul style="list-style-type: none"> ● MAINTAINING BATTEN TRUSS RELATIONSHIPS DURING CONSTR SEQUENCE ● TENSIONING OF CABLES ● EASE OF TRI TRUSS JOINING ● JOINING FORCES REQ
VERIF STRUCT QUALITY OF 20-M BEAM BY BUILDING A 3-BAY STRUCT ASSY								■		SHUTTLE PLATFORM USING 2-MW DEMO SAT. CONSTR BASE TO FAB 3, 20-M STRUCT BAYS 40M IN LENGTH (120M OVERALL) WITH INSTRUMENTED CABLES <ul style="list-style-type: none"> ● OPTICAL VERIF OF ALIGN. ● RUN COMPR TEST VIA CABLE, END PLATE, JACK TECHNIQUES
VERIF CONSTR RATES & APPROACHES FOR FULL LENGTH 20-M HIGH BEAMS						■		■		SHUTTLE - PLATFORM WHICH FAB 246-M & 493-M LONG 20-M BEAMS & MEAS OVERALL PROD. RATES
VERIF STRUCT CHAR. OF 246 & 493-M BEAMS & ANALYZE MODELING						■		■		UTILIZING BEAMS PRODUCED DURING CONSTR RATE VERIF, PERFORM VIBRATION SURVEY TO ESTAB FUND. MODES AND FREQ. PERFORM ALIGN. & MOMENT OF INERTIA CHECKS
VERIFY STRUCT CHAR. OF A 493 X 493-M STRUCT MODULE & ANAL. MODELING MADE UP OF 20-M HIGH BEAMS						■		■		<ul style="list-style-type: none"> ● STARTING WITH THE 20-M HIGH BEAMS FAB DURING CONSTR RATE VERIF, FAB 5 ADDITIONAL 246-M LONG BEAMS AND 3 ADDITIONAL 493-M LONG BEAMS USING CONST. PLATFORM ● USING MANIP & EVA, JOIN BEAMS INTO A 493-M MODULE

Fig. 5-115 Test Program for Verification/Demonstration of Manned and Remote Assembly Rates (Sheet 3 of 4)

186


VERIFICATION TEST OBJECTIVE	77	78	79	80	81	82	83	85	86	TEST APPROACH – DESCRIPTION
<p>FUNCTIONAL EQUIPMENT ASSEMBLY VERIF. BY GRD TESTING INSTL & ASSY TECHNIQUES & TOLERANCES FOR:</p> <ul style="list-style-type: none"> • SOLAR ARRAY BLANKETS • SOLAR CONCENTRATOR BLANKETS • MPTS SUBARRAY • CENTRAL MAST • ROTARY JOINT <p>VERIF MPTS ASSY & ALIGN. TECHNIQUES IN ORBITAL ENVIRON</p>										<ul style="list-style-type: none"> • INSTALL INSTRUMENTED ALIGN. CABLES & VERIFY ABILITY TO ALIGN TO WITHIN REQ TOLERANCES <p>GRD TEST OF INSTL & HANDLING TECHNIQUES IN SIM FACILITY FOR MPTS SUBARRAY, CENTRAL MAST, & ROTARY JOINT, STRUCT ATTACH. STRENGTH, FORCE & STIFFNESS MEAS FOR ALL INSTALLATIONS. UNDER TOLERANCE EXTREMES SIMULATIONS ASSESS. SHOULD INCLUDE ALIGN. CAPABILITY, MANIPULATOR HANDLING, LIGHTING/VIEWING REQMTS</p> <p>2 SHUTTLE – PLATFORM MISSIONS TO PERFORM THE FOLLOWING:</p> <ul style="list-style-type: none"> • CONSTRUCT BASIC MPTS SUBARRAY SUBSTRUCT USING AUTO FAB MACHINE. • FAB BASIC MPTS SUBARRAY STRUCT & VERIFY SUBARRAY ALIGN. • INSTALL SUBARRAY ON STRUCT USING REMOTE MANIP & COARSE ALIGN • SECURE TO SCREW JACKS & VERIFY FINE ALIGN. CAPABILITY & PROCEDURES • RUN VIBRATION TESTS, & THERMAL CYCLING TO VERIFY CONSTR INTEGRITY

Fig 5-116 Test Program for Verification/Demonstration of Manned and Remote Assembly Rates (Sheet 4 of 4)

- 1M Truss joining
- 20M high and 493M long structural module construction
- Solar array and concentrator blanket installation
- MPTS construction and subarray installation

Facilities and equipments needed to conduct these verification tests include a neutral buoyancy facility, shuttle sortie flights and a space construction platform. Major verification functions are established in the course of constructing the 150W and 2MW test satellites.



References

1. Econ Inc., "Spaced Based Solar Power Conversion and Delivery Systems Study - Interim Summary Report" March 31, 1976
2. Spectrolab/HeLiotek Divisions of Textron Inc., "Satellite Solar Power Station - Solar Photovoltaic Array Report," November 1971
3. Grumman Aerospace Corporation, "Space Based Solar Power Conversion and Delivery Systems Study - Vol. II, Engineering Analysis of Orbital Systems," June 30, 1976
4. Grumman Aerospace Corporation "Space Station Systems Analysis Study - Program Review," April 1976
5. NASA/MSFC - "Satellite Power System, Engineering and Economic Analysis Summary" NASA TMX-73344, November 1976
6. NASA/ASEE - "Prometheus, Solar Power Satellite: Analysis of Alternatives for Transporting Material to Geosynchronous Orbit," 1976
7. Boeing/Grumman, "System Concepts for STS Derived Heavy Lift Launch Vehicles Study" Contract NAS9-14710
8. Grumman "Orbital Construction Demonstration Study - Progress Report Briefing," June 23, 1976
9. Econ Inc, "Space Based Solar Power Conversion and Delivery Systems Study - Interim Summary Report" June 1976
10. NASA/MSFC "Verification Program for a Photovoltaic SPS", September 16, 1976
11. NASA/MSFC, "Space Power Demonstration System Six-Week Study" November 1976
12. D.E. Koelle "Cost Prediction of Space Projects" Presented at 2nd Symposium on Cost Reduction in Space Operations of the International Academy of Astronautics, October 14, 1972

APPENDIX A: Final Report Briefing

The final report briefing for this study was presented at the Marshall Space Flight Center on 10 March 1977. Grumman's portion of the briefing contained an overall summary of its initial study efforts and subsequent follow-on works, which is documented herein.

PRECEDING PAGE BLANK NOT FILMED

Final Report Briefing
Space-Based Solar Power
Conversion & Delivery Systems (Study)
Engineering Analysis

A-2

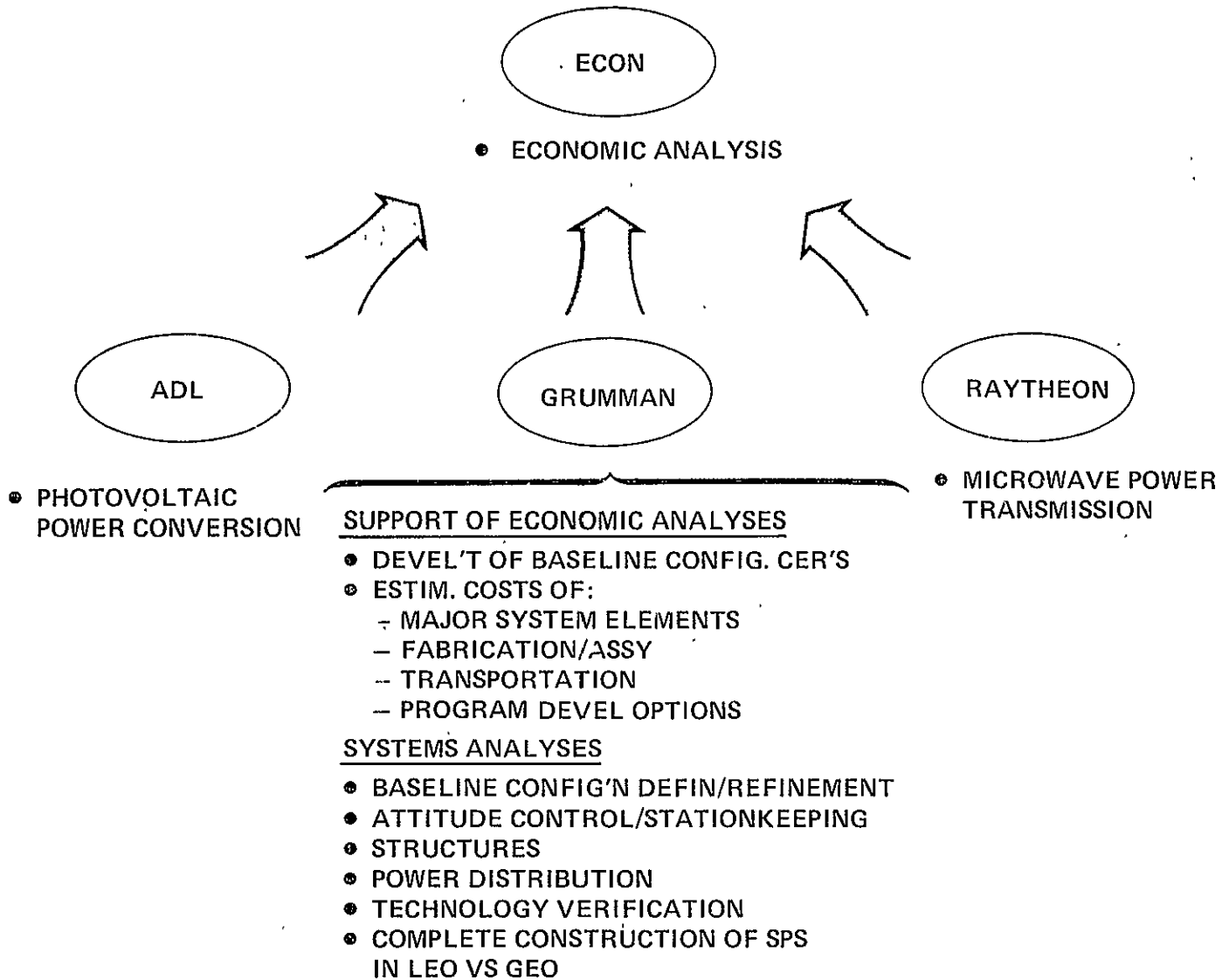
Prepared by:
Grumman Aerospace Corp.

For:
ECON, Inc

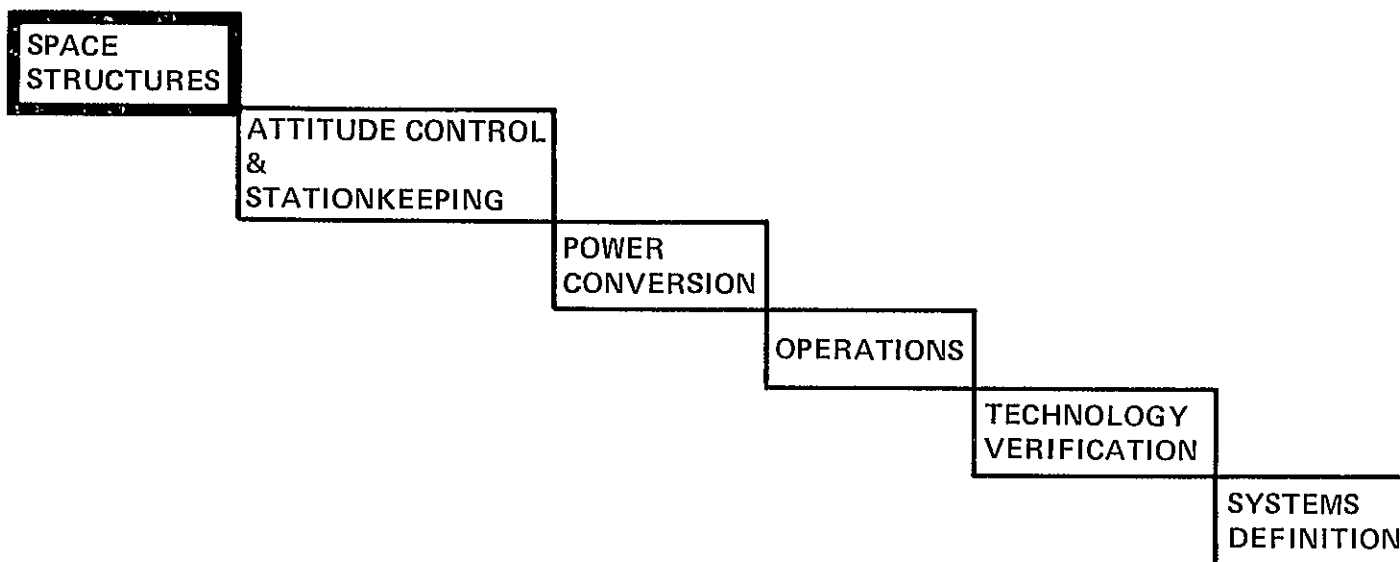
March 10, 1977

CB

GRUMMAN'S ROLE



MAJOR FINDINGS AND CONCLUSIONS



A-4

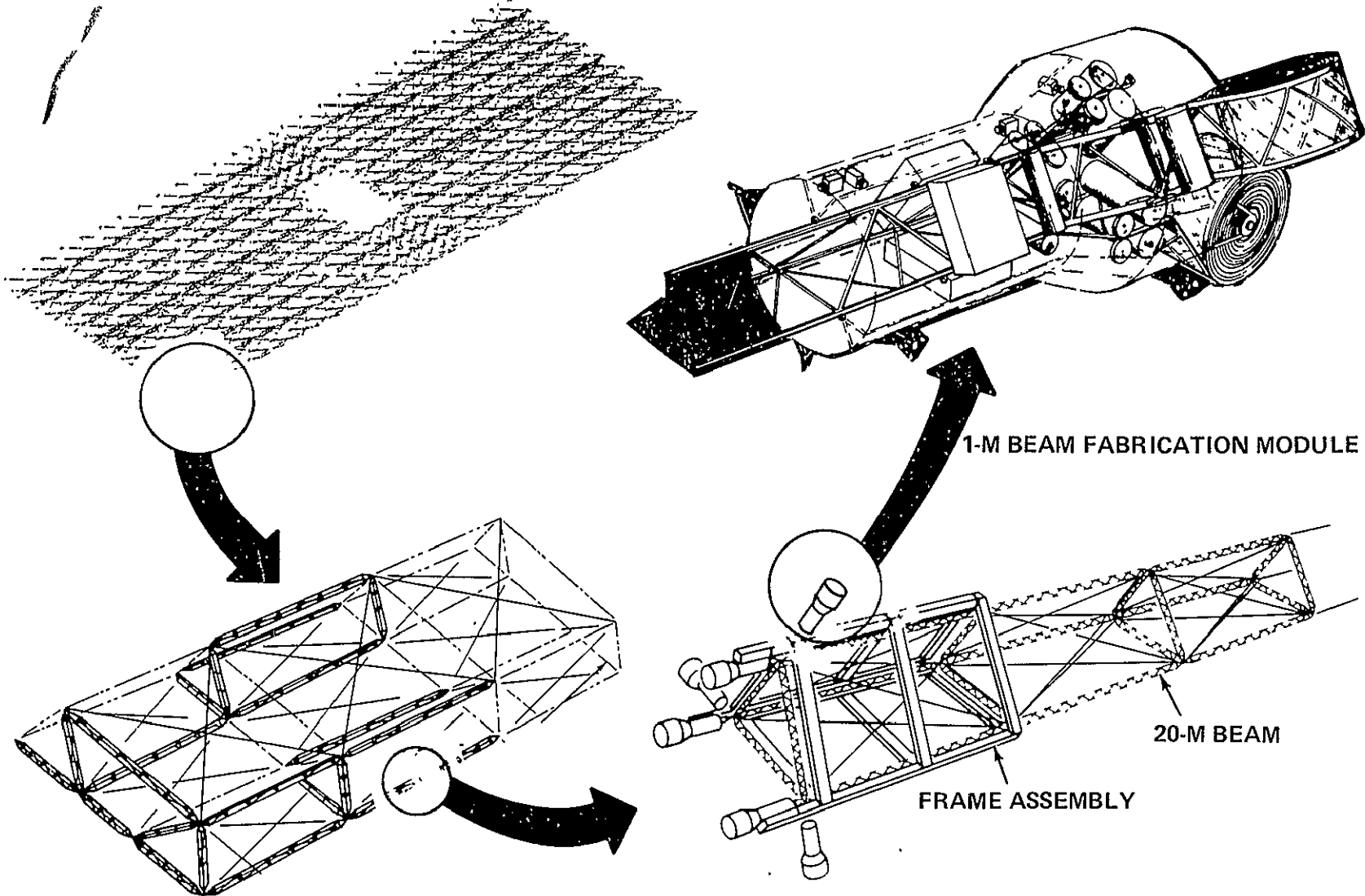
VERY LARGE AREA TRUSS-TYPE STRUCTURES

...CONFIGURED FOR OPERATION IN SPACE...

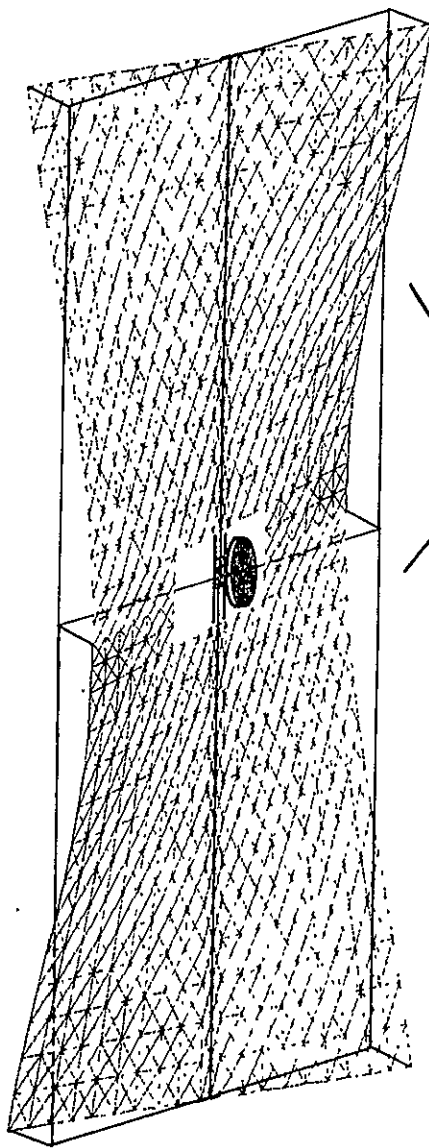
- **ARE FEASIBLE, & CAN SATISFY SPS NEEDS FOR MINIMUM WEIGHT/ STRUCTURAL STIFFNESS**
- **REPRESENT ABOUT 20% OF TOTAL SPS MASS**
- **CAN UTILIZE AUTOMATED STRUCTURAL/FABRICATION TECHNIQUES IN ORBIT**
- **ARE CONTROLLABLE AT LEO OR GEO WITH ELECTRIC PROPULSION ACS**

TRUSS-TYPE STRUCTURES FABRICATION/ ASSEMBLY

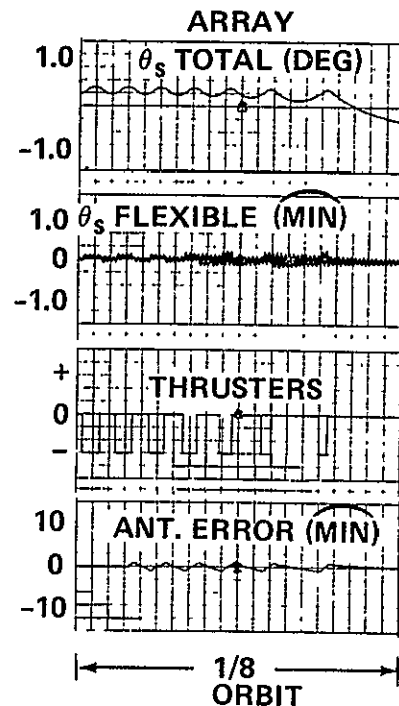
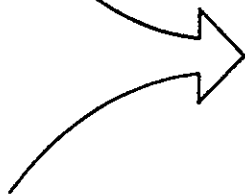
A-6



SOLAR ARRAY/MICROWAVE POINTING CONTROL

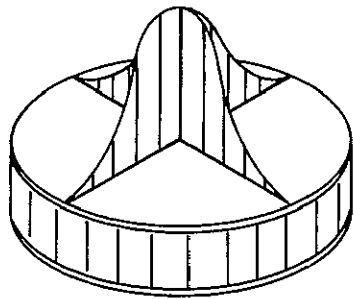


ANALOG
SIMULATION

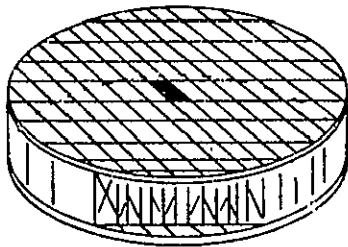


$\pm 1^\circ$ SOLAR ARRAY POINTING CONTROL
CONCURRENT WITH ± 1 ARC MIN POINTING
CONTROL OF MICROWAVE ANTENNA IS
ACHIEVABLE

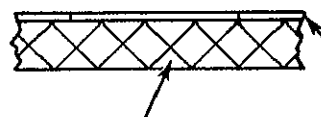
MICROWAVE ANTENNA: MATERIALS CONSIDERATIONS



TEMPERATURE DISTRIBUTION (GAUSSIAN)



TYPICAL ANTENNA SUBARRAY CONFIGURATION



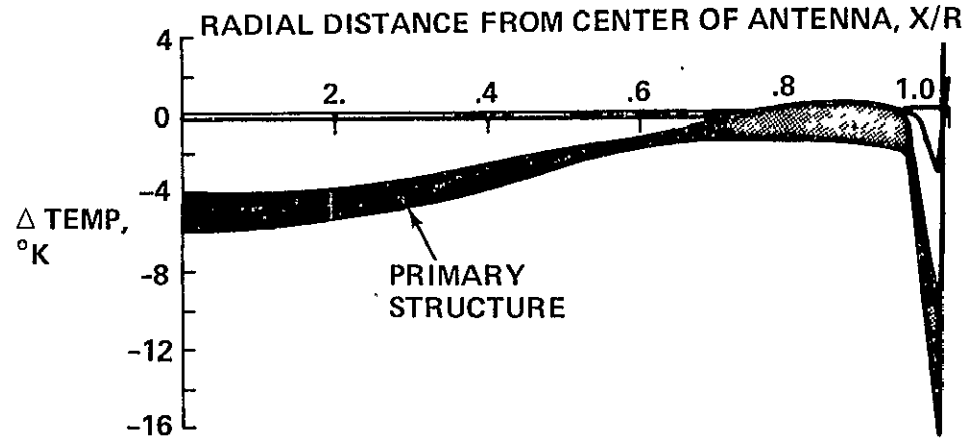
PRIMARY STRUCTURE (108 x 108M BAYS)

WAVEGUIDES/ SECONDARY STRUCTURE (18M x 18M BAYS)

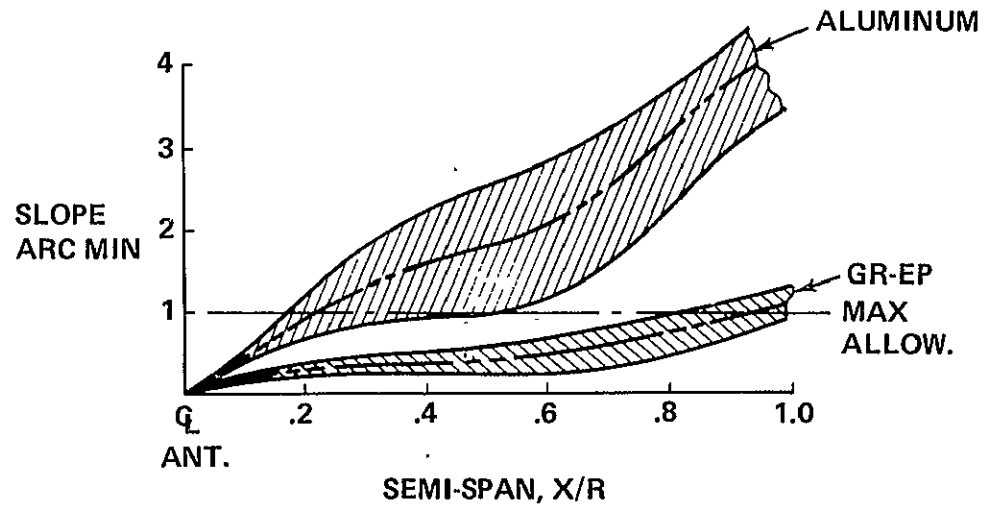
COMPOSITES ARE FAVORED FOR PRIMARY ANTENNA STRUCTURE

A-8

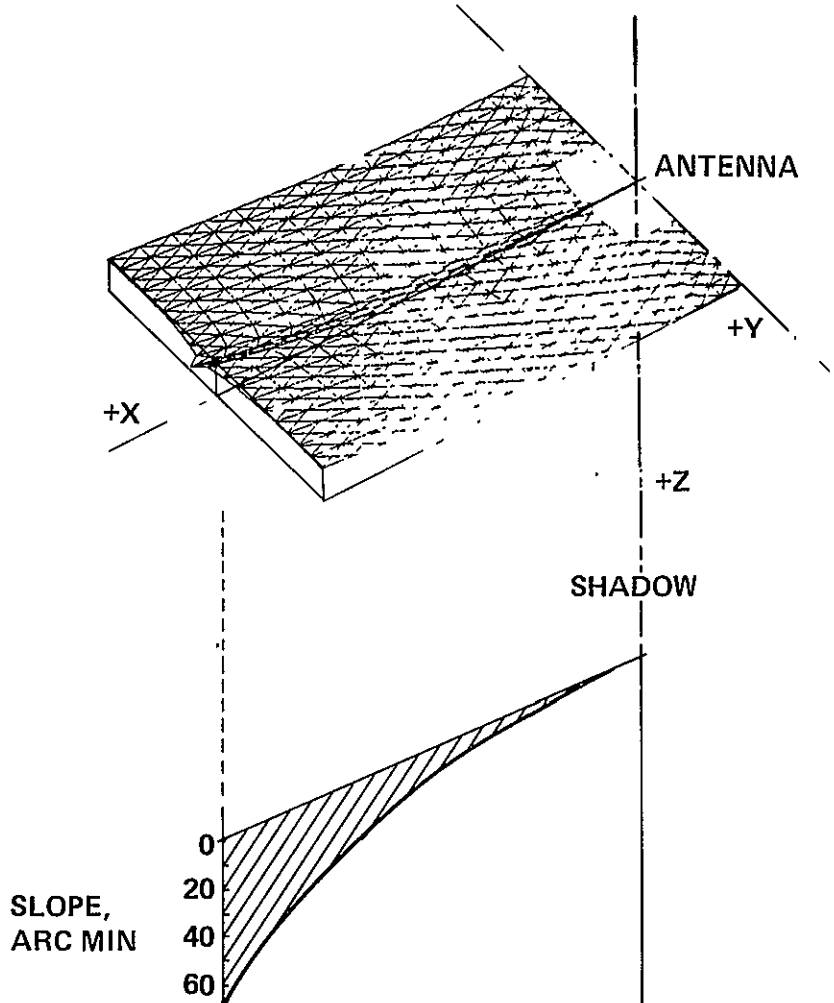
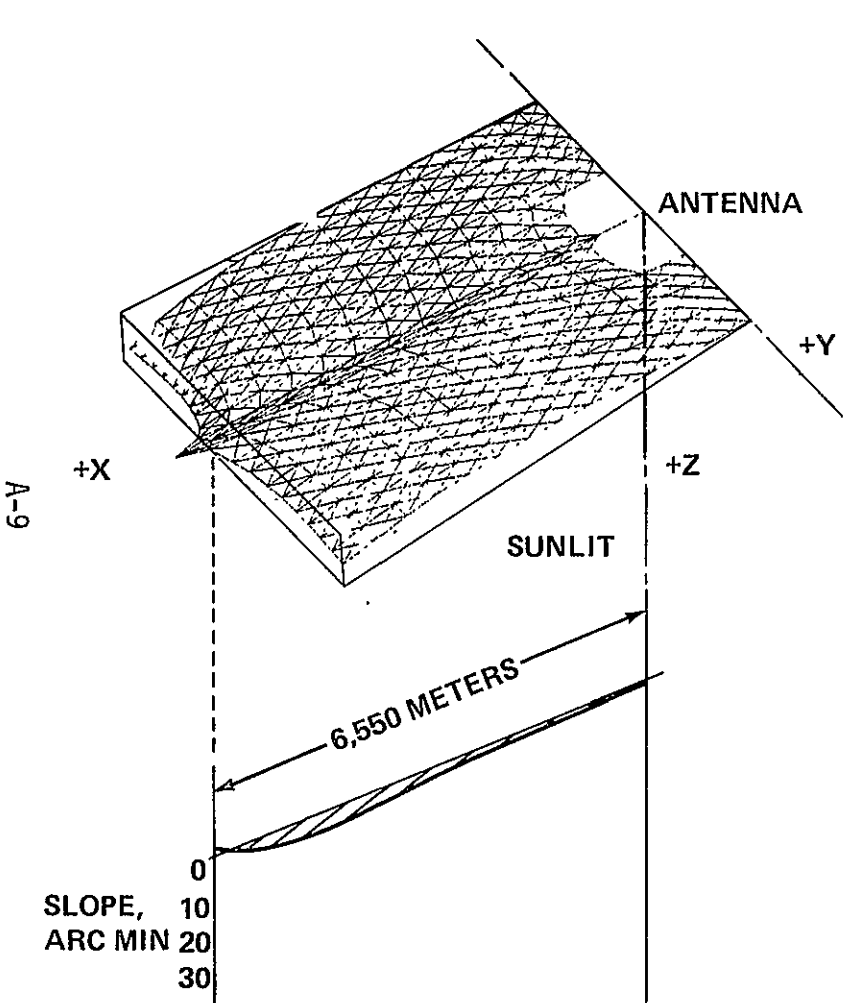
STRUCTURAL TEMPERATURE VARIATIONS



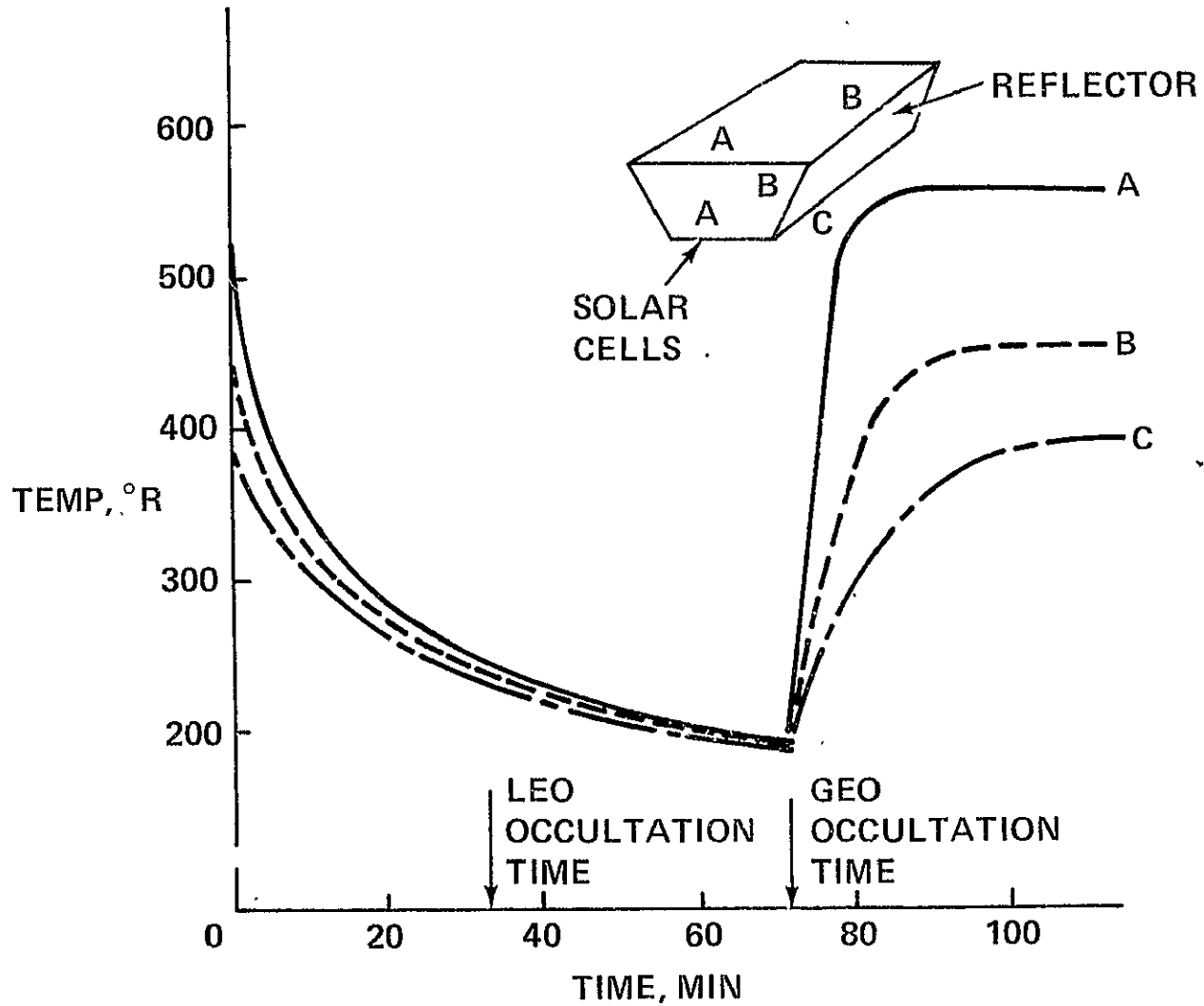
STRUCTURAL DEFLECTIONS



THERMALLY-INDUCED DEFLECTIONS DURING OCCULTATION IN GEO



STRUCTURAL TEMPERATURES DURING OCCULTATION



A-10

OCCULTATION TOLERABLE – STRUCTURAL & DEFLECTION WISE

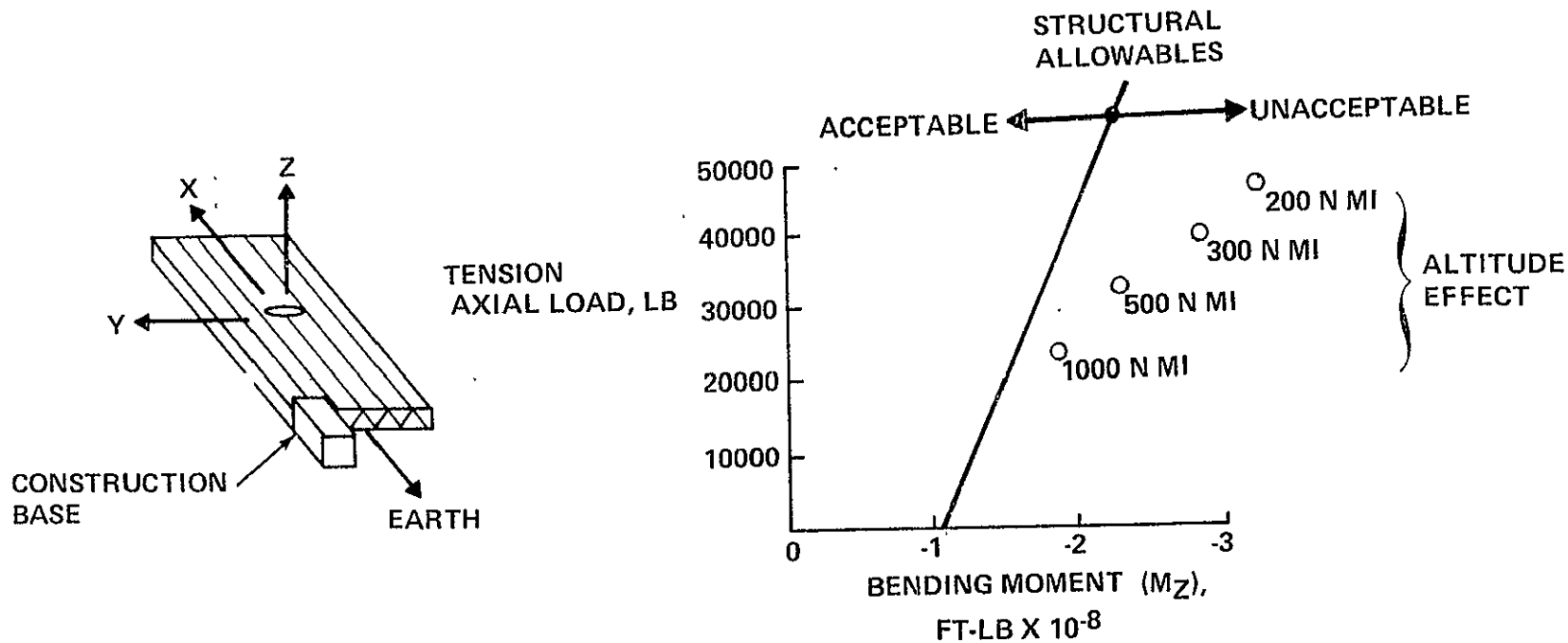
VERY LARGE AREA TRUSS-TYPE STRUCTURES

...CONSTRUCTED IN SPACE ...

- COULD ENCOUNTER HIGHER-THAN-OPERATIONAL STRUCTURAL LOADINGS DURING CONSTRUCTION IN LEO
- FACE SIZE LIMITATIONS IN LEO DUE TO SPACE DEBRIS
- SHOULD BE TRANSPORTED FROM LEO → GEO BY ELECTRIC (LOW ACCELERATION) PROPULSION SYSTEMS

LOADS DURING CONSTRUCTION

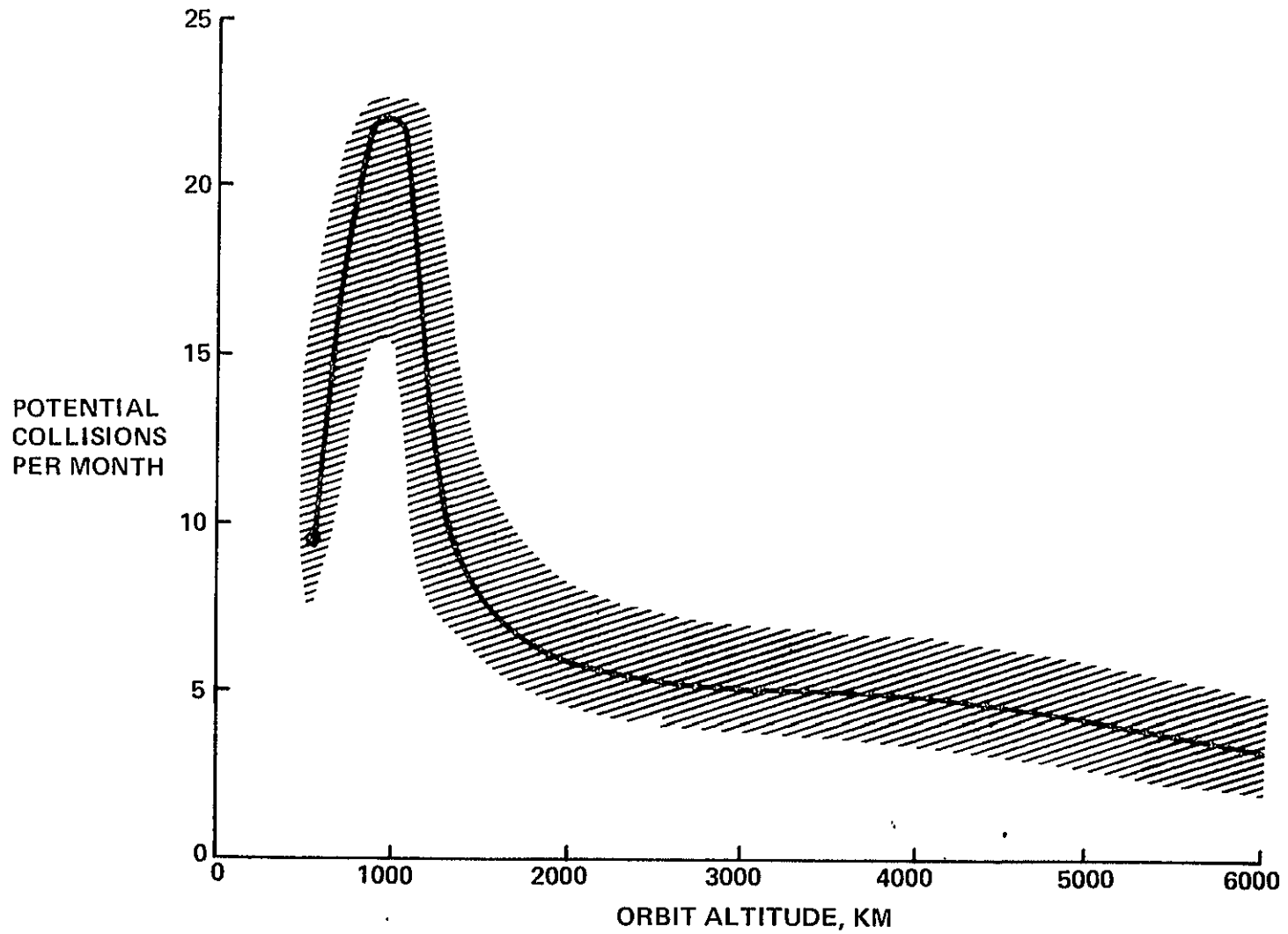
A-12



COMPLETE CONSTRUCTION OF SPS-TYPE SOLAR ARRAY STRUCTURES IN LEO IMPOSES STRUCTURAL MASS PENALTIES

LEO COLLISION PROBABILITY

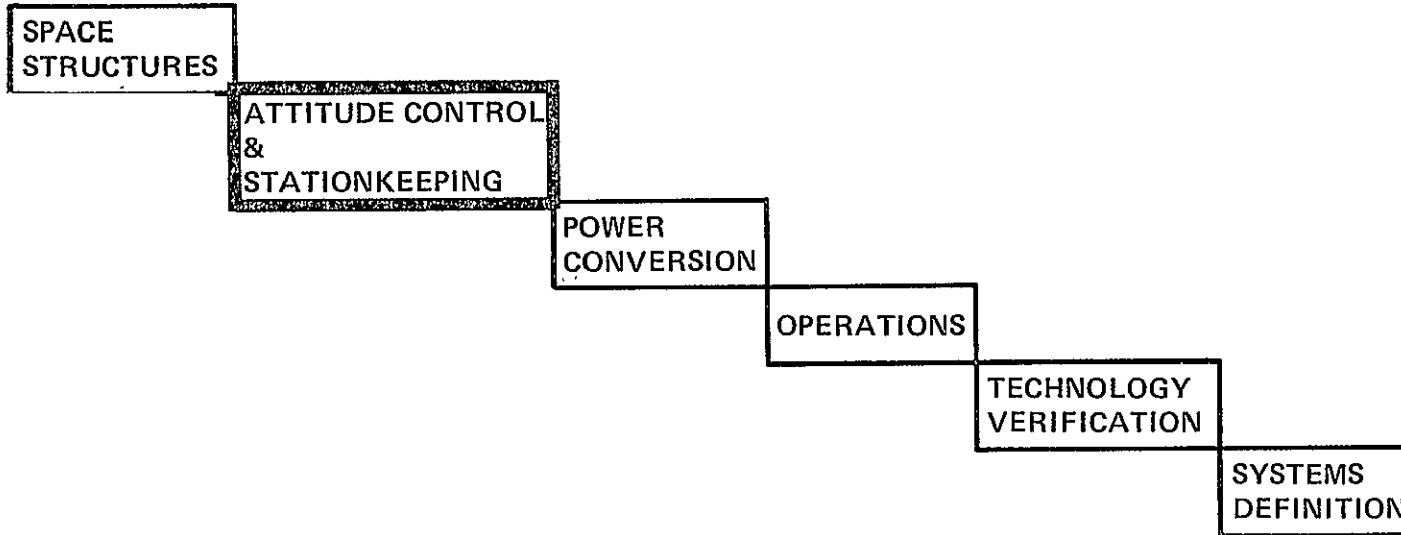
A-13



TRANSPORTATION OF SUBASSEMBLY ELEMENTS TO GEO

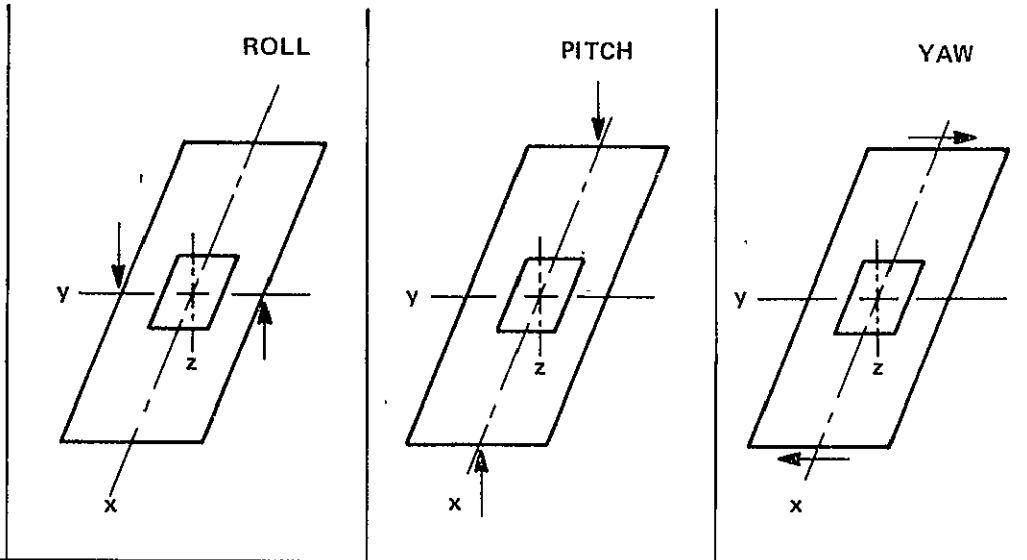
MASS KG (LB)	6.0×10^6 (13.25×10^6)	6.01×10^6 (13.24×10^6)	4.7×10^6 (10.37×10^6)	8.61×10^6 (18.99×10^6)
ALLOWABLE T/W	1.13×10^{-3}	2.9×10^{-4}	4.62×10^{-4}	4.95×10^{-4}
TRIP TIME (DAYS)	25	80	70	45

ALLOWABLE T/W RATIOS FOR LARGE SUBASSEMBLY ELEMENTS CONSTRUCTED IN LEO REQUIRE LOW THRUST ELECTRIC PROPULSION



ATTITUDE CONTROL

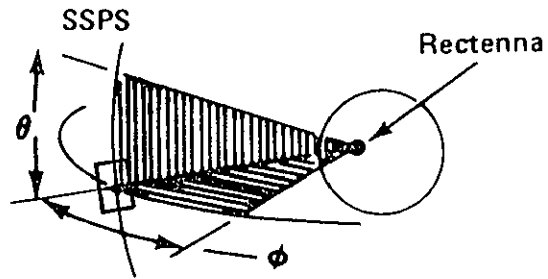
A-16



<ul style="list-style-type: none"> • STRUCTURAL LOADINGS ALLOWABLE OPERATIONAL AT GEO 	5431 N	5431 N	5431 N	TOTALS
	78.2 N	.13 N	3.57 N	
<ul style="list-style-type: none"> • PROPELLANT CONSUMPTION, KG/YR Isp = 8000 Isp = 300 	11826	1752	1292	14870
	316,090	46,720	34,378	397,188

- LOADS INDUCED BY CONTROL FORCE STRUCTURAL EXCITATION ARE TWO ORDERS OF MAGNITUDE LOWER THAN ALLOWABLES AT GEO
- HIGH-PERFORMANCE, LOW-THRUST ELECTRIC PROPULSION IS NECESSARY

STATIONKEEPING



A-17

CAUSES (PERTURBATIONS)	EFFECTS	CORRECTION DUTY CYCLE (DAYS)	ANNUAL PROPELLANT ISP = 8000-KG
• GRAVITATIONAL POTENTIAL OF THE SUN & MOON	ORBITAL INCLINATION DRIFT	365	15,695
• SOLAR RADIATION PRESSURE	ORBITAL ECCENTRICITY VARIATION ALTITUDE VARIATION	10 DAYS CONTINUOUS	58,041
• MICROWAVE RADIATION PRESSURE	SATELLITE ALTITUDE VARIATION	57 DAYS	3,297
• ELLIPTICITY OF EARTH EQUATORIAL PLANE	SATELLITE LONGITUDINAL DRIFT	57 DAYS	687
TOTAL			77,720

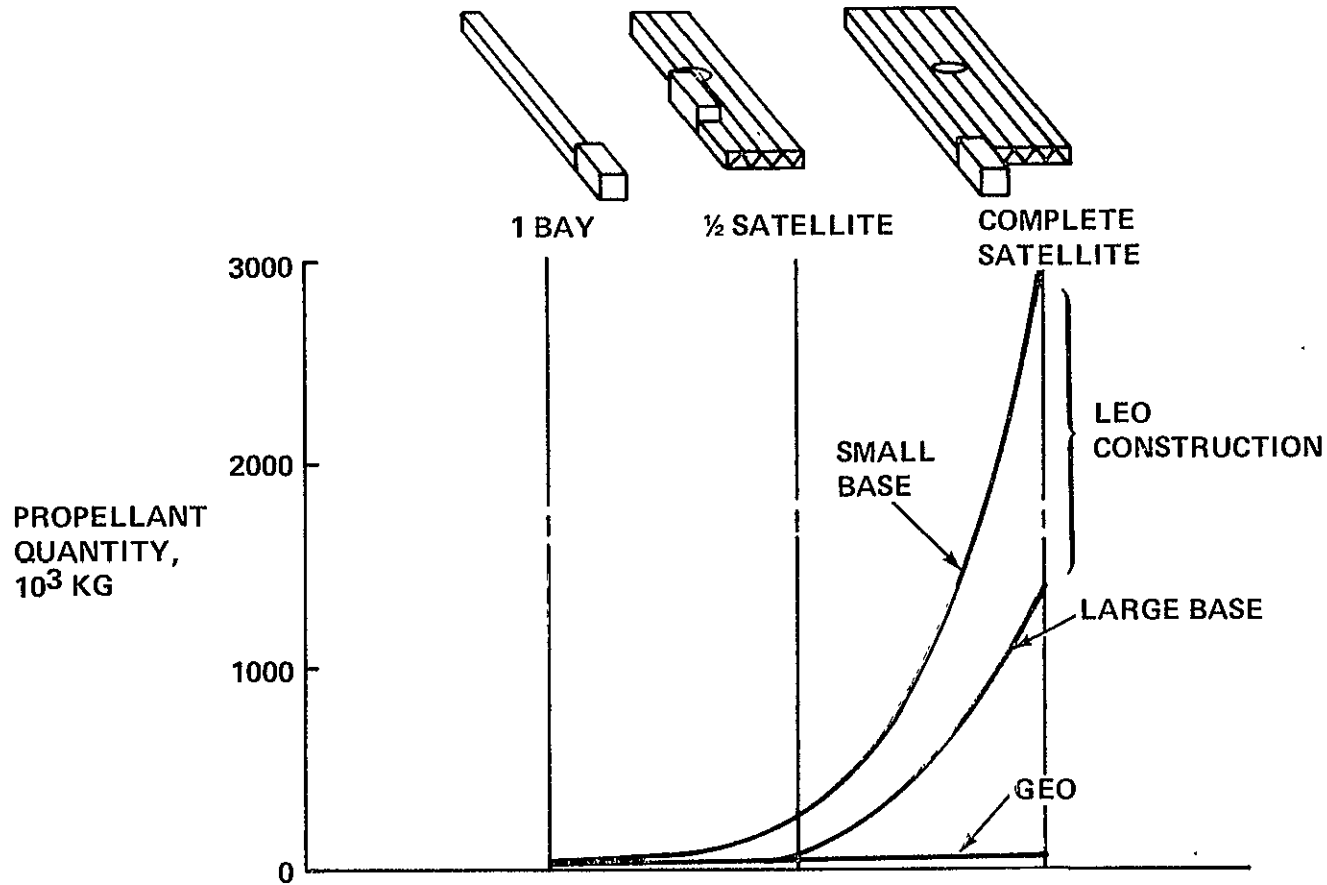
ATTITUDE CONTROL/STATIONKEEPING PROPELLANT REQUIREMENTS

- WITHIN A 120-SATELLITE CONSTELLATION SYSTEM SERVING THE U.S., A 5-GW CRYSTAL-SILICON PHOTO-VOLTAIC SPS REQUIRES PROPELLANT QUANTITIES OF:

93,000 KG/YEAR

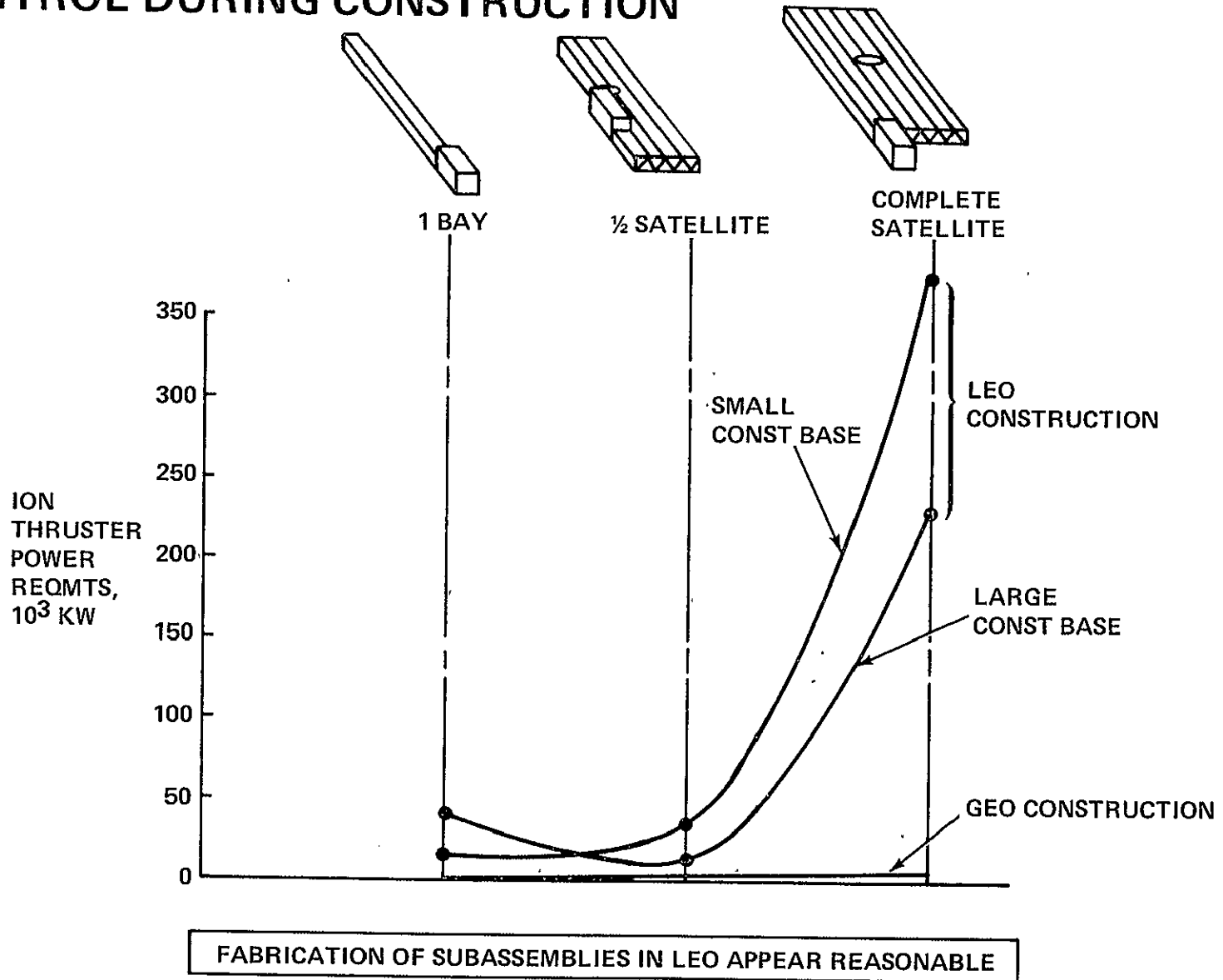
- OVER 30 YEARS, THIS REPRESENTS \approx 10% OF THE TOTAL MASS OF A SINGLE SPS SATELLITE

ATTITUDE CONTROL PROPELLANT REQUIREMENTS DURING CONSTRUCTION



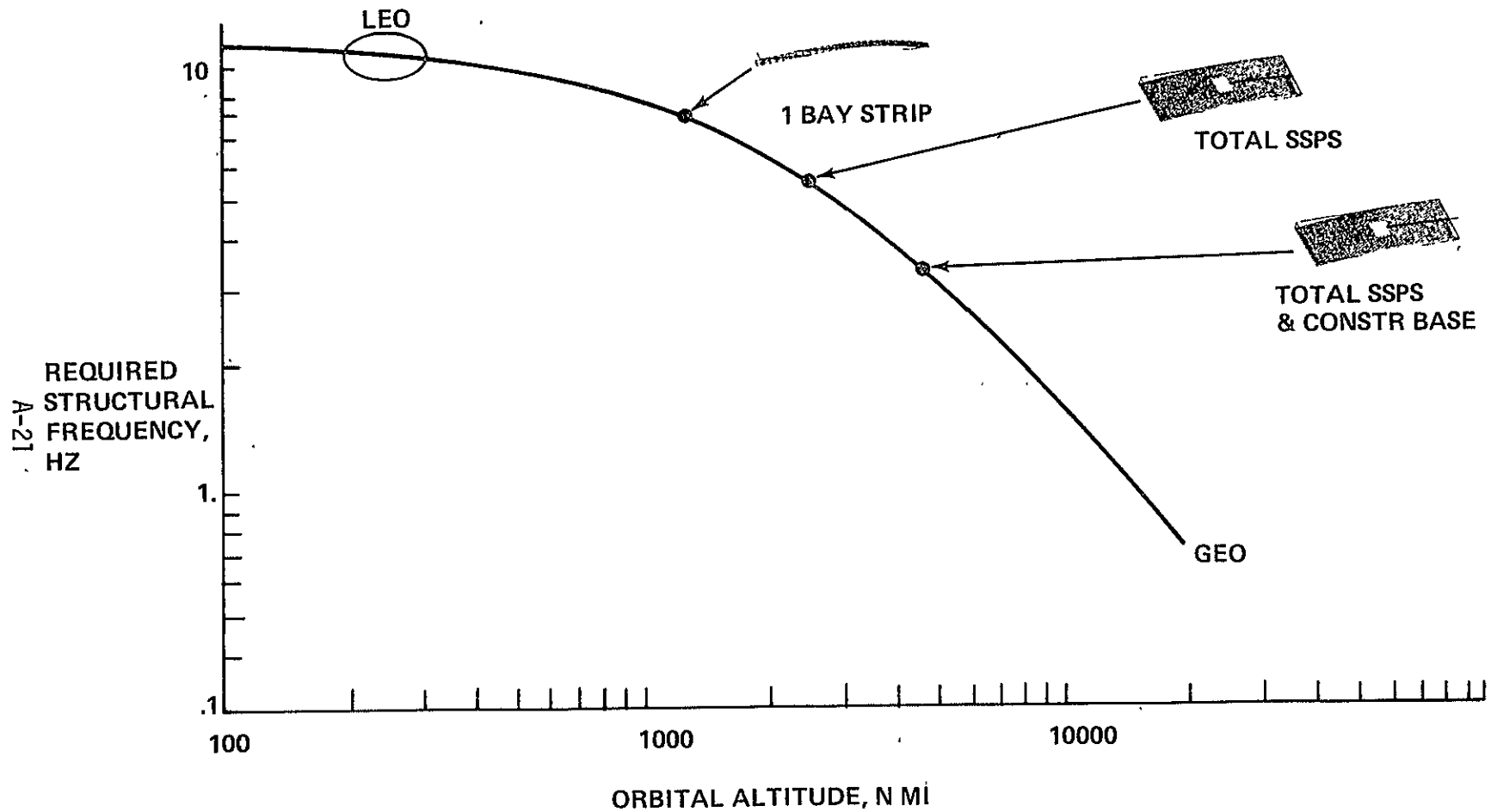
- CONSTRUCTION/ASSY OF A COMPLETE SPS IN LEO REPRESENTS ABOUT 10% OF SPS MASS AS COMPARED TO LESS THAN 0.1% AT GEO
- AIR DRAG EFFECTS IN LEO ARE INSIGNIFICANT

POWER REQUIREMENTS FOR ATTITUDE CONTROL DURING CONSTRUCTION

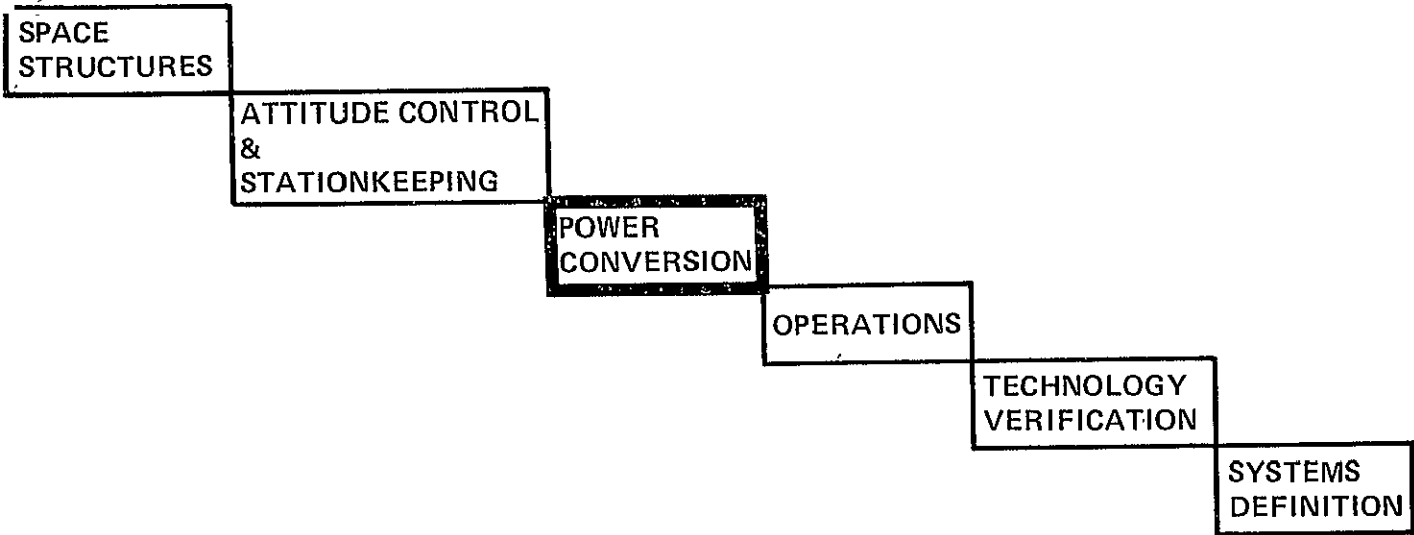


IMPACT OF STRUCTURAL-TO-CONTROL FREQUENCY RELATIONSHIPS

• FOR DESIRABLE 10:1 CHARACTERISTIC



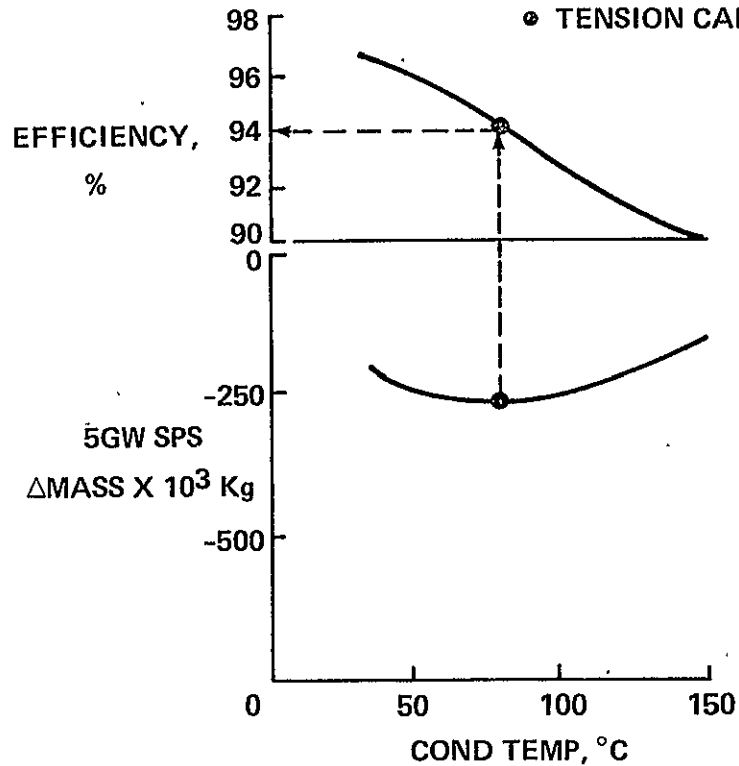
STRUCTURE/CONTROL INTERACTIONS INFLUENCE
SELECTION OF CONSTRUCTION LOCATION



POWER DISTRIBUTION EFFICIENCY

CONSIDERING:

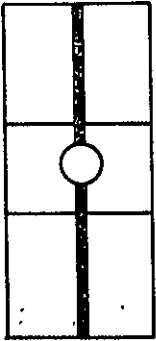
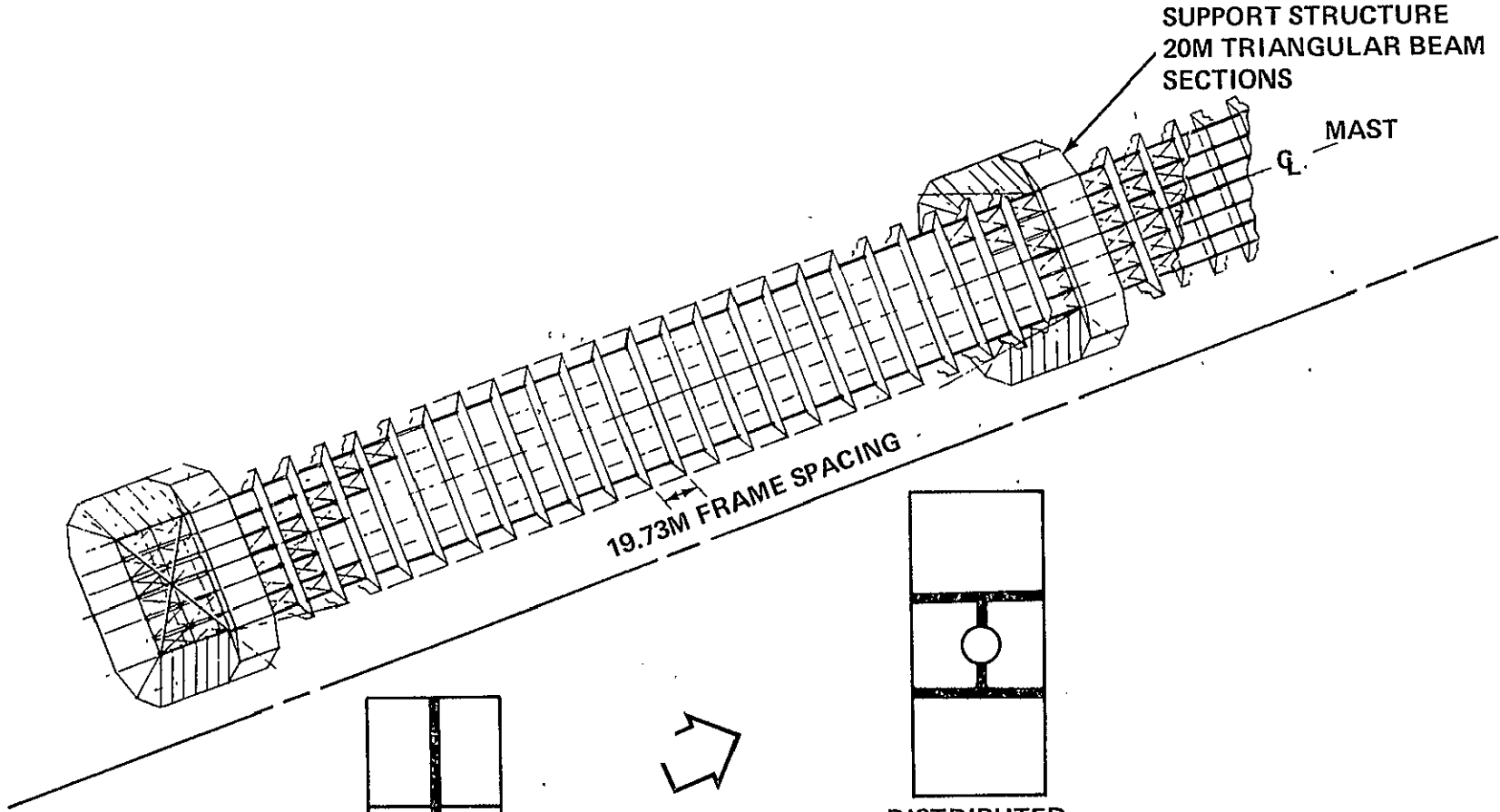
- BUS CROSS-SECTIONAL AREA, I^2R LOSSES, OPERATING TEMP
- A SOLAR CELL AREA TO COMPENSATE FOR η LOSSES
- TENSION CABLE STRUCTURAL IMPLICATIONS OF CENTRAL MAST



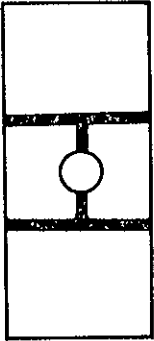
MINIMUM OVERALL SYSTEM WEIGHT
CORRESPONDS TO POWER
DISTRIBUTION EFFICIENCY OF
94% . . . FOR THIS CONFIGURATION

BASIC POWER DISTRIBUTION APPROACHES

A-24



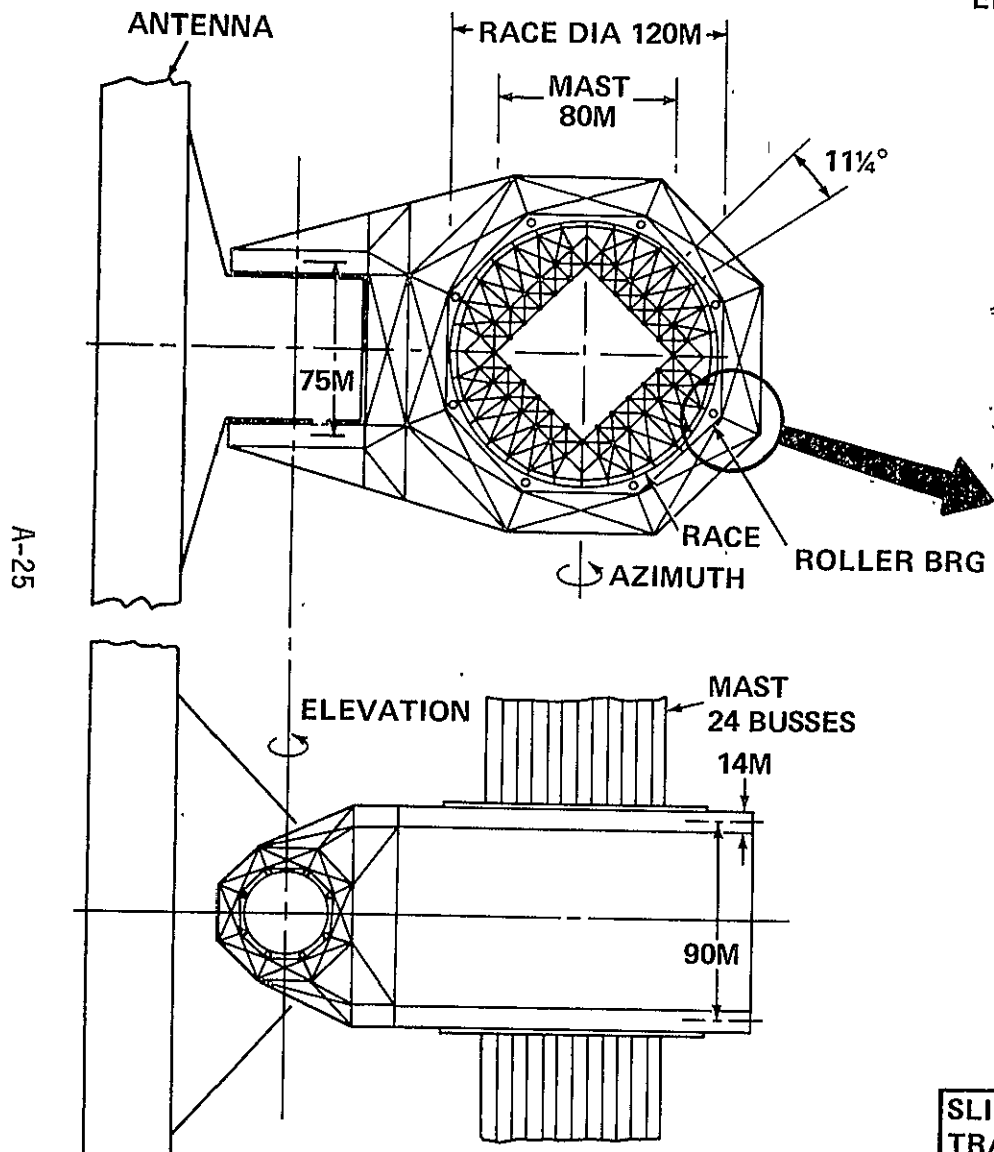
CENTRAL MAST



DISTRIBUTED

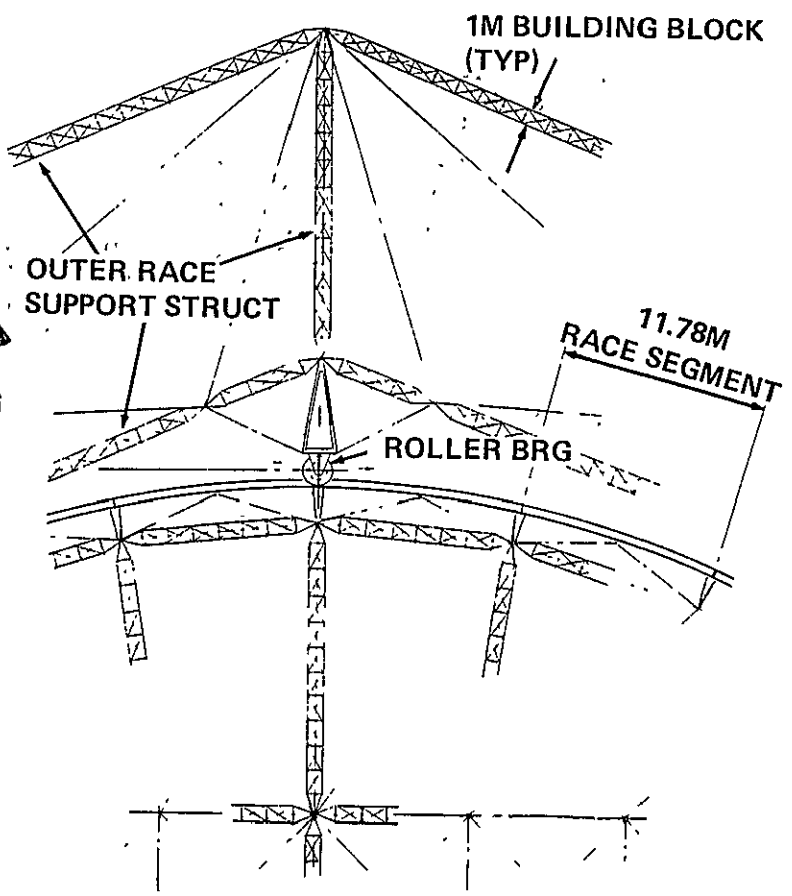
DISTRIBUTED APPROACH OFFERS SIMPLIFICATIONS IN CONSTRUCTION & ASSEMBLY

ROTARY JOINT.

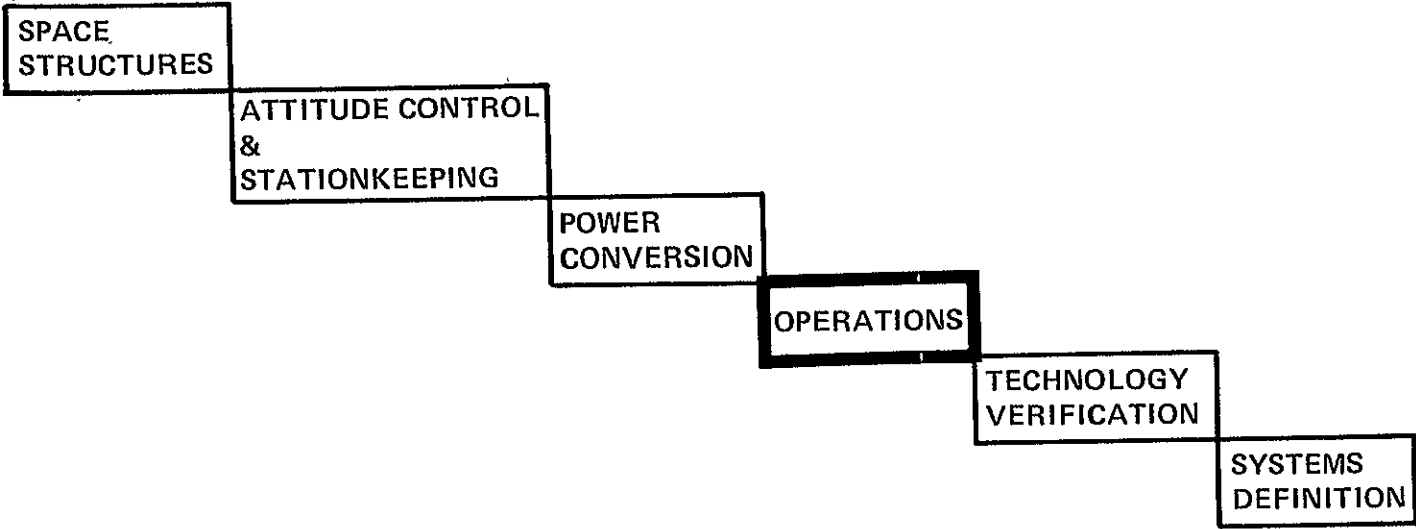


ELECTRICAL CHARACTERISTICS

- 4 PARALLEL SLIP RINGS FOR EACH ASSEMBLY
- 32 BRUSHES PER SLIP RING



SLIP RINGS/BRUSHES ARE A FEASIBLE CONCEPT FOR TRANSMITTING POWER ACROSS THE POWER DISTRIBUTION SYSTEM/ANTENNA INTERFACE

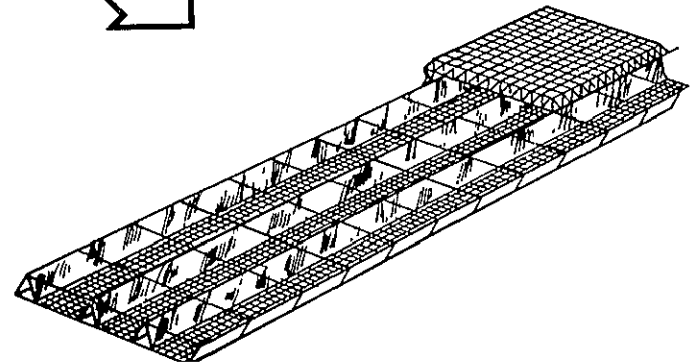
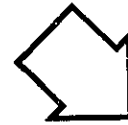
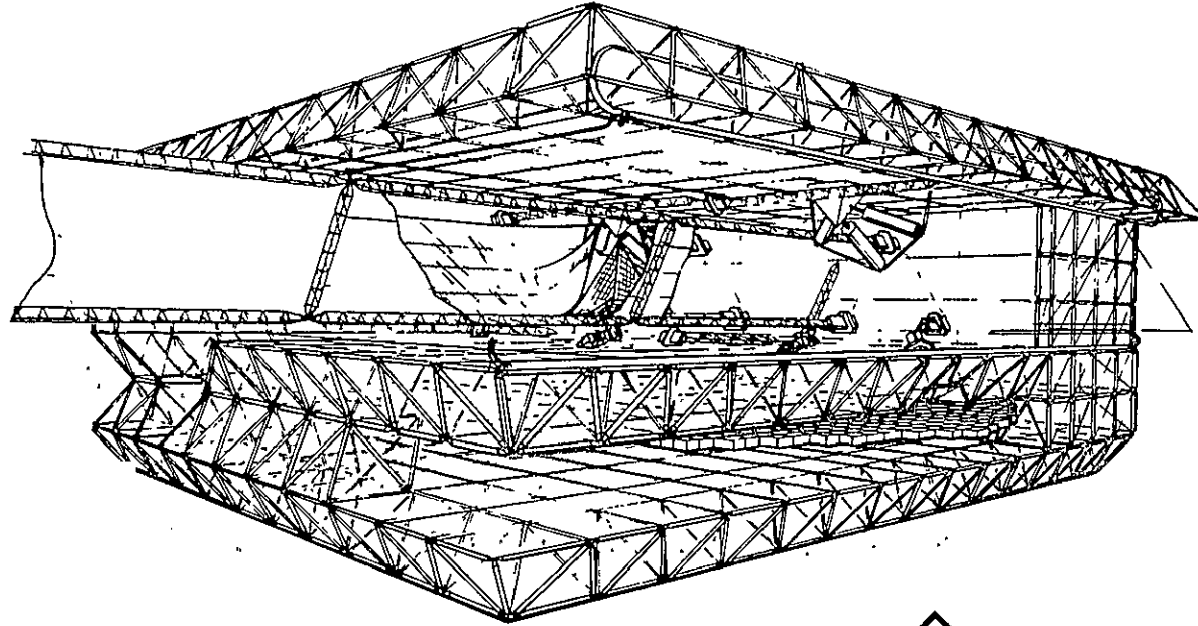


CONSTRUCTION/ASSEMBLY

**ACCEPTABLE APPROACHES FOR TRUSS-TYPE
PHOTOVOLTAIC SPS CONCEPTS ARE:**

- **CONSTRUCTION OF MAJOR SUBASSEMBLY MODULES IN LEO, WITH TRANSPORT TO GEO BY LOW ACCELERATION OTV'S**
- **CONSTRUCTION/ASSEMBLY OF THE COMPLETE SPS IN GEO**

FACTORY IN SPACE CONCEPT



A-28

FACTORY-IN-SPACE CONCEPTS

... FABRICATION/ASSEMBLY OF SPS-TYPE SYSTEMS WILL INVOLVE:

- FACTORY-TYPE ASSEMBLY-LINE OPERATIONS IN THE SPACE ENVIRONMENT...OPTIMIZED FOR PRODUCTIVITY
- CREW WORK STATIONS & MOBILITY AIDS LOCATED AT KEY SPACIAL INTERVALS, WITH ASTRO-WORKERS ACCOMMODATED IN A SHIRT-SLEEVE ENVIRONMENT
- INTERNAL TRANSPORTATION SYSTEMS FOR MOVING PEOPLE & EQUIPMENT
- A BASE MANAGEMENT ORGANIZATION/HEIRARCHY
- SUPPORTING FACILITIES INCLUDING: WAREHOUSING, CAFETERIA, RECREATIONAL, MEDICAL, LIVING, ETC.

FACTORY-IN-SPACE...REPRESENTATIVE STAFFING

...CONSTRUCTION OF COMPLETE 5 GW SPS IN LEO

● BASE MANAGEMENT	45	} PEAK ACTIVITY LEVELS & 4/YEAR RATE (3 SHIFTS)
● FACTORY WORKERS	430(2)	
● SUPPORTING PERSONNEL(1)	225	
	<hr/>	
	700	

- (1) INCLUDES MEDICS, WAREHOUSING, CAFETERIA, ETC
- (2) APPOX 100 PERSON-YEARS OF DIRECT LABOR FOR CONSTRUCTING ONE 5 GW SPS

A-30

ON-ORBIT AND EARTH CONSTRUCTION POTENTIALS

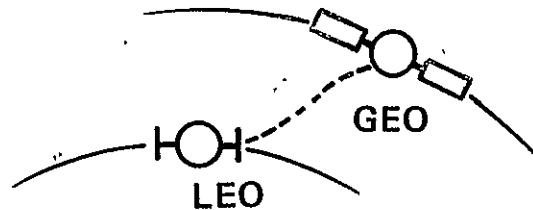
ELEMENT	EARTH FABRICATION	ON-ORBIT		ON ORBIT AUTOMATION POTENTIAL
		FAB	ASSY	
SOLAR ARRAY				
• STRUCTURE		X	X	HIGH
• BLANKETS & REFLECTORS	X		X	HIGH
MICROWAVE ANTENNA				
• STRUCTURE		X	X	HIGH
• COMPONENTS	X		X	LOW
PWR DISTRIB SYS				
• STRUCTURE		X	X	MODERATE/HIGH
• COMPONENTS	X		X	MODERATE
CONTROL SYS				
• COMPONENTS	X		X	LOW
ROTARY JOINT				
• STRUCTURE		X	X	HIGH
• COMPONENTS	X		X	LOW

*HIGH DEGREE OF AUTOMATION ENVISIONED FOR SOLAR ARRAY . . . BUT COMPARABLE AUTOMATION OF MW ANTENNA SYSTEM IS UNCERTAIN

AN OBSERVATION

MICROWAVE ANTENNA SYSTEM, ROTARY JOINT, AND CLOSE-PROXIMITY PORTIONS OF THE POWER DISTRIBUTION SYSTEM INVOLVE:

- COMPLEX FACTORY OPERATIONS LARGE PERSONNEL COMPLIMENTS
- "DENSER" ELEMENT CONFIGURATIONS SMALLER PROJECTED AREA



SUGGESTS CONSTRUCTION OF THESE ELEMENTS IN LEO WITH CONSTRUCTION, ASSEMBLY, & FINAL INTEGRATION OF THE SOLAR ARRAY IN GEO

SPACE
STRUCTURES

ATTITUDE CONTROL
&
STATIONKEEPING

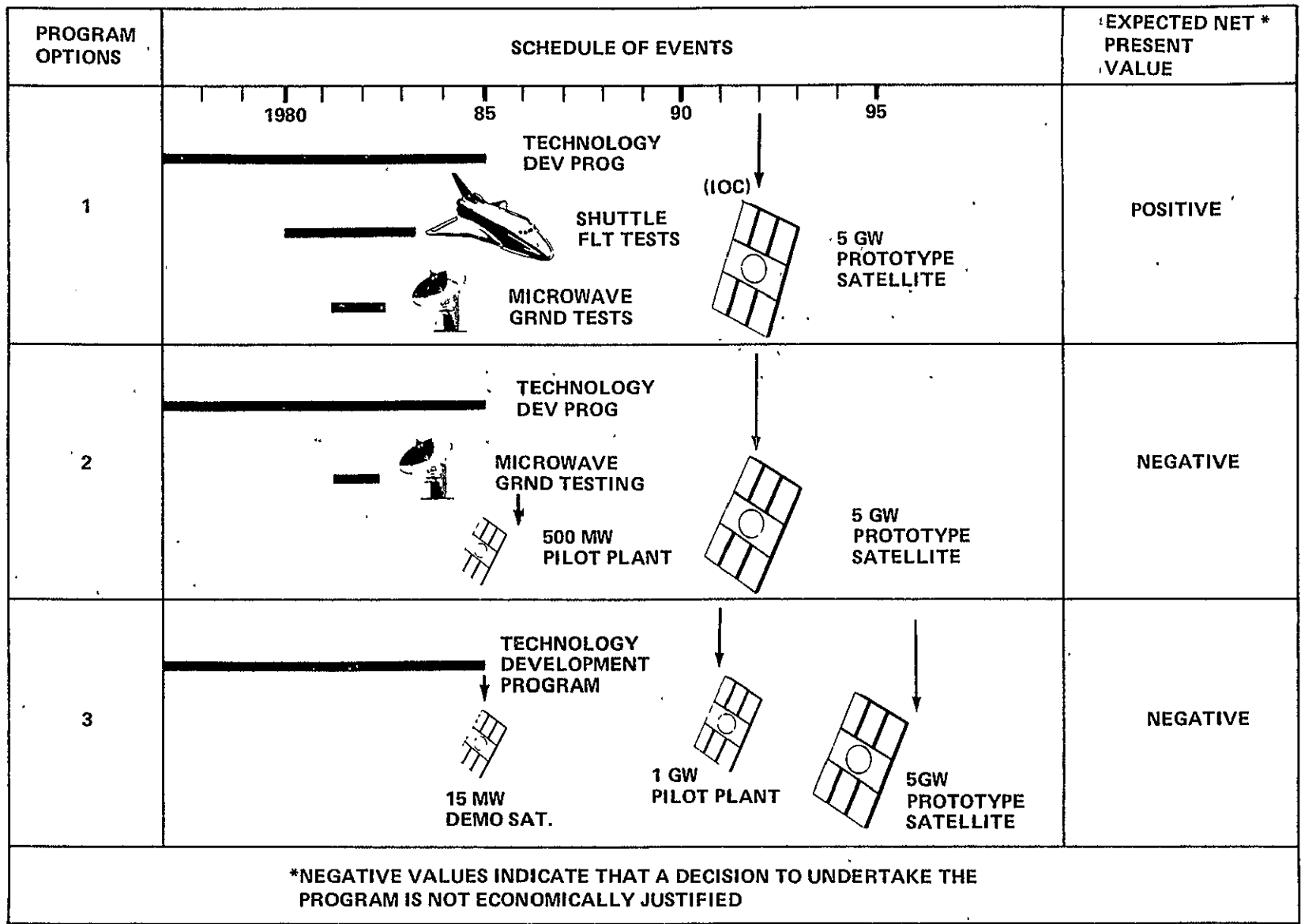
POWER
CONVERSION

OPERATIONS

TECHNOLOGY
VERIFICATION

SYSTEMS
DEFINITION

DIRECT DEVELOPMENT AND LARGE-SCALE TEST SATELLITE PROGRAM OPTIONS



A-34

SMALLER SCALE TEST SATELLITE PROGRAM OPTIONS (CONT)

PROGRAM OPTION	SCHEDULE OF EVENTS				EXPECTED NET PRESENT VALUE	ESTIMATED TECH. VERIF PROGRAM COSTS
	'80	'85	'90	'95		
5	<p>TECHNOLOGY DEVEL PROGRAM</p> <p>SHUTTLE FLT TESTS</p> <p>150-KW GEO SATELLITE (100 M LINEAR ANTENNA)</p> <p>MICROWAVE GRD TESTS</p> <p>2-MW GEO TEST SATELLITE 20 M X 20 M ANTENNA 1000M LINEAR ANTENNA (1986 IOC)</p> <p>1995 IOC</p> <p>5 GW PROTOTYPE SATELLITE</p>				POSITIVE	≈ \$3.5B

SMALLER SCALE TEST SATELLITE PROGRAM OPTIONS (CONT)

A-36

PROGRAM OPTION	SCHEDULE OF EVENTS				EXPECTED NET PRESENT VALUE	ESTIMATED TECH. VERIF PROGRAM COSTS
	'80	'85	'90	'95		
5	<p>TECHNOLOGY DEVEL PROGRAM</p> <p>SHUTTLE FLT TESTS</p> <p>150-KW GEO SATELLITE (100 M LINEAR ANTENNA)</p> <p>MICROWAVE GRD TESTS</p> <p>2-MW GEO TEST SATELLITE 20 M X 20 M ANTENNA 1000M LINEAR ANTENNA (1986 IOC)</p> <p>1995 IOC</p> <p>5 GW PROTOTYPE SATELLITE</p>				POSITIVE	≈ \$3.5B

SPACE
STRUCTURES

ATTITUDE CONTROL
&
STATIONKEEPING

POWER
CONVERSION

OPERATIONS

TECHNOLOGY
VERIFICATION

SYSTEMS
DEFINITION

RELATING TO THE LEO VS GEO ASSEMBLY QUESTION

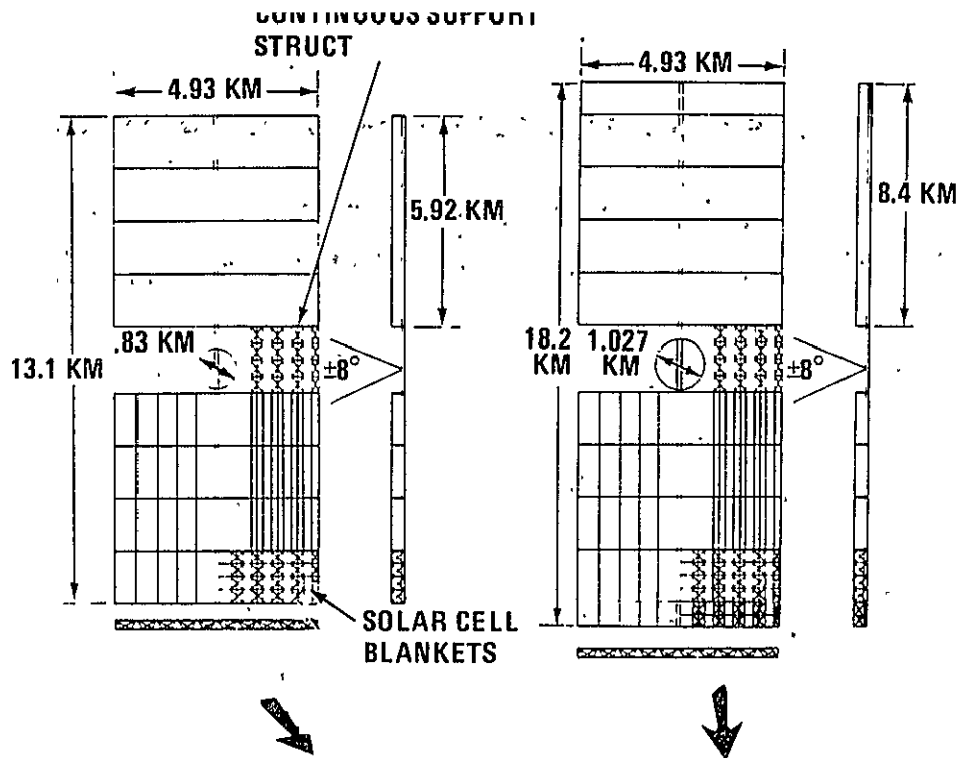
- COMPLETE ASSEMBLY OF AN OPERATIONAL SPS IN LEO, FOLLOWED BY TRANSPORT TO GEO, DOES NOT APPEAR TECHNICALLY DESIRABLE
 - COLLISION WITH SPACE DEBRIS SIZE LIMITATIONS
 - HIGHER-THAN-OPERATIONAL STRUCTURAL LOADING DURING CONSTRUCTION
 - LARGE POWER REQUIREMENTS FOR CONTROL THRUSTERS (≈ 300 MW)
 - ATTITUDE CONTROL PROPELLANT NEEDS . . . $\approx 10\%$ SPS MASS IN LEO
- VS
0.1% SPS MASS IN GEO
- MIX OF GEO VS LEO CONSTRUCTION ACTIVITY REMAINS TO BE RESOLVED

AN ISSUE:



COMPATIBLE REQUIREMENTS TO OPTIMIZE PRODUCIBILITY

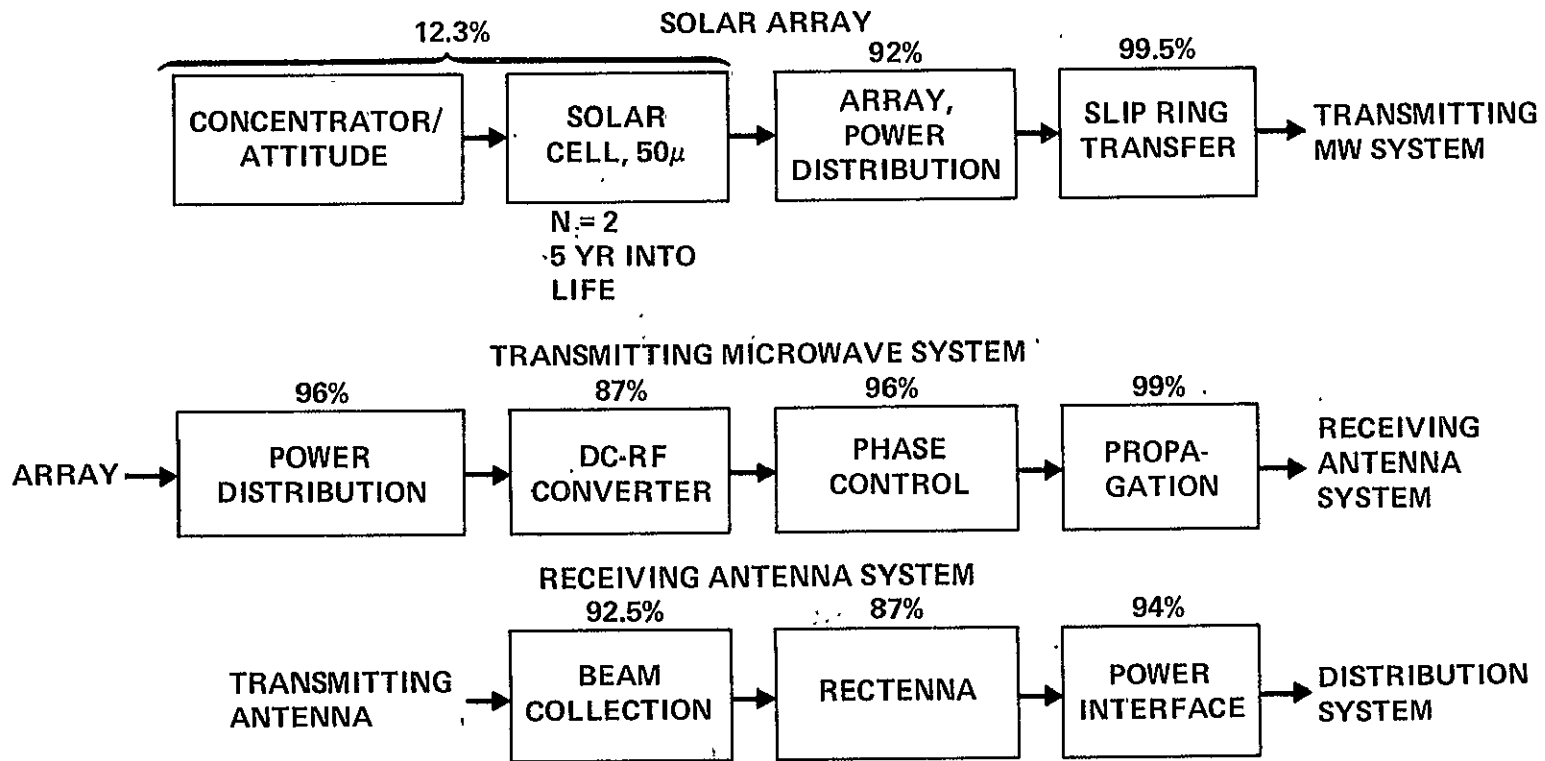
CONFIGURATION UPDATE



A-39

CHARACTERISTICS	END OF PHASE I	END OF STUDY
• POWER	5000 MW	5000 MW
• MASS	18.1×10^6 KG	27.2×10^6 KG
• SIZE	13.1 X 4.9 KM	18.2 X 4.9 KM
• ORBIT	GEOSYNCHRONOUS	GEOSYNCHRONOUS
• LIFE	30 YR	30 YR
• OPERATING FREQ	2.45 GHz	2.45 GHz
• DC-TO-DC EFFIC	55%	58%
• SOLAR CONV EFFIC	12.3%	8.0%

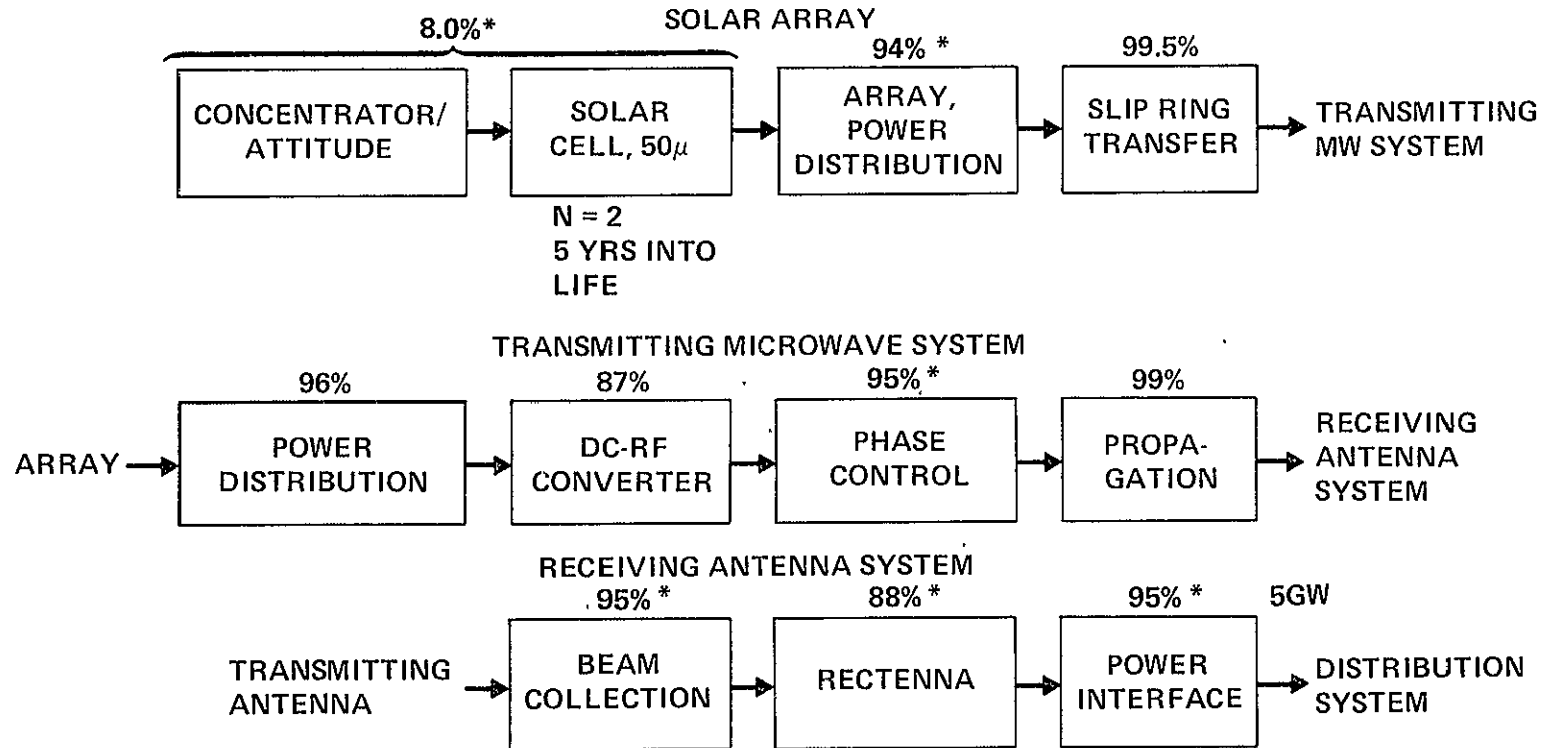
EFFICIENCY CHAIN AT START OF STUDY



A-40

REPRESENT MOST OPTIMISTIC TECHNOLOGY PROJECTIONS AS ESTABLISHED IN PHASE I STUDIES.

EFFICIENCY CHAIN AT CONCLUSION OF STUDY

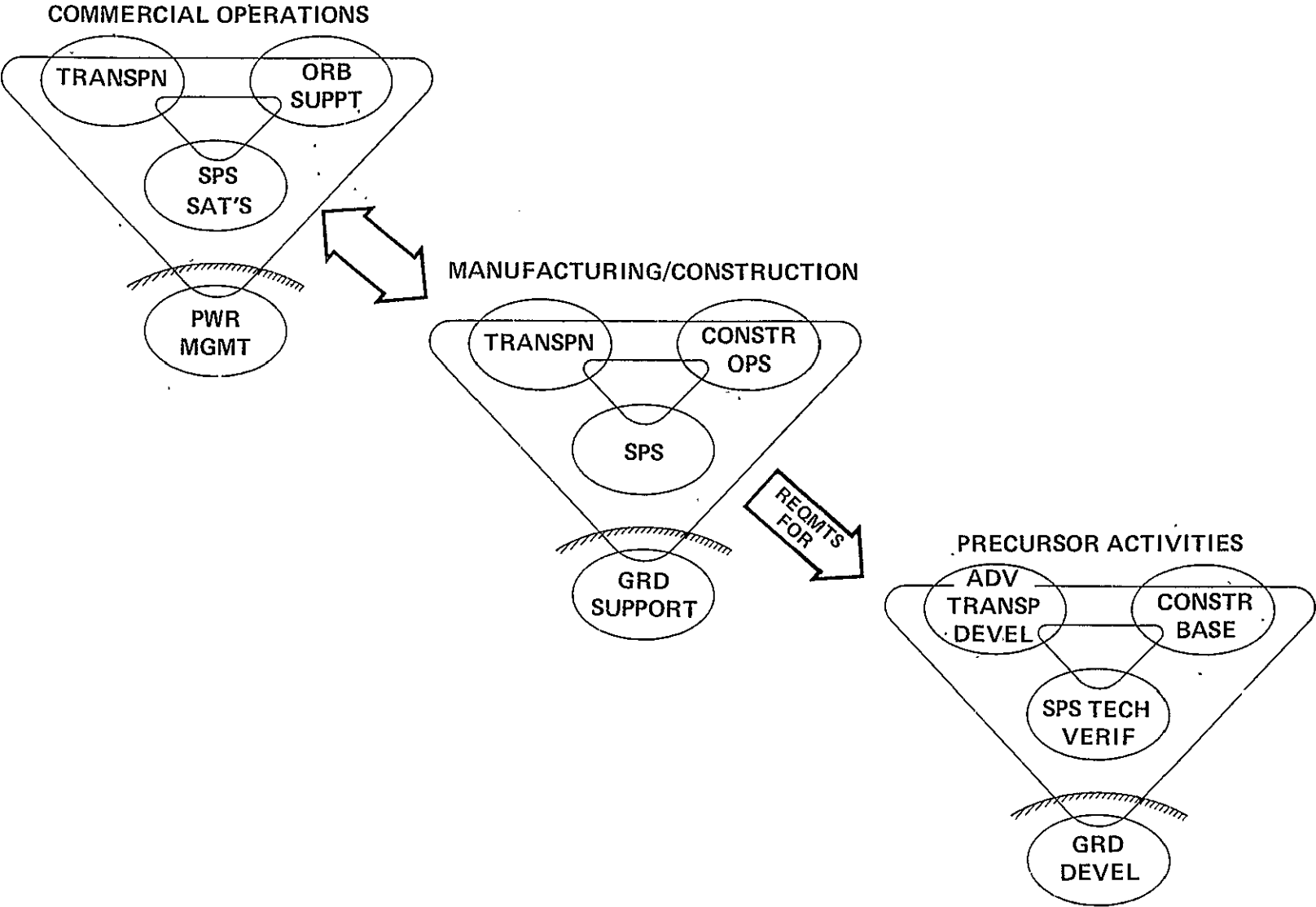


A-41

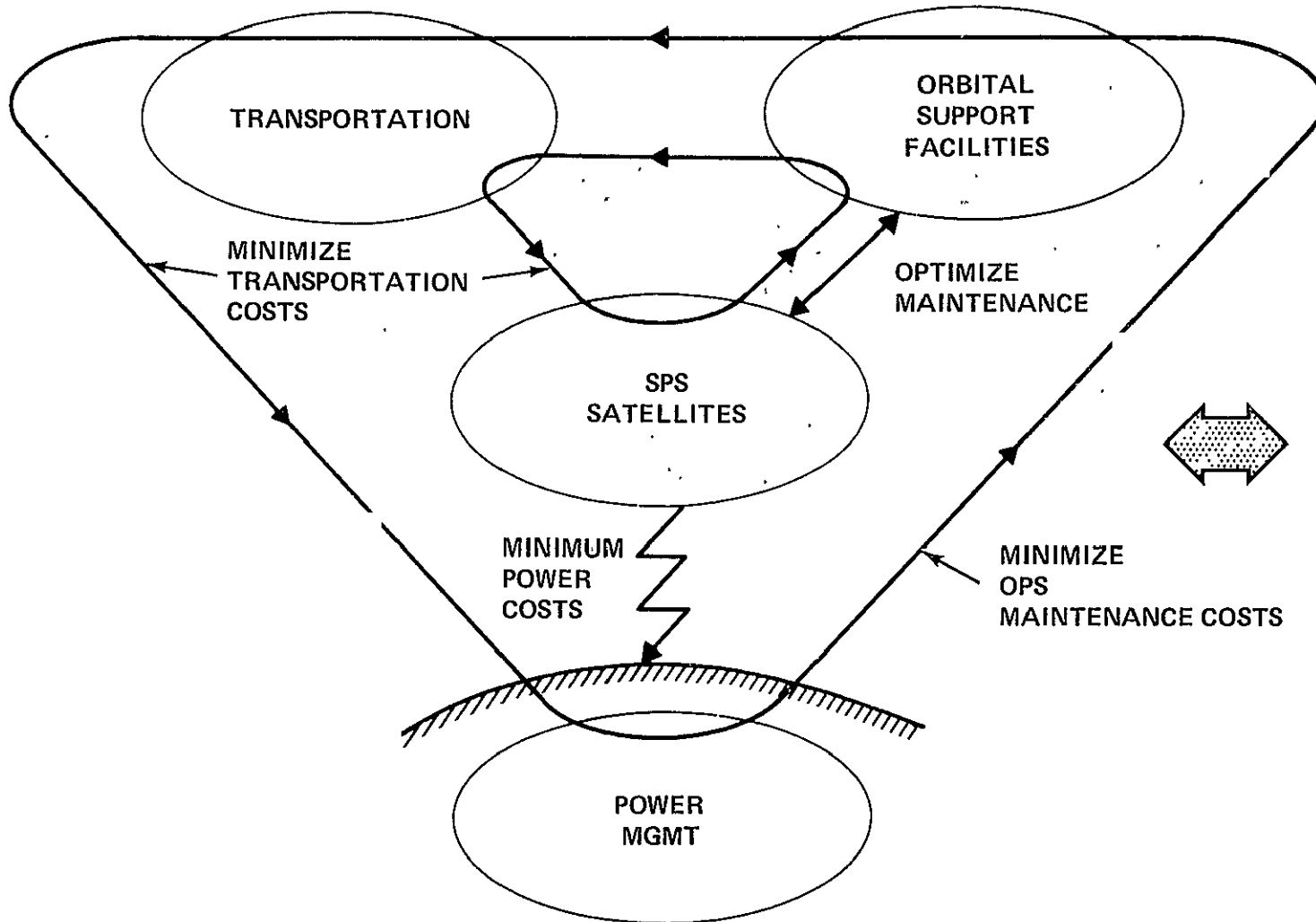
*REPRESENT MOST LIKELY VALUES OF TECHNOLOGY PROJECTIONS FOR THE 1995 TIME FRAME AS ESTABLISHED THROUGH PHASE II & III STUDIES

RECOMMENDATIONS

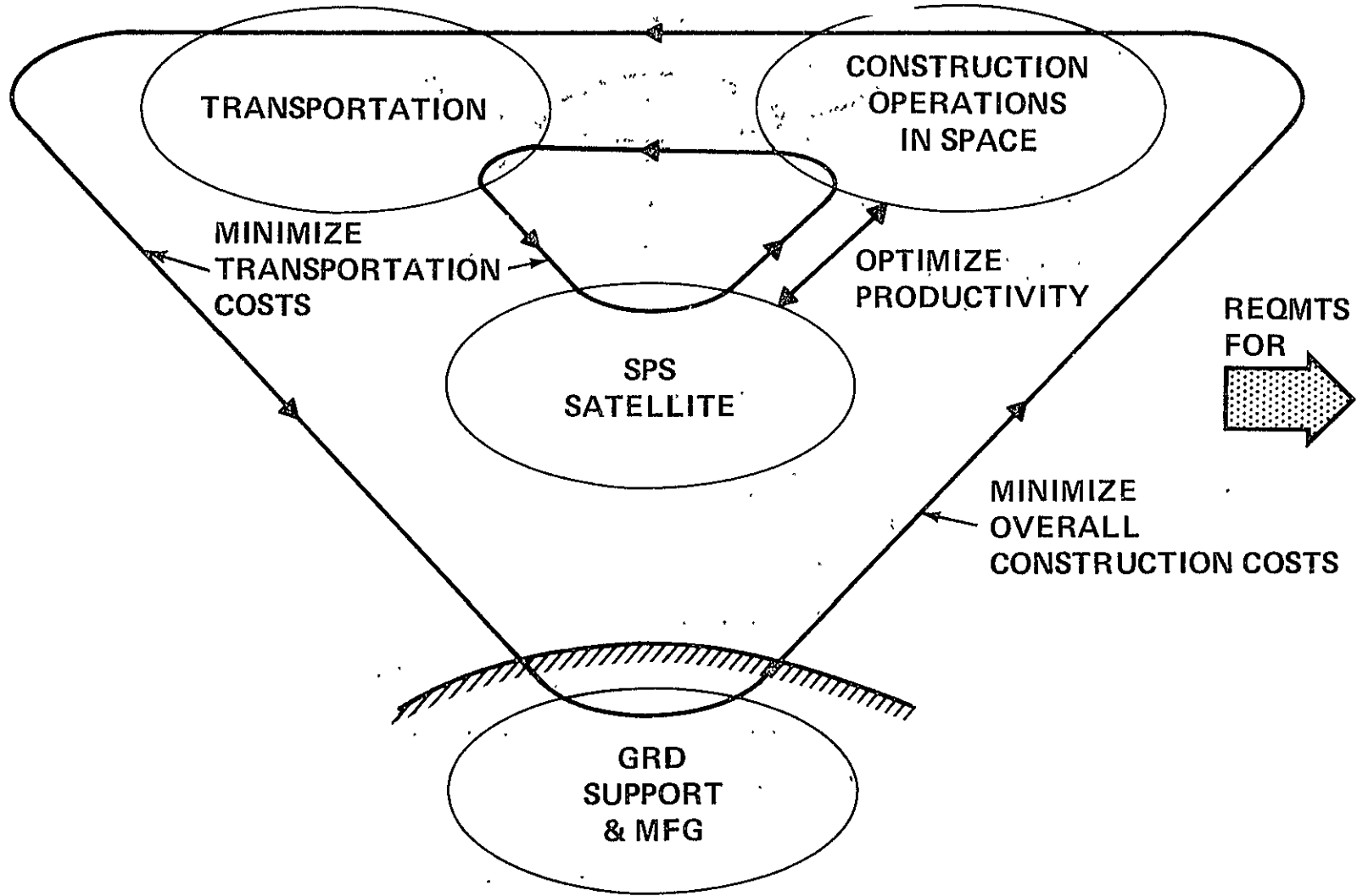
TRIADS OF SPS PROGRAM INTERACTIONS



SPS COMMERCIAL OPERATIONS TRIAD

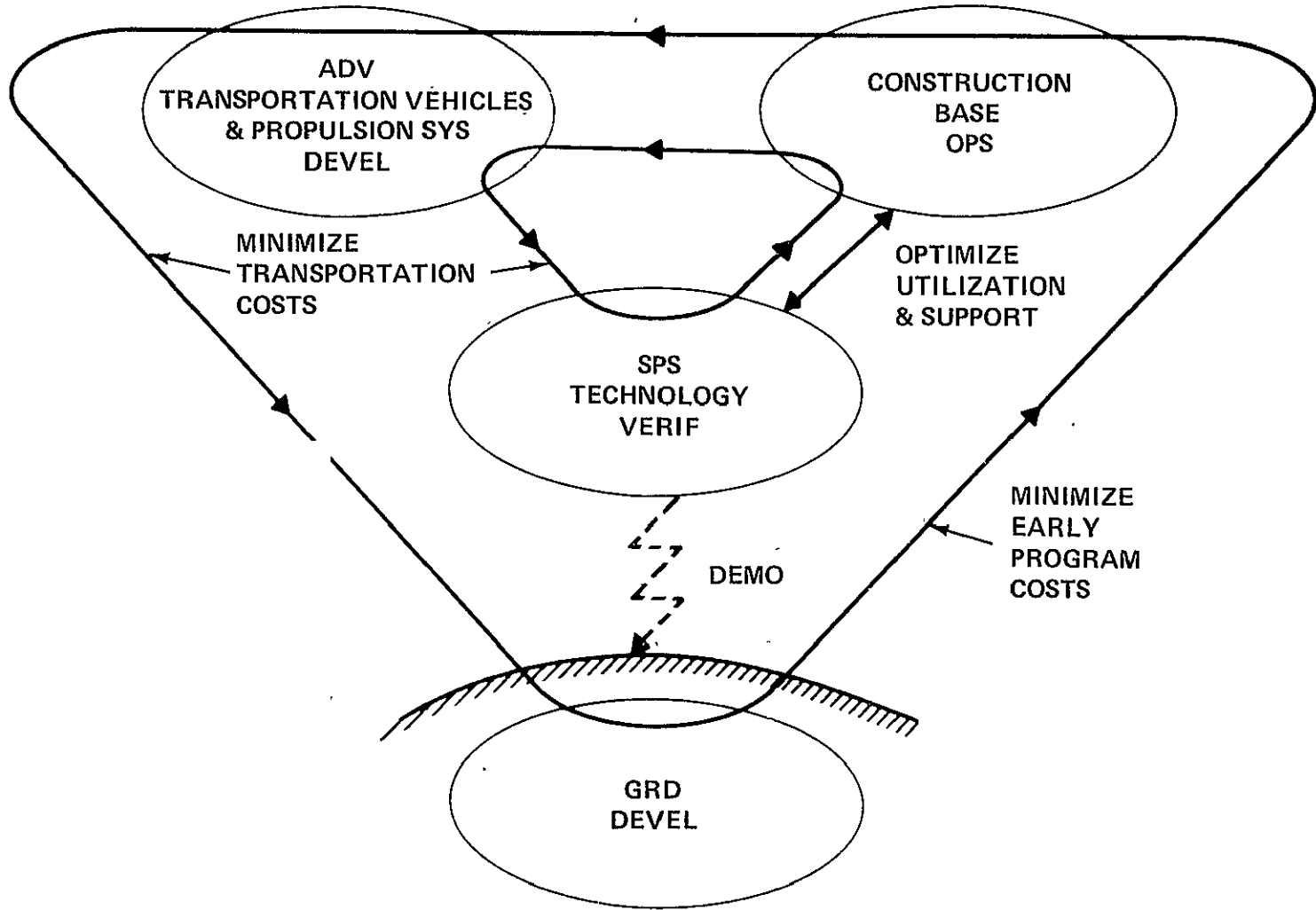


SPS MANUFACTURING AND CONSTRUCTION TRIAD



A-45

PRECURSOR ACTIVITIES TRIAD



CONFIGURATION DEVELOPMENT

DEFINITION OF GENERIC THIN-FILM PHOTOVOLTAIC SPS CONFIGURATIONS WITH FLEXIBILITY TO ACCEPT TECHNOLOGY IMPROVEMENTS



SPS TECHNOLOGY VERIFICATION

DEVELOP/EVALUATE PROGRAM OPTIONS WITHIN THE FUNDING RANGES SUGGESTING POSITIVE "EXPECTED NET PRESENT" VALUES FOR AN SPS PROGRAM (E.G., \approx \$3.0B - \$3.5B FOR GROUND/ORBITAL DEVEL)

TECHNOLOGY DEVELOPMENT

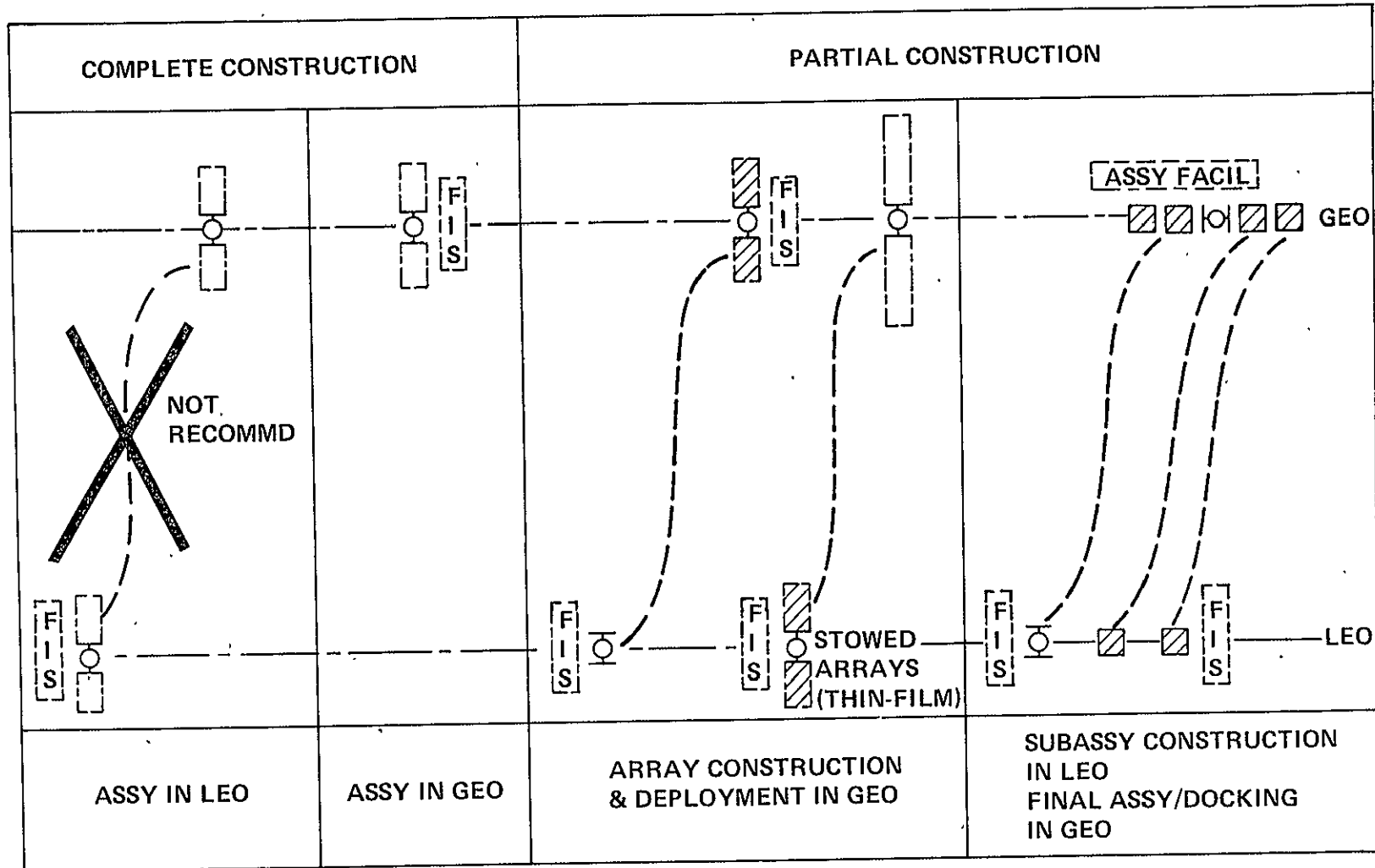
ESTABLISH PROBABLE RANGES OF PERFORMANCE REQUIREMENTS ASSOCIATED WITH LOW THRUST ELECTRIC PROPULSION SYSTEMS TO FOCUS & ACCELERATE SUPPORTIVE R & D

- GEO ATTITUDE CONTROL/STATIONKEEPING
- LEO \rightarrow GEO ORBIT TRANSFER OF LARGE SUBASSEMBLIES

MANUFACTURING AND CONSTRUCTION

- **CONTINUE DEVELOPMENT OF "BEAM MACHINES" FOR FABRICATION OF ALUMINUM/COMPOSITE TRUSS-TYPE STRUCTURES IN SPACE**
- **DEFINE/ASSESS APPROACHES FOR AUTOMATING CONSTRUCTION/ASSEMBLY OF THE MW ANTENNA SYSTEM A COMMON SPS ELEMENT**
- **EVALUATE ALTERNATE ROTARY JOINT APPROACHES & IN-ORBIT PRODUCIBILITY POTENTIALS . . . & DEFINE TECHNIQUES FOR AUTOMATING CONSTRUCTION/ASSEMBLY**
- **CONDUCT PARAMETRIC ANALYSES OF SPS MANUFACTURING & CONSTRUCTION OPTIONS TO IDENTIFY APPROACHES OPTIMIZING PRODUCTIVITY IN-ORBIT & MINIMIZING OVERALL CONSTRUCTION COSTS TO SERVE AS THE BASIS FOR ESTABLISHING REQUIREMENTS FOR PRECURSOR CONSTRUCTION BASE OPERATIONS & ADVANCED PROPULSION SYSTEMS DEVELOPMENT**

CANDIDATE SPS CONSTRUCTION SCENARIOS



[FIS] FACTORY-IN-SPACE

PRECEDING PAGE BLANK NOT FILMED

Appendix B: Inputs to ECON Inc for Economic Analysis

Inputs supplied to ECON, Inc. for use in the unit production cost model analysis are summarized in table B1. Data was supplied in the form of worst, most likely and best values, representing an estimate of the statistical range for each of the model parameters. For those parameters not shown, data was supplied by either Raytheon or A.D. Little.

Figs B-1 and B-2 show the decision tree schematics used in the economic evaluation of alternate SPS development Programs 4 and 5, respectively. Cost estimates of total program expenditures for each time phase are shown. Included in these estimates are costs for:

- Ground Development Programs
 - Solar Blanket
 - Microwave Transmission
 - Large Structures
- Shuttle Sortie Flights
- Development of a 150KW Satellite
- Development of a 2MW Satellite
- Development of a 5GW Prototype Satellite

Tables B2 and B3 summarize the state of knowledge estimated for each of the model parameters used. The data shown, in terms of percentage, represent the reduction in the uncertainties achieved in each of the parameters at each of the major decision points.

B-2

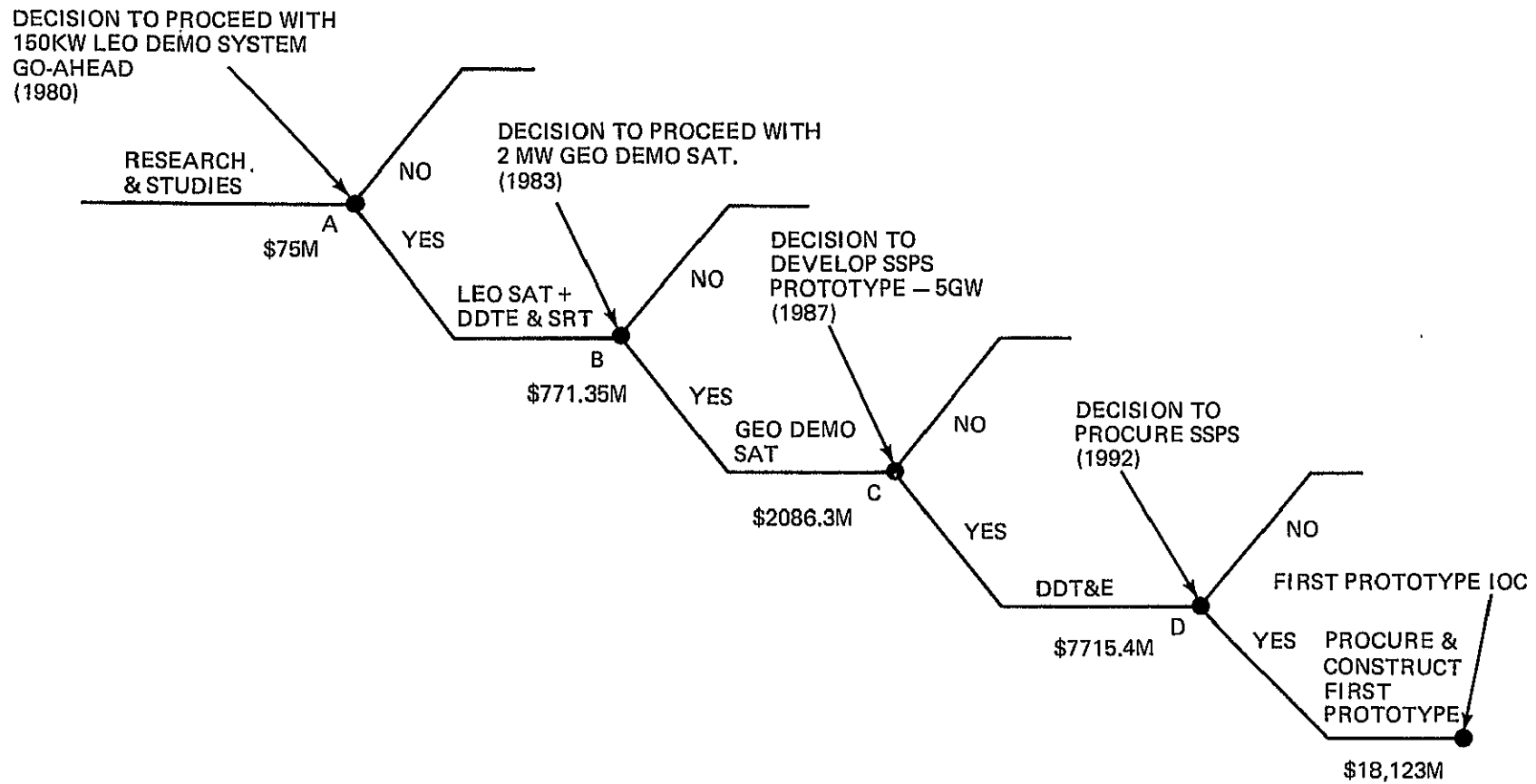


Fig B-1 Program 4 - SPS Development Program Decision Tree

B-3

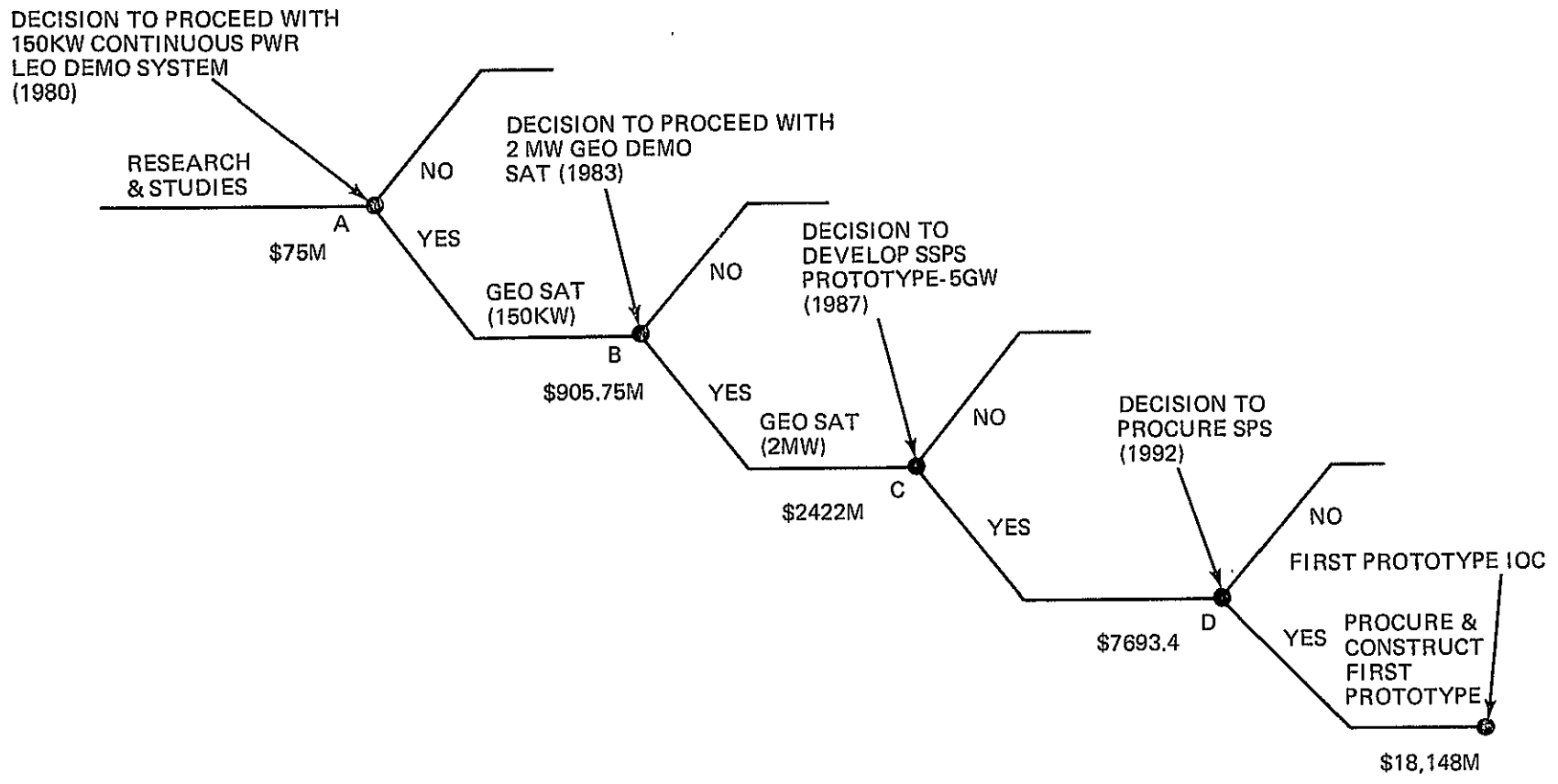


Fig B-2 Program 5 - SPS Development Program Decision Tree

TABLE B1: UNIT PRODUCTION COST MODEL INPUT VALUES

INPUT ELEMENT	UNITS	RANGE OF VALUES		
		BEST	MOST LIKELY	WORST
POWER OUTPUT AT RECTENNA BUSBAR (b.o.l.)	kW		5.258×10^6	
SOLAR CELL EFFICIENCY (b.o.l.)	Fraction	0.1440	0.1293	0.1019
SOLAR ARRAY POWER DISTRIBUTION EFFICIENCY	Fraction	0.95	0.93	0.92
ANTENNA INTERFACE EFFICIENCY	Fraction	0.99	0.98	0.97
ANTENNA POWER DISTRIBUTION EFFICIENCY	Fraction		RAYTHEON	
DC-PF CONVERTER EFFICIENCY	Fraction		RAYTHEON	
PHASE CONTROL EFFICIENCY	Fraction		RAYTHEON	
IONOSPHERIC PROPAGATION EFFICIENCY	Fraction		RAYTHEON	
ATMOSPHERIC PROPAGATION EFFICIENCY	Fraction		RAYTHEON	
BEAM COLLECTION EFFICIENCY	Fraction		RAYTHEON	
RF-DC CONVERTER EFFICIENCY	Fraction		RAYTHEON	
RECTENNA POWER DISTRIBUTION EFFICIENCY	Fraction		RAYTHEON	
PACKING FACTOR OF SOLAR BLANKET	Fraction	.99	.95	.91
SOLAR FLUX CONSTANT	kW/km ²		1353×10^3	
EFFECTIVE CONCENTRATION RATIO	Fraction	2.0	2.0	2.0
SPECIFIC MASS OF SOLAR BLANKET	kg/km ²		A.D. LITTLE	
EFFICIENCY OF SOLAR CONCENTRATOR	Fraction	.9	.86	.82
SPECIFIC MASS OF SOLAR CONCENTRATOR	kg/km ²	39820	59340	79120
RATIO: COND. STRUCT. MASS TO SOLAR ARRAY AREA	kg/km ²	4140	4625	5060
RATIO: NON-COND. STRUCT. MASS TO SOLAR ARRAY AREA	kg/km ²	35,900	39,900	43,890
SPECIFIC MASS OF CENTRAL MAST	kg/km	100×10^3	120×10^3	200×10^3
ASPECT RATIO OF SOLAR ARRAY	Fraction		1.2	
ANTENNA CLEARANCE	Fraction		1.5	
DIAMETER OF TRANSMITTING ANTENNA	km		1.027	
SPECIFIC MASS OF ANTENNA STRUCTURE	kg/kW	.0432	.048	.0528
SPECIFIC MASS OF DC-RF CONVERTERS	kg/kW		RAYTHEON	

B-4

TABLE B1: UNIT PRODUCTION COST MODEL INPUT VALUES (CONTINUED)

INPUT ELEMENT	UNITS	RANGE OF VALUES		
		BEST	MOST LIKELY	WORST
SPECIFIC MASS OF ANTENNA POWER DIST. SYSTEM	kg/kW		RAYTHEON	
SPECIFIC MASS OF WAVEGUIDES	kg/kW		RAYTHEON	
SPECIFIC MASS OF ANTENNA INTERFACE	kg/kW	.0171	.0190	.0380
SPECIFIC MASS OF PHASE CONTROL ELECTRONICS	kg/kW		RAYTHEON	
MISCELLANEOUS SATELLITE MASS	kg	70×10^3	100×10^3	360×10^3
BASIC UNIT MASS OF CONSTRUCTION BASE - SMALL	kg	2.475×10^6	2.75×10^6	3.025×10^6
BASIC UNIT MASS OF CONSTRUCTION BASE - LARGE	kg	4.95×10^6	5.5×10^6	6.05×10^6
SPECIFIC MASS OF EPS SOLAR ARRAY	kg/kW	1.5	2	5
EPS POWER REQUIREMENTS - SMALL BASE - LEO	kW	2376	2640	2904
EPS POWER REQUIREMENTS - LARGE BASE - LEO	kW	6466	7185	7903
EPS POWER REQUIREMENTS - SMALL BASE - GEO	kW	945	1050	1155
EPS POWER REQUIREMENTS - LARGE BASE - GEO	kW	2628	2920	3212
SPECIFIC MASS OF EPS BATTERIES	kg/kW	25	27	40
ORBIT KEEPING PROPELLANT MASS - SMALL BASE - LEO	kg	9000	10000	14000
ORBIT KEEPING PROPELLANT MASS - LARGE BASE - LEO	kg	9000	10000	14000
ORBIT KEEPING PROPELLANT MASS - SMALL BASE - GEO	kg	0	0	0
ORBIT KEEPING PROPELLANT MASS - LARGE BASE - GEO	kg	0	0	0
ATTITUDE CONTROL PROPELLANT MASS - SMALL BASE - LEO	kg	2.52×10^6	2.8×10^6	3.08×10^6
ATTITUDE CONTROL PROPELLANT MASS - LARGE BASE - LEO	kg	1.35×10^6	1.5×10^6	1.65×10^6
ATTITUDE CONTROL PROPELLANT MASS - SMALL BASE - GEO	kg	2.52×10^3	2.8×10^3	3.08×10^3
ATTITUDE CONTROL PROPELLANT MASS - LARGE BASE - GEO	kg	58.5×10^3	6.5×10^3	71×10^3
TOTAL SATELLITE FLEET SIZE	Number		120	
TOTAL CREW SIZE - SMALL BASE	Number	600	682	750
TOTAL CREW SIZE - LARGE BASE	Number	1600	1875	2060
NUMBER OF PERSONNEL CARRIED PER POTV FLIGHT	#/Flight	80	75	70
NUMBER OF CREW ROTATIONS PER YEAR	#/Year	3	4	6

B-5

TABLE B1: UNIT PRODUCTION COST MODEL INPUT VALUES (CONTINUED)

INPUT ELEMENT	UNITS	RANGE OF VALUES		
		BEST	MOST LIKELY	WORST
RATE OF SATELLITE CONSTRUCTION	#/Year	6	4	3
PROPELLANT CONSUMPTION PER POTV FLIGHT (RT)	kg	156×10^3	159×10^3	162×10^3
CAPACITY OF PROPELLANT STORAGE TANK	kg	-	106×10^3	-
UNIT MASS OF PROPELLANT STORAGE TANK	kg	-	3.18×10^3	-
PAYLOAD OF COTV	kg	-	250×10^3	-
UNIT MASS OF COTV (DRY)	kg	-	35×10^3	-
DESIGN LIFE OF POTV	# of Flights	-	30	-
UNIT MASS OF POTV (DRY)	kg	-	17×10^3	-
PROPELLANT CONSUMPTION PER COTV FLIGHT (RT)	kg	-	475×10^3	-
HLLV PAYLOAD TO LEO	kg	-	265×10^3	-
AIS PROPELLANT MASS-FRACTION	Fraction		.7289	
AIS TOTAL LEO-GEO MISSION ΔV	m/sec		5975	
AIS EXHAUST JET VELOCITY	m/sec		50,000	
ION PROPELLANT STORAGE TANK CAPACITY	kg		2.33×10^6	
ION PROPELLANT STORAGE TANK UNIT MASS (DRY)	kg		163×10^3	
HLLV AVERAGE LOAD FACTOR	Fraction	1.0	.9	.7
DESIGN LIFE OF HLLV UPPER STAGE	# of Flights		500	
DESIGN LIFE OF HLLV LOWER STAGE	# of Flights		300	
NUMBER OF PERSONNEL PER SHUTTLE FLIGHT	Number		75	
DESIGN LIFE OF SHUTTLE	# of Flights		100	
HLLV UPPER STAGE UNIT COST	\$	175×10^6	192×10^6	250×10^6
HLLV LOWER STAGE UNIT COST	\$	175×10^6	191×10^6	250×10^6
LAUNCH OPERATIONS COST PER HLLV FLIGHT	\$	6.5×10^6	6.9×10^6	9.0×10^6
LAUNCH OPERATIONS COST PER SHUTTLE FLIGHT	\$	12×10^6	15×10^6	20×10^6
SHUTTLE UNIT COST	\$	190×10^6	200×10^6	250×10^6
BASIC UNIT COST OF CONSTRUCTION BASE - SMALL	\$	600×10^6	892×10^6	1200×10^6

TABLE B1: UNIT PRODUCTION COST MODEL INPUT VALUES (CONTINUED)

INPUT ELEMENT	UNITS	RANGE OF VALUES		
		BEST	MOST LIKELY	WORST
BASIC UNIT COST OF CONSTRUCTION BASE - LARGE		1500 x 10 ⁶	1925 x 10 ⁶	2500 x 10 ⁶
SPECIFIC COST OF EPS SOLAR ARRAY	\$/kw	27.5 x 10 ⁶	55 x 10 ⁶	165 x 10 ⁶
SPECIFIC COST OF EPS BATTERIES	\$/kw	4000	5000	20,000
COST OF RADIATION SHIELDING - SMALL BASE - LEO	\$	5 x 10 ⁶	10 x 10 ⁶	30 x 10 ⁶
COST OF RADIATION SHIELDING - LARGE BASE - LEO	\$	15 x 10 ⁶	30	100 x 10 ⁶
COST OF RADIATION SHIELDING - SMALL BASE - GEO	\$	15 x 10 ⁶	30	100 x 10 ⁶
COST OF RADIATION SHIELDING - LARGE BASE - GEO	\$	50 x 10 ⁶	90	200 x 10 ⁶
SPECIFIC COST OF ATTITUDE CONTROL PROPELLANT	\$/kg		.33	
SPECIFIC COST OF ORBIT-KEEPING PROPELLANT	\$/kg		.33	
COTV UNIT COST	\$	12 x 10 ⁶	15 x 10 ⁶	25 x 10 ⁶
POTV UNIT COST	\$	18 x 10 ⁶	23 x 10 ⁶	40 x 10 ⁶
SPECIFIC COST OF OTV PROPELLANT	\$/kg		.55	
AIS UNIT COST	\$	150 x 10 ⁶	400 x 10 ⁶	500 x 10 ⁶
SPECIFIC COST OF ION PROPELLANT	\$/kg		.33	
OTV PROPELLANT STORAGE TANK UNIT COST	\$	12 x 10 ⁶	16 x 10 ⁶	20 x 10 ⁶
ION PROPELLANT STORAGE TANK UNIT COST	\$	12 x 10 ⁶	16 x 10 ⁶	20 x 10 ⁶
ANTENNA POWER DISTRIBUTION SPECIFIC COST	\$/kw		RAYTHEON	
PHASE CONTROL ELECTRONICS SPECIFIC COST	\$/kw		RAYTHEON	
WAVEGUIDE SPECIFIC COST	\$/kw		RAYTHEON	
DC-RF CONVERTER SPECIFIC COST	\$/kw		RAYTHEON	
ANTENNA STRUCTURE SPECIFIC COST	\$/kw	8.10	9.00	18.00
SOLAR ARRAY BLANKET SPECIFIC COST	\$/km ²	27.5 x 10 ⁶	55 x 10 ⁶	165 x 10 ⁶
SOLAR ARRAY CONCENTRATOR SPECIFIC COST	\$/km ²	1.04 x 10 ⁶	2.07 x 10 ⁶	6.22 x 10 ⁶
CONDUCTING STRUCTURE SPECIFIC COST	\$/kg	20	81	300
NON-CONDUCTING STRUCTURE SPECIFIC COST	\$/kg	20	81	300
CENTRAL MAST SPECIFIC COST	\$/kg	20	81	300

TABLE B1: UNIT PRODUCTION COST MODEL INPUT VALUES (CONTINUED)

INPUT ELEMENT	UNITS	RANGE OF VALUES		
		BEST	MOST LIKELY	WORST
MISCELLANEOUS EQUIPMENT SPECIFIC COST	\$/kg	219	437	750
RECTENNA SPECIFIC COST	\$/km ²		RAYTHEON	
BEAM ELEVATION ANGLE	Radians		RAYTHEON	
POWER INTERFACE SPECIFIC COST	\$/kW		RAYTHEON	
PHASE CONTROL SPECIFIC COST	\$/kW		RAYTHEON	

TABLE B2: STATES-OF-KNOWLEDGE AT DECISION POINTS - PROGRAM 4

INPUT ELEMENT	UNITS	IMPROVEMENTS IN STATE OF KNOWLEDGE - %			
		D.P.A. (1980)	D.P.B. (1983)	D.P.C. (1987)	D.P.D. (1992)
POWER OUTPUT AT RECTENNA BUSBAR (b.o.l.)	kW				
SOLAR CELL EFFICIENCY (b.o.l.)	Fraction	40	60	80	90
SOLAR ARRAY POWER DISTRIBUTION EFFICIENCY	Fraction	40	50	80	90
ANTENNA INTERFACE EFFICIENCY	Fraction	20	30	60	90
ANTENNA POWER DISTRIBUTION EFFICIENCY	Fraction		RAYTHEON		
DC-PF CONVERTER EFFICIENCY	Fraction		RAYTHEON		
PHASE CONTROL EFFICIENCY	Fraction		RAYTHEON		
IONOSPHERIC PROPAGATION EFFICIENCY	Fraction		RAYTHEON		
ATMOSPHERIC PROPAGATION EFFICIENCY	Fraction		RAYTHEON		
BEAM COLLECTION EFFICIENCY	Fraction		RAYTHEON		
RF-DC CONVERTER EFFICIENCY	Fraction		RAYTHEON		
RECTENNA POWER DISTRIBUTION EFFICIENCY	Fraction		RAYTHEON		
PACKING FACTOR OF SOLAR BLANKET	Fraction	20	80	90	100
SOLAR FLUX CONSTANT	kW/km ²				
EFFECTIVE CONCENTRATION RATIO	Fraction	20	40	80	100
SPECIFIC MASS OF SOLAR BLANKET	kg/km ²		A.D. LITTLE		
EFFICIENCY OF SOLAR CONCENTRATOR	Fraction	20	40	90	100
SPECIFIC MASS OF SOLAR CONCENTRATOR	kg/km ²	10	20	80	100
RATIO: COND. STRUCT. MASS TO SOLAR ARRAY AREA	kg/km ²	20	50	90	100
RATIO: NON-COND. STRUCT. MASS TO SOLAR ARRAY AREA	kg/km ²	20	50	90	100
SPECIFIC MASS OF CENTRAL MAST	kg/km	20	50	90	100
ASPECT RATIO OF SOLAR ARRAY	Fraction				
ANTENNA CLEARANCE	Fraction				
DIAMETER OF TRANSMITTING ANTENNA	km				
SPECIFIC MASS OF ANTENNA STRUCTURE	kg/kW	20	30	70	100
SPECIFIC MASS OF DC-RF CONVERTERS	kg/kW		RAYTHEON		

TABLE B2: STATES-OF-KNOWLEDGE AT DECISION POINTS - PROGRAM 4 (CONTINUED)

INPUT ELEMENT	UNITS	IMPROVEMENTS IN STATE OF KNOWLEDGE - %			
		D.P.A. (1980)	D.P.B. (1983)	D.P.C. (1987)	D.P.D. (1992)
SPECIFIC MASS OF ANTENNA POWER DIST. SYSTEM	kg/kW		RAYTHEON		
SPECIFIC MASS OF WAVEGUIDES	kg/kW		RAYTHEON		
SPECIFIC MASS OF ANTENNA INTERFACE	kg/kW		RAYTHEON		
SPECIFIC MASS OF PHASE CONTROL ELECTRONICS	kg/kW		RAYTHEON		
MISCELLANEOUS SATELLITE MASS	kg	20	30	80	90
BASIC UNIT MASS OF CONSTRUCTION BASE - SMALL	kg	20	40	80	90
BASIC UNIT MASS OF CONSTRUCTION BASE - LARGE	kg	20	40	80	90
SPECIFIC MASS OF EPS SOLAR ARRAY	kg/kW	20	40	80	90
EPS POWER REQUIREMENTS - SMALL BASE - LEO	kW	20	40	80	90
EPS POWER REQUIREMENTS - LARGE BASE - LEO	kW	20	40	80	90
EPS POWER REQUIREMENTS - SMALL BASE - GEO	kW	20	40	80	90
EPS POWER REQUIREMENTS - LARGE BASE - GEO	kW	20	40	80	90
SPECIFIC MASS OF EPS BATTERIES	kg/kW	30	50	70	100
ORBIT KEEPING PROPELLANT MASS - SMALL BASE - LEO	kg	20	70	90	100
ORBIT KEEPING PROPELLANT MASS - LARGE BASE - LEO	kg	20	70	90	100
ORBIT KEEPING PROPELLANT MASS - SMALL BASE - GEO	kg	20	40	70	90
ORBIT KEEPING PROPELLANT MASS - LARGE BASE - GEO	kg	20	40	70	90
ATTITUDE CONTROL PROPELLANT MASS - SMALL BASE - LEO	kg	20	50	90	100
ATTITUDE CONTROL PROPELLANT MASS - LARGE BASE - LEO	kg	20	50	90	100
ATTITUDE CONTROL PROPELLANT MASS - SMALL BASE - GEO	kg	20	40	70	90
ATTITUDE CONTROL PROPELLANT MASS - LARGE BASE - GEO	kg	20	40	70	90
TOTAL SATELLITE FLEET SIZE	Number				
TOTAL CREW SIZE - SMALL BASE	Number	20	40	70	90
TOTAL CREW SIZE - LARGE BASE	Number	20	40	70	90
NUMBER OF PERSONNEL CARRIED PER POTV FLIGHT	#/Flight	30	50	90	100
NUMBER OF CREW ROTATIONS PER YEAR	#/Year	30	70	90	100

TABLE B2: STATES-OF-KNOWLEDGE AT DECISION POINTS - PROGRAM 4 (CONTINUED)

INPUT ELEMENT	UNITS	IMPROVEMENTS IN STATE OF KNOWLEDGE - %			
		D.P.A. (1980)	D.P.B. (1983)	D.P.C. (1987)	D.P.D. (1992)
RATE OF SATELLITE CONSTRUCTION	#/Year	20	50	90	100
PROPELLANT CONSUMPTION PER POTV FLIGHT (RT)	kg	20	70	90	100
CAPACITY OF PROPELLANT STORAGE TANK	kg				
UNIT MASS OF PROPELLANT STORAGE TANK	kg				
PAYLOAD OF COTV	kg	20	50	90	100
UNIT MASS OF COTV (DRY)	kg				
DESIGN LIFE OF POTV	# of Flights				
UNIT MASS OF POTV (DRY)	kg				
PROPELLANT CONSUMPTION PER COTV FLIGHT (RT)	kg				
HLLV PAYLOAD TO LEO	kg				
AIS PROPELLANT MASS-FRACTION	Fraction				
AIS TOTAL LEO-GEO MISSION ΔV	m/sec				
AIS EXHAUST JET VELOCITY	m/sec				
ION PROPELLANT STORAGE TANK CAPACITY	kg	20	50	70	100
ION PROPELLANT STORAGE TANK UNIT MASS (DRY)	kg	20	50	70	100
HLLV AVERAGE LOAD FACTOR	Fraction	20	50	70	100
DESIGN LIFE OF HLLV UPPER STAGE	# of Flights	30	70	90	100
DESIGN LIFE OF HLLV LOWER STAGE	# of Flights	30	70	90	100
NUMBER OF PERSONNEL PER SHUTTLE FLIGHT	Number				
DESIGN LIFE OF SHUTTLE	# of Flights				
HLLV UPPER STAGE UNIT COST	\$	30	70	90	100
HLLV LOWER STAGE UNIT COST	\$	30	70	90	100
LAUNCH OPERATIONS COST PER HLLV FLIGHT	\$	30	70	90	100
LAUNCH OPERATIONS COST PER SHUTTLE FLIGHT	\$	100			
SHUTTLE UNIT COST	\$	100			
BASIC UNIT COST OF CONSTRUCTION BASE - SMALL	\$	20	50	70	90

TABLE B2: STATES-OF-KNOWLEDGE AT DECISION POINTS - PROGRAM 4 (CONTINUED)

INPUT ELEMENT	UNITS	IMPROVEMENTS IN STATE OF KNOWLEDGE - %			
		D.P.A. (1980)	D.P.B. (1983)	D.P.C. (1987)	D.P.D. (1992)
BASIC UNIT COST OF CONSTRUCTION BASE - LARGE		20	50	70	90
SPECIFIC COST OF EPS SOLAR ARRAY	\$/kW	20	50	70	90
SPECIFIC COST OF EPS BATTERIES	\$/kW	20	70	100	
COST OF RADIATION SHIELDING - SMALL BASE - LEO	\$	20	50	70	90
COST OF RADIATION SHIELDING - LARGE BASE - LEO	\$	20	50	70	90
COST OF RADIATION SHIELDING - SMALL BASE - GEO	\$	20	50	70	90
COST OF RADIATION SHIELDING - LARGE BASE - GEO	\$	20	50	70	90
SPECIFIC COST OF ATTITUDE CONTROL PROPELLANT	\$/kg				
SPECIFIC COST OF ORBIT-KEEPING PROPELLANT	\$/kg				
COTV UNIT COST	\$	20	50	90	100
POTV UNIT COST	\$	20	50	90	100
SPECIFIC COST OF OTV PROPELLANT	\$/kg				
AIS UNIT COST	\$	20	50	90	100
SPECIFIC COST OF ION PROPELLANT	\$/kg				
OTV PROPELLANT STORAGE TANK UNIT COST	\$	20	50	90	100
ION PROPELLANT STORAGE TANK UNIT COST	\$	20	50	90	100
ANTENNA POWER DISTRIBUTION SPECIFIC COST	\$/kW		RAYTHEON		
PHASE CONTROL ELECTRONICS SPECIFIC COST	\$/kW		RAYTHEON		
WAVEGUIDE SPECIFIC COST	\$/kW		RAYTHEON		
DC-RF CONVERTER SPECIFIC COST	\$/kW		RAYTHEON		
ANTENNA STRUCTURE SPECIFIC COST	\$/kW	20	50	70	100
SOLAR ARRAY BLANKET SPECIFIC COST	\$/km ²	20	50	70	100
SOLAR ARRAY CONCENTRATOR SPECIFIC COST	\$/km ²	10	40	80	100
CONDUCTING STRUCTURE SPECIFIC COST	\$/kg	10	50	90	100
NON-CONDUCTING STRUCTURE SPECIFIC COST	\$/kg	10	50	90	100
CENTRAL MAST SPECIFIC COST	\$/kg	10	50	90	100

TABLE B2: STATES-OF-KNOWLEDGE AT DECISION POINTS - PROGRAM 4 (CONTINUED)

INPUT ELEMENT	UNITS	IMPROVEMENTS IN STATE OF KNOWLEDGE - %			
		D.P.A. (1980)	D.P.B. (1983)	D.P.C. (1987)	D.P.D. (1992)
MISCELLANEOUS EQUIPMENT SPECIFIC COST	\$/kg	10	40	70	100
RECTENNA SPECIFIC COST	\$/km ²		RAYTHEON		
BEAM ELEVATION ANGLE	Radians		RAYTHEON		
POWER INTERFACE SPECIFIC COST	\$/kW		RAYTHEON		
PHASE CONTROL SPECIFIC COST	\$/kW		RAYTHEON		
MASS OF RADIATION SHIELDING - SMALL BASE - LEO			34,000 Kg		
MASS OF RADIATION SHIELDING - SMALL BASE - GEO			136,000 Kg		
MASS OF RADIATION SHIELDING - LARGE BASE - LEO			93,000 Kg		
MASS OF RADIATION SHIELDING - LARGE BASE - GEO			374,000 Kg		

TABLE B3: STATES-OF-KNOWLEDGE AT DECISION POINTS - PROGRAM 5

INPUT ELEMENT	UNITS	IMPROVEMENTS IN STATE OF KNOWLEDGE - %			
		D.P.A. (1980)	D.P.B. (1983)	D.P.C. (1987)	D.P.D. (1992)
POWER OUTPUT AT RECTENNA BUSBAR (b.o.l.)	kW				
SOLAR CELL EFFICIENCY (b.o.l.)	Fraction	40	70	85	90
SOLAR ARRAY POWER DISTRIBUTION EFFICIENCY	Fraction	40	60	85	90
ANTENNA INTERFACE EFFICIENCY	Fraction	20	60	75	90
ANTENNA POWER DISTRIBUTION EFFICIENCY	Fraction		RAYTHEON		
DC-PF CONVERTER EFFICIENCY	Fraction		RAYTHEON		
PHASE CONTROL EFFICIENCY	Fraction		RAYTHEON		
IONOSPHERIC PROPAGATION EFFICIENCY	Fraction		RAYTHEON		
ATMOSPHERIC PROPAGATION EFFICIENCY	Fraction		RAYTHEON		
BEAM COLLECTION EFFICIENCY	Fraction		RAYTHEON		
RF-DC CONVERTER EFFICIENCY	Fraction		RAYTHEON		
RECTENNA POWER DISTRIBUTION EFFICIENCY	Fraction		RAYTHEON		
PACKING FACTOR OF SOLAR BLANKET	Fraction	20	80	90	100
SOLAR FLUX CONSTANT	kW/km ²				
EFFECTIVE CONCENTRATION RATIO	Fraction	20	70	90	100
SPECIFIC MASS OF SOLAR BLANKET	kg/km ²		A.D. LITTLE		
EFFICIENCY OF SOLAR CONCENTRATOR	Fraction	20	90	100	100
SPECIFIC MASS OF SOLAR CONCENTRATOR	kg/km ²	10	40	90	100
RATIO: COND. STRUCT. MASS TO SOLAR ARRAY AREA	kg/km ²	20	50	90	100
RATIO: NON-COND. STRUCT. MASS TO SOLAR ARRAY AREA	kg/km ²	20	50	90	100
SPECIFIC MASS OF CENTRAL MAST	kg/km	20	50	90	100
ASPECT RATIO OF SOLAR ARRAY	Fraction				
ANTENNA CLEARANCE	Fraction				
DIAMETER OF TRANSMITTING ANTENNA	km				
SPECIFIC MASS OF ANTENNA STRUCTURE	kg/kW	20	60	90	100
SPECIFIC MASS OF DC-RF CONVERTERS	kg/kW		RAYTHEON		

B-14

TABLE B3: STATES-OF-KNOWLEDGE AT DECISION POINTS - PROGRAM 5 (CONTINUED)

INPUT ELEMENT	UNITS	IMPROVEMENTS IN STATE OF KNOWLEDGE - %			
		D.P.A. (1980)	D.P.B. (1983)	D.P.C. (1987)	D.P.D. (1992)
SPECIFIC MASS OF ANTENNA POWER DIST. SYSTEM	kg/kW		RAYTHEON		
SPECIFIC MASS OF WAVEGUIDES	kg/kW		RAYTHEON		
SPECIFIC MASS OF ANTENNA INTERFACE	kg/kW		RAYTHEON		
SPECIFIC MASS OF PHASE CONTROL ELECTRONICS	kg/kW		RAYTHEON		
MISCELLANEOUS SATELLITE MASS	kg	30	50	90	100
BASIC UNIT MASS OF CONSTRUCTION BASE - SMALL	kg	20	40	80	90
BASIC UNIT MASS OF CONSTRUCTION BASE - LARGE	kg	20	40	80	90
SPECIFIC MASS OF EPS SOLAR ARRAY	kg/kW	20	40	80	90
EPS POWER REQUIREMENTS - SMALL BASE - LEO	kW	20	40	80	90
EPS POWER REQUIREMENTS - LARGE BASE - LEO	kW	20	40	80	90
EPS POWER REQUIREMENTS - SMALL BASE - GEO	kW	20	40	80	90
EPS POWER REQUIREMENTS - LARGE BASE - GEO	kW	20	40	80	90
SPECIFIC MASS OF EPS BATTERIES	kg/kW	30	50	70	100
ORBIT KEEPING PROPELLANT MASS - SMALL BASE - LEO	kg	20	70	100	100
ORBIT KEEPING PROPELLANT MASS - LARGE BASE - LEO	kg	20	70	100	100
ORBIT KEEPING PROPELLANT MASS - SMALL BASE - GEO	kg	20	60	90	100
ORBIT KEEPING PROPELLANT MASS - LARGE BASE - GEO	kg	20	60	90	100
ATTITUDE CONTROL PROPELLANT MASS - SMALL BASE - LEO	kg	20	70	90	100
ATTITUDE CONTROL PROPELLANT MASS - LARGE BASE - LEO	kg	20	70	90	100
ATTITUDE CONTROL PROPELLANT MASS - SMALL BASE - GEO	kg	20	40	70	90
ATTITUDE CONTROL PROPELLANT MASS - LARGE BASE - GEO	kg	20	40	70	90
TOTAL SATELLITE FLEET SIZE	Number				
TOTAL CREW SIZE - SMALL BASE	Number	20	50	80	90
TOTAL CREW SIZE - LARGE BASE	Number	20	50	80	90
NUMBER OF PERSONNEL CARRIED PER POTV FLIGHT	#/Flight	30	50	90	100
NUMBER OF CREW ROTATIONS PER YEAR	#/Year	30	70	90	100

TABLE B3: STATES-OF-KNOWLEDGE AT DECISION POINTS - PROGRAM 5 (CONTINUED)

INPUT ELEMENT	UNITS	IMPROVEMENTS IN STATE OF KNOWLEDGE - %			
		D.P.A. (1980)	D.P.B. (1983)	D.P.C. (1987)	D.P.D. (1992)
RATE OF SATELLITE CONSTRUCTION	#/Year	20	50	90	100
PROPELLANT CONSUMPTION PER POTV FLIGHT (RT)	kg	20	70	90	100
CAPACITY OF PROPELLANT STORAGE TANK	kg				
UNIT MASS OF PROPELLANT STORAGE TANK	kg				
PAYLOAD OF COTV	kg	20	80	90	100
UNIT MASS OF COTV (DRY)	kg				
DESIGN LIFE OF POTV	# of Flights				
UNIT MASS OF POTV (DRY)	kg				
PROPELLANT CONSUMPTION PER COTV FLIGHT (RT)	kg				
HLLV PAYLOAD TO LEO	kg				
AIS PROPELLANT MASS-FRACTION	Fraction				
AIS TOTAL LEO-GEO MISSION ΔV	m/sec				
AIS EXHAUST JET VELOCITY	m/sec				
ION PROPELLANT STORAGE TANK CAPACITY	kg	20	50	70	100
ION PROPELLANT STORAGE TANK UNIT MASS (DRY)	kg	20	50	70	100
HLLV AVERAGE LOAD FACTOR	Fraction	20	50	70	100
DESIGN LIFE OF HLLV UPPER STAGE	# of Flights	30	70	90	100
DESIGN LIFE OF HLLV LOWER STAGE	# of Flights	30	70	90	100
NUMBER OF PERSONNEL PER SHUTTLE FLIGHT	Number				
DESIGN LIFE OF SHUTTLE	# of Flights				
HLLV UPPER STAGE UNIT COST	\$	30	70	90	100
HLLV LOWER STAGE UNIT COST	\$	30	70	90	100
LAUNCH OPERATIONS COST PER HLLV FLIGHT	\$	30	70	90	100
LAUNCH OPERATIONS COST PER SHUTTLE FLIGHT	\$	100			
SHUTTLE UNIT COST.	\$	100			
BASIC UNIT COST OF CONSTRUCTION BASE - SMALL	\$	20	50	70	90

TABLE B3: STATES-OF-KNOWLEDGE AT DECISION POINTS - PROGRAM 5 (CONTINUED)

INPUT ELEMENT	UNITS	IMPROVEMENTS IN STATE OF KNOWLEDGE - %			
		D.P.A. (1980)	D.P.B. (1983)	D.P.C. (1987)	D.P.D. (1992)
BASIC UNIT COST OF CONSTRUCTION BASE - LARGE		20	50	70	90
SPECIFIC COST OF EPS SOLAR ARRAY	\$/kW	20	50	70	90
SPECIFIC COST OF EPS BATTERIES	\$/kW	20	50	90	100
COST OF RADIATION SHIELDING - SMALL BASE - LEO	\$	20	50	70	90
COST OF RADIATION SHIELDING - LARGE BASE - LEO	\$	20	50	70	90
COST OF RADIATION SHIELDING - SMALL BASE - GEO	\$	20	50	70	90
COST OF RADIATION SHIELDING - LARGE BASE - GEO	\$	20	50	70	90
SPECIFIC COST OF ATTITUDE CONTROL PROPELLANT	\$/kg				
SPECIFIC COST OF ORBIT-KEEPING PROPELLANT	\$/kg				
COTV UNIT COST	\$	20	50	90	100
POTV UNIT COST	\$	20	50	90	100
SPECIFIC COST OF OTV PROPELLANT	\$/kg				
AIS UNIT COST	\$	20	50	90	100
SPECIFIC COST OF ION PROPELLANT	\$/kg				
OTV PROPELLANT STORAGE TANK UNIT COST	\$	20	70	90	100
ION PROPELLANT STORAGE TANK UNIT COST	\$	20	50	90	100
ANTENNA POWER DISTRIBUTION SPECIFIC COST	\$/kW		RAYTHEON		
PHASE CONTROL ELECTRONICS SPECIFIC COST	\$/kW		RAYTHEON		
WAVEGUIDE SPECIFIC COST	\$/kW		RAYTHEON		
DC-RF CONVERTER SPECIFIC COST	\$/kW		RAYTHEON		
ANTENNA STRUCTURE SPECIFIC COST	\$/kW	20	70	90	100
SOLAR ARRAY BLANKET SPECIFIC COST	\$/km ²	20	50	70	100
SOLAR ARRAY CONCENTRATOR SPECIFIC COST	\$/km ²	10	60	90	100
CONDUCTING STRUCTURE SPECIFIC COST	\$/kg	10	60	90	100
NON-CONDUCTING STRUCTURE SPECIFIC COST	\$/kg	10	50	90	100
CENTRAL MAST SPECIFIC COST	\$/kg	10	50	90	100

TABLE B3: STATES-OF-KNOWLEDGE AT DECISION POINTS - PROGRAM 5 (CONTINUED)

INPUT ELEMENT	UNITS	IMPROVEMENTS IN STATE OF KNOWLEDGE - %			
		D.P.A. (1980)	D.P.B. (1983)	D.P.C. (1987)	D.P.D. (1992)
MISCELLANEOUS EQUIPMENT SPECIFIC COST	\$/kg	10	50	80	100
RECTENNA SPECIFIC COST	\$/km ²		RAYTHEON		
BEAM ELEVATION ANGLE	Radians		RAYTHEON		
POWER INTERFACE SPECIFIC COST	\$/kW		RAYTHEON		
PHASE CONTROL SPECIFIC COST	\$/kW		RAYTHEON		

BIBLIOGRAPHY

1. Spectrolab - 6011-03 Progress Report - "Feasibility Study of Satellite Solar Power Station," 1 October 1972.
2. Spectrolab - 6011-02 "Progress Report - Feasibility Study of Satellite Solar Power Station," 1 September 1972.
3. NAS, "Solar Cells - Outlook for Improved Efficiency," 1972.
4. NSS-MO-75-109, "SSPS Engineering Analysis of Special Requirements Transportation to Low Earth Orbit," 21 February 1975.
5. JPL, "Progress Report No. 2 - Comparative Assessment of Orbital and Terrestrial Central Power Station," August 1 to November 30, 1974.
6. NASA CR-2357, "Feasibility Study of a Satellite Solar Power Station," February 1975.
7. MPTS-R-002, "Task 2 Concept Definition, Microwave Power Transmission System Studies - Mechanical Systems & Flight Operations," 12 December 1974.
8. Spectrolab, "Satellite Solar Power Station" Technical Report, November 1971.
9. ECON, "Space Based Solar Power Conversion and Delivery Systems Study" - Interim Summary Report, March 31, 1976.
10. NASA CR-2357, "Feasibility Study of a Satellite Solar Power Station," February 1974.
11. NASA CR-134886, "Microwave Power Transmission System Studies," December 1975.
12. "Cost Prediction of Space Projects," Technical paper presented at 2nd Symposium on Cost Reduction in Space Operations, International Academy of Astronautics. .
13. Grumman Report ASP-583-R-8, "Satellite Solar Power Station - Systems Engineering Report," November 1971.
14. Grumman Report ASP-583-R-11 "Satellite Solar Power Station - Technical Memoranda," June 1972.
15. Grumman Memo NSS-MO-75-111, "SSPS Engineering Analysis of Special Requirements - Orbit to Orbit Transportation," March 1975.

16. Grumman Memo ASP-611-M-1011 "Force Resulting From The Electromagnetic Radiation of Energy From the SSPS Antenna," September 1972.
17. Grumman Memo ASP-611-M-1004, "Sensitivity of Attitude Control Propellant Requirement to SSPS Deviation Angle Limits," August 1972.
18. Grumman Memo NSS-MO-75-118, "SSPS Engineering Analysis of Special Requirement - Large Solar Arrays," March 1975.
19. NASA CR-2357, "Feasibility Study of a Satellite Solar Power Station," February 1974.
20. Grumman/Raytheon, MPTS-R-002, "Microwave Power Transmission Systems Study - Task 2 Report," 12 December 1974.
21. Kaula, "Theory of Satellite Geodesy," 1966 Blarsdell Publishing Co., Waltham, Mass.
22. Rockwell Report E74-31, "Power Relay Satellite," March 1974.
23. GAC Report MPTS-R-002, "Microwave Power Transmission Systems Study - Task 2," December 1974.



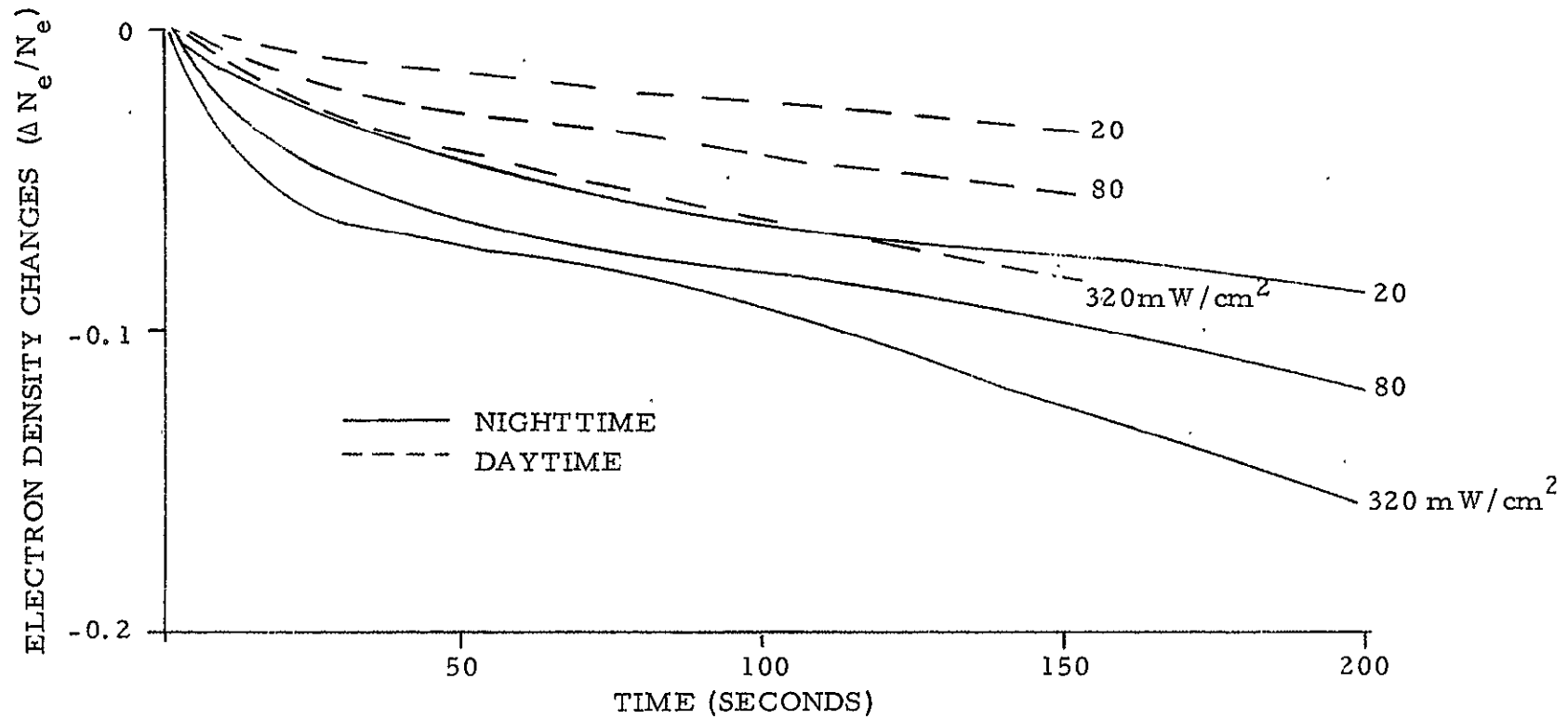


FIGURE 2.9 Decrease in electron density at the Northeast site for both daytime and nighttime ionospheres, calculated for 3 different Poynting fluxes.

2.2.3 D-REGION HEATING

2.2.3.1 Basic Processes

In the D-region, from 60 - 90 km, collisions are so frequent that thermal conductivity can be completely neglected; therefore, the energy imparted to the electrons from the power beam is transferred to the neutral gas at the same point in space at which it is absorbed.

The electron temperature under the influence of the power beam is calculated by means of a computer program which uses the method described in References 6 - 8. The electron temperature reaches a steady state in times of the order of milliseconds, although this rate, which is essentially proportional to collision frequency, becomes slower with increasing altitude.

As shown below, the absorption in the D-region increases by an order of magnitude due to the increased collision frequency of the heated electrons; however, the amount of power removed from the power beam at 2450 MHz is only in order of one part in 5000, including the effect of the high temperature electrons. Because the Poynting flux remains constant, the microwave heating problem is much simpler to solve than was the HF heating problem, which required solving three coupled differential equations for S , the electron temperature T_e , and the electron density n .⁶⁻⁸ The equation for electron temperature in the microwave case is

$$\frac{\partial T_e}{\partial t} = AS - \frac{2}{3} (U_1 + U_2 + U_3 + U_4) \quad (4)$$

where, for T_e in °K, and, for $f = 2450$ MHz, and S in (mW/cm^2) ,

$$A = .0216 \nu_{en}$$

and ν_{en} is the effective Sen-Wyller collision frequency^{6, 9-10}

$$\nu_{en} = 2.49 \times 10^{-11} n_2 T \quad (5)$$